ALLIGATOR RIVERS ANALOGUE PROJECT

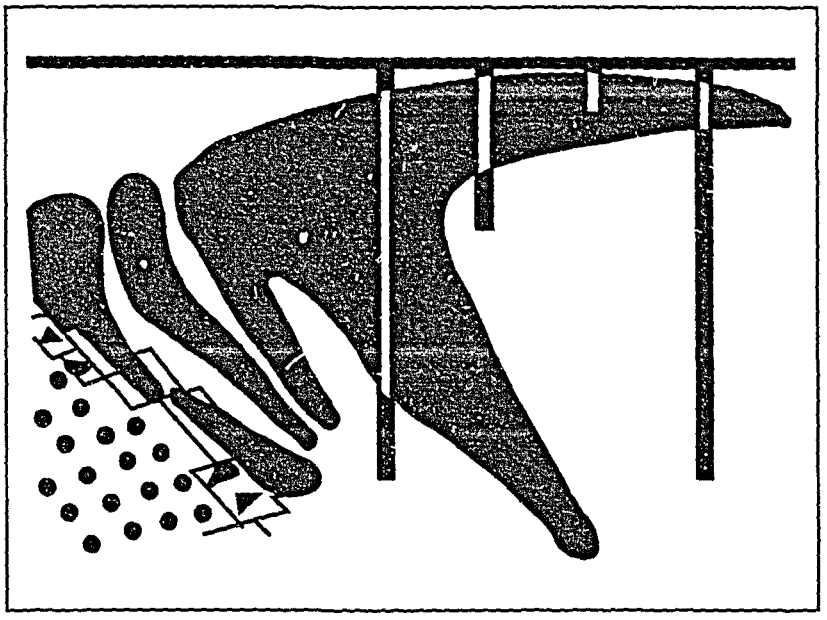

ISBN 0-642-59933-5

DOE/HMIP/RR/92/077

SKI TR 92:20-7

FINAL REPORT
VOLUME 7

GROUNDWATER CHEMISTRY

1992

AN OECD/NEA INTERNATIONAL PROJECT MANAGED BY:
AUSTRALIAN NUCLEAR SCIENCE AND TECHNOLOGY ORGANISATION

ALLIGATOR RIVERS ANALOGUE PROJECT

FINAL REPORT

VOLUME 7

GROUNDWATER CHEMISTRY

Lead author: Timothy E. Payne[1]

Contributing authors:
Robert Edis[1], Andrew L. Herczeg[2], Keiichi Sekine[3],
Toshihiro Seo[4], T. David Waite[1], and Nobuyuki Yanase[3].

[1]Australian Nuclear Science and Technology Organisation
Private Mail Bag 1, Menai, NSW, 2234, Australia

[2]Commonwealth Scientific and Industrial Research Organisation
Division of Water Resources, Private Bag No.2, Glen Osmond, SA, 5064, Australia

[3]Japan Atomic Energy Research Institute
Environmental Radiochemistry Laboratory, Tokai Research Establishment,
Tokai-Mura, Naka-Gun, Ibaraki-Ken, Japan

[4]Power Reactor and Nuclear Fuel Development Corporation
Waste Isolation Section, Chubu Works, 929-31, Sonodo, Jorinji,
Izumi-cho, Toki City, Gifu Pref, 509-51, Japan

PREFACE

The Koongarra uranium ore deposit is located in the Alligator Rivers Region of the Northern Territory of Australia. Many of the processes that have controlled the development of this natural system are relevant to the performance assessment of radioactive waste repositories. An Agreement was reached in 1987 by a number of agencies concerned with radioactive waste disposal, to set up the International Alligator Rivers Analogue Project (ARAP) to study relevant aspects of the hydrological and geochemical evolution of the site. The Project ran for five years.

The work was undertaken by ARAP through an Agreement sponsored by the OECD Nuclear Energy Agency (NEA). The Agreement was signed by the following organisations: the Australian Nuclear Science and Technology Organisation (ANSTO); the Japan Atomic Energy Research Institute (JAERI); the Power Reactor and Nuclear Fuel Development Corporation of Japan (PNC); the Swedish Nuclear Power Inspectorate (SKI); the UK Department of the Environment (UKDoE); and the US Nuclear Regulatory Commission (USNRC). ANSTO was the managing participant.

This report is one of a series of 16 describing the work of the Project; these are listed below:

No.	Title	Lead Author(s)
1	Summary of Findings	P Duerden, D A Lever, D A Sverjensky and L R Townley
2	Geologic Setting	A A Snelling
3	Geomorphology and Paleoclimatic History	K-H Wyrwoll
4	Geophysics, Petrophysics and Structure	D W Emerson
5	Hydrogeological Field Studies	S N Davis
6	Hydrogeological Modelling	L R Townley
7	Groundwater Chemistry	T E Payne
8	Chemistry and Mineralogy of Rocks and Soils	R Edis
9	Weathering and its Effects on Uranium Redistribution	T Murakami
10	Geochemical Data Bases	D G Bennett and D Read
11	Geochemical Modelling of Secondary Uranium Ore Formation	D A Sverjensky
12	Geochemical Modelling of Present-day Groundwaters	D A Sverjensky
13	Uranium Sorption	T D Waite
14	Radionuclide Transport	C Golian and D A Lever
15	Geochemistry of ^{238}Pu, ^{129}I, ^{99}Tc and ^{36}Cl	J T Fabryka-Martin
16	Scenarios	K Skagius and S Wingefors

CONTENTS

LIST OF TABLES

LIST OF FIGURES

ABBREVIATIONS

AES	Atomic Emission Spectroscopy
ANSTO	Australian Nuclear Science and Technology Organisation
ASV	Anodic Stripping Voltammetry
BF	Ultrafilter Back-Flush (in colloid separation experiments)
CC	Colloid Concentrate
CSIRO	Commonwealth Scientific and Industrial Research Organisation
DIC	Dissolved Inorganic Carbon
DO	Dissolved Oxygen
dpm	Disintegrations per Minute
EC	Electrical Conductivity
EDS	Energy Dispersive Spectroscopy
ICPAES	Inductively Coupled Plasma Atomic Emission Spectroscopy
ICPMS	Inductively Coupled Plasma Mass Spectrometry
JAERI	Japan Atomic Energy Research Institute
KPA	Kinetic Phosphorescence Analysis
MINTEQA2	A chemical speciation computer program
PDB	A marine carbonate standard with a reference $^{13}C/^{12}C$ ratio
PET	Polyethylene
PMC	Percent Modern Carbon
PNC	Power Reactor and Nuclear Fuel Corporation (Japan)
PVC	Polyvinylchloride
SEM	Scanning Electron Microscopy
SMOW	Standard Mean Ocean Water
SWL	Standing Water Level
TAO	Tamm's Acid Oxalate
TDS	Total Dissolved Solids
TEM	Transmission Electron Microscopy
TOC	Total Organic Carbon
TU	Tritium Unit
UF	Ultrafiltrate
UKDOE	United Kingdom Department of the Environment
USNRC	United States Nuclear Regulatory Commission
V-SMOW	Vienna Standard Mean Ocean Water
WATEQ4F	A chemical speciation computer program

EXECUTIVE SUMMARY

Groundwaters in the mineralised zones at Koongarra exhibit elevated levels of uranium and the radionuclides of its decay series. The pH is slightly acidic or neutral, and the major ion chemistry is dominated by magnesium and bicarbonate. Groundwaters are quite dilute, with total dissolved solids (TDS) below 200 mg/L. In many groundwater samples, partial pressures of CO_2 are substantially elevated relative to those of surface waters.

Uranium concentrations within the orebody are up to four orders of magnitude above background concentrations. Down-gradient, there is a gradual decrease over approximately 200 metres. The $^{234}U/^{238}U$ activity ratio is strongly dependent on depth. In groundwaters of the weathered zone, $^{234}U/^{238}U$ ratios are often substantially below unity. These low ratios are correlated to those in accessible (readily leached) uranium of the solid phase. In the unweathered zone the groundwater $^{234}U/^{238}U$ ratios generally exceed unity.

Uranium appears to be mobile in the weathered zone as uranyl carbonate complexes. Other inorganic uranium complexants are not present at levels sufficient to influence uranium speciation, with the possible exception of phosphate. Uranyl phosphate minerals occur in the secondary uranium mineralisation and the levels of phosphate in some Koongarra groundwaters are unusually high. Total organic carbon levels are generally low, suggesting that uranium complexation by organic species plays a minor role.

The measured concentrations of thorium isotopes in Koongarra groundwaters were extremely low, with $^{230}Th/^{234}U$ ratios below 0.001. Therefore, ^{230}Th is substantially less mobile than ^{234}U and can be regarded as immobile for modelling purposes. Radium is mobile in deeper groundwaters, and may be precipitated, together with manganese and ferric oxyhydroxides, at the base of the weathered zone. The distributions of ^{238}U and other isotopes, such as ^{210}Pb, suggested that the direction of present-day radionuclide migration is towards the south.

Dissolved CO_2 in Koongarra groundwater plays an important role in weathering of minerals such as chlorite. This process is responsible for the elevated levels of Mg^{2+} and HCO_3^-. Groundwater in the centre of the orebody has a low proportion of ^{14}C. Therefore, the CO_2 is not, in the main, derived from the root zone of plants. Based on ^{13}C data, a possible ultimate source of the CO_2 is bacterial degradation of organic material, such as the dispersed graphite in the Cahill formation. Another significant input of CO_2 into the system may be the CO_2 present in up-gradient (Kombolgie) groundwaters.

Iron seems to play an important role in the system. The state of saturation of groundwaters with respect to amorphous iron minerals is correlated to measured redox values, and some iron-rich colloids are present. Iron minerals adsorb uranium strongly, and adsorption may be a more important mechanism for uranium retardation than mineral precipitation as solubility products for uranium minerals are rarely approached, except in the immediate vicinity of the orebody.

Seasonal changes in the composition of deeper groundwaters (from depths below the permanent water table) are relatively minor. However, in the zone of fluctuating saturation, seasonal effects appear to be quite marked. Water chemistry in this zone, during the wet season, is similar to rainwater. These shallower groundwaters, sampled at the end of the wet season, tended to be extremely dilute in major constituents, and had a pH/Eh state which was intermediate between rainwater and the groundwater samples from the permanently saturated zone. There is some evidence that as water levels drop during the dry season, the chemistry becomes less dilute and approaches the chemistry of deeper samples, either by mixing processes, evapotranspiration or a combination of both.

On the basis of isotopic and chemical evidence, there are two major potential inputs of groundwater in the system. The first of these is flow from the vicinity of the Koongarra fault into the Cahill formation which hosts the uranium mineralisation. A second major source is infiltrating waters which permeate downwards from the surface, and cause a gradual mixing and dilution of the characteristics of groundwaters from the mineralised zone. As a result, the chemistry of shallow groundwaters is dependent on depth.

The input of significant quantities of water across the fault from the Kombolgie formation is suggested by the similar isotopic composition of water molecules (δ^2H values) of groundwaters from the orebody and those from the Kombolgie formation. Furthermore, borehole KD1 (which intersects the Kombolgie formation), yields large quantities of oxidising and CO_2-charged groundwater when continuously pumped, and primary uranium minerals in the region adjacent to the fault have been subjected to in-situ alteration. One explanation of these observations is groundwater flow from fractures in the Kombolgie through the fault zone, causing in-situ alteration in the zone close to the fault. However, flow downwards in the vicinity of the fault may also explain this in-situ alteration.

Groundwaters up-gradient and within the orebody are characterised by quite negative deuterium (δ^2H) values, in the range -25 ‰ to -40 ‰. Down-gradient of the orebody the groundwaters become more dilute, and the δ^2H composition of the water molecules becomes less negative and tends to approach the average values of rainwaters and surface waters. These changes are accompanied by an increase in the radiocarbon content. Tritium is present in some shallower groundwaters. These phenomena appear to be adequately explained by a gradual mixing with local recharge as groundwater moves down-gradient. However, the data for tritium and ^{14}C suggest that mixing processes are quite slow, and most of the precipitation over the site is dispersed by evapotranspiration and run-off.

In general, groundwater in the system does not seem to move perpendicularly to the fault, but at an angle to it. In the vicinity of borehole PH88 (due south of the ore-zone), uranium concentrations were quite high, given the distance from the orebody. Concentrations of Mg^{2+} and HCO_3^- were also elevated at PH88, and some other isotopes (eg. ^{210}Pb), appear to be dispersed in this direction. On a Piper tri-linear diagram, groundwaters from this area plot close to those from the centre of the ore-body, indicating that the two groundwater types are closely related.

Colloids are a relatively unimportant mechanism for radionuclide transport in Koongarra groundwaters, and the total number of colloidal particles is very low. Uranium migrates mostly as dissolved species, whereas thorium and actinium are mostly associated with larger, relatively immobile particles (>1.0 μm). However, of the small amount of ^{230}Th that passes through a 1.0 μm filter, a significant proportion is associated with colloidal particles. These colloids mostly consist of iron oxides and clay minerals and carry a small proportion of the uranium in the groundwater. The clay minerals in the colloids reflect the mineralogy of the solid phase from the vicinity of the water sampling point. Actinium appears to be slightly more mobile than thorium and is associated with colloids to a greater extent, although generally present in low concentrations.

In summary, groundwater enters the Cahill formation from the vicinity of the Koongarra fault. The groundwater in the mineralised zone has elevated levels of HCO_3^-, Mg^{2+}, uranium isotopes, and ^{238}U-series radionuclides; and low levels of ^{14}C. Uranium is present in a true dissolved (rather than colloidal) form, probably as uranyl carbonate complexes. As it moves down-gradient, the groundwater is gradually diluted and mixed with local recharge derived from seasonal rainwaters. Dilution and adsorption appear to be the main processes which reduce uranium concentrations once the groundwater is outside the immediate vicinity of the primary ore-zone.

ACKNOWLEDGEMENTS

We gratefully acknowledge the financial support of the organisations which sponsored the Alligator Rivers Analogue Project (ARAP).

Peter Duerden directed ARAP with great skill and good humour, and guided the groundwater studies described in this volume. Robin Lowerson assisted in an almost infinite variety of administrative and organisational matters. Invaluable technical support both in the field and at Lucas Heights was provided by David Garton. We thank Andrew Jenkinson for finalising many of the data tables included in this volume.

A large number of chemical and isotopic analyses were carried out during this project, mostly in ANSTO and CSIRO laboratories. We acknowledge all those involved, particularly Tim Nightingale, David Hill, Graeme Calf, Ralph Matthews, Marie Emmett, Steve McEvoy, John Dighton, Lloyd Smith, Fred Leaney, Robert Stokes, Steve Short, Henri Wong, and Les Dale. Many of those named also provided valuable technical input and advice.

Bob Treloar and other personnel from the Northern Territory Department of Mines and Energy provided capable field assistance. Denison Australia kindly allowed access to Koongarra and provided support in the field.

The colloid investigations described in Section 9 continued previous work financially supported by the USNRC and the UKDOE.

We thank June Fabryka-Martin for detailed comments on the final draft, and Dimitri Sverjensky who provided valuable input on many occasions. We warmly acknowledge productive interactions with other participants in ARAP throughout this study.

1 INTRODUCTION

1.1 Scope of this Volume

The objective of this volume is to provide an account of the groundwater sampling and analysis program undertaken at Koongarra, as part of the Alligator Rivers Analogue Project. The primary emphasis is descriptive rather than interpretative, but inferences regarding flow-paths and chemical evolution of groundwater, or interactions with solid phases may be drawn from the data which are presented.

1.2 Parameters Investigated

Chemical parameters were investigated in groundwaters at various locations and depths in the vicinity of the Koongarra orebody. Measurements of the pH, redox state, conductivity, and bicarbonate alkalinity provided a starting point for interpreting water chemistry. Values of these parameters, which may vary with water storage, were measured in the field.

Groundwater samples were obtained using submersible pumps, or, in a few cases, bailers. Appropriate filtration, chemical treatment, and storage conditions were selected for the various samples, which were then transported to the laboratory for analysis. The concentrations of major cations and anions, such as magnesium and phosphate, were determined using a variety of standard techniques. Numerous elements were routinely analysed using quantitative or semi-quantitative ICPMS.

Uranium series radionuclides and environmental isotopes were measured using radiochemical techniques and mass spectrometry. The distributions of isotopes such as deuterium, tritium, ^{210}Pb, ^{13}C and ^{14}C enabled groundwater mixing and flow-paths to be studied.

On some field trips, colloids and particles entrained in Koongarra groundwaters were collected and analysed to study the relative importance of colloids and migration in true solution.

1.3 Outline

The composition of groundwater usually reflects the geologic strata through which it passes, and may evolve as the groundwater intersects different rock units (Drever, 1988). Koongarra groundwaters exhibit characteristic compositions depending on the location and depth of the sampling point. These compositions are modified by processes such as precipitation, mineral dissolution, dilution, sorption, and out-gassing. The occurrence and distributions of major species at Koongarra are presented in this volume, using both cross-sections and contour plans. Chemical and isotopic data for groundwater analyses carried out during the project are included in the Appendices. Detailed modelling of the chemical data is presented in other volumes in this series.

2 KOONGARRA BOREHOLES AND GENERAL HYDROLOGY

2.1 Borehole Construction and Pumping

Numerous boreholes exist at Koongarra and may be used for groundwater sampling. These boreholes fall into the following categories:

a) **PH, C and M holes**. These boreholes have a metal casing through the weathered zone to prevent them from collapsing. Therefore, groundwaters are sampled from depths geater than about 18 m using these boreholes. The PH holes were drilled in the 1970's during the exploration of Koongarra. The M and C series were constructed during the ARAP project.

Groundwater from these boreholes was usually obtained using a submersible pump suspended between inflatable packers (Figure 2.1a). This defined a short interval as the source of the water. If packers were not used when pumping from these boreholes, the source of the groundwater was limited by the casing, and the bottom of the hole. However, unless the lower end of the casing was sealed (usually by a cement plug) there may have been inflow of groundwater from slightly shallower depths (Figure 2.1b). For some groundwater sampling, only one packer (either above or below the pump) was used. The source of the water in these cases was limited by the packer and either the base of the casing or the bottom of the hole.

b) **KD1 and KD2**. These boreholes were cased to depths well into the unweathered rock. Sections of the casing were slotted and groundwater could be obtained from the slotted intervals.

During groundwater sampling, packers were inflated inside the casing immediately above and below the slotted sections, with the pump between the packers. Therefore, water samples were obtained entirely from the slotted intervals.

c) **W-series**. The W-series boreholes were constructed to obtain groundwaters from within the weathered zone. They were cased with two PVC pipes, open at two separate intervals (Figure 2.1c). These were at depths 13-15 m (referred to as W1a, W2a, etc), and 23-25 m (W1b, W2b, etc). These boreholes were backfilled with cement and gravel to close off the required depth intervals.

Small electric submersible pumps were used to obtain water from the sampling intervals of the W-series boreholes. The presence of gypsum cement caused a perturbation of water chemistry in some of the W-series boreholes (usually in the 13-15 m sampling interval). Whilst this effect diminished with time and with the continued pumping of the boreholes, it was considered that some data were affected and these suspect analyses were excluded from final data compilations.

d) **AD-holes**. These were drilled with an auger drill to obtain water from the intermittently saturated zone close to the surface (Figure 2.1d). Each AD-hole was cased with a PVC tube, with a stainless steel screen at the sampling depth. Hence, water was sampled from a single depth, which was within 12 m of the surface.

The AD-holes tended to have relatively low rates of water inflow, probably due to their small diameter and the presence of clays in the near-surface layers at Koongarra. They were sampled either using a small submersible pump or a bailer. In the latter case they were bailed out entirely and new water allowed to flow in prior to samples being taken.

All boreholes were covered (except when samples were being taken) to minimise entry of airborne contamination and rainwater.

2.2 Borehole Location

The locations of boreholes utilised for water sampling during the ARAP are shown on Figure 2.2 (PH, C, M, and W-series) and Figure 2.3 (AD-holes). The co-ordinates of the boreholes relative to the standard mine grid are given in Table 2.1. Note that the mine grid (shown on Figure 2.2) is not oriented towards true north (see Volume 2 of this series for further information).

The direction of uranium dispersion in the secondary orebody suggests that the general direction of migration in the system is away from the fault, towards the south or south-east. Standing water level contours (Volume 5 of this series), whilst subject to substantial seasonal changes, confirm this general direction of groundwater flow. It therefore seems reasonable, in interpreting some of the chemical data, to restrict attention to boreholes which are on a transect through the orebody from north to south. The boreholes in the region between the dashed lines on Figure 2.2 lie up-gradient, within and down-gradient of the orebody, assuming that the direction of flow is generally to the south or south-east. On this figure, a distance scale based on a direction perpendicular to the fault serves as an approximate measure of flow distance. (Note that the distance scale on Figure 2.2 is the perpendicular distance from the 3000m E line on the mine grid. Borehole KD1 is located within a few metres of this grid-line). This transect will be utilised in presenting data, together with plan views, which show the entire area around the deposit.

TABLE 2.1

KOONGARRA BOREHOLES SAMPLED DURING ARAP

Borehole	Location (m)		When Sampled[a]
	N	E	
PH14	6048	3171	1,2,3,7
PH15	6046	3119	1,2
PH27	6537	3109	2
PH49	6109	3147	1,2,3,4,5
PH55	6109	3216	1,2
PH56	5928	3170	1,2
PH58	6109	3246	1,2
PH61	5926	3094	1,2
PH80	5865	3231	1,2,3
PH88	5865	3322	1,2
PH92	5865	3337	2
PH93	5865	3353	6
PH94	6109	3399	1,2
PH96	5911	3370	1,2
PH110	5621	3170	2
PH139	6233	3322	2
PH146	5623	2927	3,7
C1	5804	3322	6,7
C4	5865	3199	6
C5	5926	3132	4
C6	5933	3216	3,6,7
C7	5988	3149	4
C8	5989	3200	3
C9	6124	3185	3,5
C10	6109	3056	3

Borehole	Location (m)		When Sampled[a]
	N	E	
M1	6170	3124	3,5
M2	6170	3162	3,4,5,7
M3	6170	3216	3
M4	6046	3246	3,5
M5	5941	3315	6
W1	6109	3117	4,5,6,7
W2	6048	3200	4,5,6,7
W3	5865	3153	4,5
W4	6139	3147	3,4,5,6,7
W5	6109	3274	4,5,6,7
W6	6106	2975	7
W7	6018	3315	4,5,6,7
KD1	6081	2998	1,2,5
KD2	5945	3268	6,7
AD1			6,7
AD2			6,7
AD6			7
AD8			6,7
AD9			7
AD11			7
AD12			7
AD13			7
AD14			7

a Dates of field trips were as follows:

1. May 1988
2. November 1988
3. May 1989
4. October 1989
5. May 1990
6. November 1990
7. April 1991

b Depths of sampling and other details are given in Table 3.1. Chemical data are tabulated in appendices.

c Further details of total depth and cased depth of boreholes are given in Table 4.1 of Volume 2 of this series.

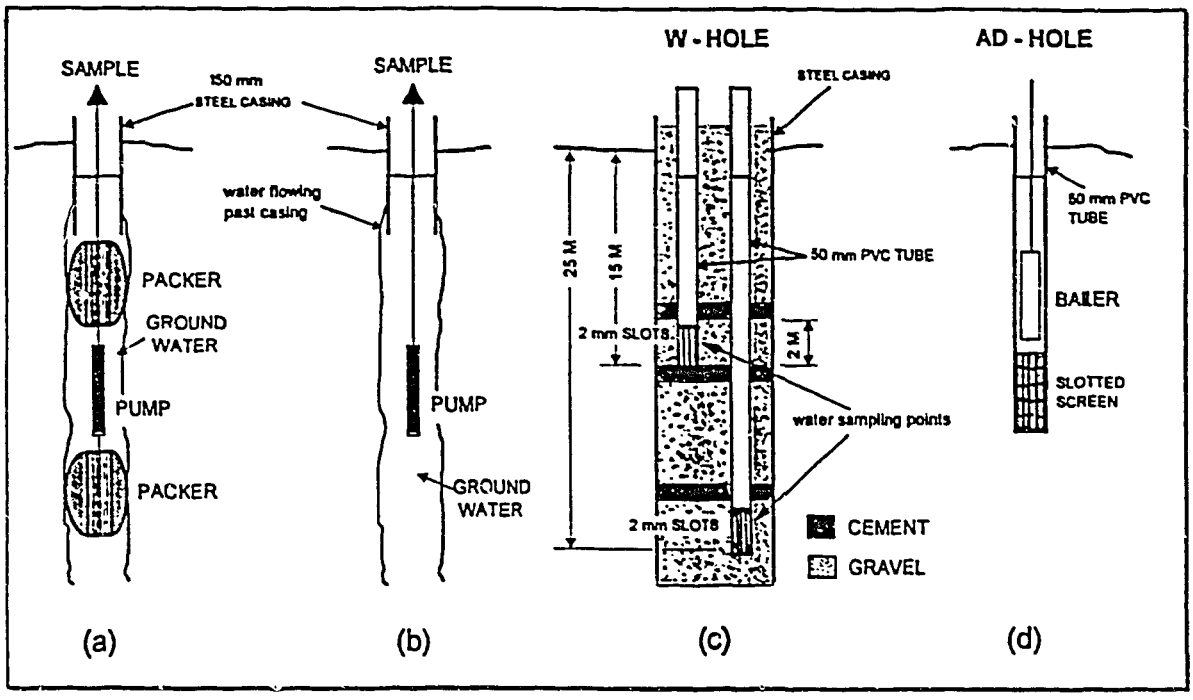

FIGURE 2.1 Groundwater sampling from Koongarra boreholes
- a) Double packer sampling
- b) Pumping without packers
- c) W-series borehole (showing separate sampling intervals)
- d) AD-hole

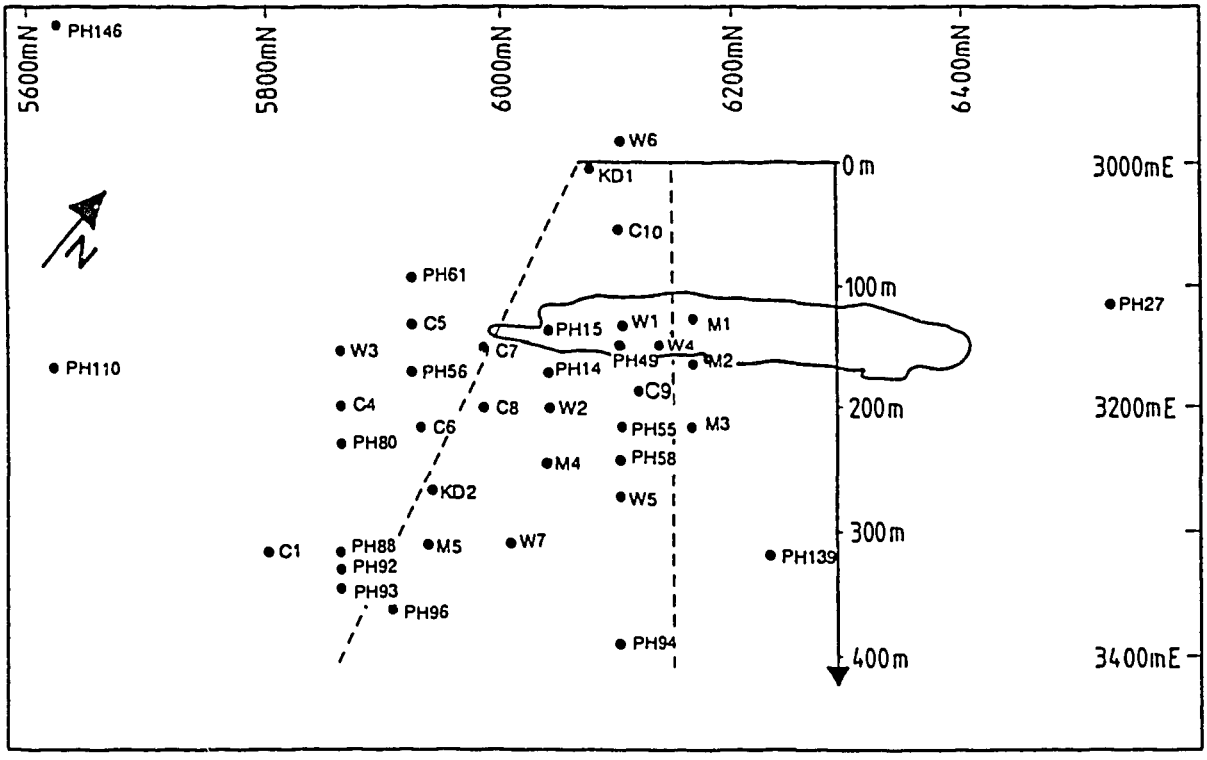

FIGURE 2.2 Koongarra plan showing position of primary orebody, boreholes sampled during ARAP and transect selected for projected cross-sections of groundwater chemistry (between dashed lines)

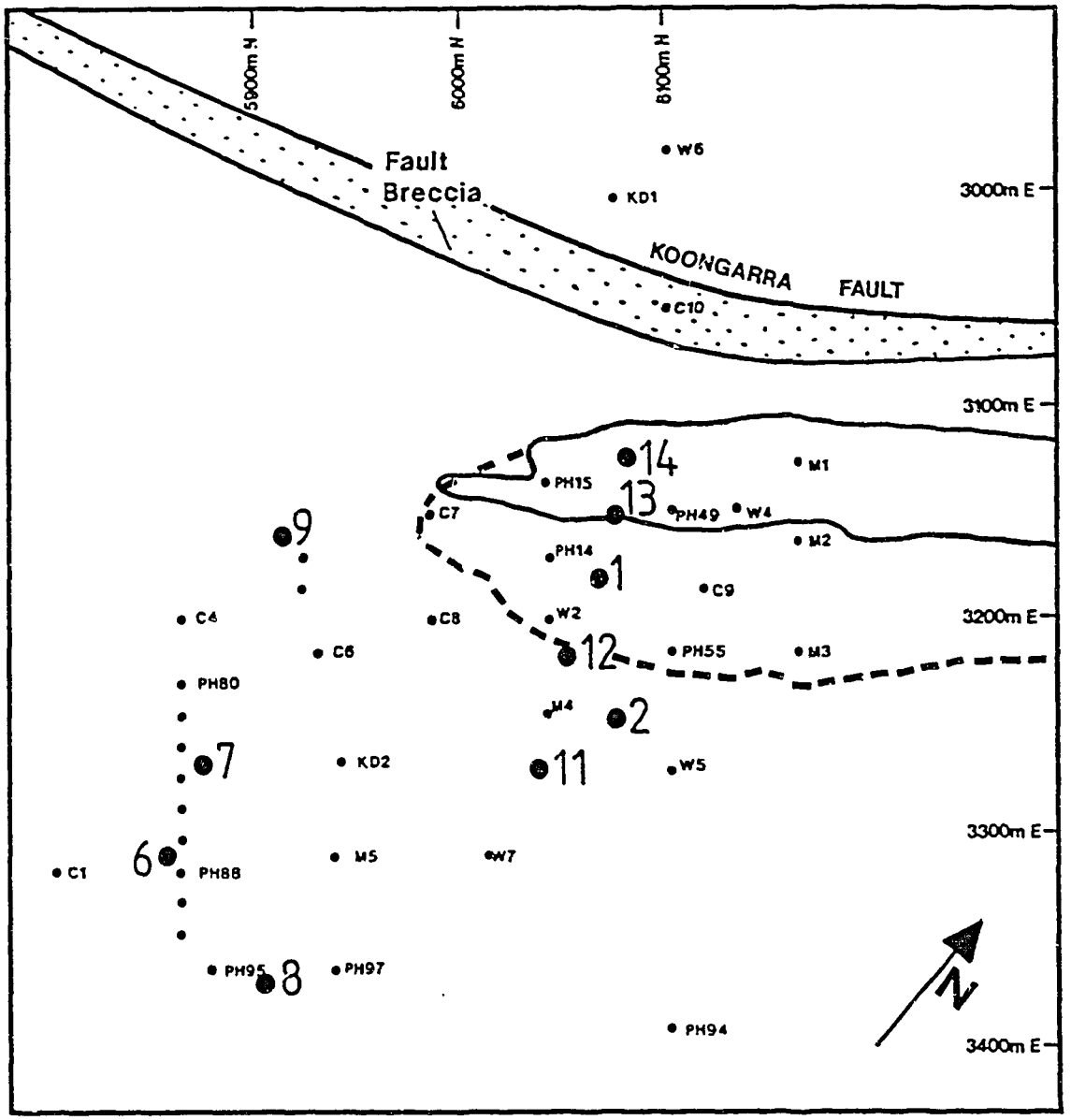

FIGURE 2.3 Location of Auger Drill (AD) shallow water sampling boreholes (large symbols). The dashed line shows the approximate extent of the dispersion fan.

3 SAMPLING AND ANALYSIS

3.1 Field Sampling

Details of the major field trips to Koongarra during the ARAP are given in Table 3.1. This table shows all the boreholes and depths sampled during the ARAP, for which chemical data is provided in the Appendices. Some boreholes were sampled on several occasions, primarily to determine whether there were significant seasonal variations in groundwater chemistry. For this reason, field trips were generally undertaken at the beginning, and at the end, of the dry season. In some instances samples for specific investigations were obtained, including large volume sampling for thorium isotopes, ^{14}C, and groundwater colloids. Samples for the studies of the geochemistry of ^{36}Cl, ^{129}I and ^{239}Pu (detailed in Volume 15 of this series) were also taken.

Typical arrangements for groundwater sampling in the field are shown in Figure 3.1 (a)-(c). The apparatus used was dependent on the samples being collected (particularly in terms of volume required) and, in some cases, the rate of water inflow into the borehole. The sampling system included the following key components:

- submersible pumps, or bailers, to obtain water samples,
- pre-filters to remove large particles,
- a measurement cell (for pH, Eh, conductivity and DO electrodes),
- a final membrane filter selected for each application (generally 0.45 μm except for colloid sampling where a 1.0 μm membrane was used), and
- various taps and run-off lines to enable samples to be taken at any point in the system.

Special care was taken to avoid air contacting the groundwater during sampling. This was of particular importance in the colloid sampling, where oxidation could have led to the precipitation of iron. However, the possibility of oxidation during sampling cannot be excluded for some samples from AD-holes, which were obtained with a bailer on account of the low rate of flow of water into these holes.

The usual sampling procedure was to pump the borehole using a submersible electric or diaphragm pump whilst monitoring the pH and conductivity. When these parameters became stable it was considered that the standing water had been eliminated and aquifer water was being sampled. In the case of bailed samples, the borehole was entirely bailed out and left overnight for inflow to occur.

After the chemistry became stable, the alkalinity was determined by titration (Barnes, 1964), and other field parameters were measured (details are given in Table 3.2). On some occasions, in-field measurements of other parameters, such as phosphate, ferrous iron and sulfide, were undertaken.

For most chemical analyses, samples were taken after filtration through a 0.45 μm membrane. This separation is accepted as defining the dissolved or soluble fraction (Batley and Gardner, 1977). However, this is largely an operational definition, as fine suspended particles or colloids may pass through the membrane and be included in the filtrate. A smaller pore-size membrane, such as an ultrafilter, may give a better indication of truly dissolved species. While filtration through a 0.45 μm membrane is a standard technique in water analysis, it should be regarded as a practical separation procedure rather than a true measure of dissolved species. The nature and significance of fine particles and colloids in Koongarra groundwaters is discussed in detail in Section 9.

Separate samples were generally taken for each chemical determination, due to the different requirements of the various analyses. For example, glass bottles were used for total organic carbon (TOC) samples, and PET bottles for cation samples. Concentrated nitric acid (Aristar^{R} high purity) was added to groundwater samples for cation and radionuclide analysis. Samples for anion analysis were not acidified, but were stored in a refrigerator (<4°C). For other samples, treatment (acidification, refrigeration, etc) was as appropriate for each analysis. For many analyses of trace constituents, pre-concentration steps were carried out in the field to avoid the necessity of large volumes being transported to the laboratory. Pre-concentration techniques included adsorption on ferric hydroxide (for Th, and some U analyses), precipitation (^{14}C and ^{36}Cl), and ion exchange (^{129}I and ^{239}Pu).

3.2 Analysis

Elemental analyses were carried out using a number of techniques including ICPMS, ICPAES, anion exchange chromatography, and spectrophotometry. Many of the routine elemental analyses of groundwater samples collected during the ARAP were carried out by the CSIRO Centre for Advanced Analytical Chemistry, Lucas Heights. The ICPMS results included quantitative data run with internal standards for elements of particular interest, and semi-quantitative results for a large number of trace constituents (see Appendix 1.6 for more details). Copper measurements were attempted using both ASV and ICPMS.

Phosphate was determined using a standard ascorbic acid / molybdenum blue spectrophotometric method (Appendix 1.5). Other anions were determined by various techniques, primarily anion exchange chromatography (for chloride and sulfate) or an ion sensitive electrode (for fluoride). TOC was measured using a photocatalytic oxidation technique (Appendix 1.7). Where possible, field tests were also carried out for important parameters and compared with subsequent laboratory values. This proved to be particularly useful in the case of phosphate where field determinations using Chemettes^{R} showed an excellent correspondence to subsequent measurements in the laboratory (see Appendix 1.5).

Uranium was measured using α-spectrometry, quantitative ICPMS and KPA. Other radiochemical techniques were also used for particular radionuclides (Th, Ra, Ac, Rn, ^{14}C, tritium, etc). For full details of analytical techniques for uranium-series radionuclides and other groundwater constituents, refer to Appendix 1.

3.3 Stability and Reproducibility of Data

Determination of the accuracy of data involves an assessment of several different issues.

Analytical reproducibility refers to whether repeated analysis of the same sample (either by the same or different techniques) gave results which agreed within experimental error. Although it was impractical to duplicate large numbers of analyses, replicate analyses of various parameters by different techniques were obtained regularly in order to validate the analytical data. In the important case of uranium, there was extensive inter-comparison of results obtained by different methods. The agreement between the various techniques (ICPMS, KPA, α-spectrometry, γ-spectrometry) was generally extremely good over several orders of magnitude (Figures 3.2 and 3.3). For the May 1988 set of groundwater samples, duplicate sample sets were analysed independently for a large number of parameters in the laboratories of PNC (Japan), and CSIRO (Australia). The results (Appendix 6.1) showed good agreement between the two laboratories.

Chemical data were examined for consistency between data-sets, and clearly anomalous values were rejected or, when possible, submitted for repeat determinations.

Sampling Stability. Groundwater samples were only taken after pumping the boreholes until the chemistry was constant, based on field parameters. On some occasions, extra samples were taken to give an indication of the stability of elemental concentrations as boreholes were pumped. The analytical results (Figure 3.4) showed that there continued to be slight fluctuations in some values even after several hours pumping. This may be attributed to variations in water chemistry as groundwater was drawn in from greater distances. In general, if only one set of samples was taken from a borehole, this would be after at least two hours pumping, and Figure 3.4 indicates an acceptable stability for most parameters at this time. Uranium, Mn and Fe concentrations tended to be more unstable than other elements. This could reflect continuing change in redox conditions as boreholes were pumped, and local heterogeneity in the concentrations of these species in the vicinity of the borehole.

The changes in concentrations of major and minor species over 5 hours of pumping at these boreholes (Figure 3.4) showed that magnesium achieved constant values shortly after the commencement of pumping, but iron and uranium levels continued to change throughout the entire period. The change in uranium concentration at borehole W4b (by a factor of approximately two) is not an extreme case. A variation of an order of magnitude (at borehole PH14) has been reported (Ivanovich et al., 1988) although on that occasion the borehole was subjected to the rapid pumping of several thousand litres over a 2-day period.

Reproducibility of sampling protocol. Sampling procedures were standardised and repeated as closely as possible for each field trip. However, factors such as operational requirements, time-constraints, equipment failure, and changes in personnel might be expected to lead to some lack of reproducibility when

comparing results from different field trips. Field data collected for several boreholes over a number of field trips usually showed an excellent correspondence and indicated that, in general, sampling was carried out in a reproducible fashion. Changes in chemistry between field trips may also result from seasonal effects, and this is discussed in detail in Section 5.

A case where seasonal effects can be excluded is data obtained for boreholes W1 and W4 during the October 1989 field trip. The entire sampling procedure was repeated (after an interval of about one week), and the data (Table 3.3) therefore provide an indication of the sampling variability. The two data sets are generally extremely consistent. Again the most significant variations are in the data for Fe, Mn, and U.

The variation in uranium concentration reflects the heterogeneous nature of its distribution in Koongarra groundwaters. However, it should be appreciated that the variation in the measured U concentration at a particular borehole (generally around a factor of two), is small relative to the variation in U between boreholes, which ranges over about four orders of magnitude at Koongarra. (The magnitude of fluctuations amongst samples from the one borehole compared to variations between boreholes may be assessed from Figure 5.1(f), which is discussed in Section 5.2).

TABLE 3.1

DETAILS OF BOREHOLES AND DEPTHS SAMPLED ON MAJOR FIELD TRIPS TO KOONGARRA

1) May 1988		2) November 1988		3) May 1989		4) October 1989	
Bore	Depth (m)	Bore	Depth (m)	Bore	Depth (m)	Bore	Depth (m)
KD1	40-42	KD1	40-42	C6	35-40	C5	25-27
KD1	80-82	KD1	70-72	C8	24-26	C7	25-27
				C8	38-40		
PH14	20-26	PH14	20-26	C9	34-40	M2	37-39
PH15	19-21	PH15	19-21	C10	27-40		
PH49	16-28	PH49	28-30			PH49	25-27
PH49	28-30	PH49	44-46	M1	24-26	PH49	45-47
PH55	26-28	PH55	26-28	M1	35-50		
PH55	40-42	PH55	40-42	M1	46-48	W1a	13-15
PH56	26-28	PH56	26-28	M2	40-46	W1a*	13-15
PH56	43-45	PH56	43-45	M3	20-22	W1b	23-25
PH58	25-27	PH58	25-27	M3	26-28	W1b*	23-25
PH58	38-40	PH58	38-40	M3	34-40	W2a	13-15
PH61	26-28	PH61	26-28	M4	34-40	W2b	23-25
PH61	43-45	PH61	43-45			W3a	13-15
PH80	17-20	PH80	17-20	PH14	20-26	W3b	23-25
PH88	28-30	PH88	28-30	PH49	27-29	W4a	13-15
PH88	38-40	PH88	38-40	PH49	33-35	W4a*	13-15
PH94	26-28	PH94	26-28	PH80	17-19	W4b	23-25
PH94	40-42	PH94	40-42	PH146	17-89	W4b*	23-25
PH96	16-26	PH96	16-26	PH146*	17-89	W5a	13-15
						W5b	23-25
Limited data for:		Samples obtained without packers		W4	23-25	W7a	13-15
PH49 (44-46m)						W7b	23-25
		PH27	20 m	Koongarra Creek			
		PH92	20 m				
		PH96	20 m				
		PH110	20 m				
		PH139	20 m				

* Signifies repeat sampling.

TABLE 3.1 (Continued)

5) May 1990		6) November 1990		7) April 1991			
Bore	Depth (m)	Bore	Depth (m)	Bore	Depth (m)	Bore	Depth (m)
C9	28-30	AD1	9.5	AD1	9.5	W1a	13-15
		AD2	9.0	AD1*	9.5	W1b	23-25
KD1	65-76	AD8	9.0	AD2	9.0	W2a	13-15
				AD6	4.0	W2b	23-25
M1	27-29	C1	22-23	AD8	9.0	W4a	13-15
M2	42-44	C4	23-40	AD9	7.0	W4b	23-25
M4	28-30	C6	23-25	AD9*	7.0	W5a	13-15
				AD11	2.5	W5b	23-25
PH49	18-20	KD2	24-32	AD12	5.0	W6b	23-25
				TAD12	1.5	W7a	13-15
W1a	13-15	M5	27-29	AD13	9.0	W7b	23-25
W1b	23-25	M5	28-40	AD14	10.5		
W2a	13-15						
W2b	23-25	PH93	22-23	C1	22-23	Rain	
W4a	13-15			C6	23-24	Creek near KD1	
W4b	23-25	W1a	13-15				
W5a	13-15	W1b	23-25	KD2	24-26		
W5b	23-25	W2a	13-15				
W7a	13-15	W2b	23-25	M2	36-40		
W7b	23-25	W4a	13-15				
		W4b	23-25	PH14	20-26		
		W5a	13-15	PH146	17-89		
		W5b	23-25				
		W7a	13-15				
		W7b	23-25				

* Signifies repeat sampling

TABLE 3.2

FIELD MEASUREMENT PROCEDURES

Parameter	Meter/Electrode	Standardisation
pH	Hanna (HI8424) pH meter OR Philips pH/mV meter (PW9419) and electrode (CA1EG)	Activon buffers pH 4.00 and 7.00 (freshly prepared)
Eh	Activon digital pH/Mv meter (Model 205) Sensorex ORP electrode (Ag/AgCl reference)	Zobell's solution (3.33×10^{-3}M $K_4Fe(CN)_6$ + 10^{-3} M $K_3Fe(CN)_6$ + 0.1 M KCl) (Nordstrom, 1977)
EC	Hanna conductivity meter (HI8733) and cell	Standard KCl solutions
DO	Hanna DO meter (HI8543) and polarographic probe (HI76406)	Zero point - with zero oxygen solution Full scale - atmospheric oxygen According to manufacturer's instructions
$[HCO_3^-]$	Determined by titration against standard acid (HCl) (Barnes, 1964) Endpoint determined by monitoring pH	

In some cases equivalent instruments to the above were substituted for operational reasons.

TABLE 3.3

COMPARISON OF GROUNDWATER DATA OBTAINED FOR BOREHOLES W1 AND W4 FOR SEPARATE SAMPLES OBTAINED DURING THE OCTOBER 1989 FIELD TRIP

(The second sample set is denoted by *)

A Field Data, Anions, Si and U

Bore	Depth (m)	pH	Eh mV	EC µS/cm	HCO_3 mg/L	Cl mg/L	PO_4 µg/L	Si mg/L	U µg/L
W1 a	13-15	6.55	220	195	98	7.4	<5	6.7	2.51
W1 a*	13-15	6.80	195	200	93	6.2	10	6.8	7.33
W1 b	23-25	7.09	255	230	120	8.2	415	6.7	38.6
W1 b*	23-25	6.75	235	215	107	6.9	370	6.9	50.5
W4 a	13-15	5.85	330	135	66	5.8	30	9.8	414
W4 a*	13-15	5.75	305	133	60	6.4	35	9.7	386
W4 b	23-25	6.80	140	240	165	2.9	90	9.7	364
W4 b*	23-25	6.85	125	250	159	4.1	80	9.7	318

B Cations and Trace Metals (data for W4 only)

Bore	Depth (m)	Mg mg/L	Na mg/L	K mg/L	Fe µg/L	Mn µg/L
W4 a	13-15	12.3	1.7	0.5	17	421
W4 a*	13-15	11.4	1.7	0.5	37	532
W4 b	23-25	27.3	1.1	0.6	35	60
W4 b*	23-25	26.8	1.2	0.7	510	69

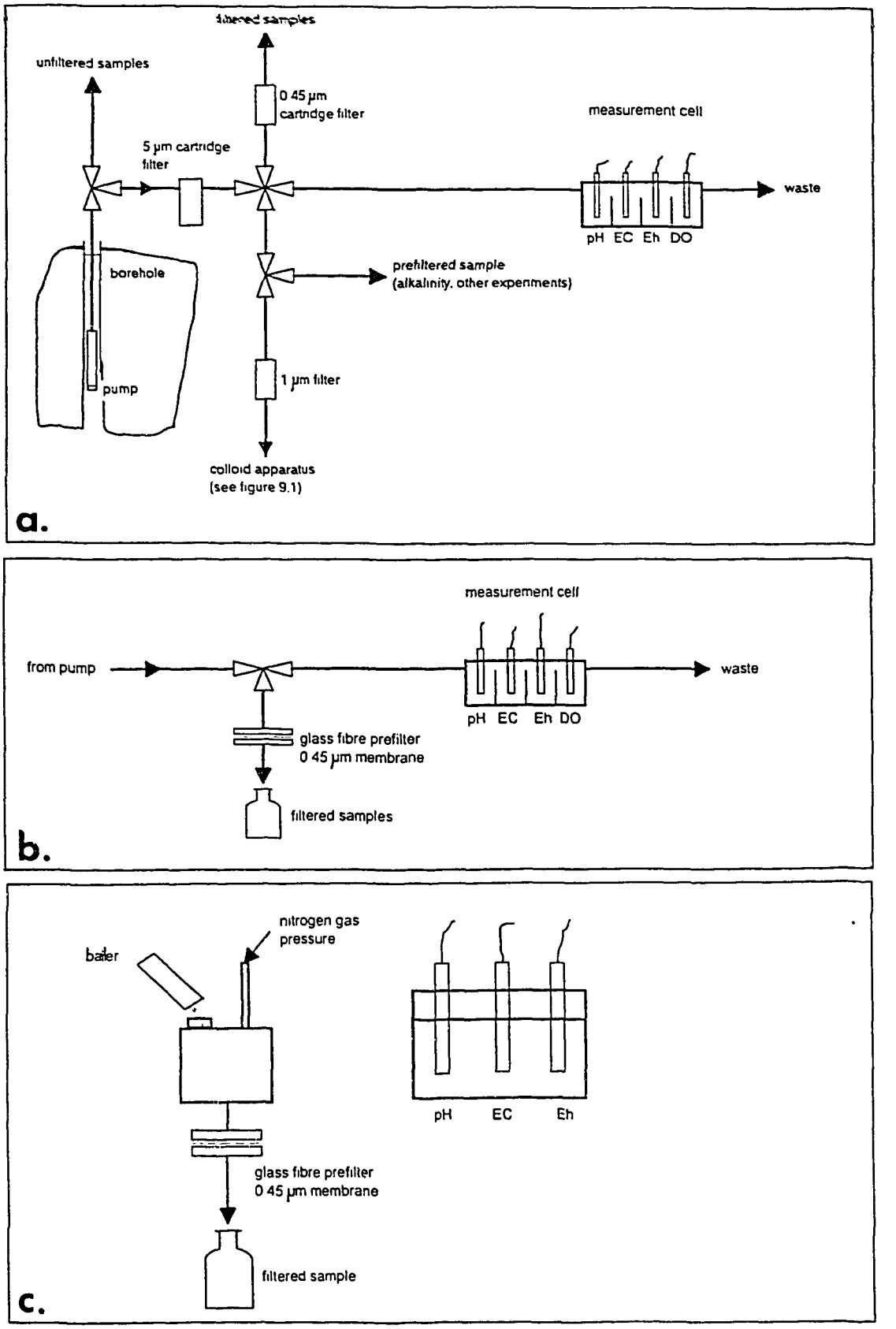

FIGURE 3.1 Field sampling and measurement equipment
- a) Large volume sampling
- b) Small volume pumping
- c) Bailed samples

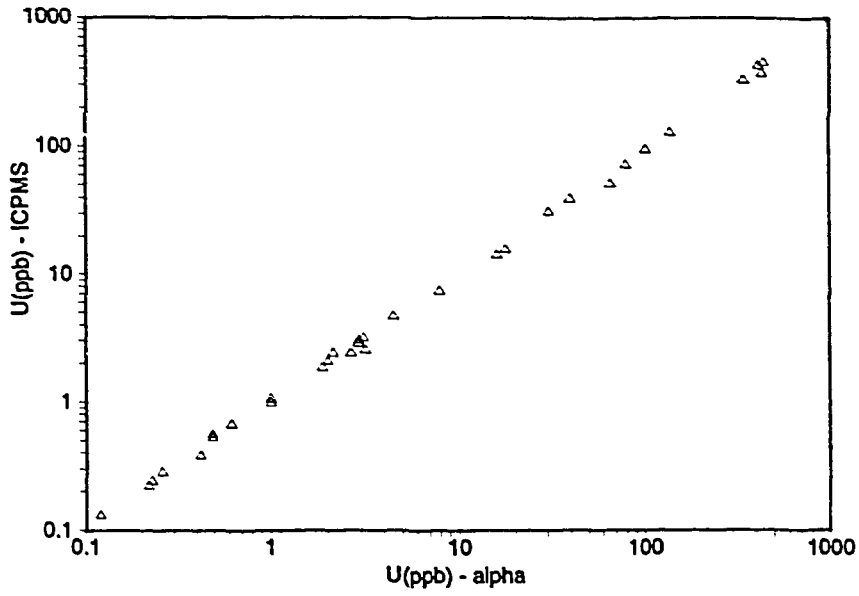

FIGURE 3.2 Comparison of α-spectrometry and ICPMS uranium concentration data

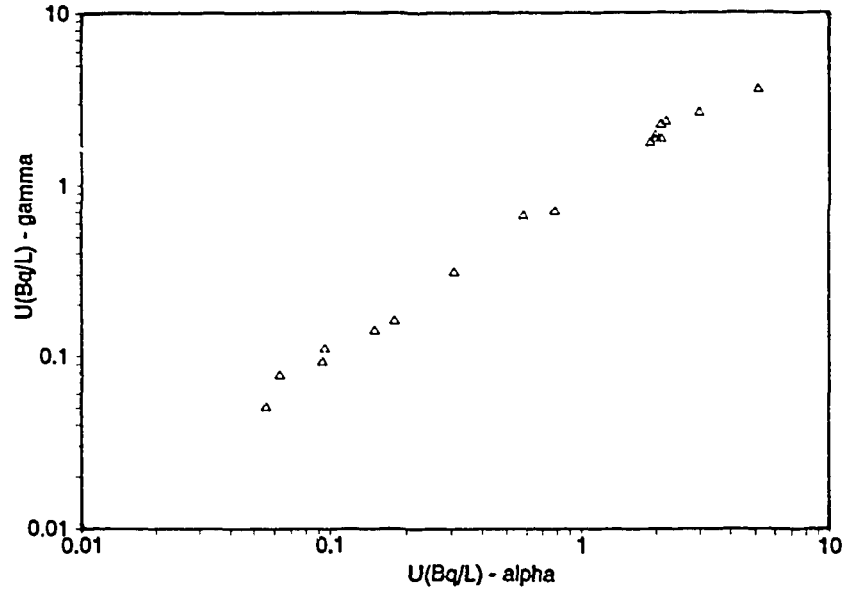

FIGURE 3.3 Comparison of α-spectrometry and γ-spectrometry uranium concentration data

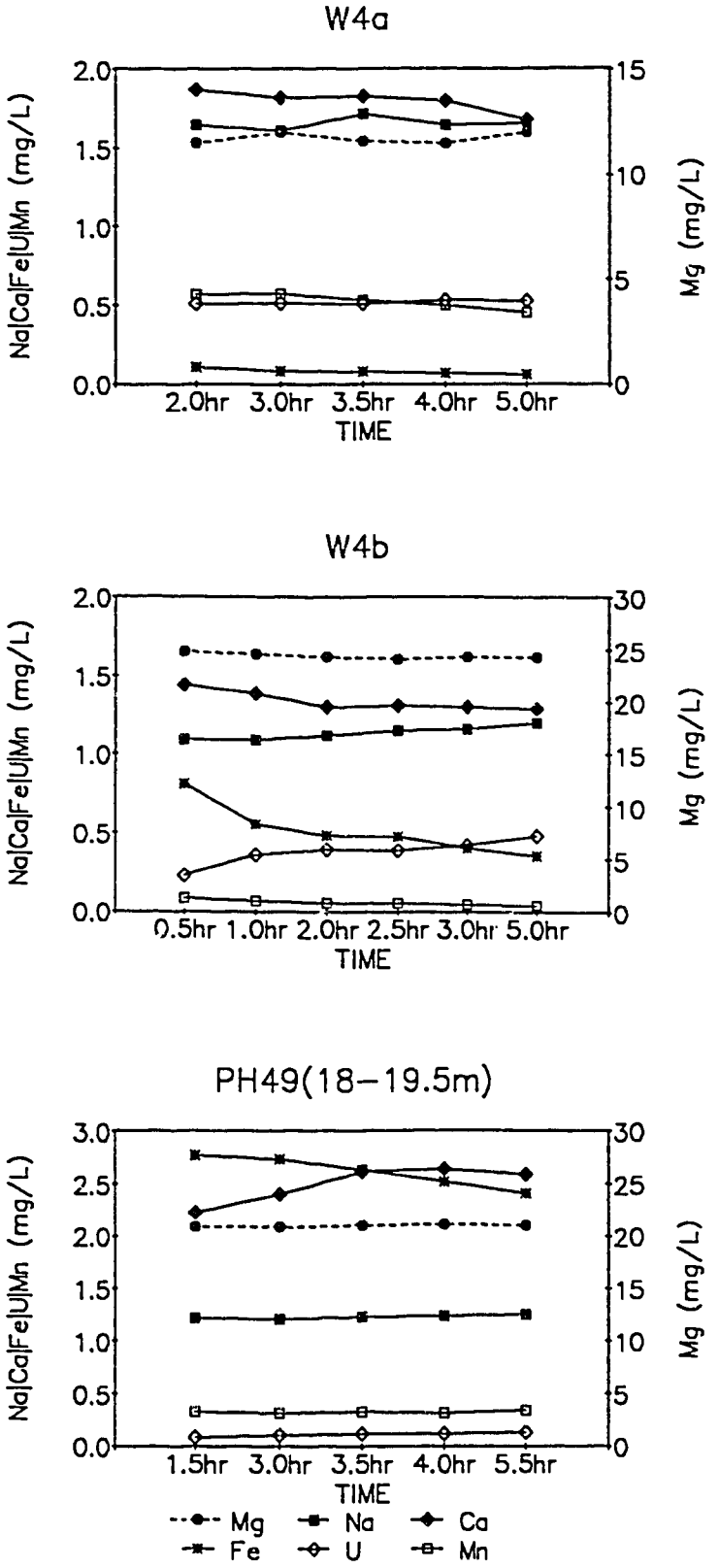

FIGURE 3.4 Elemental concentrations in groundwater - effect of pumping time (boreholes W4a, W4b, PH49 - May 1990 field trip)

4 GENERAL CHARACTERISTICS OF KOONGARRA WATERS

4.1 Chemical Composition of Rainfall

Local rainfall, which mostly occurs during the wet season between October and early April, is the ultimate source of water in the Koongarra system. Rainfall averages 1650 mm/yr, while pan evaporation averages 2500 mm/yr. Potential evaporation is distributed evenly throughout the year, and invariably greatly exceeds rainfall outside the months of the wet season. The isotopic composition of rainfall is discussed in Section 8. Full details of rainfall occurrence at Koongarra are given in Volume 6 of this series.

A detailed study of the characteristics of rainfall of the Alligator Rivers Region has been reported by Noller et al. (1990). The mean pH of rainfall was 4.4, and the mean composition of rainwater in the Nourlangie Creek Catchment (close to Koongarra) was dominated by Na and Cl (0.25 and 0.50 mg/L respectively). Rainfall always contains some traces of sea-salt, originating from the evaporation of droplets of seawater to a fine aerosol of NaCl (Drever, 1988). Minor amounts of Mg, Ca and K (all below 0.1 mg/L) were also reported.

Rainwater, sampled at Koongarra on a field trip in April 1991, had a pH of 5.2, significantly below neutral, and contained very dilute levels of total dissolved constituents, as indicated by its low conductivity of 17 μS/cm. This data is in reasonable agreement with the mean values reported by Noller et al. (1990). For comparison, typical conductivity values for Koongarra groundwaters are in the range 100-250 μS/cm, with brines or seawater several orders of magnitude higher.

A small creek at Koongarra was also sampled in April 1991. At this time of year, it would be expected that this water would have a similar chemistry to rainwater. This was confirmed by field measurements of its pH and conductivity, which were 4.6 and 18 μS/cm, respectively.

Surface waters sampled during the 1977/1978 wet season were slightly acidic (pH 5), with low alkalinity, conductivity and correspondingly low levels of dissolved constituents (Noranda, 1978). In the most dilute waters sampled, Na and Cl were the only ions present in significant amounts (0.57 mg/L and 0.51 mg/L respectively). These compositions probably reflect recent rainfall.

The combined data indicate that the local rainfall is fairly acidic. Noller et al. (1990) concluded that the acidity was partly attributable to weak organic acids (formate and acetate). Likely natural sources of acidity include burning of vegetation, soil dust, lightning, biogenic emissions, volcanoes, etc; and there may be anthropogenic emissions from the Ranger uranium mine (about 40 km from Koongarra), and other locations. Presumably, at the remote and undeveloped Koongarra site the anthropogenic sources of acidity are relatively minor.

4.2 Main Characteristics of Groundwaters

Selected parameters for a groundwater sample from near the centre of the ore body (borehole PH49) are listed in Table 4.1. This groundwater composition shows the major features of water chemistry for a mineralised aquifer at Koongarra. The main characteristics of the PH49 sample are:

a) the pH is close to neutral,

b) the conductivity is low, indicating a dilute groundwater with low levels of dissolved constituents,

c) magnesium is the dominant cation, reflecting the chlorite content of the host rock. This Mg dominance, represented in Figure 4.1, is characteristic of groundwaters from uranium orebodies in the Alligator Rivers region (Giblin and Snelling, 1983),

d) the main anion is bicarbonate,

e) the groundwater contains elevated concentrations of uranium and radionuclides in its decay series,

f) low levels of total organic carbon are present,

g) the groundwater is slightly oxidising with respect to U^{4+}/U^{6+},

h) significant levels of Si are present.

The major components of Koongarra groundwaters, which were often present at levels above 0.1 mg/L, included:

Ca, Cl, F, Fe, HCO_3, K, Mg, Mn, Na, PO_4, Si, SO_4, and U.

Groundwater data for these major constituents are given in Appendix 3 of this report. Aluminium and Zn were sometimes detected at these levels but may have been particulate.

The bar graph in Figure 4.1 only shows the total concentrations of cations in a single groundwater sample. A more detailed analysis of the characteristics of major groundwater types at Koongarra, using Piper tri-linear diagrams, is presented in Section 10 of this report.

Measurable amounts of numerous other elements were present at trace levels (below 100 μg/L). These included:

B, Ba, Br, I, Mo, Rb, Sr, Ti, V, and W.

Quantitative and semi-quantitative data for trace constituents in Koongarra groundwaters are included in Appendices 4 and 5. It is particularly important to note that Appendix 5 contains blank values (measured in de-ionised water) for numerous elements. Measured values of these components were, for many samples, comparable to or below the values measured in the blanks.

4.3 Uranium Mobility in Koongarra Groundwaters

The chemistry of Koongarra groundwaters is a major factor influencing the mobility of uranium in the system. The pH and Eh conditions, together with the elemental composition of groundwater, determine the state of saturation with respect to solid mineral phases which may potentially be present. In addition, the chemical speciation of uranium (which influences its adsorption behaviour) is a function of the concentrations of complexing ligands.

Koongarra groundwaters are quite low in total organic carbon (Appendix 6), therefore inorganic species, such as carbonate and phosphate are likely to be the main uranyl complexants. In the absence of significant amounts of phosphate, uranyl carbonate species dominate uranyl speciation in the pH range above 5.0.

Published stability constants for the formation of the $UO_2(HPO_4)_2^{2-}$ species (Dongarra and Langmuir, 1980) indicated that phosphate could be a significant uranyl complexant in Koongarra groundwaters. Although these constants have since been questioned, phosphate is also of importance on account of the widespread occurrence of uranium phosphate minerals (such as saleeite and renardite) at Koongarra. Therefore, numerous groundwater phosphate determinations were made. The measured values of phosphate in Koongarra groundwaters (Appendix 3) were up to about 700 µg/L. The potential importance of phosphate in influencing uranium mobility in the system is addressed in Volumes 10 and 12 of this series.

Another consideration when discussing uranium mobility in Koongarra groundwaters is the pH/Eh state of the system. Figure 4.2 shows that for samples from depths greater than 16 m (i.e. well into the permanently saturated zone), pH/Eh conditions tended to be in the regime of significant uranium solubility (uranium present in its oxidised (U(VI)) state). Therefore, Koongarra groundwaters would generally be expected to dissolve uraninite (UO_2), which is present in the primary ore-zone. Many Koongarra groundwaters lie in the pH regime where equilibrium UO_2^{2+} concentrations in excess of 10^{-6} M are expected. However, groundwater uranium concentrations at Koongarra are generally below 10^{-6} M. It can thus be concluded that these groundwaters tend to be significantly undersaturated with respect to major uranium minerals. For such groundwaters, adsorption is likely to be a more important retardation mechanism for uranium than the precipitation of uranium minerals. The chemical speciation of uranium and state of saturation of Koongarra groundwaters are further discussed in Volume 12 of this series.

TABLE 4.1

CHEMICAL COMPOSITION OF A GROUNDWATER FROM THE No.1 OREBODY

Borehole	**PH49**
Depth	28-30 m
Date	May 1988
pH	6.74
Eh (mV)	+130
EC (µS/cm)	236
Mg^{2+}	26.4
Ca^{2+}	3.9
Fe^{2+}	0.8
K^{+}	0.7
Na^{+}	1.4
Si	8.9
HCO_3^-	154
Cl^-	3.7
F^-	0.2
PO_4^{3-}	0.310
SO_4^{2-}	2
U (µg/L)	274
TOC	1.5

Units are mg/L except where otherwise stated

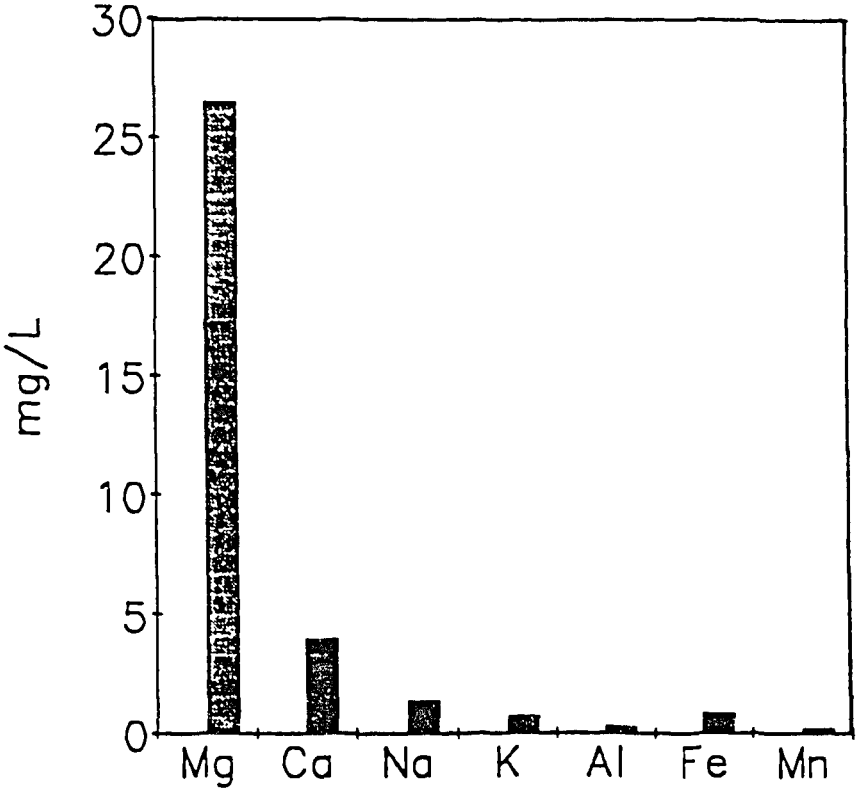

FIGURE 4.1 Chemical composition of PH49 groundwater

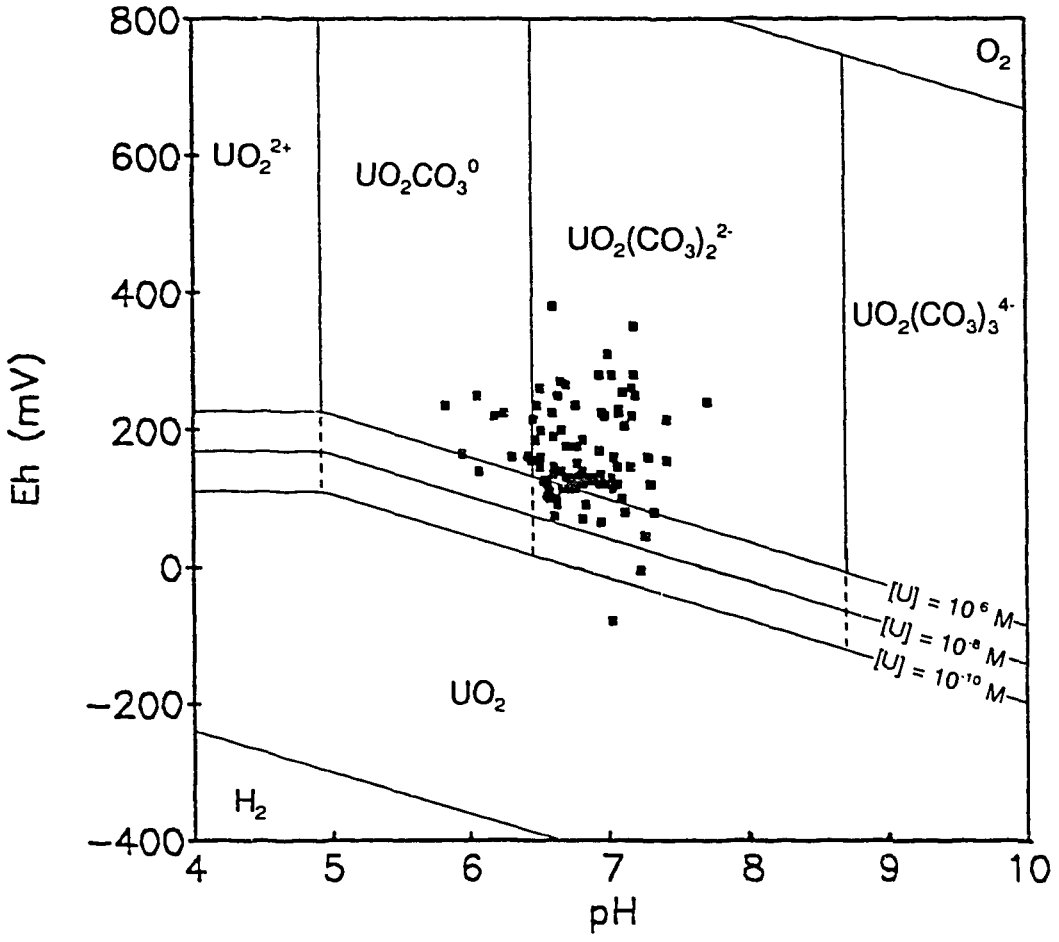

FIGURE 4.2 pH/Eh state of Koongarra groundwater samples (depths greater than 16 m). Approximate stability fields and solubility contours (from Brookins, 1988) are shown.

5 SEASONAL EFFECTS ON GROUNDWATER COMPOSITION

5.1 Potential Significance of Seasonal Variations

Koongarra has a monsoonal climate, with rainfall concentrated in the months from November to March. Standing water levels in boreholes fluctuate annually over 10 m or more. During the wet season, the water level in some boreholes can rise to ground-level. This raises the possibility that the chemical conditions and movement of radionuclides in groundwater could be strongly dependent on the season. A possible scenario could involve rapid migration after major rainfall events with the system relatively dormant for the remainder of the time. Therefore, the redistribution of uranium at Koongarra might be due to numerous discrete events, rather than progressive migration. In order to test this hypothesis, groundwater was sampled from a number of Koongarra boreholes several times throughout the ARAP project, over intervals spanning both wet and dry seasons.

5.2 Groundwater Compositions

PH-series Boreholes. The PH boreholes (which existed prior to the start of ARAP) were sampled on two occasions in 1988. Samples were taken in May, when water levels were high, and in November, just prior to the onset of the wet season. The two sets of results (Table 5.1), showed a similar major ion chemistry. The conductivity showed no consistent changes, which might have indicated dilution or evaporation/transpiration processes. Correspondingly, the concentrations of HCO_3^- and Mg^{2+}, the dominant ions in these groundwaters (and therefore the main contributors to the conductivity), were similar in the two data sets. There were, however, substantial differences in minor and trace constituents, such as uranium and iron. The concentrations of these elements have been shown to vary during sampling as water is pumped from Koongarra boreholes, and significant variations have been measured between samples separated by an interval of only one week (Section 3.3). In these cases, seasonal effects could be excluded from consideration. It is therefore likely that the changes in Fe and U concentrations between the sample sets obtained at these PH boreholes are due to sampling variability rather than being a seasonal effect.

The results suggest that there is no significant seasonal variation in the major ion chemistry of these groundwaters, and seasonal changes in the values of minor parameters (such as Fe and U) are comparatively small and masked by sampling variability. However, the PH holes are cased to about 20 m depth (the base of the weathered zone), and therefore do not provide an opportunity to sample shallow groundwaters which might be considered more likely to show seasonal effects.

W-series Boreholes. The W-holes, which were drilled in 1988, have sampling points at 13-15 m depth and also 23-25 m depth. These depths are in the weathered zone and transition zones respectively. Possible seasonal variations in groundwaters from these boreholes were studied by taking a sequence of samples over several field trips from October 1989 to April 1991. Data for sampling points W4a, W4b, W2b and W5b are presented in Figure 5.1 (a)-(f). These boreholes are

within and down-gradient of the orebody (see Figure 2.2). The diagrams show the key parameters pH, conductivity, magnesium, bicarbonate, phosphate and uranium concentrations.

For most of these parameters, slight differences were detected between samples from different field trips. However, these were not generally related to the time of year when samples were obtained. The differences between the boreholes were far greater than any seasonal change and were reproducible within each sampling set (Figure 5.1). The most likely seasonal effect is at W4a where there may have been an influx of more acidic, dilute waters (as evidenced by pH, conductivity, Mg and HCO_3^- concentrations) during the wet season commencing in November 1990.

The relatively constant pH, conductivity and major ion chemistry of these groundwaters implies that seasonal change in groundwater chemistry is a relatively minor consideration in chemical modelling of these groundwaters. The spatial variation is of far greater significance. The pH and the concentrations of bicarbonate and phosphate were reproducible, which implies that the speciation of uranium is likely to be similar throughout the year at these depths in the weathered zone, which are permanently saturated.

In the case of uranium (note: plotted on a log scale), variations between samples tended to be much greater than most other parameters, but again, were not obviously correlated with season. As shown in Section 3.3, changes in uranium concentrations occurred during continuous pumping of boreholes, therefore, the differences between samples taken on different field trips do not infer a seasonal effect, but may be ascribed to variation during sampling. Figure 5.1(f) shows that, while there were significant changes in uranium concentrations between samples taken at each of these W-series boreholes, these variations were slight compared to the differences between boreholes.

Auger Drill (AD) holes. A series of shallow water sampling holes were augered in 1990 and early 1991. The sampling depths of the AD holes are within the zone where the water table fluctuates, so it is only possible to sample water from these boreholes during months when water levels are high. Water from these boreholes, when sampled in April 1991, generally had a low pH, low conductivity, and low concentrations of phosphate and carbonate anions (Table 5.2, see also Section 6). Therefore, the chemistry was similar to rainwater. It should be noted that the casing was tight in these holes, they were capped to exclude rainwater, and standing water was discarded before taking samples. Therefore, these samples probably provide an accurate indication of the water chemistry in near-surface layers shortly after the wet season.

Uranium concentrations in samples from AD-holes were mostly below those found in deeper groundwaters from the same area. The highest concentration (74.6 µg/L) was measured in a sample from AD13, which is directly over the centre of the orebody. This sampling point is very close to W4a, but at a slightly shallower depth, and the groundwater chemistry of the two boreholes was very similar.

Unfortunately, the data set for the AD holes does not extend over a significant period, which is partly due to the absence of water in these holes for several months of the year when the water table is low. There were major changes in the chemistry of groundwater from AD1 and AD2 after the 1990-91 wet season and this can be attributed to a seasonal influx of water. For example, the conductivity of AD1 groundwater fell from 110 μS/cm in November 1990 to 30 μS/cm in April 1991, with a drop in pH from 6.7 to 5.9. By July 1991 the conductivity had risen to 70 μS/cm and the pH to 6.8. Presumably, in the dry season, evaporation and slow mixing processes result in the chemistry of these waters becoming more saline. The effects of seasonal draining, and the accompanying cycles of saturation and unsaturation, are probably the major factors influencing groundwater/solid interactions in these near surface zones.

A pit (referred to as a temporary sample point TAD12) was excavated near AD12 during the May 1991 field trip, and gave an opportunity to sample water from the top surface of the water table. This water proved to be very similar to rainwater with a pH of 5.55, conductivity of 24 μs/cm, and low Mg and U concentrations (1.1 mg/L and 0.5 μg/L respectively).

5.3 Conclusions and Implications for Modelling

There does not appear to be a substantial seasonal variation in groundwater chemistry for samples obtained from depths greater than about 16 m. Whilst changes in some parameters (such as iron and uranium concentrations) occurred between samples taken on different field trips, these can be attributed to variations during pumping of the boreholes. Fluctuations in these minor constituents continue after the borehole has been pumped to stable conductivity, by which time concentrations of major species are relatively constant. Generally these fluctuations are small compared to the differences between the various sampling points.

There is a seasonal effect in the shallow AD-holes, which show the influence of rainfall in the wet season. However, the shallow seasonal groundwaters at Koongarra do not generally contain high levels of uranium complexants, or uranium itself, and are unlikely to mobilise significant amounts of uranium.

The lack of a significant seasonal change in major ion groundwater chemistry, with the exception of the shallow AD holes, has important implications. In general, it is apparent that seasonal factors are much less significant than spatial variations and do not need to be incorporated in any chemical modelling of these groundwaters.

TABLE 5.1

GROUNDWATER DATA FOR MAY AND NOVEMBER 1988

SAMPLES FROM DEPTHS GREATER THAN 25 m

Bore	Depth (m)	Month	pH	EC µS/cm	HCO_3^- mg/L	Mg mg/L	Fe mg/L	U µg/L	Si mg/L
PH49	28-30	May	6.74	236	154	26.4	0.78	265	8.9
		Nov	6.84	230	159	25.0	1.10	93.9	9.2
PH55	26-28	May	6.57	193	127	17.9	5.60	0.40	14.0
		Nov	6.55	179	117	19.0	2.30	0.36	14.7
PH55	40-42	May	6.53	198	124	18.3	0.70	1.00	12.1
		Nov	6.60	180	120	19.0	3.50	0.98	14.5
PH56	26-28	May	6.50	177	108	16.0	0.87	12.0	10.1
		Nov	6.72	167	116	18.0	0.93	7.19	10.0
PH56	43-45	May	6.95	169	113	16.7	0.53	11.4	9.4
		Nov	6.93	183	120	19.0	0.71	4.30	8.8
PH58	25-27	May	6.57	198	125	18.0	0.52	1.61	14.4
		Nov	6.70	188	118	19.0	2.40	2.04	15.2
PH58	38-40	May	6.60	172	114	17.7	0.28	0.56	15.8
		Nov	6.59	187	114	18.0	1.10	1.05	15.7
PH61	26-28	May	6.92	170	107	16.4	0.05	3.95	8.1
		Nov	7.24	208	140	19.0	0.83	2.97	6.6
PH61	43-45	May	7.03	225	151	18.0	0.26	5.49	7.2
		Nov	7.30	227	156	21.0	0.59	2.38	6.5
PH88	28-30	May	6.54	148	88	14.1	0.32	2.13	14.5
		Nov	6.92	138	87	15.0	1.10	2.83	14.9
PH88	38-40	May	6.62	134	81	13.0	1.05	3.60	14.1
		Nov	6.82	141	92	15.0	1.20	2.37	14.9
PH94	26-28	May	7.17	74	38	5.7	0.04	0.17	12.1
		Nov	7.06	74	38	6.0	0.06	0.24	12.1
PH94	40-42	May	6.77	90	56	6.1	0.19	0.57	10.4
		Nov	6.94	75	38	6.1	0.05	0.28	12.1
KD1	40-42	May	5.95	106	69	3.6	18.9	4.61	6.1
		Nov	6.07	126	81	4.8	22.0	0.52	5.3

TABLE 5.2

GROUNDWATER DATA FOR SHALLOW (AD) BOREHOLES

	pH	EC µS/cm	Mg mg/L	HCO_3^- mg/L	Cl mg/L	PO_4 µg/L	U µg/L
AD1 (9.5 m)							
Nov 90	6.71	110	12.1	53	5.2	10	52.5
Apr 91	5.90	30	1.3	11	2.8	<5	5.14
Apr 91*	5.70	31	0.5	10	3.1	<5	7.14
May 91	5.95	44	2.3	20			
Jul 91	6.84	70					
AD2 (9.0 m)							
Nov 90	7.69	191	13.1	119	3.5	35	2.55
Apr 91	6.70	62	3.9	31	2.9	<5	0.73
May 91	6.51	86		25			
Jul 91	6.56	70					
AD6 (4.0 m)							
Apr 91	6.40	56	2.5	21	3.2	<5	0.49
Jul 91	6.28	63					
AD8 (9.0 m)							
Nov 90	6.59	97	4.0	50	2.4	20	1.13
Apr 91	6.44	60	2.9	30	2.5	<5	0.63
AD9 (7.0 m)							
Apr 91	5.96	42	2.2	18	1.9	<5	0.13
Apr 91*	5.68	38	1.8	14	2.2	<5	0.16
AD11 (2.5 m)							
Apr 91	5.74	33	0.6	14	1.4	<5	0.9
AD12 (5.0 m)							
Apr 91	6.76	115	7.6	54	4.2	<5	2.03
May 91	6.81	158	13.5	101			
TAD12 (1.5 m)							
Apr 91	5.55	24	1.1	6	2.0	<5	0.47
AD13 (9.0 m)							
Apr 91	6.43	149	9.2	76	6.9	<5	77.9
May 91	6.46	158	11.3	84			
Jul 91	6.84	151					
AD14 (10.5 m)							
Apr 91	5.80	101	3.2	41	6.9	<5	2.94
May 91	6.68	68	3.8	27			
Jul 91	6.02	70					

* Denotes second sampling on this field trip.

TAD12 was a temporary sampling point close to AD12.

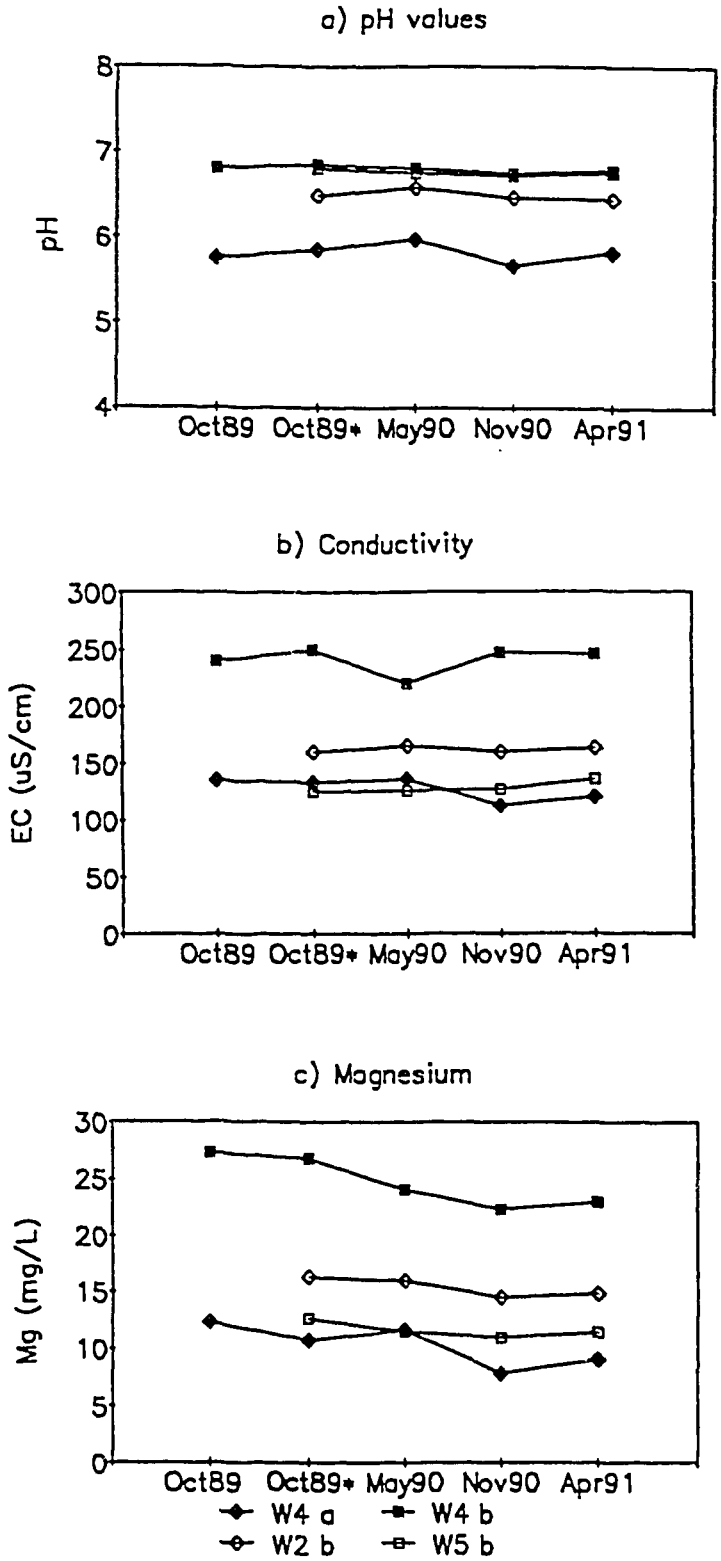

* denotes second sampling on October 1989 field trip

FIGURE 5.1 Variations in groundwater chemistry for selected boreholes. Field trips October 1989 to April 1991

a) pH
b) conductivity
c) magnesium

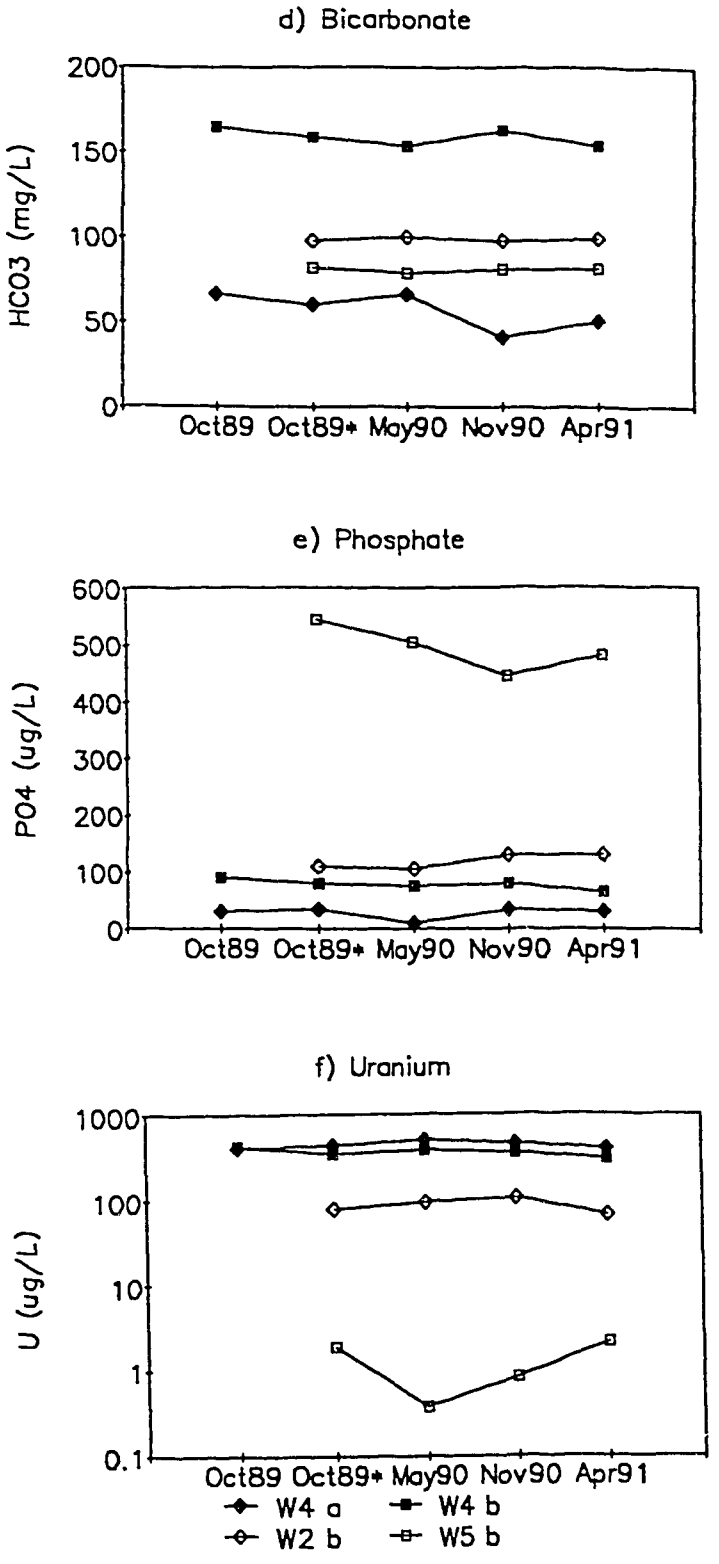

FIGURE 5.1 (continued)

d) bicarbonate
e) phosphate
f) uranium

6 MAJOR SPECIES AND SPATIAL TRENDS IN GROUNDWATER CHEMISTRY

6.1 Presentation of Results

This chapter provides an overview of the chemical compositions of Koongarra groundwaters, with particular emphasis on the variations of groundwater chemistry as a function of position and depth within the vicinity of the No.1 orebody. The subject matter of the chapter includes major groundwater parameters such as pH, redox potential, conductivity, and elemental composition.

Complete chemical data for samples collected during ARAP sampling field trips are presented in Appendices 3 to 6 of this report. Because of the large amount of analytical data, a "Guide to Appendices" has been included at the start of the Appendices section. The general approach has been to tabulate major chemical data for groundwater samples collected on each field trip in Appendix 3. This appendix includes data for the major parameters:

pH, Eh, conductivity, HCO_3, Cl, F, SO_4, PO_4, Mg, Na, K, Ca, Si, Fe, Mn, and U.

Appendices 4 and 5 provide quantitative and semi-quantitative data for trace constituents which have been determined for samples from the various field trips. Table 3.1 lists boreholes and depths sampled during each field trip and provides an index to chemical data tabulations.

In the main part of the report, much of the data is presented in the form of figures, either as:

a) contour plans, or

b) "projected cross sections".

The contour plans consist of a map of the area of the No. 1 orebody, showing the boreholes where groundwater samples have been obtained, and indicating the contours of each parameter (eg. the groundwater conductivity contour plan in Figure 6.1). The data set used for these contour plans only includes samples from depths greater than 16 m. This is within the permanently saturated zone, where, as was shown in Section 5, groundwater chemistry does not show a substantial seasonal variation. The contours are hand-drawn, rather than being computer generated. This allows them to be drawn with some discretion being shown bearing in mind the geology of the site. In most cases there is sufficient data for confidence in the indicated contours.

The "projected cross-section" has been developed to indicate the spatial and depth variation of parameters along a broad transect through the orebody. This transect is shown in Figure 2.2, and includes the AD holes in the same area of the orebody. As the boreholes are not co-linear, it has been necessary to combine

them on a distance scale where they are projected onto a single axis (eg. for conductivity in Figure 6.2). This approach allows data for a large number of boreholes to be utilised, enabling greater confidence to be placed in the resulting figures. Each point on the projected cross-sections (and contour plans) represents a sampling point for which data are available in the appendices to this volume. The origin for the x axis of the projected cross-sections is the 3000 m E line on the mine grid. This grid line is approximately parallel to the fault and passes close to KD1 (see Figure 2.2). Note that the vertical scale in Figure 6.2 (and other projected cross-sections) is greatly expanded relative to the horizontal scale.

The projected cross-sections of groundwater chemistry should be interpreted with reference to the geology of the site. A detailed description of Koongarra geology is included in Volume 2 of this series. Figure 6.3 shows the main features of the orebody, and the section used in the projected cross-sections in this volume.

On the projected cross-sections of groundwater chemistry, approximate contours of chemical parameters are indicated. It is emphasised that, whilst the selected transect approximately coincides with what is believed to be a groundwater flow direction, the objective of the approach is to show the spatial variation in parameter values. It is not intended to infer that water moves from left to right across the transect with chemical changes being a direct result of groundwater flow.

6.2 Conductivity

Conductivity is a simple parameter to measure, and reflects the level of total dissolved solids (TDS). At Koongarra, where groundwater chemistry is dominated by Mg^{2+} and HCO_3^-, the conductivity usually gives a good indication of the concentration of these ions in the groundwater.

A plan view of conductivity contours at Koongarra is shown in Figure 6.1. The highest EC values, and by inference, the highest levels of dissolved solids, coincide with the region of the uranium orebody at Koongarra. There is a gradual decrease in EC moving away from the orebody in all directions, with an elongation parallel to the fault. Groundwaters with high EC values extend some distance from the orebody in the direction of PH80 and C1. The highest groundwater conductivity, about 300 μS/cm, is quite low relative to many Australian groundwaters, which are often highly saline.

The conductivity of sampled groundwaters as a function of depth and distance is shown in Figure 6.2. The highest EC values occur in the immediate vicinity of the orezone, indicating that this is a region of active weathering. This figure shows that the near-surface groundwaters, obtained from the shallow AD-series boreholes, are much more dilute than deeper groundwaters.

6.3 pH and Redox State

The pH (acidity), and redox potential (which is an indicator of the likely oxidation states of key species such as Fe and U), are important parameters which can be measured by electrodes in unperturbed fresh groundwater samples. As discussed in Section 4.3, Koongarra groundwaters tend to lie in a pH/Eh regime in which U(VI) is dominant and uranium minerals are significantly soluble. Thus, simple pH/Eh considerations suggest potential uranium mobility in the system. Uranium speciation and solubility are discussed in detail in Volume 12 of this series.

Figure 6.4 shows the pH of Koongarra groundwaters in cross-section. The pH of samples from the unweathered or transition zones in the Cahill formation (which hosts the uranium mineralisation) is fairly uniform, usually between 6.5 and 7.2. In the shallow AD boreholes, groundwater pH values below 6.5 occur when the near-surface zone is saturated after the wet season. Samples from KD1, up-gradient of the deposit in the Kombolgie formation, also have a significantly lower pH (5.5-6.5) than the deeper samples from the Cahill formation. In-situ pH/Eh measurements of Kombolgie groundwater, obtained in borehole KD1 with a submersible probe, are discussed in Section 6.13.1.

The pH/Eh conditions of a number of groundwater samples obtained after the 1990/91 wet season are plotted on Figure 6.5. The groundwaters from depths over 16 m plot in a field of relatively high pH and lower redox potential. The pH/Eh of the shallower AD samples trends towards those of surface- and rain-waters. This diagram suggests a gradation in groundwater pH/Eh conditions as a function of depth.

There has been some controversy about the accuracy and value of Eh measurements (Lindberg and Runnells, 1984). The Eh measurements made at Koongarra correlate well with dissolved Fe values (see Section 6.10.1 below), and give a convenient approximation to the redox state of the system. However, the true situation is probably far more complex than a single Eh value reflects, with several couples and the possibility of non-equilibrium conditions occurring. Therefore the Eh values should only be interpreted as being a useful qualitative indicator of redox conditions.

6.4 Magnesium

Magnesium is important at Koongarra because it is released by weathering of the chloritised schists of the mine series host rocks. A generalised equation (from Volume 11 of this series) is as follows:

$$\underset{\text{chlorite}}{Mg_5Al_2Si_3O_{10}(OH)_8} + 10\ CO_2 + 3\ H_2O \Rightarrow \underset{\text{kaolinite}}{Al_2Si_2O_5(OH)_4} + 5\ Mg^{2+} + SiO_2 + 10\ HCO_3^- \qquad (6.1)$$

During weathering, dissolved CO_2 is consumed, with the release of silica, Mg^{2+} and HCO_3^- to solution.

Groundwaters from the immediate vicinity of the Koongarra orebody contain elevated concentrations of magnesium (Figure 6.6), generally exceeding 20 mg/L. Figure 6.6 shows an apparent dispersion of magnesium towards the south/southwest. A comparison of Figures 6.1 and 6.6 shows a close correspondence between the contours of conductivity and Mg, which is not surprising, given that Mg^{2+} is the dominant cation in most Koongarra groundwaters.

The cross section shows much lower Mg concentrations in shallow (<16 m) groundwaters (Figure 6.7), while high Mg concentrations occur at depths of at least 50 m (well into the unweathered zone) in the vicinity of the orebody.

Figure 6.8 shows the magnesium concentration in groundwaters from the sector shown on Figure 2.2, plotted as a function of distance, using the same distance scale. Magnesium levels increase sharply in the mineralised zones and decrease moving down-gradient. The variation in Mg is by about a factor of 5, much smaller than the range of uranium which varies over several orders of magnitude (detailed in Section 7.1). This can be attributed both to the more localised U distribution in the rock, and to the more rapid reduction in U concentrations by adsorption. It appears likely that gradual dilution by meteoric water plays a major role in the reduction of Mg concentrations, although processes such as ion-exchange, precipitation or adsorption probably also contribute. Magnesium values return to up-gradient values about 250 m down-gradient of the orebody.

6.5 Other Major Cations

The concentrations of cations other than Mg^{2+} in Koongarra groundwaters are relatively low (see Figure 4.1). Sodium and potassium concentrations are around 1-2 mg/L, and calcium up to about 5 mg/L in the Cahill formation. In a region of dolomites to the southwest of the orebody, the concentrations of Ca are higher, and approximately equal to those of Mg.

6.6 Bicarbonate and Dissolved CO_2

The major anion in Koongarra groundwaters is invariably bicarbonate (HCO_3^-), with concentrations of up to 160 mg/L at the centre of the orebody. Bicarbonate is released, together with Mg, during the weathering of chlorite by CO_2-charged groundwaters (Equation 6.1). The dissolved CO_2 in Koongarra groundwaters may arise from equilibration with soil gas CO_2, from bacterial oxidation of carbon-containing minerals (such as graphite), or it may enter the system as dissolved CO_2 in up-gradient groundwaters (discussed in Section 8). Several sources probably contribute to some extent.

The distribution of HCO_3^- concentrations in Koongarra groundwaters (Figures 6.9 and 6.10) is very similar to that of Mg, with maximum concentrations in the zone of uranium mineralisation. Similarly, the plot of alkalinity (to which bicarbonate is the

major contributor), as a function of distance from 3000m E grid-line (Figure 6.11) resembles the corresponding figure for Mg (Figure 6.8).

Due to the high levels of bicarbonate and the near-neutral pH, Koongarra groundwaters are unstable when brought to the surface and release CO_2. The partial pressure of CO_2 in many Koongarra groundwaters is around 10^{-2} atm. This is approximately 30 times higher than is present in the earth's atmosphere, but is typical of $p(CO_2)$ produced in the soil zone by the decay of organic matter and respiration of plant roots (Freeze and Cherry, 1979). It is possible that the aquifer intersecting the orebody may be partially confined by a heavy clay layer in the weathered zone. There is evidence that the $p(CO_2)$ decreases as the groundwaters move down-gradient (Figure 6.12), which may be partially attributed to loss of CO_2 by out-gassing to the atmosphere. Whilst out-gassing could explain the decrease in $p(CO_2)$ moving down-gradient, this process would not reduce alkalinity (Figure 6.11), so processes such as dilution and weathering must also be occurring.

It is important when interpreting this groundwater data to recognise that the total DIC in groundwaters can be much greater than that present as the HCO_3^- ion alone. This is because other forms of DIC may be present, such as dissolved CO_2, which is often referred to as H_2CO_3*. The amount of H_2CO_3* can be calculated from the HCO_3^- content and the pH, with the equilibrium between the HCO_3^- and H_2CO_3 species being strongly dependent on the pH. The contribution of H_2CO_3* to the DIC exceeds that of the HCO_3^- ion below a pH of about 6.4. Figure 6.13 shows that total DIC in Koongarra groundwaters is significantly greater than the HCO_3^-, particularly in up-gradient groundwaters from KD1 (expressed as mmol/L of C). This is almost entirely due to the contribution of H_2CO_3*, which is greatest in the KD1 groundwaters which have a lower pH (Section 6.3). In Figure 6.13, there appears to be a conversion of the form of DIC from H_2CO_3* to HCO_3^- moving along the transect to the centre of the orebody, followed by a steady decrease in DIC. The data are consistent with the dissolved CO_2 (present in up-gradient waters) being converted to HCO_3^- in weathering reactions (such as that represented by Equation 6.1). This is followed by a gradual mixing with a more dilute component in the down-gradient part of the transect.

6.7 Phosphate

Considerable effort has been put into measuring phosphate concentrations in Koongarra groundwaters because of the occurrence of uranyl phosphate minerals, such as saleeite, in the weathered zone. Furthermore, aqueous phosphate has been reported to be a strong complexant of the uranyl ion (Dongarra and Langmuir, 1980; Langmuir, 1978). Therefore, it is possible that phosphate could play an important role in mineral solubility and uranium speciation. However, the importance of the uranyl phosphate complex has been widely questioned (Markovic and Pavkovic, 1983; Tripathi, 1983). This issue is further addressed in Volume 10 of this series.

The measured concentrations of phosphate in Koongarra groundwaters (Appendix 3) were up to about 700 µg/L. Elevated phosphate concentrations were found in

two distinct zones (Figure 6.14). These were the upstream edge of the mineralised zone (PH15, W1b and M1), and a number of boreholes fringing the dispersion fan on the down-gradient side. In the zone of the dispersion fan where uranyl-phosphate minerals are abundant in the solid phase (i.e. the vicinity of boreholes PH14 and C9), the measured groundwater phosphate concentrations, (somewhat surprisingly), were relatively low. The projected cross-section (Figure 6.15) confirmed the presence of the two distinct regions of elevated phosphate concentrations, both confined to depths greater than about 15 m below the surface. Shallower samples tended to have lower phosphate concentrations, with phosphate in groundwater from the AD-holes generally below detection limits. Up-gradient of the orebody in the Kombolgie sandstone, phosphate concentrations were also very low.

In some cases, elevated phosphate concentrations were highly localised, particularly in the primary orebody. For example, the measured PO_4 concentration in groundwater from borehole M1, when sampled in May 1989, was 635 µg/L for the 46-48 m depth interval, but only 40 µg/L for the 24-26 m interval. As Figures 6.14 and 6.15 show, the phosphate-rich zone down-gradient of the orebody is widespread and represented by a large number of samples in the data set. The elevated phosphate concentrations are clearly present in two large lobes and only at depths exceeding about 15 m.

6.8 Chloride and Other Anions

Chloride concentrations were generally rather low (below 10 mg/L). Whilst significantly above rainwater values, the measured levels could be attributed to input during percolation from the surface through the soil zone, with evaporation probably playing an additional minor role. It should be noted that atmospheric fallout of a fine aerosol of NaCl (originating from the oceans) probably deposits a significant amount of Cl to the land surface at Koongarra. This source, in addition to the Cl contained in rainfall, may add a significant amount of Cl to the system. Measured groundwater chloride concentrations appeared to be somewhat variable pointing to an apparent analytical or sampling variation.

Other potentially important anions such as fluoride were present at low levels (<1 mg/L) and were not sufficiently abundant to play a role in uranium speciation.

6.9 Silicon

Silicon concentrations are about 5-15 mg/L in Koongarra groundwater, probably present as the uncharged $Si(OH)_4$ species. The measured levels of Si make it, together with Mg, one of the main contributors to TDS in Koongarra groundwaters. The contours for Si (Figure 6.16) showed a zone of enrichment around borehole W5, coinciding with one of the lobes of elevated phosphate concentrations. The main trend in Si concentrations was a steady increase moving down-gradient. This contrasted to the distributions of Mg, U and HCO_3, which showed clear maxima in the ore-zone, and to the two distinct lobes of elevated phosphate concentrations. As discussed in Volume 2 of this series, the chloritised schists of the mine-series

tend to be depleted in silica (as well as enriched in Mg), so there tends to be an increase in dissolved Si, as well as a decrease in Mg concentrations, in groundwaters moving away from the orebody.

6.10 Iron

Iron is important in the Koongarra system due to the tendency of uranium to be associated with iron minerals such as ferrihydrite (Volume 8 of this series). Furthermore, iron-rich colloids appear to be present in Koongarra groundwaters (see Section 9).

The measured concentrations of dissolved iron in Koongarra groundwaters ranged from <1 to 22000 μg/L. Iron concentrations were correlated to the Eh (redox potential) of the groundwater, with high Fe values occurring when the measured Eh was lowest. This reflects the much greater solubility of Fe^{2+}, relative to Fe^{3+}. In-field spectrophotometric determinations of Fe^{2+} confirmed that the dissolved iron was present in the ferrous (+2) oxidation state.

6.10.1 Relationship between dissolved Fe and measured Eh

The value and accuracy of redox determinations has been the subject of some debate. It has been stated that determinations using various redox couples and also platinum electrodes are virtually useless, and rarely agree except by chance (Lindberg and Runnells, 1984).

It is difficult to prove conclusively that the measured redox values for Koongarra groundwaters, which were determined using a platinum electrode, are correct. However, it can be shown that the measured Eh and dissolved iron concentrations are consistent with each other. This was done by calculating expected dissolved iron levels from the measured Eh and pH values for Koongarra groundwaters, and comparing these values with measured dissolved Fe values. It was assumed in the computations that ferrihydrite was the solid phase controlling dissolved Fe concentrations. A second assumption was that the Fe^{2+}/Fe^{3+} couple is the dominant redox couple in these groundwaters. The chemical speciation code MINTEQA2 (Allison et al., 1990) was used in these calculations.

The results (Figure 6.17) showed considerable scatter, but a significant correlation between measured and predicted Fe concentrations was observed. Significant discrepancies (up to an order of magnitude) were attributed to uncertainties in field determinations of pH and Eh, to which these calculations are highly sensitive.

Overall, this exercise showed that field redox measurements using a platinum electrode are of some value at Koongarra. The success of the approach may be attributed to the fact that only the total Fe concentration was required, rather than separate in-field determinations of both members of a redox couple, which may be present at very low levels. Furthermore, Koongarra groundwaters exhibit an extremely large range of dissolved Fe concentrations, for which the ICPAES analysis is both sensitive and accurate.

6.11 Trace Metals

Manganese was commonly detected in Koongarra groundwaters with concentrations up to 1 mg/L, although more often around 100 μg/l. Manganese oxides may be an important phase in the fixation of U and other radionuclides at Koongarra (Volume 8 of this series).

Copper-containing minerals, such as metatorbernite ($Cu(UO_2)_2(PO_4)_2.8H_2O$) are present at Koongarra. Therefore, the measurement of Cu in groundwaters was undertaken using anodic stripping voltammetry as well as quantitative ICPMS. Despite the low detection limits of these techniques, it was not possible to accurately measure Cu levels, which were extremely low, probably below 1 μg/L.

6.12 Organic Matter

Total organic carbon was measured in numerous samples (Appendix 6) but concentrations were generally less than 2 mg/L, and often not significantly above the detection limit of approximately 300 μg/L. These results suggest that Koongarra groundwaters have relatively low levels of organic constituents, and that these materials probably do not play a major role in the system.

6.13 Depth Relationships in the Cahill and Kombolgie Formations

It has already been commented that samples of seasonal groundwaters from shallow depths at Koongarra have a characteristic chemistry, which is, in many respects, similar to rainwater. During a field trip in May 1991, water samples were obtained from a number of boreholes across the deposit, including shallow groundwaters from the AD-holes. Figures 6.18 (a)-(c) show that the values of pH, conductivity and magnesium concentrations in these samples were related to the sample depth. The pH tended to increase with depth, from values around 5.5 (similar to rainwater), towards the values of 6.5-7.5 found in the unweathered Cahill Formation. Similarly, the conductivity and Mg concentrations show a general rise with increasing depth.

The amounts of HCO_3^- and total DIC (Figure 6.18d) generally increased with depth. The trend in HCO_3^- concentrations was very similar to that for Mg^{2+} and conductivity, as would be expected. The total DIC was fairly constant in samples from within about 10 m of the surface (about 1 mmol/L), but was greater in deeper samples (2-3 mmol/L). Therefore, in this case, the changes in HCO_3^- concentrations and DIC cannot be explained solely by a conversion of $H_2CO_3^*$ to HCO_3^- with increasing depth.

The data presented in Figure 6.18 suggest that there is an input of local recharge rainwater at the surface of the weathered Cahill formation during the wet season. As this water infiltrates downwards, its water chemistry evolves towards the chemistry of deeper groundwaters (for more detail, see Volume 12 of this series).

Within the unweathered Cahill formation, water samples from different depths in the same borehole generally have a similar major ion chemistry (Table 5.1), although usually having a different isotopic composition. One major reason for this chemical similarity is that the layering in the Cahill formation dips very steeply, so water samples recovered at different depths may still be close together stratigraphically, and hence have similar geochemistry.

6.13.1 Down-hole Probe Measurements

The down-hole probe consists of a sonde, equipped with sensors for pH, redox, DO, EC, and temperature measurements, which is lowered into a borehole. It provides in-situ data for these parameters, and may be used to profile chemical conditions in the borehole as a function of depth. In general, the profiles obtained for boreholes in the Cahill formation were rather uniform.

However, the down-hole probe profiles obtained for KD1, in the Kombolgie sandstone (Figure 6.19) showed that, at a depth of about 70 m, acidic, oxidising and oxygen-containing groundwater was present in the borehole. The presence of DO at this depth was surprising, given that deep Koongarra groundwater samples obtained in rigorously air-free conditions usually gave negligible DO values. In an in-situ measurement with a down-hole probe the ingress of atmospheric oxygen down the borehole is highly unlikely, hence the DO must be present in the groundwater. An important aspect of this data was that the profiles obtained after the borehole was pumped with a high capacity submersible pump and allowed to settle were similar to the previous results (Figure 6.19), and indicated that the aquifer at this depth was a major source of water in the borehole.

The data suggest that KD1 intersects an aquifer, possibly a fracture system, containing oxidising and relatively acidic groundwater. Samples pumped from KD1 invariably had high partial pressures of CO_2 (Section 6.6 above). A groundwater of this chemistry, if it traversed the fault into the adjacent Cahill formation, could be responsible for the in-situ alteration of uraninite observed in core samples taken from the No.1 orebody in regions close to the fault (Snelling, 1980), as well as the weathering of chlorite (Equation 6.1).

However, the evidence for water movement across the fault from the Kombolgie sandstone is not conclusive. There is no significant water inflow into W6, drilled into the Kombolgie, over its depth of 25 m. Another up-gradient borehole, C10, drilled to a depth of 40 m, did not intersect any aquifers. The drilling log for KD1 showed no water inflow within 30 m of the ground surface, but substantial water intersections at greater depths (Noranda, 1978). In-flowing groundwater was encountered throughout the interval between 30 m and the bottom of the hole at 120 m. Therefore, if groundwater moves across the fault from the Kombolgie sandstone into the Cahill formation, this movement may occur at considerable depths.

6.14 Comments

The distributions of elements provide much information about the system. The primary ore-zone is characterised by high conductivity, Mg, HCO_3 and U, and these tend to decrease moving away from the orebody. There is an anomalous zone down-gradient with high phosphate and silica.

The data from the AD-holes suggests that shallow seasonal groundwaters have a dilute rainwater-like chemistry. In the permanently saturated zone, at depths greater than about 16 m, it appears that seasonal effects have little influence on groundwater chemistry. The data suggest that as rainwater infiltrates downward it gradually acquires the characteristics of the deeper groundwaters.

The chemical data provide some information about the sources and flow-paths of groundwater in the system. The major inputs seem to be rainwater infiltrating across the area of the deposit, together with a source in the vicinity of the fault. This could be groundwater moving through fractures within the Kombolgie sandstone which traverses the fault and enters the system. This groundwater is acidic, oxidising, and contains significant amounts of dissolved CO_2, and may therefore be responsible for in-situ alteration of uranium minerals near to the fault. Down-gradient, groundwater flow paths appear to be at an acute angle rather than perpendicular to the fault, with an elongation of groundwater haloes towards borehole PH88, suggesting that groundwater may move in this direction. Groundwater sources and flow-paths are discussed further in Section 10 of this report.

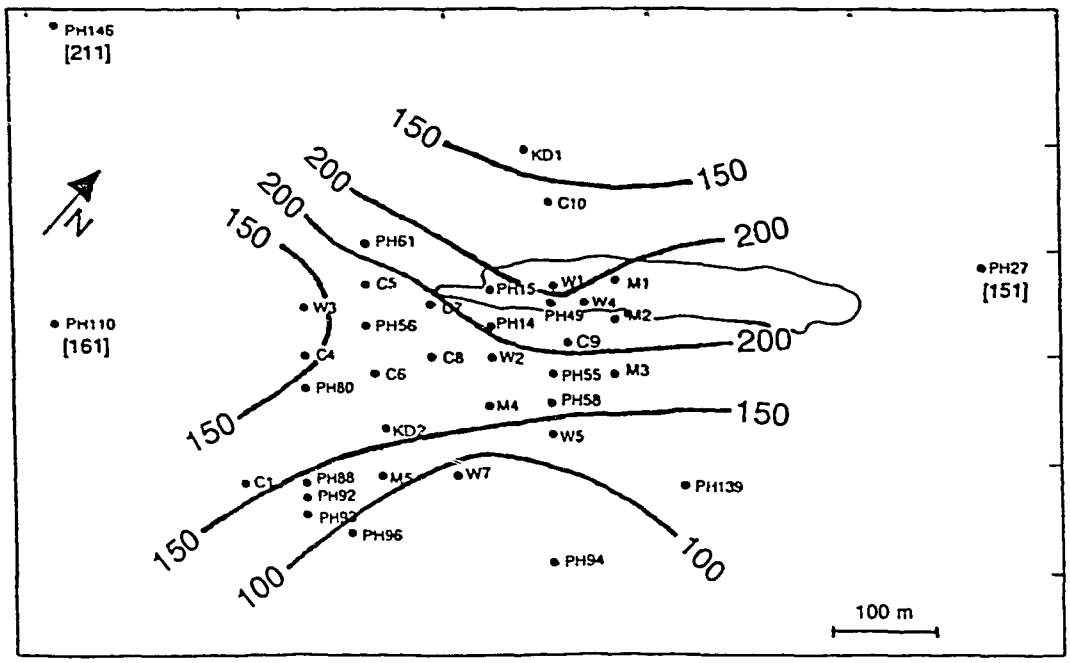

FIGURE 6.1 Groundwater conductivity (µs/cm) - contour plan
Conductivity values of outlying boreholes are indicated

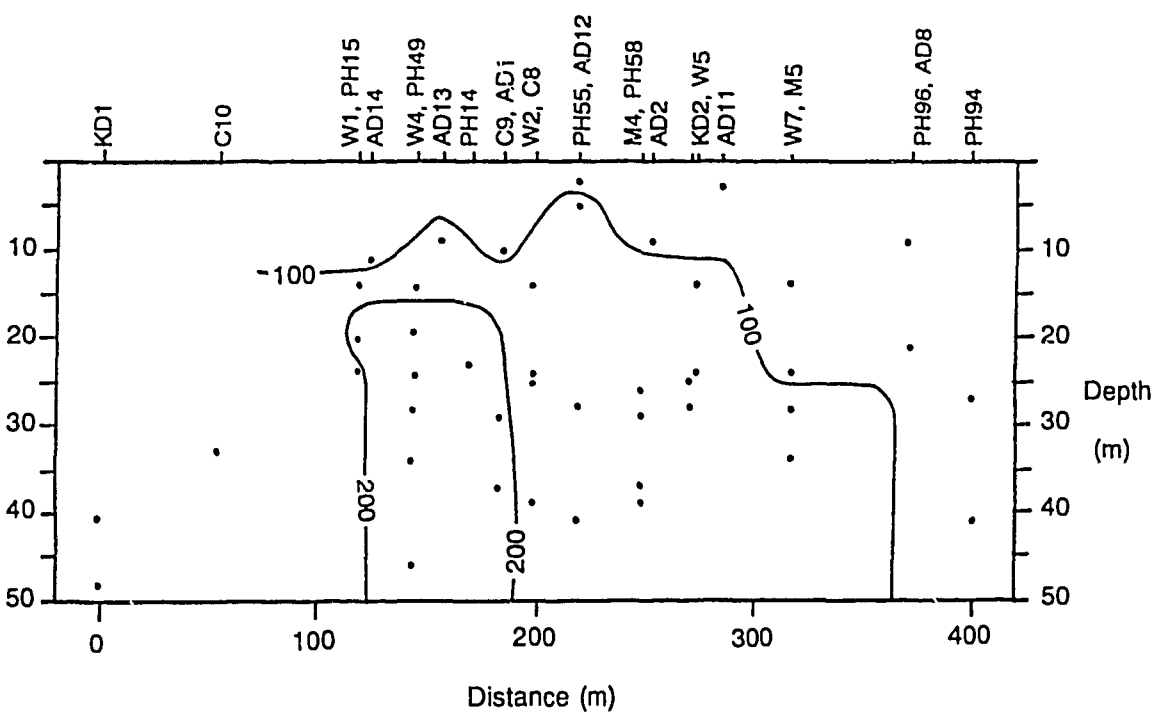

FIGURE 6.2 Conductivity of groundwater (µs/cm) - projected cross-section

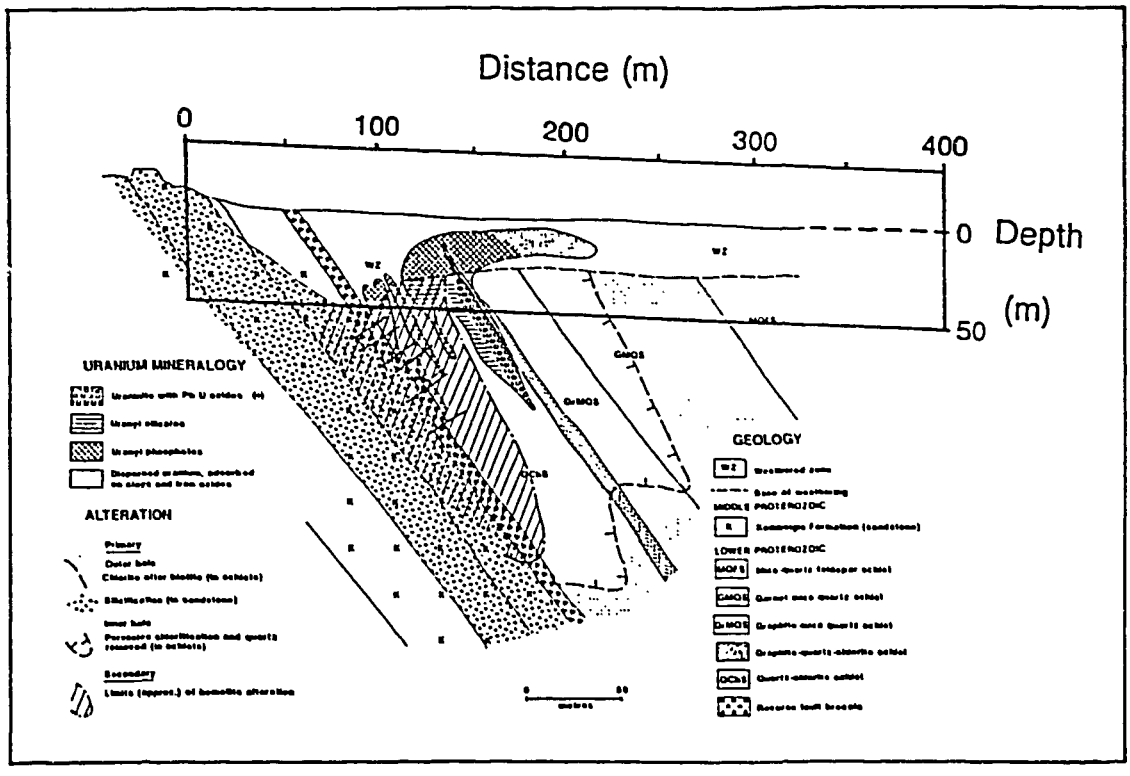

FIGURE 6.3 Simplified cross-section through the No. 1 orebody, showing the section used in presenting groundwater chemical data

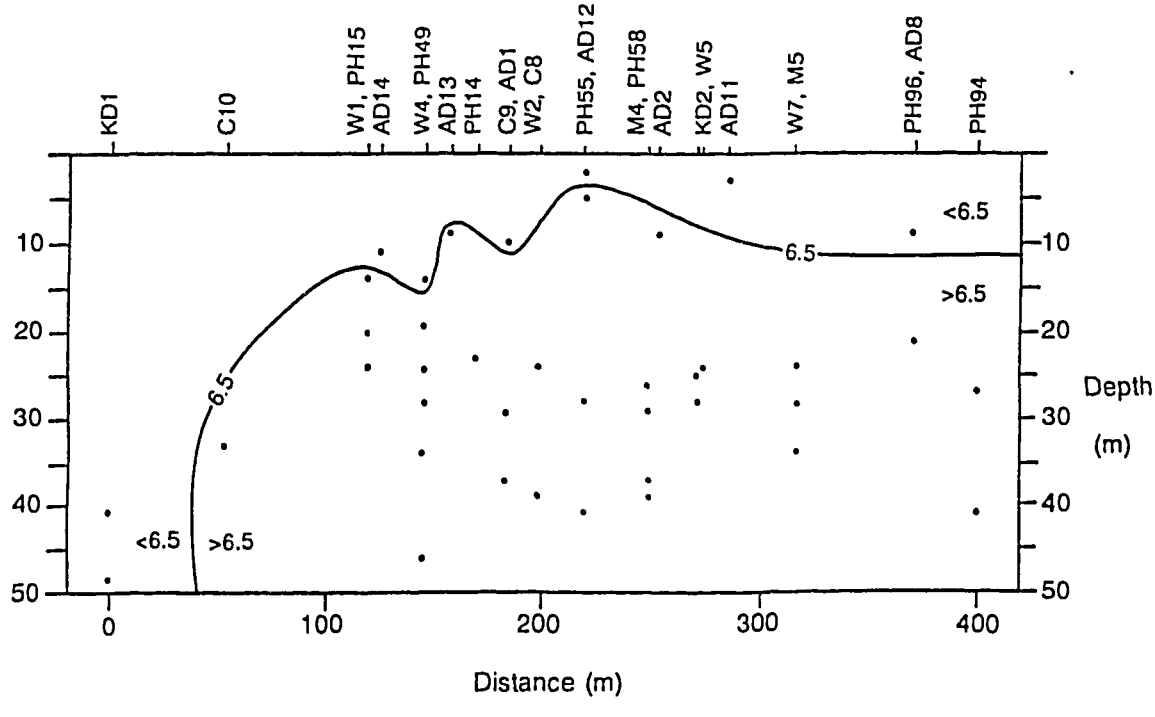

FIGURE 6.4 Groundwater pH - projected cross-section

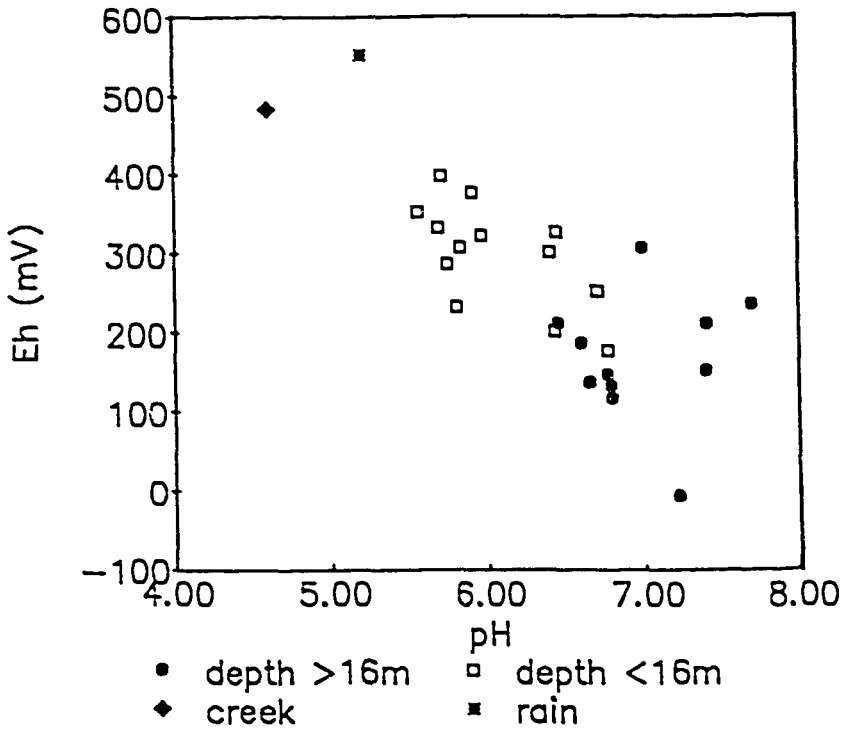

FIGURE 6.5 pH/Eh diagram for Koongarra groundwater showing the field occupied by shallow groundwaters (data from April 1991 field trip)

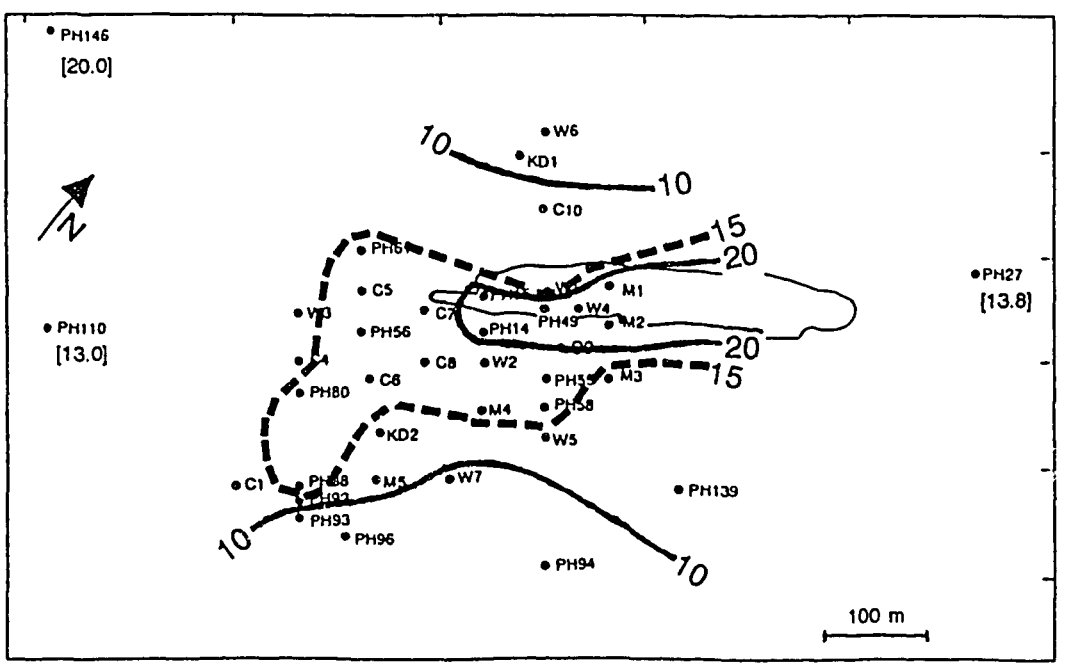

FIGURE 6.6 Magnesium in groundwater - contour plan. Data for outlying boreholes are indicated. The position of the 15 mg/L contour is uncertain.

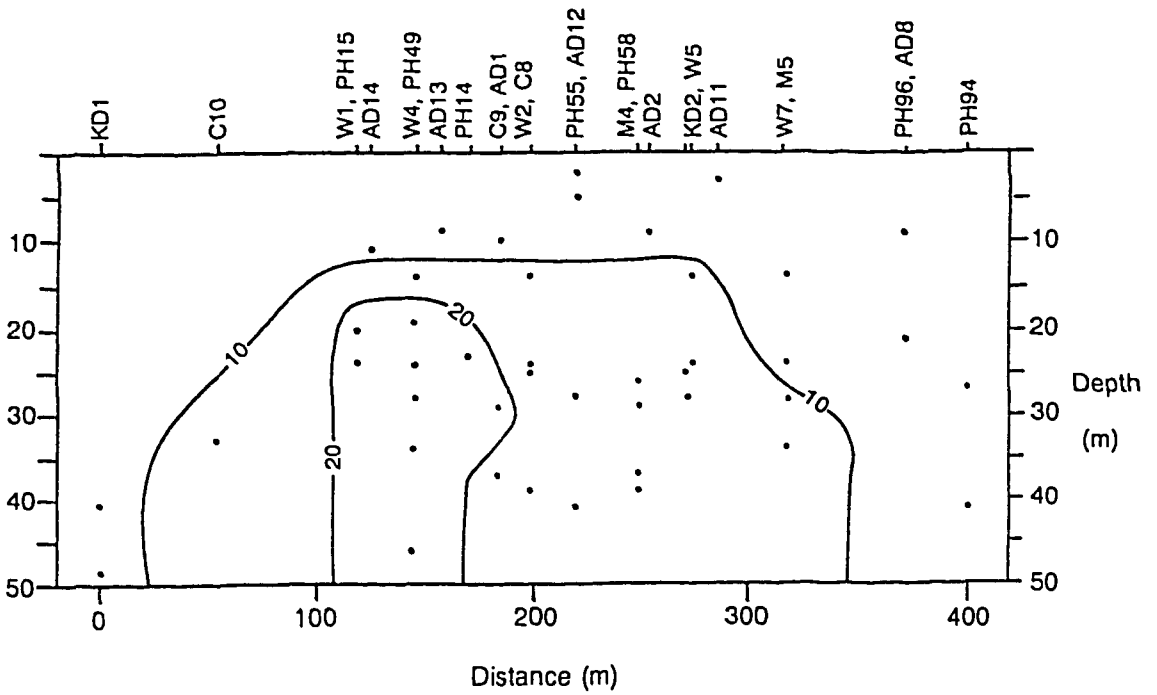

FIGURE 6.7 Magnesium in groundwater (mg/L) - projected cross-section

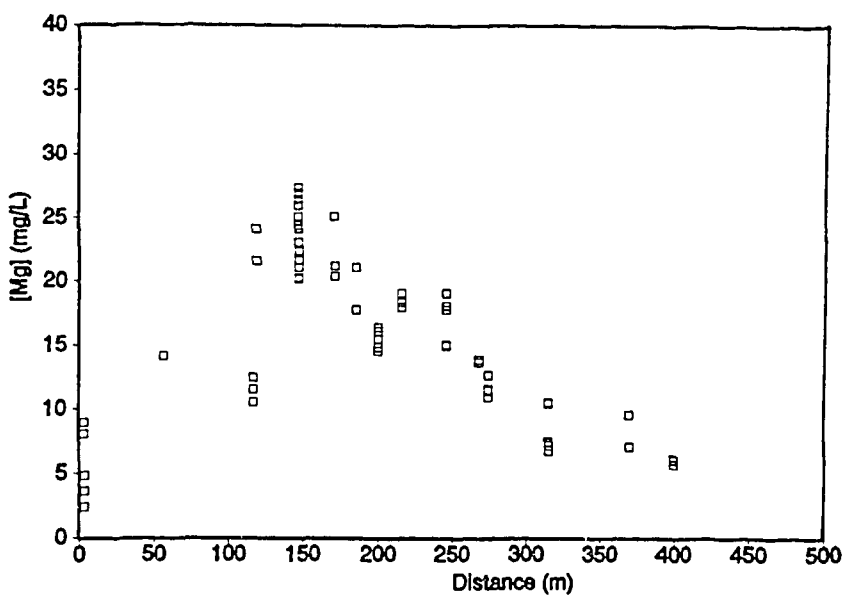

FIGURE 6.8 Magnesium concentrations as a function of distance from KD1

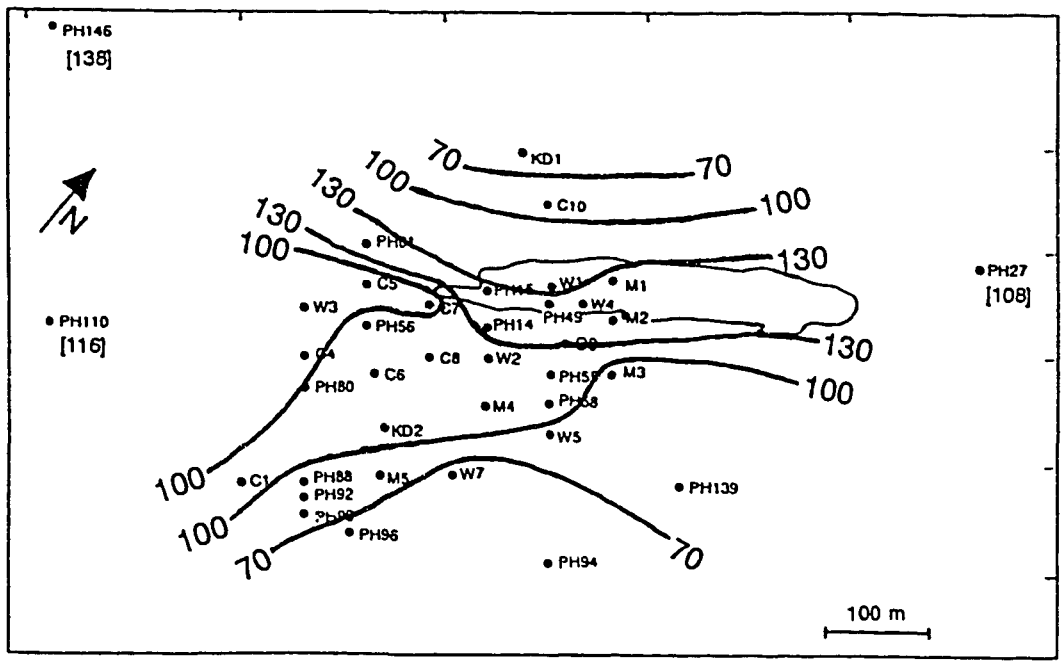

FIGURE 6.9 Bicarbonate in groundwater (mg/L) - contour plan

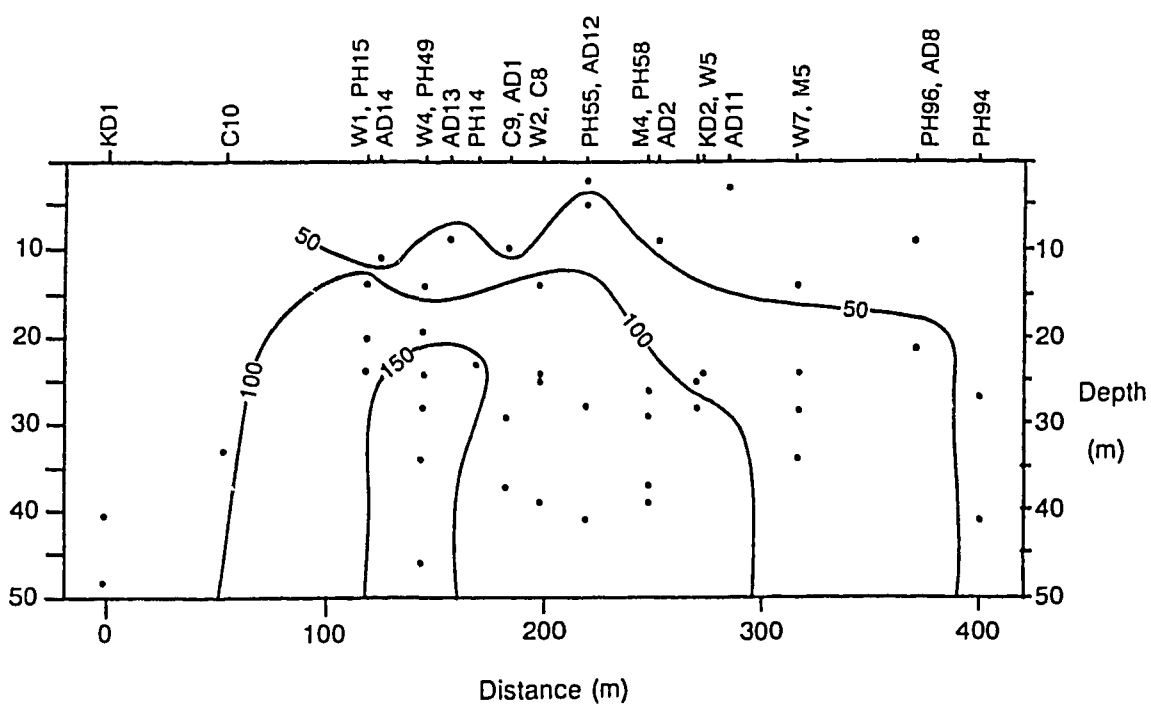

FIGURE 6.10 Bicarbonate in groundwater (mg/L) - projected cross-section

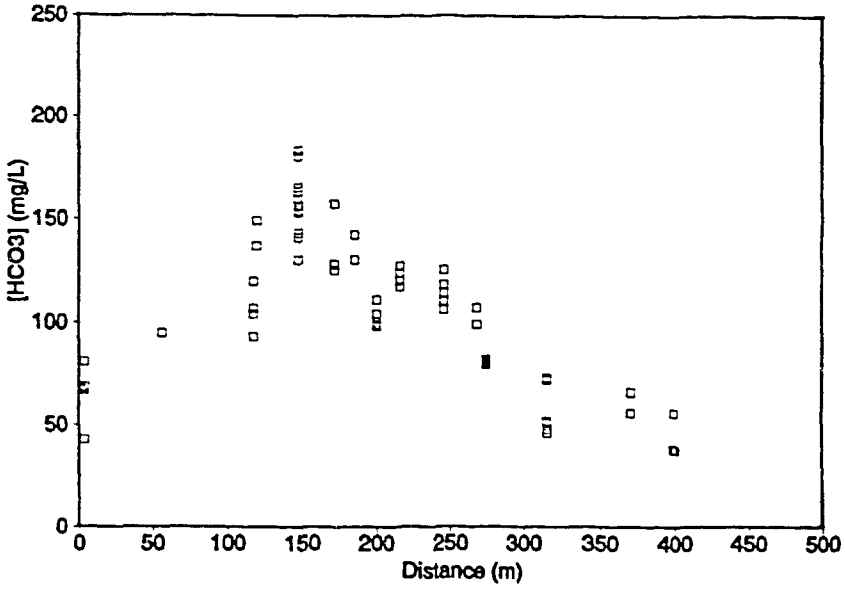

FIGURE 6.11 Groundwater alkalinity as a function of distance from KD1

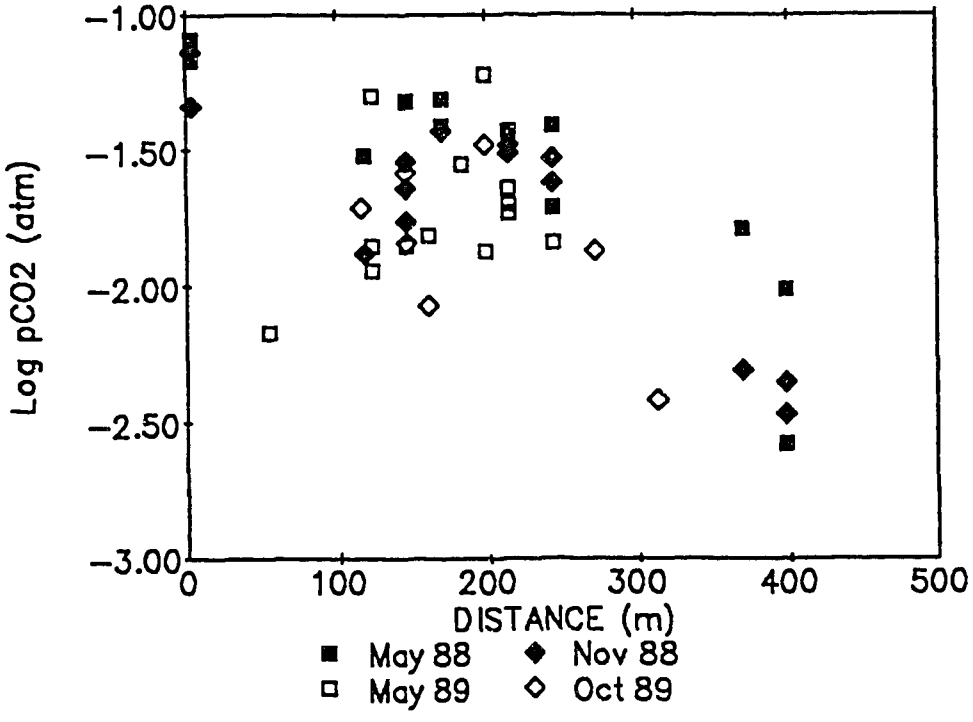

FIGURE 6.12 Partial pressure of CO_2 as a function of distance from KD1

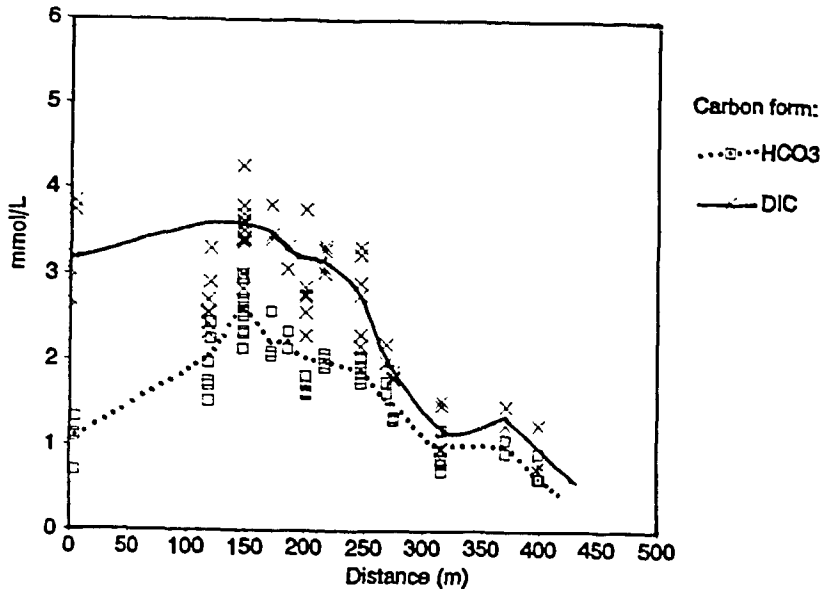

FIGURE 6.13 Inorganic carbon as DIC, and as HCO_3^-, as a function of distance from KD1 (units are mmol/L)

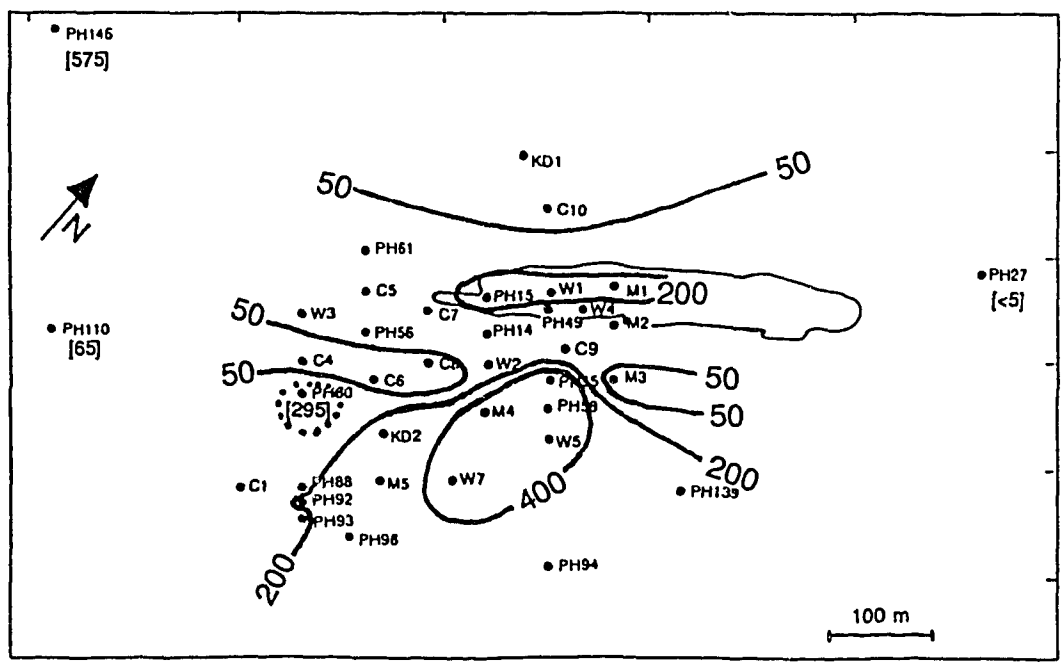

FIGURE 6.14 Phosphate in groundwater (µg/L) - contour plan. Contours in the vicinity of PH80 are uncertain.

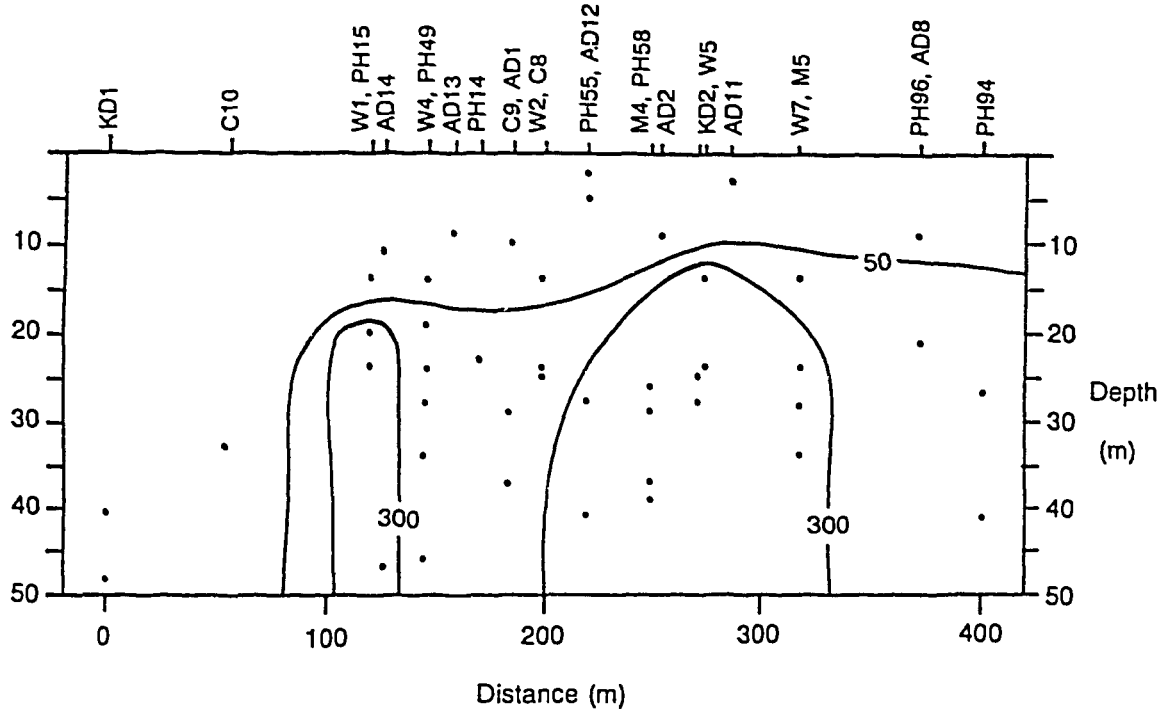

FIGURE 6.15 Phosphate in groundwater (µg/L) - projected cross-section

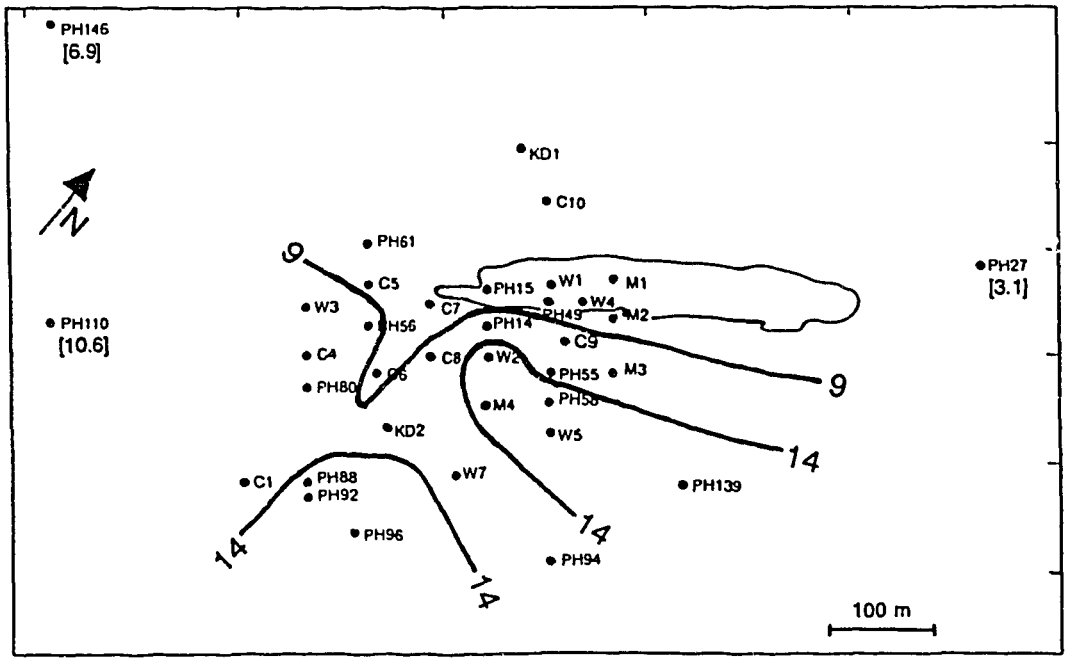

FIGURE 6.16 Silicon in groundwater (mg/L) - contour plan

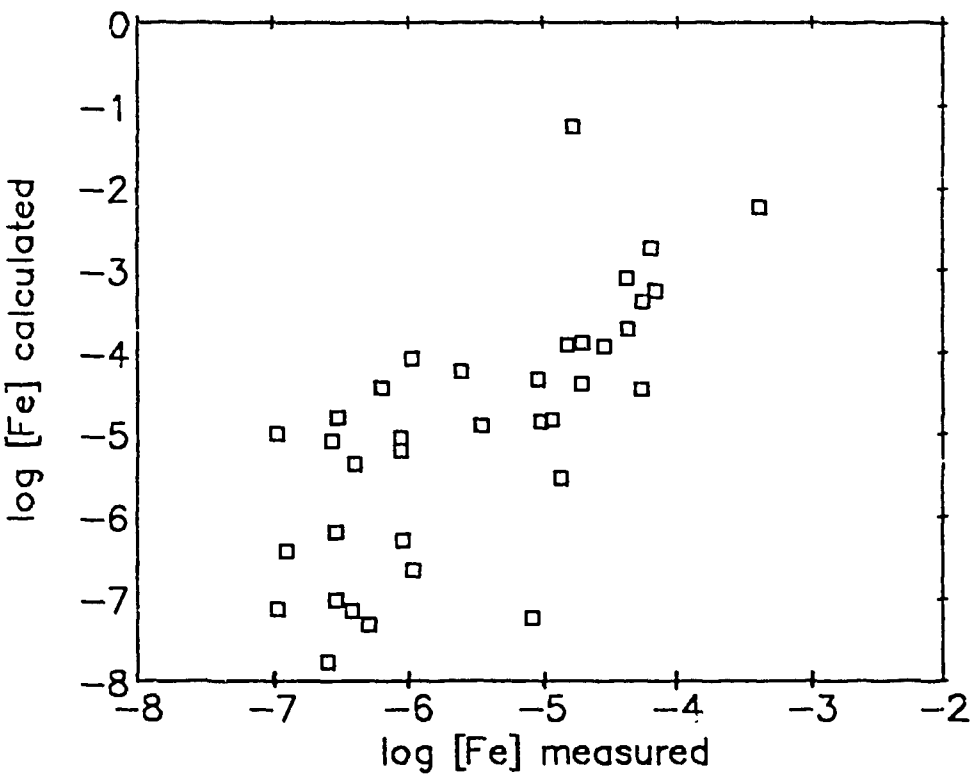

FIGURE 6.17 Relationship between total iron measured by ICP-AES and values calculated from the measured Eh and pH using MINTEQA2

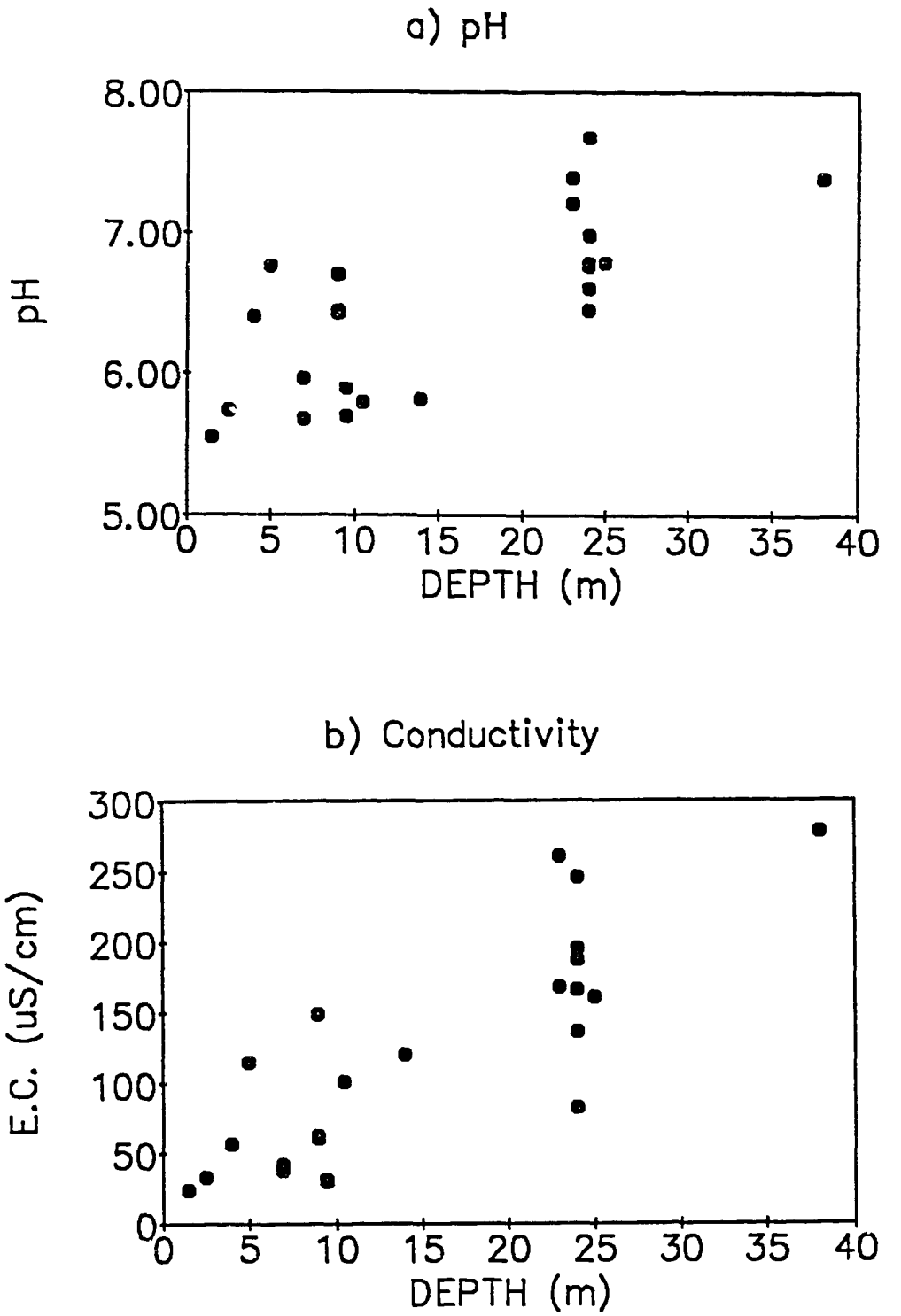

FIGURE 6.18 Depth dependence of major groundwater parameters - April 1991 field trip

a) pH
b) conductivity

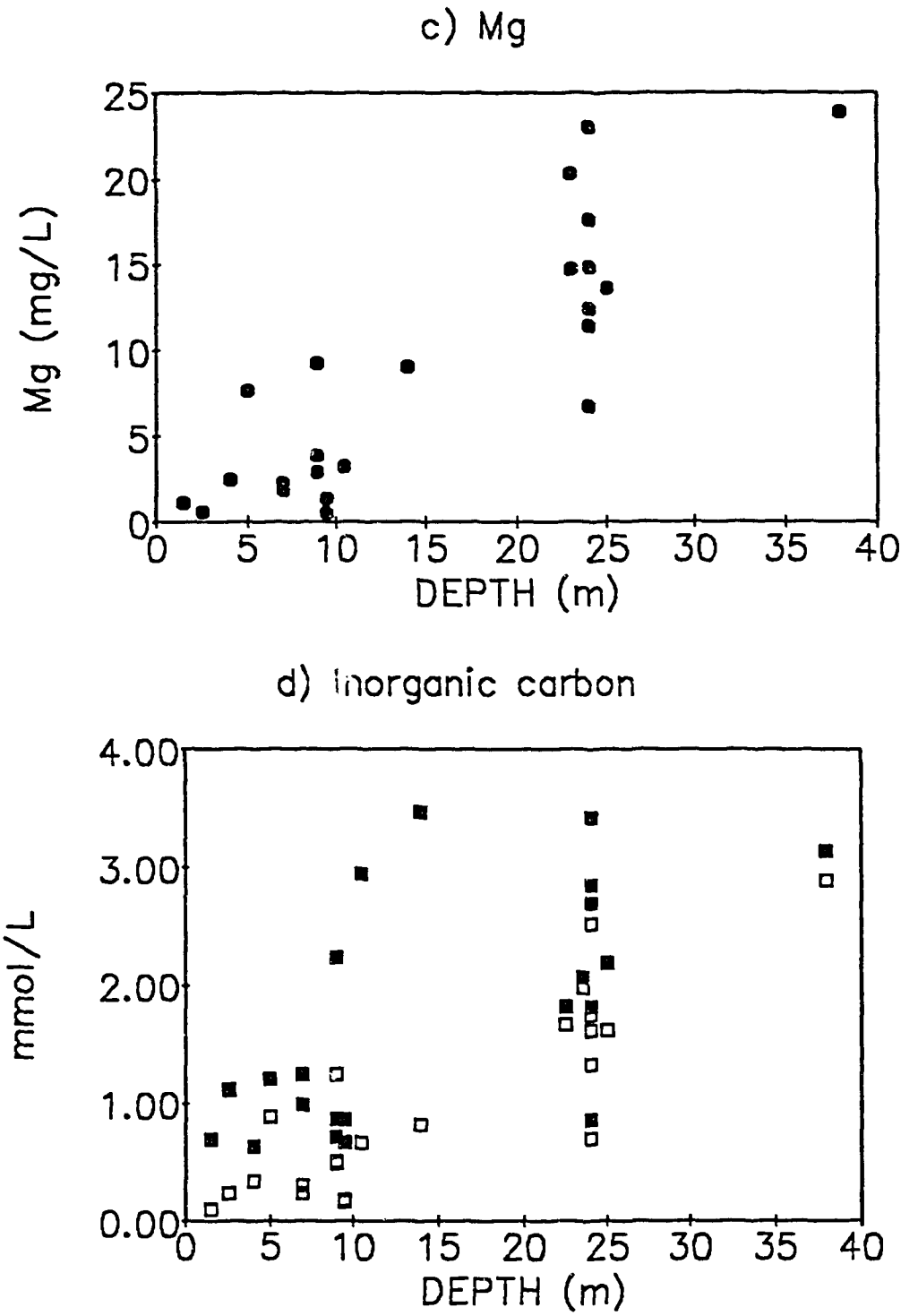

FIGURE 6.18 Depth dependence of major groundwater parameters - April 1991 field trip (continued)

c) magnesium

d) inorganic carbon as HCO_3^- and DIC (HCO_3 - open symbols, DIC - closed symbols)

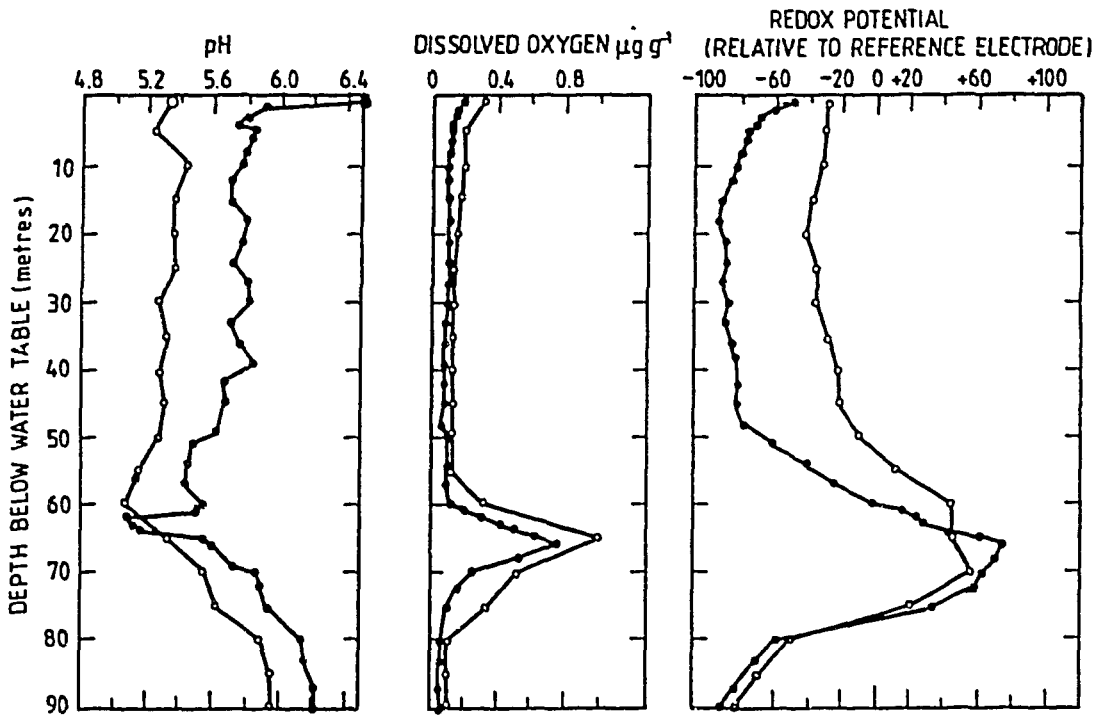

FIGURE 6.19 pH, dissolved oxygen and redox potential as a function of depth in KD1.
Closed symbols - before pumping
Open symbols - 5 days after pumping
Note: Potential of reference electrode is about +270 mV.

7 URANIUM SERIES ISOTOPES

7.1 Uranium-238

A large number of measurements of the groundwater concentrations of ^{238}U and its decay products have been made during the Alligator Rivers Analogue Project. Some data on ^{232}Th and ^{235}U, and the nuclides of their respective decay chains, have also been obtained. The radiochemical data for ^{238}U, and the isotopes of its decay series, are tabulated in Appendix 2.

The distribution of ^{238}U in Koongarra groundwaters from depths greater than 16 m (Figure 7.1) shows that ^{238}U concentrations are (not surprisingly) highest in the immediate vicinity of the orebody. In this zone, groundwater ^{238}U levels exceed 100 μg/L. The contour plan suggests that the extent of ^{238}U dispersion to the south (towards borehole PH80) is greater than the dispersion towards the south-east, in the direction of PH94. Groundwater from PH80, which is some 100 m from the recognised limits of the No.1 orebody, has ^{238}U concentrations of about 5 μg/L, which is significantly above background levels. In general, ^{238}U concentrations return to background levels much closer to the orebody in the direction perpendicular to the fault, towards PH94. This suggests the possibility of a significant component of groundwater movement away from the orebody towards PH80.

The boreholes at Koongarra can be arranged in approximate order of increasing distance from the fault, based on the east coordinate on the mine grid. This order approximates a groundwater flow line, assuming flow is towards the south or south-east. Groundwater uranium data for boreholes in the transect shown on Figure 2.2, and for depths greater than 12 m, are given in Table 7.1. A plot of ^{238}U concentrations in groundwater, as a function of distance from the 3000m E grid-line, can then be constructed (Figure 7.2). This figure shows a sharp increase in ^{238}U concentrations, up to four orders of magnitude above background levels, when moving groundwaters intersect the orebody. Moving further away from the fault, there is a gradual decrease to background levels. It appears that background uranium levels in this region are lower than in the Kombolgie sandstone, which may be attributed to the more strongly sorbing nature of the clay-rich weathered schists relative to the sandstone. The extent of elevated uranium concentrations in groundwater is greater than the extent of the economic ore-zone as defined for mining purposes, which extends over approximately 75 m. Considerable scatter is seen in the data, and this is attributed to the heterogeneous distribution of uranium in the system.

The projected cross section of the uranium dispersion (Figure 7.3) shows that high ^{238}U concentrations persist at depth near the primary orebody but seem to extend unevenly down-gradient in the weathered zone. Close to the surface, the uranium concentrations in the seasonal groundwaters sampled at the end of the wet season were relatively low.

7.2 Uranium-234 Concentrations and $^{234}U/^{238}U$ Activity Ratios

At secular equilibrium, the activities of ^{234}U and its precursor ^{238}U are equal, but it is common for natural groundwaters to have $^{234}U/^{238}U$ activity ratios considerably above 1.0. A number of mechanisms to explain this preferential mobilisation of ^{234}U have been suggested (Osmond et al., 1983), including:

a) lattice damage induced by radioactive decay,

b) location of daughter atoms in weakly bound or interstitial sites,

c) oxidation state change from +4 to +6 during decay, leading to enhanced solubility of the daughter, or

d) direct α-recoil from the solid into the aqueous phase.

The process of α-recoil results from a sudden movement of a daughter nucleus when an α-particle of several MeV energy is emitted. The distance through which the recoiling nucleus is displaced is approximately 20 nm (Sheng and Kuroda, 1986). If a ^{238}U atom near the surface of a mineral grain decays, emitting an α-particle, the daughter ^{234}Th nucleus could be recoiled into the surrounding groundwater. The ^{234}Th will probably rapidly adsorb to a mineral surface, where it is still accessible to the aqueous phase, or may remain in solution for the duration of its short (24 day) half-life. In either case, its subsequent decay to ^{234}U will lead to an excess of ^{234}U in the aqueous phase relative to ^{238}U.

Koongarra groundwaters are unusual in that the measured $^{234}U/^{238}U$ ratio is often below 1.0. This is generally considered to be distinctly anomalous (Osmond and Cowart, 1982). The projected cross section (Figure 7.4) shows that the measured $^{234}U/^{238}U$ ratios were below unity in groundwaters from the weathered zone. Extraordinarily low values, below 0.7, were found in groundwater samples from borehole W2.

Figure 7.5 shows the $^{234}U/^{238}U$ ratios in Koongarra groundwater samples plotted as a function of depth. On the basis of this figure, it is possible to divide the water samples into 3 depth ranges:

a) 0-20 m. Groundwaters from the weathered zone, with $^{234}U/^{238}U$ below 1.0.

b) 20-30 m. The transition zone, with a range of $^{234}U/^{238}U$ ratios.

c) > 30 m. Unweathered zone groundwaters with $^{234}U/^{238}U$ greater than unity.

In over 50 water samples analysed, there is only one borehole (PH88) which does not fit this pattern. The isotope data for PH88 are anomalous in several other respects and are discussed further below.

The data show that the main factor determining whether the $^{234}U/^{238}U$ ratio in these water samples exceeds unity is the depth from which the samples are obtained, with weathered zone conditions favouring preferential mobility of ^{238}U.

The apparently lower mobility of ^{234}U in the weathered zone has been attributed to α-recoil emplacement of daughter nuclides in inaccessible mineral phases, reducing their availability for leaching (Nightingale, 1988). Another possibility is that low activity ratios have developed near the surface of mineral phases due to a previous net loss of ^{234}U by alpha-recoil of its parent (^{234}Th) into solution (Osmond and Cowart, 1982). Sudden, rather than gradual shifts in conditions have then occurred, and the U at, or near, the boundary of the rock surface has been put into solution, causing an increase in U concentration and a decrease in activity ratio in solution.

There was a close correspondence between the $^{234}U/^{238}U$ ratio in the groundwater and the ratios in accessible phases of core samples, extracted from core samples under mild leaching conditions with the Tamm's Acid Oxalate (TAO) reagent (reported in Volume 8 of this series). The correspondence between groundwater $^{234}U/^{238}U$ ratios and those extracted with the TAO reagent suggests that groundwater values are derived from adsorbed uranium or readily soluble minerals.

Groundwater from borehole PH88, in the depth interval between 38 and 40 metres, consistently showed elevated uranium concentrations together with low isotope ratios. These were the only samples obtained from depths greater than 30 m which had a $^{234}U/^{238}U$ isotope ratio below unity. This may indicate a greater depth of weathering or fracturing at this location, and it is significant that tritium and ^{14}C data (of a PH88 sample from this depth) indicated the presence of modern water. A possible explanation for this data is that groundwater flows from the weathered zone of the secondary ore-body into this area, transporting uranium with a low $^{234}U/^{238}U$ ratio, but relatively high total uranium concentration, towards PH88. Therefore, the vicinity of this borehole could be an exit-point for water from the system. Such a scenario would also explain the relatively high U concentration (and low $^{234}U/^{238}U$) in groundwater from borehole PH80 (depth 17-20 m), which is nearby. However, in this latter case, samples could not be obtained from depths exceeding 20 m.

The generally low $^{234}U/^{238}U$ ratios in groundwaters of the weathered zone provide support for the "recoil emplacement" mechanism mentioned above, as they imply that ^{234}U is, compared to ^{238}U, relatively immobile. The fact that low $^{234}U/^{238}U$ ratios are generally confined to the weathered zone, which is intersected by the water table, can be explained by considering the likely outcome of an α-recoil process in saturated and unsaturated conditions. If an α-particle is emitted when the system is not saturated, the recoiling ^{234}Th nucleus is likely to travel through intervening pore space into a mineral phase before coming to rest. When the pore spaces are filled with water, the recoiling nucleus is more likely to come to rest in the aqueous phase. Therefore, immobilisation of ^{234}U by recoil emplacement is favoured in unsaturated conditions. This reasoning implies that $^{234}U/^{238}U$ ratios below unity are more likely to be found in near surface systems, intersected periodically by the

water table. Further discussion of the possible mechanisms giving rise to fractionation between ^{238}U and ^{234}U in the Koongarra system is contained in Volume 8 of this series.

7.3 Thorium Concentrations and $^{230}Th/^{234}U$ Activity Ratios

The question of thorium mobility is important for two reasons. These are:

a) thorium immobility is commonly assumed in modelling the Koongarra system, and

b) thorium is a chemical analogue of several components of HLW including Np(IV) and Pu(IV).

The measured $^{230}Th/^{234}U$ ratio in Koongarra groundwaters was below 0.022 in all samples (Table 7.2). In samples with significant uranium concentrations (>10 μg/L), this ratio was always below 0.001. This data substantiates the immobility of ^{230}Th, relative to ^{238}U, in the system.

The immobility of ^{230}Th can also be demonstrated by computing partition ratios (P), which are the ratio of the amount of ^{230}Th bound by the solid phase (g/g) to the concentration in the aqueous phase (g/mL). Partition ratios for ^{230}Th at Koongarra are usually of the order of 10^6 to 10^9 mL/g (Volume 8 of this series). These values are about three orders of magnitude higher than for ^{238}U and indicate that thorium is extremely immobile.

The data in Table 7.2 show that only very low levels of ^{232}Th were present in Koongarra groundwaters. This is because ^{232}Th is very insoluble, and has a relatively low specific activity. Therefore, it was not usually seen in alpha-spectra for Koongarra groundwater samples.

7.4 Radium-226 and Radon-222

Radium-226 is the product of the α-decay of ^{230}Th, and ^{222}Rn is the daughter of ^{226}Ra. Although ^{226}Ra and ^{222}Rn have relatively short half-lives (1600 years and 3.8 days, respectively), they may migrate in geological systems and therefore be out of equilibrium with their precursors.

The distributions of ^{226}Ra in cross-section and plan-view are shown in Figures 7.6 and 7.7. As with ^{238}U, ^{226}Ra concentrations are highest in the vicinity of the orebody and fall off rapidly in the direction of PH94 and W7. However, a lobe of elevated concentrations appears to extend to the south, towards PH80 and PH88. Figure 7.7 shows that ^{226}Ra levels tended to be greater in groundwaters from the unweathered zone than in the shallower weathered zone groundwaters. A similar trend also occurs in Figure 7.8, which shows $^{226}Ra/^{238}U$ ratios plotted as a function of depth. All samples from depths greater than 30 m have $^{226}Ra/^{238}U$ ratios which exceed unity. Therefore, in this zone, ^{226}Ra is more mobile than its precursor ^{238}U. As with the $^{234}U/^{238}U$ ratios, the pattern of $^{226}Ra/^{238}U$ ratios shows that distinctly

different geochemical conditions prevail in the unweathered zone compared to the unweathered zone. However, no general statement can be made about the values of $^{226}Ra/^{238}U$ ratios in the weathered zone, which cover a broad range.

The relative mobility of ^{226}Ra in the unweathered zone can be attributed to co-precipitation of radium from shallower, more oxidising groundwaters with iron and manganese oxides. Accumulations of radium are often found around mineral springs where Fe and Mn oxides precipitate (Dickson and Snelling, 1980). Another possible reason for the lower concentrations of ^{226}Ra in groundwaters of the weathered zone is radium adsorption by clay minerals. Radium appears to be relatively mobile in the more reducing conditions of deeper groundwaters. This is a contrast to the behaviour of uranium, which tends to be more mobile in oxidising conditions where the U^{6+} oxidation state is favoured. Significant levels of ^{226}Ra were present in groundwaters from KD1, which intersects the Kombolgie formation. These values could indicate radium mobility in the Kombolgie sandstone or, possibly, remnant pockets of uranium mineralisation.

Radon is a radioactive inert gas, and can arise in groundwater by decay of its precursors both in the groundwater, as well as on mineral surfaces and in the adjacent rock. The release of ^{222}Rn into groundwater from the contacting solid by diffusion can result in a large excess over its precursors. Some very high values of ^{222}Rn have been measured at Koongarra (Appendix 2).

High excess concentrations of ^{226}Ra and ^{222}Rn, relative to their parent ^{238}U, are often present in hot water springs, and, the activity of ^{222}Rn is generally higher than ^{226}Ra owing to the greater solubility and mobility of Rn in groundwater. As shown by the data in Appendix 2, ^{222}Rn is present at levels greatly in excess of those of ^{238}U and ^{226}Ra in Koongarra groundwaters.

The reported range of $^{222}Rn/^{226}Ra$ activity ratios in groundwaters is from 10^2 to 10^4 (Lee et al., 1979; Stenstrand et al., 1979; Strain et al., 1979; Asikainen and Kahlos, 1980; Hussain and Krishnaswami, 1980; Asikainen, 1981; King et al., 1982). The ratios obtained for Koongarra groundwaters (5×10^3 to about 10^6) are shifted towards higher values (Appendix 2). There may have been loss of ^{222}Rn during sampling, in which case the measured $^{222}Rn/^{226}Ra$ ratios are minimum values, and the true value would be even higher. Therefore, the excess of ^{222}Rn over ^{226}Ra in some Koongarra groundwater samples (up to a factor exceeding 10^5) is even greater than reported in the previous studies.

The $^{222}Rn/^{226}Ra$ activity ratios of the shallower groundwaters would be expected to be higher than those of deeper groundwaters, due to the mechanisms (noted above) of Ra adsorption on clay minerals, and the co-precipitation of Ra with Mn and Fe. In addition, the greater accessibility of the matrix to groundwater in the weathered zone would favour ^{222}Rn release into the groundwater. At the present time, the $^{222}Rn/^{226}Ra$ data is not conclusive, although, as previously commented, there is evidence that ^{226}Ra levels are lower in shallower groundwaters.

7.5 Lead-210

Lead-210 is produced, via a number of short-lived intermediates, from the decay of ^{222}Rn. High concentrations of ^{210}Pb were measured in groundwater samples from a number of Koongarra boreholes, particularly from the centre of the orebody (Appendix 2). While the measured activities of ^{210}Pb varied over several orders of magnitude, from <0.024 Bq/L to 99.9 Bq/L, the measured $^{210}Pb/^{222}Rn$ activity ratios only ranged from 14×10^{-5} to 158×10^{-5}. This shows that a major factor determining the activity of ^{210}Pb in these groundwaters is the level of its precursor ^{222}Rn, a result which is reasonable considering the short half-lives of the intermediate radionuclides in the decay chain.

The contours of ^{210}Pb activities (Figure 7.9) suggest an elongation of the radiochemical halo from the orebody in the direction of PH80, where the concentration of ^{210}Pb was significantly elevated. The PH88(38-40 m) sample, which was noted as showing an unexpectedly high $^{234}U/^{238}U$ activity ratio (Section 7.2), also showed an unusually high ^{210}Pb activity. This sample, and the sample from PH80, had the highest ^{210}Pb content obtained outside the zones of primary and secondary uranium mineralisation. Indeed, the ^{210}Pb activities at PH80 and PH88, were higher than groundwaters from PH55, which intersects the dispersion fan. These data indicate the possibility of groundwater flow towards PH80 and PH88 rather than towards PH55 (Figure 7.9).

A scavenging residence time (τ) for ^{210}Pb of 1 day was calculated from the $^{210}Pb/^{222}Rn$ activity ratio (R) for groundwaters at Gujarat, India (Hussain and Krishnaswami, 1980), using the equation:

$$\tau = 11061\ [R/(1-R)]$$

(11061 days is the mean lifetime of ^{210}Pb).

At Koongarra, ^{210}Pb a residence time of about 6 days can be calculated from the mean $^{210}Pb/^{222}Rn$ activity ratio (5.0×10^{-4}), although it is not known if the model is applicable to the Koongarra site. The longer residence time, and the higher relative levels, of ^{210}Pb suggest a slow adsorption reaction of ^{210}Pb to the solid phase, and the possible presence of a semi-stable form of ^{210}Pb in Koongarra groundwater.

7.6 Isotopes of the Uranium-235 Series

The ^{235}U-series has not been studied in detail, since its radionuclides are much less abundant than members of ^{238}U chain (due to the relatively low ratio of ^{235}U to ^{238}U). However, evidence for mobility of ^{227}Ac was obtained in colloid studies (Section 9). Of all the radionuclides studied, ^{227}Ac showed the most association with colloids. Actinium was considered to have a mobility intermediate between thorium and uranium. These results are interesting because americium and curium (which may be present in radioactive waste), share with actinium a trivalent oxidation state.

TABLE 7.1

URANIUM CONCENTRATIONS IN GROUNDWATER

(Boreholes in the transect on Figure 2.2 arranged in order of increasing distance from the fault - AD Holes excluded)

Borehole	Distance (m)[a]	[U] (ppb)	Depth (m)	Field Trip[b]
W6	-25	2.63	23-25	7
KD1	-2	4.60	40-42	1
KD1	-2	3.60	80-82	1
KD1	-2	0.52	40-42	2
KD1	-2	0.55	70-72	2
KD1	-2	3.43	65-76	5
C10	56	0.70	27-40	3
W1 a	117	2.51	13-15	4
W1 a	117	7.33	13-15	4
W1 b	117	38.60	23-25	4
W1 b	117	50.50	23-25	4
W1 a	117	4.64	13-15	5
W1 b	117	63.00	23-25	5
W1 a	117	8.83	13-15	6
W1 b	117	106.00	23-25	6
W1 a	117	7.76	13-15	7
W1 b	117	45.90	23-25	7
PH15	119	137.00	19-21	1
PH15	119	30.50	19-21	2
M1	124	128.00	24-26	3
M1	124	248.00	35-50	3
M1	124	109.00	46-48	3
M1	124	489.00	27-29	5
W4 b	147	393.00	23-25	3
W4 a	147	414.00	13-15	4
W4 a	147	439.00	13-15	4
W4 b	147	364.00	23-25	4
W4 b	147	318.00	23-25	4
W4 a	147	511.00	13-15	5
W4 b	147	389.00	23-25	5
W4 a	147	459.00	13-15	6
W4 b	147	355.00	23-25	6
W4 a	147	393.00	13-15	7

Borehole	Distance (m)[a]	[U] (ppb)	Depth (m)	Field Trip[b]
W4 b	147	287.00	23-25	7
PH49	147	265.00	28-30	1
PH49	147	93.90	28-30	2
PH49	147	127.00	44-46	2
PH49	147	107.00	27-29	3
PH49	147	71.20	33-35	3
PH49	147	108.00	25-27	4
PH49	147	131.00	45-47	4
PH49	147	118.00	18-20	5
M2	162	3.11	40-46	3
M2	162	7.35	37-39	4
M2	162	52.20	42-44	5
M2	162	36.10	36-40	7
PH14	171	52.30	20-26	1
PH14	171	15.60	20-26	2
PH14	171	46.60	20-26	3
C9	185	26.40	34-40	3
C9	185	57.20	28-30	5
W2 a	200	14.10	13-15	4
W2 b	200	71.20	23-25	4
W2 a	200	59.60	13-15	5
W2 b	200	95.50	23-25	5
W2 a	200	83.30	13-15	6
W2 b	200	107.00	23-25	6
W2 a	200	47.00	13-15	7
W2 b	200	67.30	23-25	7
C8	200	9.71	24-26	3
C8	200	2.27	38-40	3
M3	216	22.00	20-22	3
M3	216	28.80	26-28	3
M3	216	31.00	34-40	3
PH55	216	0.40	26-28	1
PH55	216	1.00	40-42	1
PH55	216	0.66	26-28	2
PH55	216	0.98	40-42	2
M4	246	4.08	34-40	3
M4	246	3.85	28-30	5
PH58	246	1.61	25-27	1
PH58	246	0.56	38-40	1

Borehole	Distance (m)[a]	[U] (ppb)	Depth (m)	Field Trip[b]
PH58	246	2.04	25-27	2
PH58	246	1.05	38-40	2
KD2	268	2.87	24-32	6
KD2	268	1.54	24-26	7
W5 a	274	0.38	13-15	4
W5 b	274	1.82	23-25	4
W5 a	274	0.22	13-15	5
W5 b	274	0.38	23-25	5
W5 a	274	0.63	13-15	6
W5 b	274	0.83	23-25	6
W5 a	274	1.37	13-15	7
W5 b	274	2.08	23-25	7
M5	315	3.72	27-29	6
M5	315	5.17	28-40	6
W7 a	315	0.13	13-15	4
W7 b	315	0.22	23-25	4
W7 a	315	5.40	13-15	5
W7 b	315	0.56	23-25	5
W7 a	315	1.30	13-15	6
W7 b	315	0.59	23-25	6
W7 a	315	1.18	13-15	7
W7 b	315	0.32	23-25	7
PH96	370	0.25	16-26	1
PH96	370	0.30	16-26	2
PH94	399	0.17	26-28	1
PH94	399	0.57	40-42	1
PH94	399	0.24	26-28	2
PH94	399	0.28	40-42	2

a Perpendicular distance from the 3000 m E line on the mine grid, in the direction moving away from the fault.

b Dates of field trips were as follows:

1. May 1988
2. November 1988
3. May 1989
4. October 1989
5. May 1990
6. November 1990
7. April 1991

TABLE 7.2

^{232}Th, ^{230}Th AND $^{230}Th/^{234}U$ IN KOONGARRA GROUNDWATERS

SAMPLES COLLECTED DURING NOVEMBER 1988 FIELD TRIP

(Errors in Brackets)

Hole	Depth (m)	^{232}Th (dpm/L)	^{230}Th (dpm/L)	^{234}U (dpm/L)	$^{230}Th/^{234}U$
PH14	20-26	0.0007(0.0010)	0.0014(0.0011)	11.6(0.5)	1.2×10^{-4}
PH15	19-21	0.0008(0.0010)	0.0034(0.0011)	22.5(0.7)	1.5×10^{-4}
PH49	28-30	0.0002(0.0016)	0.050(0.005)	76.5(2.2)	6.5×10^{-4}
PH49	44-46	<0.006	0.036(0.0006)	105(3)	3.4×10^{-4}
PH55	40-42	0.000(0.003)	0.001(0.005)	0.83(0.06)	$<7 \times 10^{-3}$
PH56	26-28	0.0009(0.0014)	<0.0017	4.93(0.16)	$<4 \times 10^{-4}$
PH61	43-45	0.0006(0.0015)	0.0024(0.0022)	1.63(0.08)	1.5×10^{-3}
PH88	38-40	<0.0009	0.0055(0.0017)	1.52(0.08)	3.6×10^{-3}
PH94	40-42	0.0015(0.0010)	0.0052(0.0012)	0.24(0.04)	2.2×10^{-2}
PH96	16-26	0.0018(0.0019)	0.0114(0.0025)	0.21(0.02)	5.5×10^{-2}

All measurements were corrected for detector backgrounds and chemical blanks.

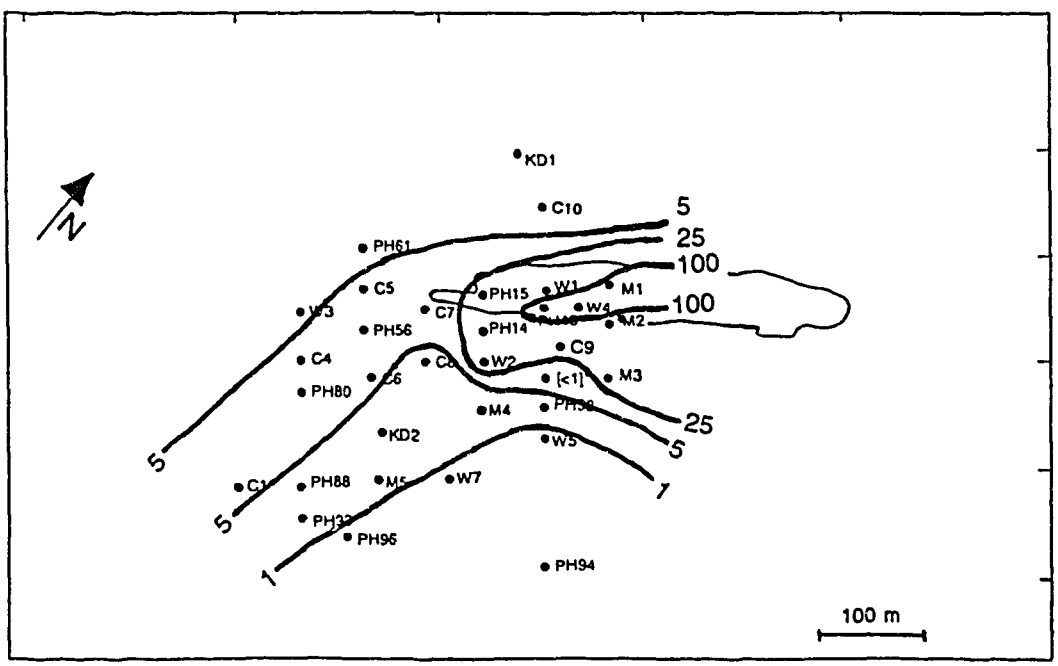

FIGURE 7.1 Uranium concentrations in groundwater (μg/L) - contour plan. The anomalously low value for PH55 (<1 μg/L) is shown. This point was excluded in drawing contour lines.

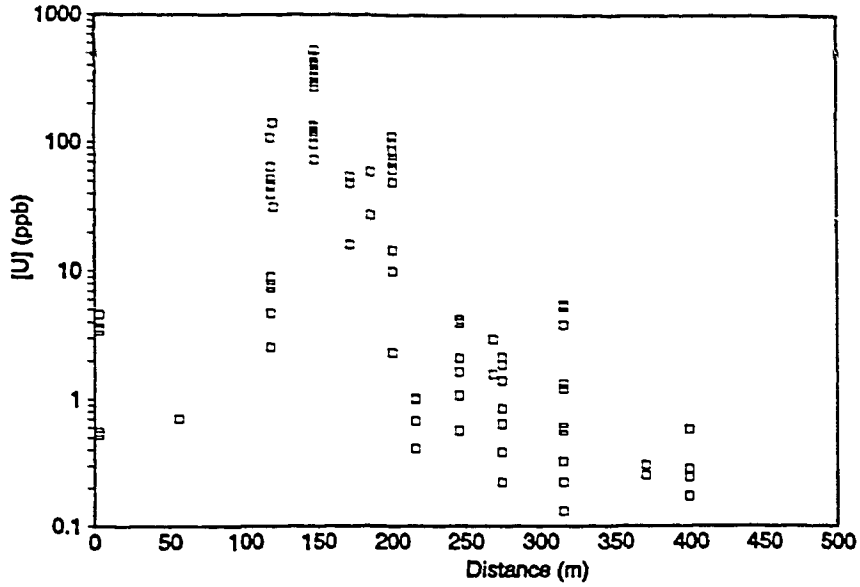

FIGURE 7.2 Uranium concentrations in groundwater as a function of distance from the 3000m E line on the mine grid

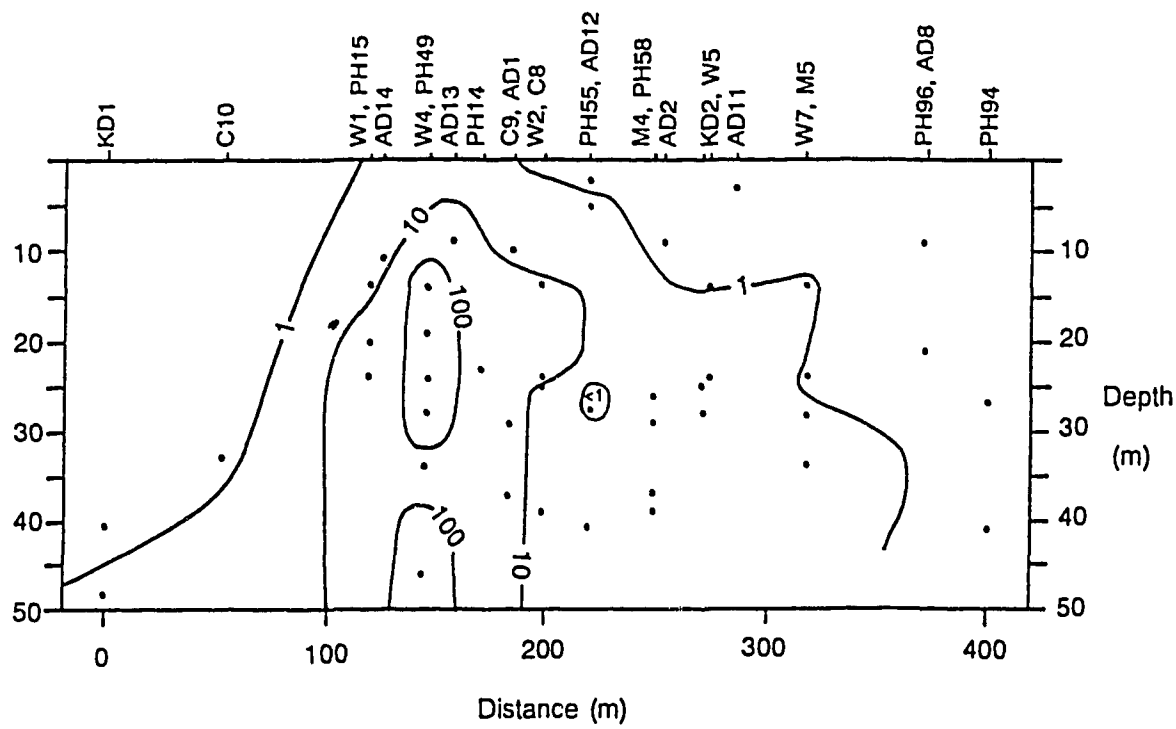

FIGURE 7.3 Uranium in groundwater (µg/L) - projected cross section

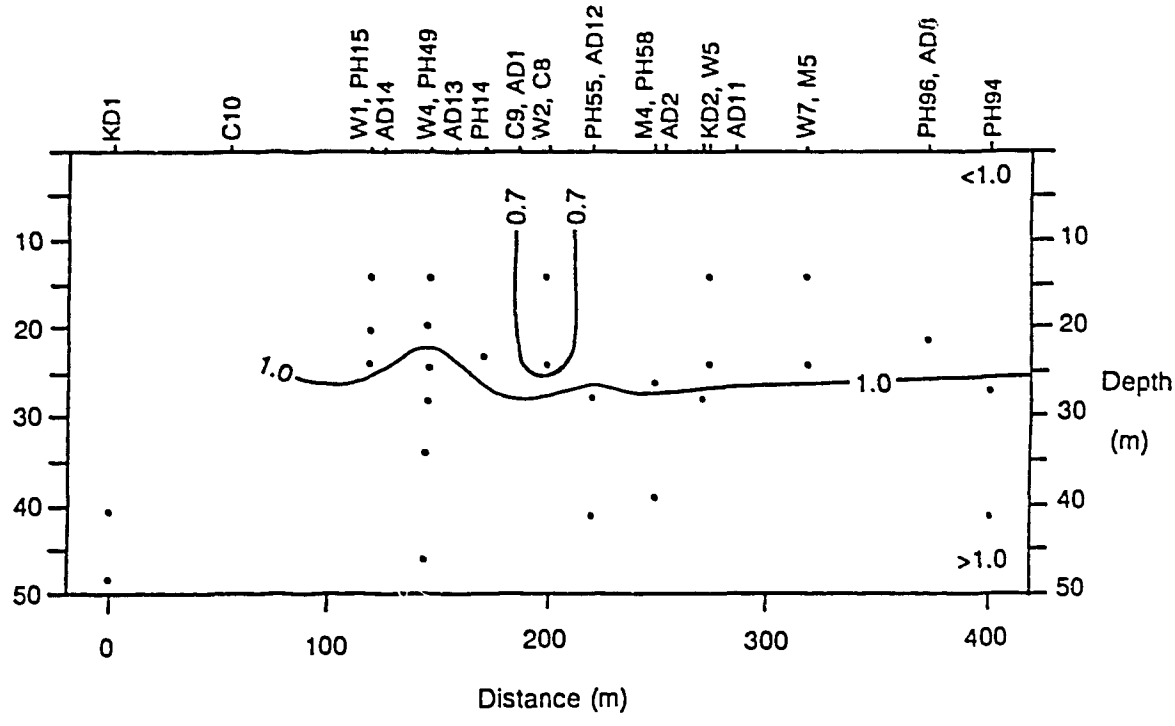

FIGURE 7.4 $^{234}U/^{238}U$ in groundwater - projected cross-section

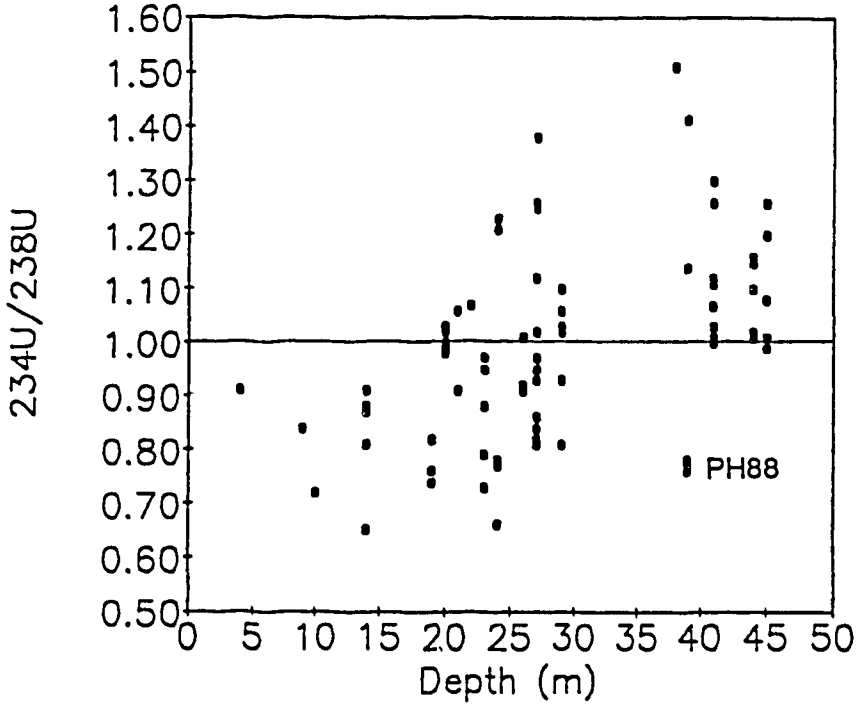

FIGURE 7.5 $^{234}U/^{238}U$ activity ratio in groundwater as a function of depth

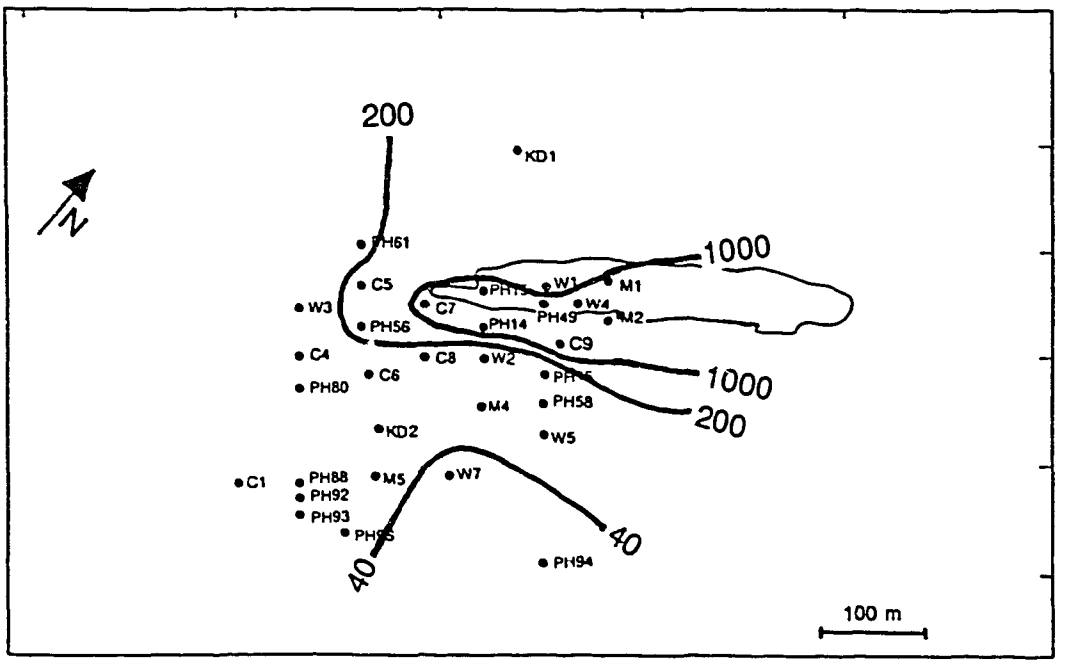

FIGURE 7.6 Radium-226 activities in groundwater (mBq/l) - contour plan

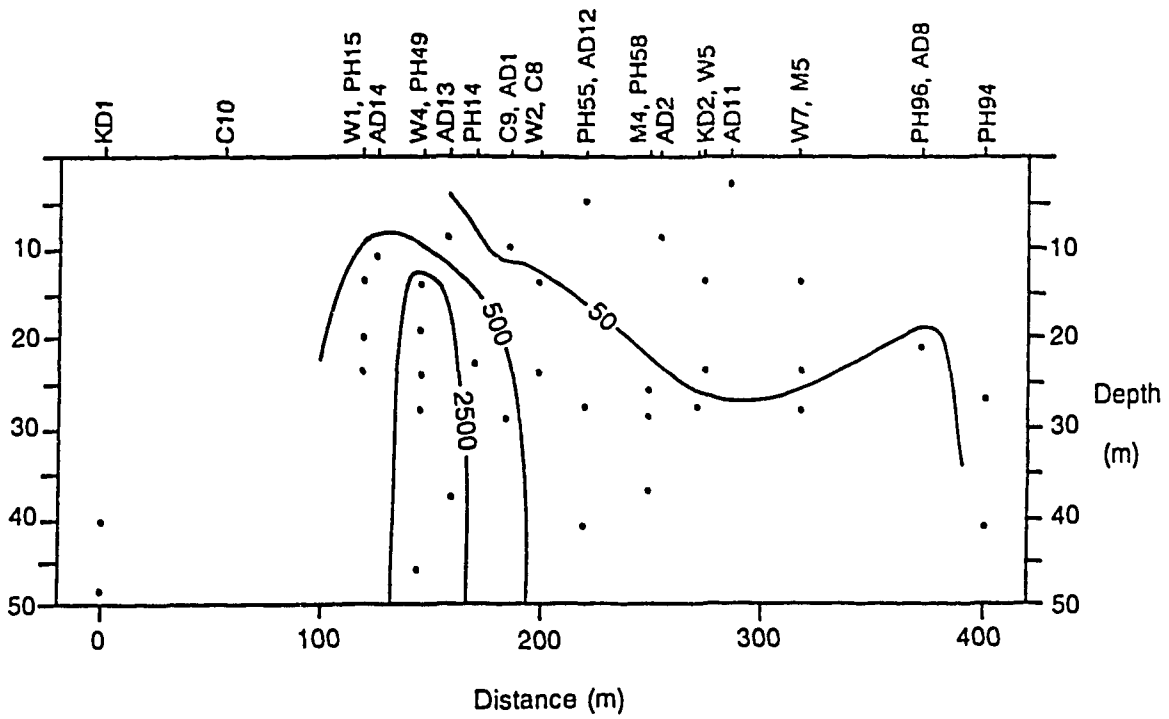

FIGURE 7.7 Radium-226 in groundwater (mBq/L) - projected cross-section

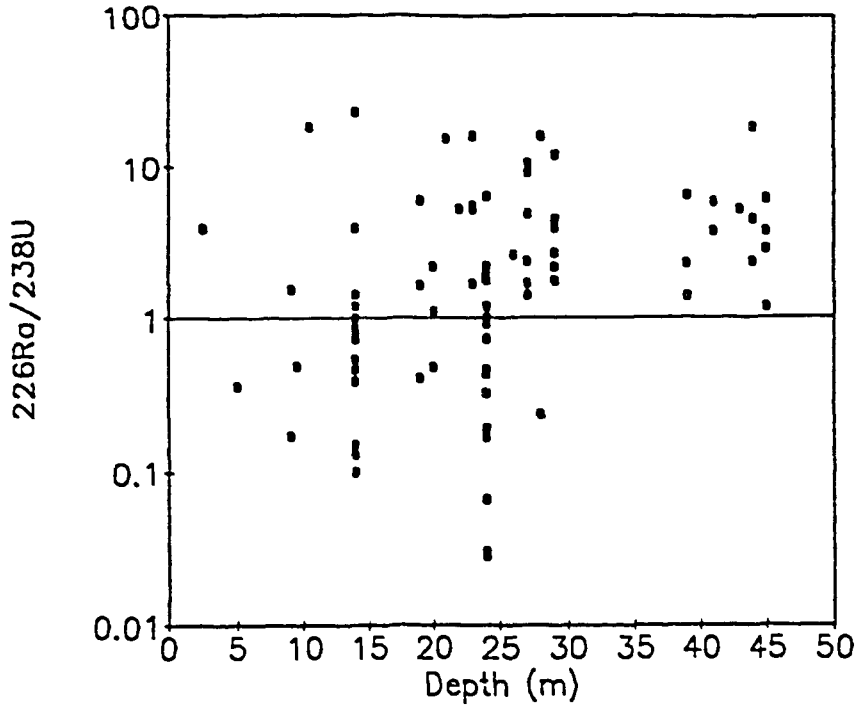

FIGURE 7.8 $^{226}Ra/^{238}U$ in groundwater as a function of depth

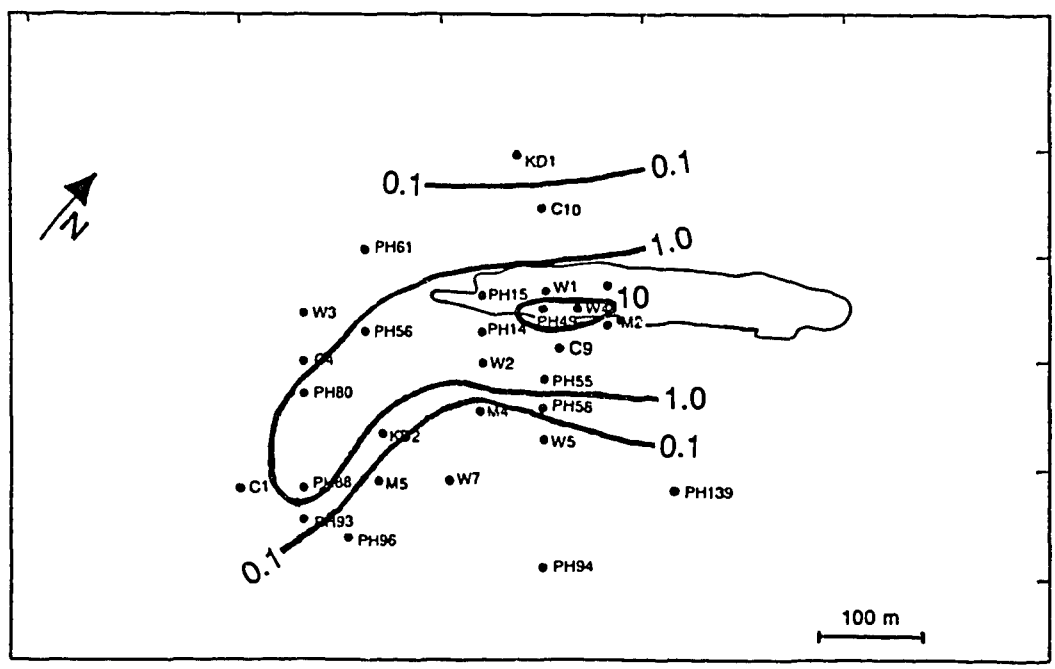

FIGURE 7.9 ^{210}Pb in groundwater (Bq/L) - contour plan

8 ENVIRONMENTAL ISOTOPES

8.1 Introduction

A large quantity of isotopic data has been obtained during the ARAP. This has provided information about the sources of groundwater in the system, and the mixing and dilution processes which occur down-gradient of the orebody. Concentrations of the following environmental isotopes have been determined:

- deuterium and ^{18}O,
- tritium, and
- carbon isotopes (^{14}C and ^{13}C).

Full tabulations of isotopic data are included in Appendix 2.

8.2 Carbonate Equilibria and Carbon Isotopes

The mineral-solution reactions that occur in the Koongarra groundwaters are induced, at least in part, by the action of dissolved CO_2 on carbonate or silicate minerals. One probable reaction is the CO_2-induced weathering of chlorite to kaolinite, according to Equation 6.1. Potential sources of CO_2 include :

a) Degradation of plant material, and root respiration, within the soil zone above the orebody, followed by downward percolation of CO_2-charged water.

b) CO_2 produced within the vicinity of the orebody from oxidation or bacterial degradation of sedimentary organic matter.

c) CO_2 present in up-gradient groundwaters, and carried into the zone of the orebody by lateral groundwater movement.

In general, sources of carbon in groundwaters can be identified by studying the concentrations of ^{13}C. These concentrations are reported relative to a marine carbonate reference material known as the PDB standard. The $\delta^{13}C$ of dissolved carbonate species in the ocean is about 0‰, and that of atmospheric CO_2 is about -7‰ (Drever, 1988). The ^{13}C method is particularly useful for distinguishing between carbon derived from organic matter and that derived from carbonate minerals. Typically, CO_2 derived from organic matter has a $\delta^{13}C$ of -30‰ to -20‰, whereas CO_2 derived from carbonate is about 0‰ (Drever, 1988).

Donnelly and Ferguson (1980) measured $\delta^{13}C$ in Koongarra graphite (range -20‰ to -14‰), vein carbonates (about -14‰ to -8‰) and bedded carbonates (about 0‰). There are other potential sources of ^{13}C in groundwaters, for example, biogenic CO_2 from the soil zone, with a $\delta^{13}C$ typically around -20‰. However, this latter source would be likely to contain significant levels of ^{14}C, whereas dissolution

of minerals such as graphite would release "dead carbon" containing very low levels of ^{14}C. Therefore, in principle, it would be possible to use ^{13}C and ^{14}C to determine the origin of the carbon contained in Koongarra groundwaters.

At Koongarra, groundwaters with the highest dissolved inorganic carbon (DIC) displayed the most negative $\delta^{13}C$ composition, of about -20‰. A plot of $\delta^{13}C$ versus the inverse of DIC (Figure 8.1) shows a range from -21‰ to -15‰. The $\delta^{13}C$ of plant material is close to the observed end-member DIC in Koongarra groundwaters, and it is therefore probable that the ultimate origin for the DIC is a biogenic material. The dissolution of carbonate minerals would tend to enrich the DIC in ^{13}C with increasing DIC, which is the opposite of that observed. Thus, on the basis of measured $\delta^{13}C$ values, carbonate minerals can be excluded as the source of the CO_2.

The radiocarbon (^{14}C) content of the dissolved inorganic carbon was measured in groundwaters from numerous boreholes at Koongarra (data tabulated in Appendix 2). The ^{14}C concentrations (expressed as percent modern carbon - PMC) ranged from 55% to >100%. Values greater than 100% indicate input of carbon from the post 1950s, when atmospheric weapons testing resulted in atmospheric CO_2 reaching values of about 200% in the southern hemisphere.

The proportion of radiocarbon in the groundwaters tended to increase along a transect from north to south, moving away from the 3000m E grid-line (this transect is described in section 6.1). Figure 8.2 shows that relative ^{14}C activities are lowest in groundwater samples from the vicinity of the primary uranium mineralisation, a result which is also seen in the contour plan of the ^{14}C data (Figure 8.3). The ^{14}C values generally increase towards 100% modern carbon in the direction moving away from the fault. Whilst Figures 8.2 and 8.3 clearly establish the presence of groundwaters with a low proportion of ^{14}C close to the orebody, only two boreholes (C10 and KD1) have been drilled to the north of the orebody. For this reason, interpretation of the ^{14}C data in this vicinity is somewhat speculative.

The ^{14}C data, taken at face value, give apparent "ages" of between zero and 8000 years for the groundwaters, with the age decreasing with increasing distance from the Koongarra fault. However, this simple interpretation of ^{14}C indicating a groundwater age is not appropriate for the Koongarra system where mixing and input of "dead" carbon are major considerations.

The uncertainties associated with the ^{14}C measurements preclude a conclusion of a smooth gradation of ^{14}C content along the transect, although there is sufficient evidence to say that those waters down-gradient appear to have more ^{14}C (which translates to younger ^{14}C "age") than those groundwaters in the up-gradient regions and in the ore-zones. Up-gradient and within the orebody, there appears to be input of "old" CO_2 (that is, depleted in ^{14}C), leading to groundwaters with a high $p(CO_2)$, but a relatively low proportion of ^{14}C. The ^{13}C values are quite negative for these high DIC waters (Figure 8.1).

It should be noted that radiocarbon is an indication of mean residence time of dissolved inorganic carbon (DIC) within the system. Water residence time can only be inferred if the appropriate corrections are applied for possible reactions with ^{14}C-free carbonate within the aquifer matrix, or oxidation of old organic carbon. In either case, there would be an apparent older ^{14}C "age" for the carbon, and by inference, the water. The former case has already been excluded on account of the measured ^{13}C content of DIC.

A possible origin for CO_2 could be bacterial oxidation of a "dead" carbon source, such as the abundant graphite or trace organic materials in the Cahill formation, which would be relatively depleted in ^{13}C but have little or no ^{14}C. This process would require the presence of sufficient amounts of bacteria in Koongarra groundwaters. There have been previous reports of in-situ degradation of carbonaceous material within aquifers (Chapelle et al., 1988; Grossman et al., 1989). If this occurs at Koongarra, then the "ages" as calculated are much older than the true ages, and ^{13}C data cannot be used to correct for "dead" CO_2 derived from graphite.

Another process which could release CO_2 with the measured ^{13}C and ^{14}C content is the oxidation of graphite by oxygen-carrying groundwater. There is some dissolved oxygen in groundwaters in the Kombolgie (Section 6.13.1). However, the D.O. content of the groundwaters sampled from borehole KD1 was less than 1 mg/L and this probably could not produce the amount of CO_2 observed, unless the system is was open to an oxygen source such as the atmosphere. However, if the system was open to the atmosphere, the ^{14}C content would increase to "modern" values. Therefore, this scenario can be considered unlikely to play a dominant role.

A more plausible scenario is that the CO_2 is transported into the Cahill formation, dissolved in the groundwaters from the Kombolgie. This scenario would require groundwater flow across the fault. Groundwaters from KD1 (in the Kombolgie sandstone) have high $p(CO_2)$ values, relatively high DIC (Section 6.6), and a ^{13}C of around -20‰. In addition, some groundwater samples obtained from KD1 had quite low levels of ^{14}C. A sample obtained during the May 1988 field trip from 80-82 m depth had a value of 82.9% modern carbon, but a KD1 sample analysed during the previous USNRC-sponsored investigation at Koongarra yielded a value of 63.8%, which is amongst the lowest reported for a Koongarra water sample. Whilst this latter sample was obtained without packers, so its depth of origin is unknown, a reasonable interpretation of the data is that the fractures in the Kombolgie sandstone contain groundwaters with different ^{14}C contents, some of which are quite low. The total DIC in KD1 samples is amongst the highest in Koongarra groundwaters (mostly being $H_2CO_3^*$, rather than HCO_3^-), therefore the input of CO_2 into the system across the fault from the Kombolgie cannot be excluded. The low PMC value (54.5%) of groundwaters from borehole C10 (which is between KD1 and the orebody) also supports the possibility that groundwaters with low proportions ^{14}C may enter the orebody from its northern side. However, as noted above, there are insufficient sampling points in this vicinity to allow a definite conclusion on this point.

It appears that there is a correlation between PMC and HCO_3^- concentration (Figure 8.4), with the PMC increasing with decreasing HCO_3^-, especially in the concentration range 1.5 to 3 meq/L. This observed trend in ^{14}C could result from mixing of two end-member waters that have undergone different types of water-rock interaction, rather than representing a real age of the flow system.

It was shown in Section 6.6 that partial pressures of CO_2 in Koongarra groundwaters exceed equilibrium with the atmosphere, with a general decrease moving down-gradient, away from the fault. The proportion of $CO_2(aq)$ contributing to DIC also decreases along the inferred flow path from 40% to 10%. The decrease in the observed ratio of $CO_2(aq)/HCO_3$ is accompanied by an increase in ^{13}C, due to the approximately 8‰ fractionation between dissolved CO_2 and HCO_3^- (Figure 8.5). The apparent loss of CO_2 may be caused by a number of possibilities which include:

- consumption during weathering of silicate minerals,
- degassing due to depressurisation, or
- simple mixing between two end-members having different $p(CO_2)$ and isotopic compositions.

The ^{14}C data for W-series wells (Appendix 2) tended to display younger ^{14}C "ages" at shallow (13-15 m) depths, compared to the deeper (23-25 m) sampling points. Whilst not conclusive, this may suggest a different origin of groundwaters at the two depths. The PH88 bore (38-40 m) recorded PMC values of 100% indicating recharge of essentially new water. It has already been commented (Chapter 7) that at this depth this borehole has an unusually low $^{234}U/^{238}U$ ratio, and an anomalous ^{210}Pb content. The young ^{14}C age suggests that this area of the site could be an exit point for recently recharged water from the system.

8.3 Deuterium and Oxygen-18

The stable isotopic composition of groundwaters (δ^2H and $\delta^{18}O$) is governed largely by the source of recharge water (principally rainfall), with slight modification of that signature by evaporation within the soil zone. The values of ^2H and ^{18}O are usually reported relative to standard mean ocean water (SMOW). Although the mean annual isotopic composition of rainfall at a given location is relatively constant, the variations from one event to another can be very great.

There is a large range of monthly values for the isotopic composition of precipitation at Darwin, with the deuterium composition ranging over 100‰ and the oxygen-18 composition varying by over 12‰ (Figure 8.6). The data plot on, or near, the world meteoric water line. A plot of deuterium versus amount of rainfall (Figure 8.7) shows that the heaviest rains tend to be more depleted in deuterium. As well as this tendency towards lighter values for larger rainfall events, rainfall is generally more depleted in deuterium at the end of the wet season. The running weighted mean isotopic composition for Darwin is : δ^2H= -29.7‰; $\delta^{18}O$= -5.04‰.

Koongarra is located about 50 km inland, at about 25-45 m above sea level. It is possible that these factors may modify the isotopic signature of rainfall relative to that measured at Darwin, which is at sea-level and on the coast. The stable isotopes of groundwater at Koongarra generally plot close to the meteoric water line (Figure 8.8), but tend to be lighter than the running mean of precipitation at Darwin. This may be because rainfall at Koongarra is lighter than mean Darwin precipitation, although insufficient rainfall data is available. Alternatively, recharge may predominantly occur during significant rain events, or towards the end of the wet season, both of which tend to have the most depleted isotopic compositions. It is also possible that the isotopic composition of the groundwaters represents a past climatic regime when the isotopic composition of rainfall tended to be more negative than it is at present.

As discussed in Section 6.4, groundwaters within the orebody tended to have the highest Mg concentrations. This is reflected by a transect of conductivity (Figure 8.9a), which is effectively dominated by Mg^{2+} and HCO_3^-. The values of δ^2H, plotted on the same transect, show that groundwaters within and up-gradient of the orebody have a lighter isotopic composition than those down-gradient of the orebody (Figure 8.9b). In these transects, the origin of distance, and the distance scale, are as shown in Figure 2.2.

If δ^2H and conductivity are plotted against one another, deuterium appears to be related to conductivity (Figure 8.10), with δ^2H values tending to be more negative at higher conductivity. This is not the result of evaporation (which would tend to enrich the water in heavy isotopes and dissolved solids), and there is no obvious trend away from the meteoric water line (Figure 8.8).

Water from KD1 displays a similar isotopic composition to waters just across the fault zone, which suggests hydraulic connectivity across the fault. The Kombolgie waters are much lower in dissolved solutes, which indicates that most of the weathering takes place on the south side of the fault zone. There is no indication that the oxygen isotopes have been modified by hydration reactions involving Mg-silicates. Therefore, only a small proportion of water molecules take part in the chemical weathering reactions.

Down-gradient of the orebody, the correlation between δ^2H and conductivity suggests gradual mixing of two groundwater types. One of these is enriched in Mg and relatively depleted in deuterium, the other is "heavier" and carries less Mg. There appears to be a continuum of mixing between the two "end-members". It should be emphasised that the range of δ^2H values at Koongarra (from approximately -25‰ to -40‰) is not great, compared, for example, to Darwin rainfall, which extends from about +20‰ to -70‰, as shown in Figure 8.6. Therefore, while trends in the data are apparent, the interpretation is somewhat speculative. Nonetheless, the precision of the measurement of δ^2H (1‰) is substantially less than the scatter in the data.

One scenario which explains the data is shown by the numbered arrows on Figure 8.10. The groundwaters in the Kombolgie (KD1) plot in a field of negative δ^2H

values and relatively low conductivity. Moving across the fault to the primary ore zone, the conductivity increases but the δ^2H composition is basically unchanged (transition 1). As noted above, the similar δ^2H composition of waters from KD1 and from the primary ore zone provides evidence for some water movement across the fault. Alternatively, the KD1 water may be unrelated to the orebody and the similarity in δ^2H values could be merely coincidental.

Regardless of the interpretation of the KD1 data (and of the issue of groundwater moving across the fault), it is possible to be more certain about the trends moving down-gradient from the ore-zones. In this direction, there appears to be gradual mixing with groundwaters which are more dilute (ie lower conductivity) and are less depleted in deuterium. Therefore, there is a trend towards less negative δ^2H values and lower conductivity (transition 2 on Figure 8.10). The groundwaters appear to move towards the position of rain and creek water on Figure 8.10. However, too much should not be made of these two points because of the variability in rainfall isotopic composition as shown in Figure 8.8. It is more significant that trend-line (2) in Figure 8.10 also moves towards the weighted average mean of Darwin rainfall. Thus, there are several lines of evidence which tend to point towards a gradual mixing with, and dilution with local recharge water moving down-gradient.

The δ^2H data for the shallow AD-holes (tabulated in Appendix 2) generally reflect the trends in the deeper samples from the W, C, PH and M holes. Samples from close to the fault exhibited more negative δ^2H values, with a slight increase moving away from the fault. However, on the basis of the limited data available, it could also be argued that the δ^2H data for AD-samples are related to depth. The small number of samples, and the various depths from which samples were obtained make this data-set inadequate to provide further information about the system.

8.4 Tritium

Generally, tritium can be used to indicate the presence of young groundwaters (less than 30 years). In low and middle latitudes, groundwaters having more than about 1 tritium unit (TU) fall into this category (IAEA, 1983).

Measured tritium values were generally low throughout the Koongarra system, indicating residence times of at least some decades. Significant tritium levels (> 1.0 TU) were generally restricted to the AD-holes and the shallower depths of the W-holes. A limitation in interpreting the tritium data is that there is a significant error in the measurement (0.3 TU). However, near the centre of the orebody, where weathering is somewhat deeper there seemed to be deeper penetration of tritium (Figure 8.11). An interesting feature of the data was the presence of elevated levels of tritium at substantial depths (over 20 m) in groundwater from boreholes PH94, PH88 and possibly W7. These boreholes are some distance down-gradient, and this data could indicate the presence of fractures extending to some depth. This is particularly so for PH88, where the anomalous tritium data is concordant with anomalous values for several other isotopes.

8.5 Conclusions

A possible source of water entering the ore-body is groundwater flow from the sandstones of the Kombolgie formation. This formation is heavily fractured and water may travel through the fractures and move across the Koongarra fault into the Cahill formation, which hosts the uranium deposit. Evidence for conduits for water across the fault lies in the similar isotopic composition of water molecules (δ^2H values) of Kombolgie groundwaters and those of groundwaters from the mineralised zones.

Dissolved carbon dioxide is an important agent of weathering in the immediate vicinity of the orebody. There is evidence that this CO_2 enters the system dissolved in groundwaters moving across the fault from the Kombolgie, with a high DIC content (consisting largely of $H_2CO_3^*$), but quite negative $\delta^{13}C$ composition and depleted in ^{14}C. Alternatively, the ^{14}C and ^{13}C values in the groundwaters are consistent with bacterial degradation of a carbon-containing material, such as graphite, which is dispersed throughout the area of the deposit. In either case, the proportion of ^{14}C in dissolved inorganic carbon (DIC) in groundwaters from the immediate vicinity of the ore-body would be comparatively low, as is observed.

Down-gradient of the orebody, the groundwaters become more dilute, and the δ^2H composition of the water molecules becomes less negative and tends to approach average values of rainwaters and surface waters. The proportion of radiocarbon in increases. Tritium is present in some shallower groundwaters. These phenomena appear to be adequately explained by a gradual mixing with local recharge as groundwaters move down-gradient.

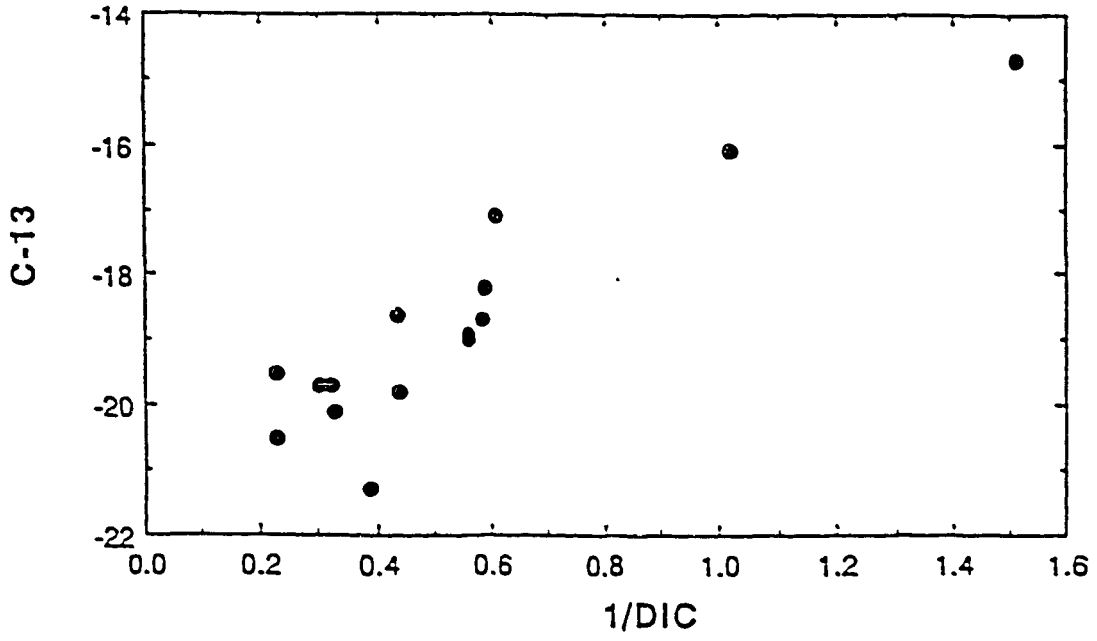

FIGURE 8.1 $\delta^{13}C$ concentrations of groundwaters versus the inverse of DIC

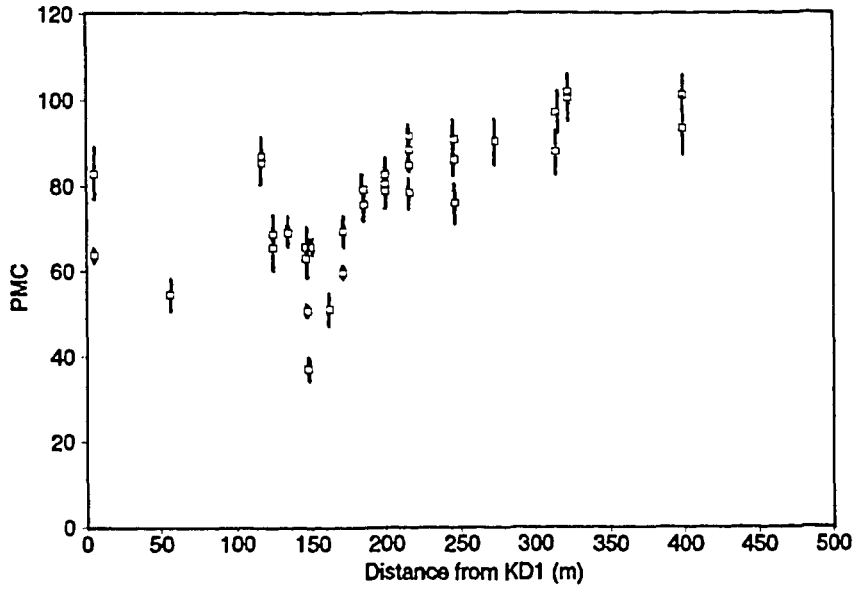

FIGURE 8.2 Transect of ^{14}C expressed as percent modern carbon (PMC)

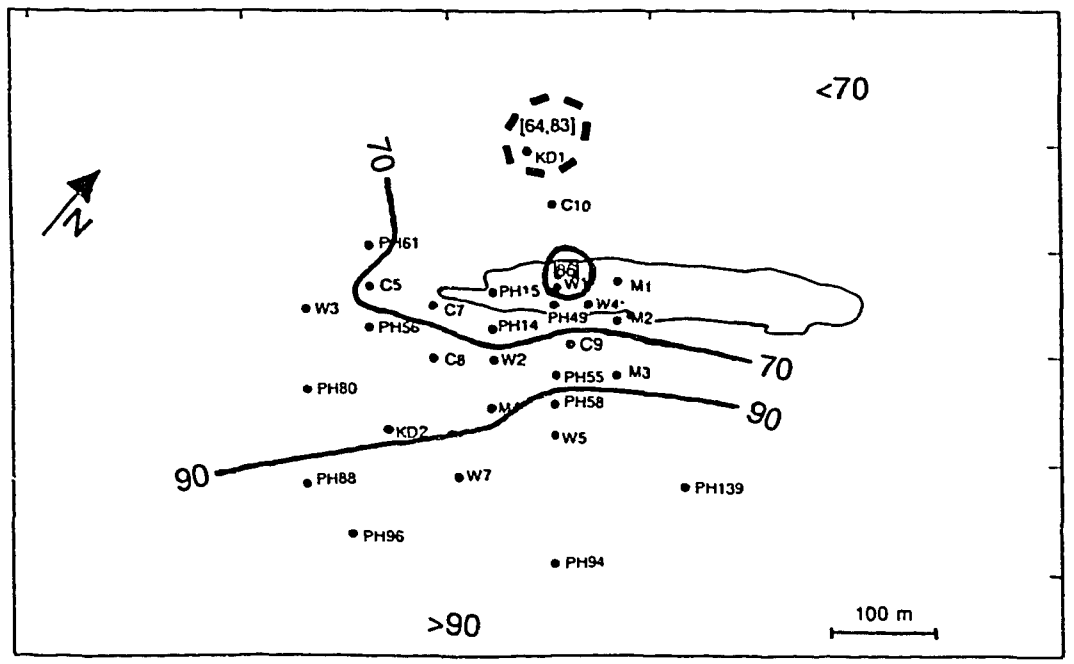

FIGURE 8.3 Contour plan of ^{14}C expressed as PMC. The contours to the north of the orebody (boreholes W1, C10 and KD1) are uncertain

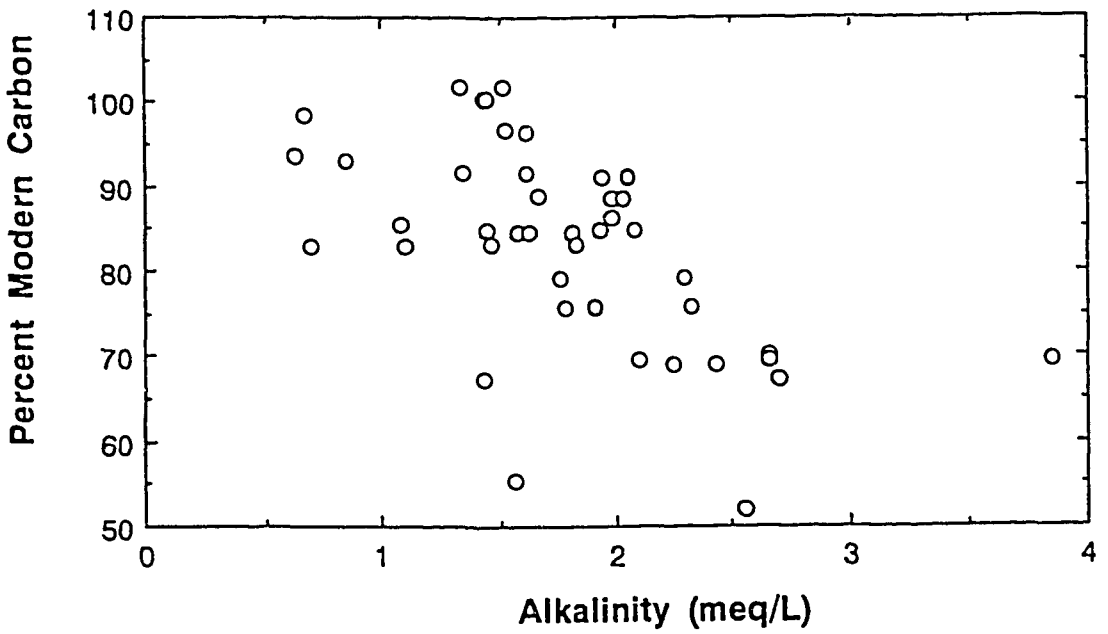

FIGURE 8.4 Radiocarbon (PMC) versus alkalinity for Koongarra groundwaters

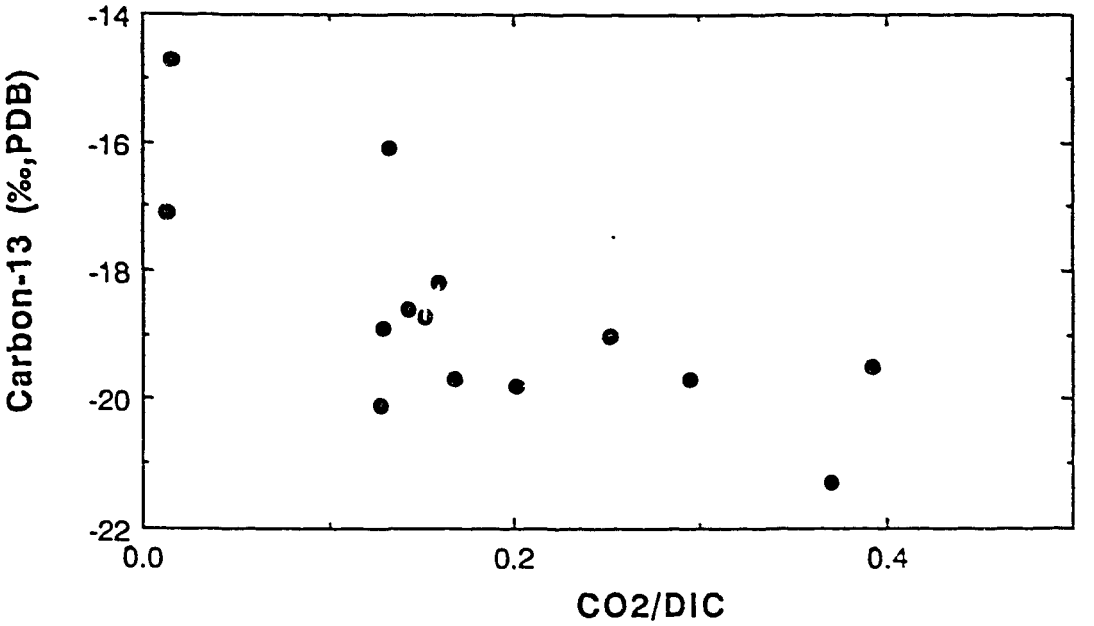

FIGURE 8.5 $\delta^{13}C$ concentration of groundwaters versus $CO_2(aq)/DIC$

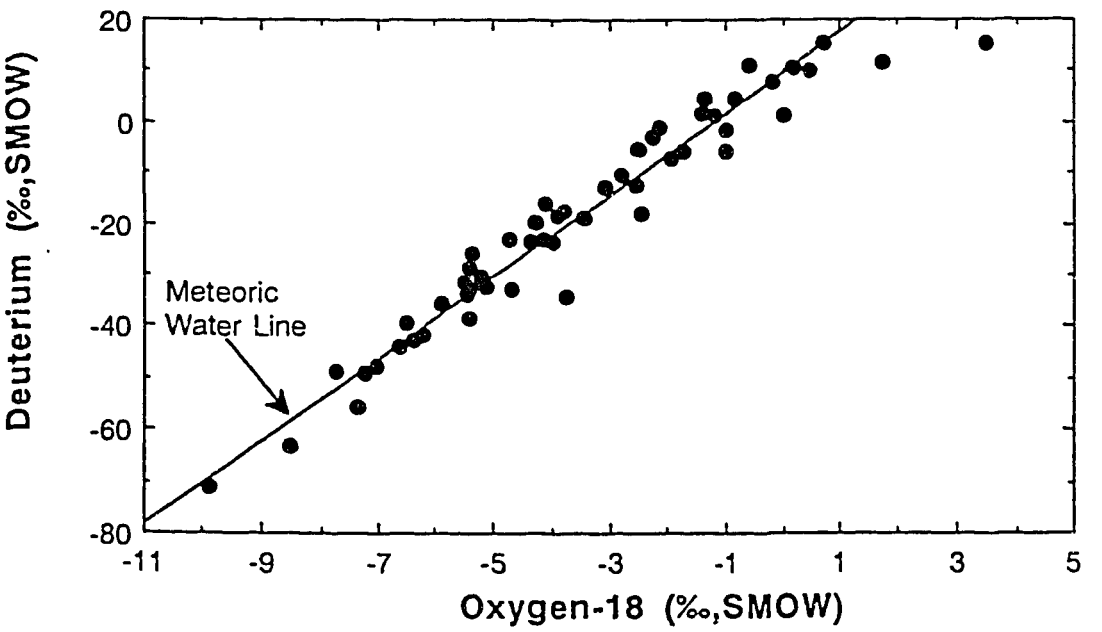

FIGURE 8.6 Variation of the isotopic composition of mean monthly rainfall at Darwin (1963-1987)

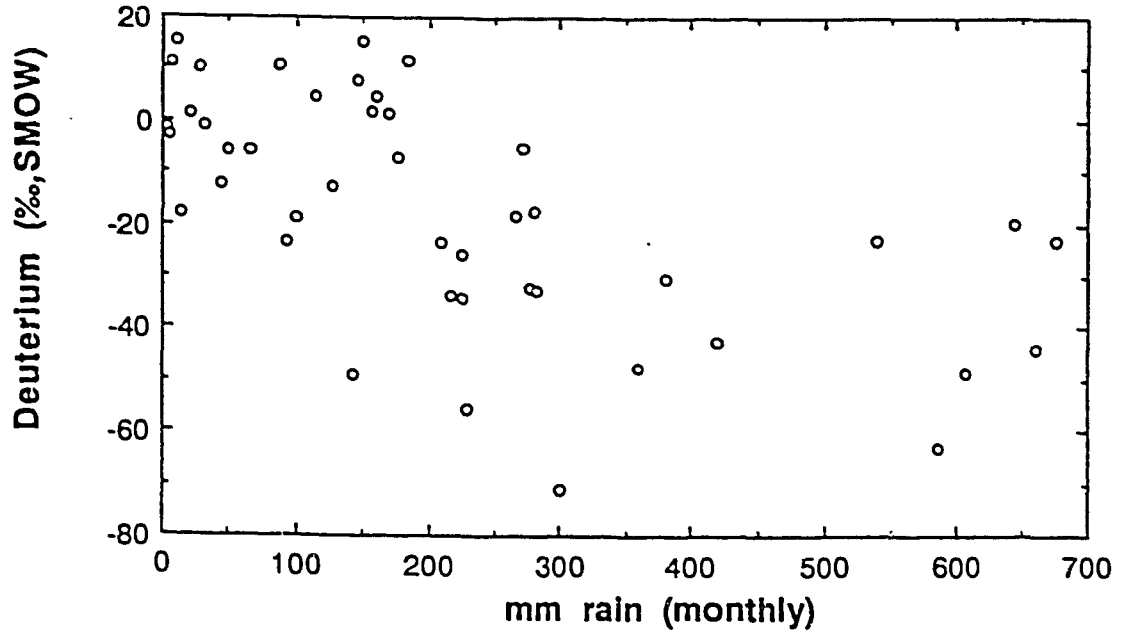

FIGURE 8.7 δ^2H composition of mean monthly rainfall as a function of rainfall amount

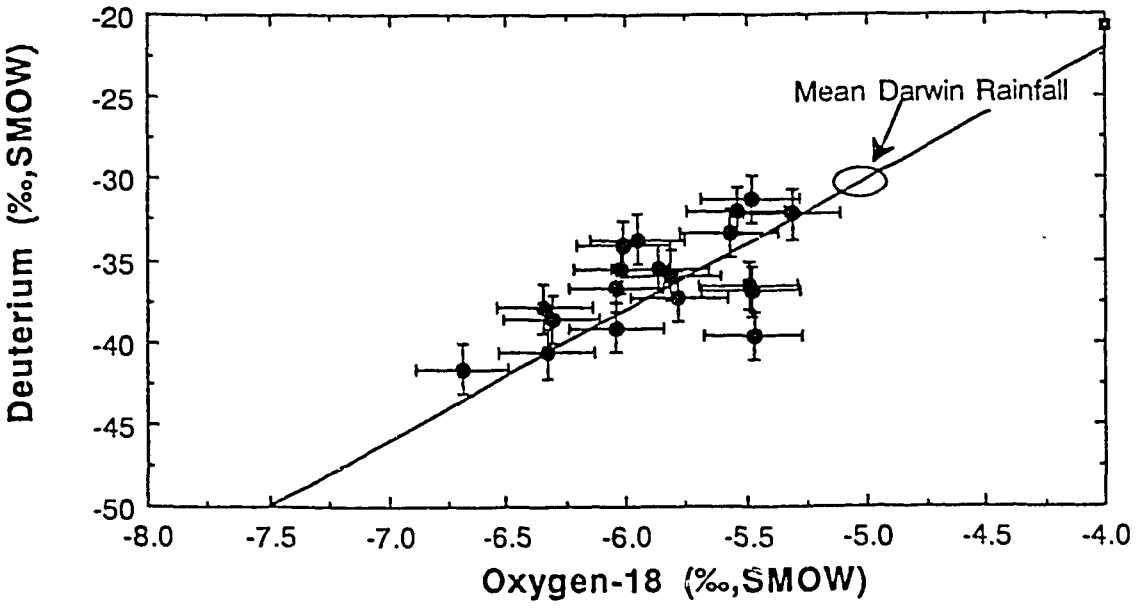

FIGURE 8.8 Deuterium and ^{18}O composition of Koongarra groundwaters

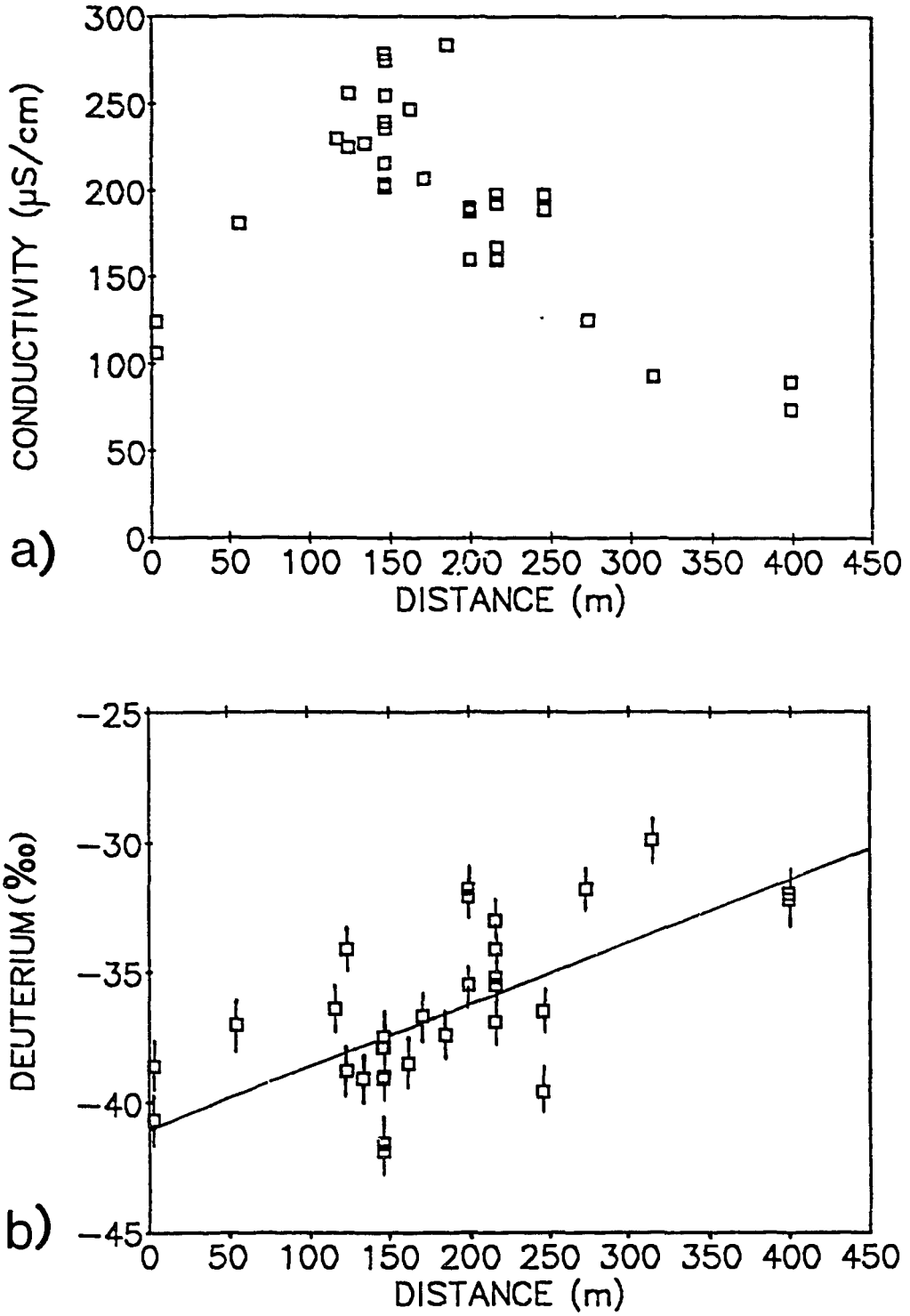

FIGURE 8.9 Conductivity and deuterium as a function of distance from KD1
a) conductivity
b) deuterium
Data for samples from depths > 16 m

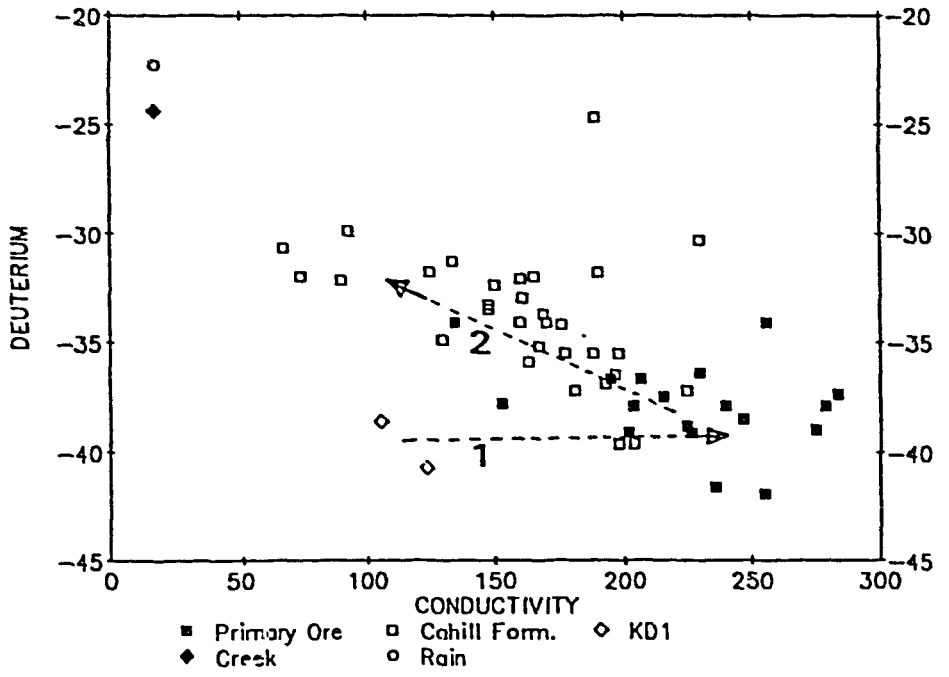

FIGURE 8.10 Deuterium in Koongarra groundwaters as a function of conductivity showing inferred trends

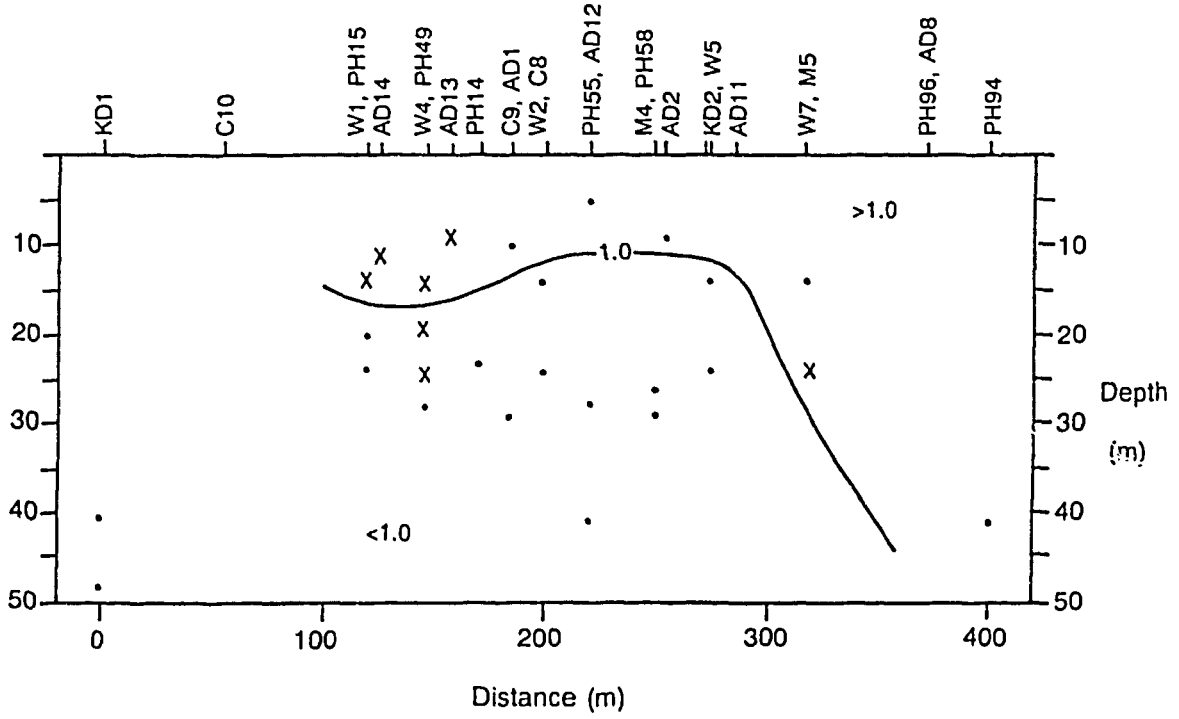

FIGURE 8.11 Tritium - projected cross-section. The contour of 1.0 t.u. is shown. The position of this contour is uncertain because several points (indicated by crosses) were close to 1.0 t.u. (within experimental error)

9 GROUNDWATER COLLOIDS AND FINE PARTICLES

9.1 Background to Colloid Study

A primary aim of the Alligator Rivers Analogue Project was to identify the major mechanisms of radionuclide migration at Koongarra and to develop a quantitative model of the evolution of the dispersion fan. Colloidal particles may provide a mechanism for radionuclide transport by groundwaters. The role of colloids has been studied at a number of proposed sites for nuclear waste repositories, and in several natural analogue systems (Kim et al., 1984; Degueldre et al., 1989; Dearlove et al., 1991; Vilks et al., 1988; Miekeley et al., 1989). A previous study of the association of radionuclides with colloids in groundwaters of the Alligator Rivers Region was carried out with the financial support from the USNRC (Short et al., 1988).

In this section, the significance of groundwater colloids in transporting radionuclides at Koongarra is evaluated and the nature of these particles is discussed. Colloid studies at Koongarra commenced with support from the UKDOE, and were reported in detail by Ivanovich et al. (1988). This study was continued as part of the ARAP project, and the entire colloid program is reviewed in this chapter.

9.2 Colloid Sampling and Analysis

Two different sampling systems were used to concentrate the colloids from the groundwater. In the first of these, large volumes (1000 L) of groundwater were processed using a hollow fibre ultrafiltration system, with the objective being to maximise the amount of colloidal material subjected to chemical and physical analysis. In a second approach, much smaller volumes (600 mL) were ultrafiltered through flat membranes in a stirred cell. Both colloid sampling procedures were carried out on-site at the borehole.

The large volumes used in the hollow fibre ultrafiltration system were obtained using a submersible pump without packers. The smaller volumes, used in the later experiments with the stirred cell, were pumped using packers to restrict the inflow of water to discrete depth intervals.

9.2.1 Hollow fibre ultrafiltration

Groundwater was pumped through pre-filters (5 μm and 1 μm) into an Amicon DC10LA hollow fibre ultrafiltration system (Figure 9.1). This consists of a closed loop around which groundwater is pumped, maintaining a high velocity of water along the hollow fibre membranes. Ultrafiltrate continuously passes through the membranes and is replaced by an equivalent amount of fresh water. Hence, the groundwater in the ultrafiltration system is gradually enriched in colloids. Approximately 1000 litres were concentrated to about 10 litres. This operation was done in the field, under an oxygen-free atmosphere (2% CO_2, 98% N_2) to minimise oxidation or other transformation of the samples.

The second pre-filter (Nuclepore 1.0 μm) defined the upper size limit of the colloids. Subsequently, the Nuclepore filters were examined by scanning electron microscopy (SEM) to verify that pores had not become blocked during the concentration step. The lower size limit of the colloids was determined by the ultrafiltration membranes which had a nominal cut-off at 10000 molecular weight (about 1.5 nm - Dearlove et al., 1991). The colloid concentrates and ultrafiltrates were stored in airtight containers, and sub-samples were subsequently mounted on electron microscope grids. The hollow fibre ultrafilters were back-flushed after each experiment with 0.1 M HCl and this solution was retained for subsequent analysis. Full details of the sampling procedure have been reported (Ivanovich et al., 1988).

9.2.2 Stirred cell ultrafiltration

In these experiments, inflatable borehole packers were used to limit the origin of the sampled groundwaters. Groundwaters were sampled in various depth intervals from a number of boreholes in the vicinity of the Koongarra deposit. The groundwater was pre-filtered as before and passed into a stirred cell in an oxygen-free glovebox (Figure 9.2). The groundwater was forced through a flat ultrafilter (30000 MW cut-off) using gas pressure (2% CO_2, 98% N_2). In some experiments, the colloids were concentrated into a small volume in the stirred cell, and then mounted onto electron microscope grids using centrifugation. Alternatively, the entire volume was passed through the ultrafilters, which were then sealed into plastic bags for analysis.

9.2.3 Analysis

The colloid concentrates, and samples of filtered and ultrafiltered groundwater, were analysed using alpha spectroscopy, ICPMS and other chemical techniques (see Appendix 1). Electron microscope grids, filter membranes, and the particles from the colloid concentrates were examined using SEM, TEM and EDS. Ultrafiltrate samples were also examined for evidence of particle formation after field sampling. The chemical composition of material retained by pre-filters and the flat ultrafilters was determined after ashing or chemical digestion.

9.3 Elemental Content of Colloids

The major cation data for the ultrafiltrates (UF) and colloid concentrates (CC) obtained in the experiments with the hollow-fibre system showed only minor differences (Table 9.1), considering that the CC contained colloids which were concentrated by a factor of about a hundred. A significant amount of Fe (approximately 1% of the Fe in 1 μm-filtered groundwater) was retained on the ultrafilter membrane and was found in the ultrafilter backflush (BF) fractions. The detection of Fe-containing particles in the CC (by EDS) suggested that at least part of this Fe was colloidal, although some may have resulted from sorption on the ultrafilter membrane. Colloidal Fe in groundwaters has been previously reported (Short et al., 1988, Miekeley et al., 1989). Chemical analysis did not provide evidence for enrichment of other elements in the colloids (except possibly Al)

although some other elements were detected in the EDS and radiochemical analyses (see below).

The total organic carbon (TOC) in Koongarra groundwaters is low (11 mg/L - Appendix 6) and the levels in the CC were generally not above the usual range. Therefore, there does not appear to be a significant organic colloid component over 10000 MW. Colloidal organic carbon was not detected in a previous study of groundwaters from the Alligator Rivers region (Short et al., 1988), but has been reported in groundwaters with much higher levels of TOC (Dearlove et al., 1991).

In the experiments with the stirred cell, ICPMS analyses of 1.0 μm-filtered groundwater and ultrafiltrates were the same within experimental error. Chemical analyses of the ultrafiltration membranes were carried out after digestion in concentrated nitric acid, but provided no conclusive evidence of association of any major cation with colloids. This was consistent with the small amount of colloidal material found in the previous experiments with the hollow fibre system.

9.4 Characterisation of Colloids and Fine Particles

Colloids in groundwaters from weathered or partially weathered rock were mainly clay particles, particularly kaolinite (crystalline platelets and spheres, 0.1-1.0 μm across, Si and Al in EDS spectra). Chlorite platelets were observed in samples from less weathered rock (Si, Al, and Mg in EDS). Clay particle concentrations, estimated by manual counting, were about 10^5-10^8 particles per litre. The highest concentrations were in groundwaters from the vicinity of a graphitic hanging wall unit in high grade ore material.

It was possible to study the distribution of colloid minerals as a function of both depth and position, because the packer systems developed during ARAP enabled samples to be obtained from well defined depths. The occurrence of major minerals in the colloids is presented in cross-section in Figure 9.3. Colloids of kaolinite occurred in the weathered zone, with chlorite, quartz, uranium, lead and uranyl silicates found in deeper samples. The presence of these minerals corresponded to their occurrence in the solid phase, with the chlorite and kaolinite being the principal minerals in the unweathered and weathered zones respectively (Murakami et al., 1991 - see also Volumes 8 and 9 of this series).

Fine quartz grains (highly to weakly crystalline, blocky or spheroidal, up to 1 μm across, Si in EDS) were the major colloidal constituent of water from unweathered rock, with an estimated concentration of up to about 10^7 particles per litre.

Non- to weakly crystalline Fe-rich particles (probably ferrihydrite) were observed in both the CC and UF samples, with about ten times more Fe particles in the CC fractions. Their presence in ultrafiltrates indicated a proportion of post sampling formation of these colloids. Crystalline sub-angular to blocky Fe-rich particles, about 0.3 μm across, were observed in the CC samples only, and were probably present in the groundwater before sampling.

Crystalline particles with EDS spectra dominated by U and Pb were found in a CC sample from the high grade ore zone. These particles were crystalline, spheroidal, 0.04-0.3 μm across, and were present at about 10^8 particles per litre. The estimated contribution of these particles to the U concentration of the groundwater was below 1%.

A few titanium-rich colloids were detected. These were probably anatase (TiO_2) particles, 0.06-0.17 μm across, often occurring in dendritic clusters up to 1 μm long. Three particles containing Si, Fe, and Mn (0.1 μm) and one particle of native gold (0.08 μm) were also observed.

Particles on the 1 μm pre-filters were examined by SEM/EDS and were found to consist of kaolinite, chlorite, mica and iron oxides. Iron oxides were present as separate particles and as coatings on clays.

9.5 Uranium-238 and Thorium-230 Distributions

The amounts of colloidal ^{238}U and ^{230}Th in the hollow fibre ultrafiltration experiments are given in Table 9.2. The data indicate the amount of these radionuclides retained by the ultrafilter, as a percentage of the total ^{238}U and ^{230}Th which passed through the 1.0 μm filter. The results show that a much greater proportion of ^{230}Th than ^{238}U was associated with colloids, in agreement with other studies (Short et al., 1988; Miekeley et al., 1989). However, the total amount of ^{230}Th in the <1 μm size range was extremely low, bordering on detection limits.

The data for colloidal ^{238}U and ^{230}Th in Table 9.2 include radionuclides found in both the CC and BF fractions. The BF may include radionuclides adsorbed from solution by the ultrafilter, as well as colloidal material. The large groundwater volumes passed through the ultrafilter would be expected to saturate sorption sites, reducing the amount of adsorption. Also, as there were large quantities of radionuclides associated with particulate material in the >1 μm size ranges (see below), it seems likely that the material in the BF (as well as the CC) is the 'tail' of this particle size distribution. Nonetheless, adsorption by the ultrafilter membrane may have a significant effect. Therefore, the amounts of colloidal ^{238}U and ^{230}Th in Table 9.2 may be considered to be upper limits. If the radionuclides found in the BF are excluded from consideration, the amounts of colloidal ^{238}U and ^{230}Th (based only on enrichment in the CC) are in the range 0.1-0.4% for ^{238}U and 5-35% for ^{230}Th. Whilst these figures are substantially lower than those in Table 9.2, the percentage of colloidal ^{230}Th is significant and remains much greater than is the case for ^{238}U.

Data for colloidal ^{238}U was also obtained for the samples obtained in the stirred cell experiments with the 30000 MW membrane (Table 9.3). On account of the low ^{230}Th levels, and the smaller volumes processed, it was not possible to measure ^{230}Th in these samples. The amount of colloidal ^{238}U was generally in the range 0.1 to 0.5%. One higher result of 6.5% was obtained for a groundwater sample obtained some distance from the ore body, where total U concentrations (and therefore measurement precision) were much lower.

As boreholes PH49 and PH14 intersect the high grade ore zone, it was possible to undertake a detailed study of the particle size distribution of ^{238}U and ^{230}Th in groundwater from these boreholes. The distribution of ^{238}U and ^{230}Th in particles in size ranges defined by the 5 μm filter, the 1 μm filter, and the ultrafilter; and in solution are given in Table 9.4.

Even when the quantities of ^{238}U associated with large particles are considered, it can be seen that the ^{238}U was mostly present in dissolved forms, which passed through the ultrafilter. The uranium is probably present as U(VI) carbonate complexes, which are relatively mobile in groundwaters. In contrast, virtually all the ^{230}Th was retained by the 5 μm and 1 μm pre-filters. The extremely low levels of ^{230}Th in the ultrafiltrate and colloids reflect the immobility of Th(IV), particularly considering the high levels of ^{230}Th which are present in the solid phase near these boreholes.

The results show that only a small proportion of the total ^{238}U and ^{230}Th in the sampled groundwaters is carried by colloidal particles. Almost all (65-87% of the total) of the ^{238}U is dissolved. On the other hand, ^{230}Th is mostly associated with particles above 1 μm in size, with less than 1% passing through the 1 μm filter. Of this small fraction, a major proportion was associated with colloids.

A detailed study of the $^{234}U/^{238}U$ and $^{230}Th/^{234}U$ ratios in accessible and residual phases was carried out on the larger particles retained on the 1 μm and 5 μm filters. These filters were treated to remove precipitated or adsorbed phases, using a 2-3 day leach in 0.5 M HCl, after briefly heating to 70°C. The procedure was similar to those previously employed for this purpose by other workers (Agemian and Chau, 1976; Malo, 1977). However, a relatively longer leaching time was employed, because the bulky nature of the filters was expected to inhibit the leaching process.

The results (Table 9.5) showed that for PH14 samples, the accessible phases of particles contained the same $^{234}U/^{238}U$ isotope ratio as the groundwater, indicating that these phases contained uranium adsorbed from, and readily exchangeable with, solution. The residual phases tended to have higher $^{234}U/^{238}U$ ratios, and contained inaccessible uranium. In the case of PH49, the $^{234}U/^{238}U$ ratios in acid-extracted phases for particles retained by the 1 μm and 5 μm filters were similar to each other, but differed from that of the UF. A possible explanation for this is mixing of particle bearing groundwaters from different aquifers during sampling (because of the large volumes required, packers were not used for the experiments with the hollow fibre ultrafiltration rig).

The $^{230}Th/^{234}U$ isotope ratios (Table 9.5b) showed the immobility of thorium relative to uranium, with the ratio in the UF several orders of magnitude below unity. This deficiency of thorium was reflected by the $^{230}Th/^{234}U$ ratio in accessible phases of groundwater particles, which was also below unity.

9.6 Evidence for Colloidal Transport of Actinium-227

The thorium α-spectrum for many of the colloidal and fine particle fractions showed an unusual feature - prominent peaks of ^{227}Th, which is a daughter of ^{227}Ac. Peaks of ^{227}Th, and its decay products ^{219}Rn and ^{211}Bi, were present in the thorium α-spectrum for particles in the 1-5 μm size range obtained at borehole PH14 (Figure 9.4a). This spectrum is for "accessible" phases, which were extracted from the particles retained on the 1.0 μm Nuclepore filter using 0.5 M HCl. Isotope data suggested that this phase contained radionuclides which were adsorbed or precipitated from solution (discussed above). The spectrum in Figure 9.4a may be compared with the thorium α-spectrum for material retained on the hollow fibre ultra-filter at PH14 (Figure 9.4b). In both cases, peaks of ^{227}Th and its decay products are prominent.

The ^{227}Th/^{230}Th activity ratio in bulk rock samples is usually close to that of their respective precursors (^{235}U and ^{238}U), and values between 0.032 and 0.052 have been reported for weathered rock samples from the Alligator Rivers region (Golian et al., 1984). The ^{227}Th/^{230}Th ratios in Figures 9.4a and 9.4b are approximately 3.0. As ^{227}Th has a half life of 19 days, and several months elapsed before analysis, this indicates the presence of excess amounts of its parent, ^{227}Ac in these samples. Elevated levels of actinium have been reported in ocean water (Nozaki and Horibe, 1983) and acidic mine-waters (Dickson and Meakins, 1984).

The ^{227}Th/^{230}Th isotope ratios in accessible and inaccessible phases are given in Table 9.6. Excess ^{227}Th (indicating the presence of elevated levels of ^{227}Ac) was found in the ultrafilter backflush fraction, which contains mobile radionuclides which had passed through the 1 μm pre-filter in either fine colloidal or dissolved forms. Similarly, the accessible phases on the fine particles, which contain potentially mobile radionuclides adsorbed from solution, also contained excess ^{227}Ac. It therefore appears that unexpectedly large amounts of ^{227}Ac are associated with fine particles and mobile colloidal or dissolved groundwater phases. It is significant that the residual (inaccessible) phases in the 1 μm and 5 μm particles did not have a ^{227}Ac content elevated above normal values.

At least 95% of the ^{227}Ac in these groundwaters was retained by the pre-filters, and the level of ^{227}Ac in the ultrafiltrate was below detection limits, indicating that it is comparatively immobile (compared to uranium). However, the excess ^{227}Ac found on the ultrafilter indicates some mobility of ^{227}Ac in the <1 μm size range, possibly adsorbed on a fine clay or Fe-colloid. This result may be significant in the assessment of nuclear waste repositories since the dominant oxidation state of actinium is +3, in common with curium and americium.

9.7 Nature and Significance of Colloids

The colloids and particles included clay minerals, particularly kaolinite and chlorite, together with fine quartz grains. The distribution of these groundwater colloids tended to reflect their distribution in the solid phase. Iron was present as particle coatings, and in a separate colloidal form.

The amount of ^{238}U associated with colloids (expressed as a percentage of the total ^{238}U which passed through the 1.0 μm filter) ranged up to 6.5%. The corresponding figures for ^{230}Th were 10-85%. However, the amount of ^{230}Th which passed through the 1.0 μm filter was extremely small, and ^{230}Th was associated to a much greater extent with larger particles, which are unlikely to be mobile in natural groundwaters.

The results for one experiment showing the major features of ^{238}U and ^{230}Th distributions are summarised in Figure 9.5. The graph shows the total amount of each radionuclide carried by unfiltered groundwater, and then after passing through each successive filter. The majority of uranium was present in dissolved forms which passed through the ultrafilter. In contrast, the thorium was almost entirely found in large particles.

The total mass of particles in the colloidal size range was quite small, probably below 0.05 mg/L (Table 9.7). The mass of colloids was too small to be measured directly and an upper limit was estimated from the elemental data. However, the mass of larger particles (> 1 μm) in groundwaters from boreholes intersecting the orebody was readily determined after ashing the 1 μm and 5 μm pre-filters. The results (Table 9.7) show that a significant mass of these larger particles was present in the sampled groundwaters. It is likely that these particles are normally immobile and are entrained during pumping of the boreholes.

In some fine particle and colloidal fractions, the $^{227}Th/^{230}Th$ activity ratio in the thorium alpha spectrum was unusually high, indicating the presence of substantial quantities of ^{227}Ac. This suggested that actinium could be present as a mobile colloid phase. Actinium appears to be slightly more mobile than thorium and is associated with colloids to a greater extent, although generally present in low concentrations. These results for Th(IV) and Ac(III), suggest the possibility of colloidal transport of trivalent and tetravalent actinides in the vicinity of a nuclear waste repository.

Overall, there was very little colloidal material in these groundwaters. Uranium migrates mostly as dissolved species, whereas thorium and actinium are mostly associated with larger, relatively immobile particles (>1.0 μm). However, of the small amount of ^{230}Th that passes through a 1.0 μm filter, a significant proportion is associated with colloidal particles. These colloids mostly consist of iron oxides and clay minerals, and carry a small proportion of the uranium in the system.

Colloids are relatively unimportant in transporting radionuclides in Koongarra groundwaters, with only iron, uranium, actinium, and thorium showing a significant association with colloids.

TABLE 9.1

PARTITIONING OF CATIONS IN 1 μm-FILTERED GROUNDWATER BETWEEN COLLOID CONCENTRATE (CC), ULTRAFILTRATE (UF) AND ULTRAFILTER BACKFLUSH (BF)
(Hollow Fibre Ultrafiltration Experiments)

Hole	Fraction	K	Na	Mg	Ca	Al	Fe	Mn	Si
KD2	UF (mg/L)	0.65	1.69	15.5	0.92	<0.02	1.14	0.037	12.5
	CC (mg/L)	0.63	1.63	11.1	0.70	0.02	1.06	0.027	9.8
	BF*	-	-	-	-	(0.1%)	0.8%	-	-
PH55	UF (mg/L)	1.07	1.58	17.1	1.28	<0.02	0.77	0.067	12.5
	CC (mg/L)	1.11	1.62	18.2	1.38	0.02	0.80	0.070	12.6
	BF*	-	-	-	-	(0.05%)	0.5%	-	-
PH14a	UF (mg/L)	0.71	1.49	21.7	2.29	0.04	0.43	0.36	9.2
	CC (mg/L)	0.74	1.44	22.2	2.38	<0.02	0.46	0.37	9.0
	BF*	-	-	-	-	(0.15%)	1.4%		
PH14b	UF (mg/L)	0.65	1.36	19.8	1.50	0.02	0.14	0.20	9.5
	CC (mg/L)	0.69	1.37	18.2	1.43	<0.02	0.13	0.17	9.0
	BF*	-	-	-		(0.2%)	1.1%	-	-
PH49	UF (mg/L)	0.58	1.12	24	1.60	0.02	0.40	0.13	8.3
	CC (mg/L)	0.60	1.09	23	1.60	<0.02	0.46	0.13	8.0
	BF*	-	-	-	-	(0.4%)	1.1%		

* Percentage of total found in ultrafilter backflush. In cases not assigned a numeric value, ultrafilter retention was below 0.03%. Data for Al in BF fraction are bracketed because the values were close to detection limits.

TABLE 9.2

PARTITIONING OF ^{238}U AND ^{230}Th IN 1 μm-FILTERED GROUNDWATER

(Hollow fibre ultrafiltration experiments)

Borehole	^{238}U		^{230}Th	
	UF (ppb)	Colloid	UF (mBq/L)	Colloid
KD2	0.079	1.8%	<0.007	-
PH55	0.40	2.5%	0.073	33%
PH14(a)*	87.7	1.4%	0.160	12%
PH14(b)*	205	1.1%	0.062	27%
PH49	178	1.4%	0.053	82%

* There were two colloid sampling experiments at PH14.

TABLE 9.3

URANIUM ASSOCIATED WITH COLLOIDS

(Stirred Cell Experiments)

Hole	Sampling Depth (m)	U_C ppb	U_{UF} ppb	% of U on Colloid
W1	23-25 m	0.24	61	0.4
W4	13-15 m	2.6	470	0.5
W4	23-25 m	1.0	300	0.3
M1	27-29 m	0.52	620	0.1
PH49	18-20 m	0.60	110	0.5
M2	42-44 m	0.12	46	0.3
W5	23-25 m	0.21	3.0	6.5

U_C - uranium on collolid.
U_{UF} - uranium in ultrafiltrate.

TABLE 9.4

DISTRIBUTIONS OF ^{238}U AND ^{230}Th AMONGST COLLOIDS, PARTICLES (>1 μm) AND ULTRAFILTRATES

(Hollow Fibre Ultrafiltration Experiments)

Experiment	Particles >5 μm (mBq/L)	Particles 1-5 μm (mBq/L)	Colloids <1 μm (mBq/L)	Ultrafiltrate (mBq/L)	Ultrafiltrate as Percentage of Total*	Colloid as Percentage of Total*
^{238}U						
PH14(a)	60.7(1.8)	81.0(2.3)	15.7(0.7)	1090(40)	87.4(3.3)	1.26(0.06)
PH14(b)	547(17)	507(13)	27.5(2.0)	2550(70)	70.2(1.8)	0.76(0.06)
PH49	722(12)	452(10)	31.0(2.5)	2220(50)	64.8(2.0)	0.91(0.07)
^{230}Th						
PH14(a)	12.8(0.7)	20.5(0.8)	0.022(0.003)	0.160(0.030)	0.48(0.09)	0.07(0.01)
PH14(b)	64.3(1.7)	16.0(0.7)	0.023(0.003)	0.062(0.017)	0.08(0.02)	0.03(0.01)
PH49	445(10)	348(10)	0.250(0.033)	0.053(0.008)	0.007(0.001)	0.032(0.004)

Errors are given in brackets.

* The total includes ultrafiltrate and particles in all size ranges.

TABLE 9.5

ISOTOPE RATIOS IN ULTRAFILTRATES, ACID-EXTRACTABLE PARTICLE PHASES, AND RESIDUAL PARTICLE PHASES

(Hollow Fibre Ultrafiltration Experiments)

A $^{234}U/^{238}U$

	PH14(a)	PH14(b)	PH49
Ultrafiltrate	0.75(0.02)	0.78(0.01)	1.02(0.01)
Particles:			
>5 μm - acid extraction	0.80(0.01)	0.78(0.01)	0.90(0.01)
1-5 μm - acid extraction	0.74(0.02)	0.75(0.01)	0.88(0.02)
>5 μm - residual phases	0.93(0.01)	0.84(0.04)	1.08(0.01)
1-5 μm - residual phases	0.92(0.02)	0 90(0.03)	1.17(0.02)

B $^{230}Th/^{234}U$

	PH14(a)	PH14(b)	PH49
Ultrafiltrate	2.0×10^{-4}	3.1×10^{-5}	2.3×10^{-5}
Particles:			
>5 μm - acid extraction	0.012	0.026	0.37
1-5 μm - acid extraction	0.17	0.0072	0.69
>5 μm - residual phases	0.86	0.40	1.03
1-5 μm - residual phases	0.91	0.80	1.39

The accuracy of $^{230}Th/^{234}U$ is +/-20% for the ultrafiltrates and +/-5% for all other phases.

TABLE 9.6

$^{227}Th/^{230}Th$ IN PARTICULATE FRACTIONS AND ULTRAFILTER BACKFLUSH

(Hollow Fibre Ultrafiltration Experiments)

Filter	PH14a	PH14b	PH49
5 μm - extractable phase	2.37	0.99	0.14
5 μm - residual phase	0.04	0.07	0.05
1 μm - extractable phase	0.22	2.87	0.09
1 μm - residual phase	0.04	0.05	0.05
Ultrafilter backflush	3.1	3.5	2.8

The radiometric equilibrium value of $^{227}Th/^{230}Th$ is 0.046.

TABLE 9.7

MASS OF PARTICLES IN EACH SIZE RANGE
(boreholes intersecting the orebody - PH14, PH49 and PH55*)

Size range	Particle mass
1.5 nm# - 1 μm	< 50 μg/L
1 μm - 5 μm	1 - 10 mg/L
> 5 μm	5 - 35 mg/L

* Data are for hollow fibre ultrafiltration experiments. Note that results for KD2 were about an order of magnitude lower.

\# 10000 MW

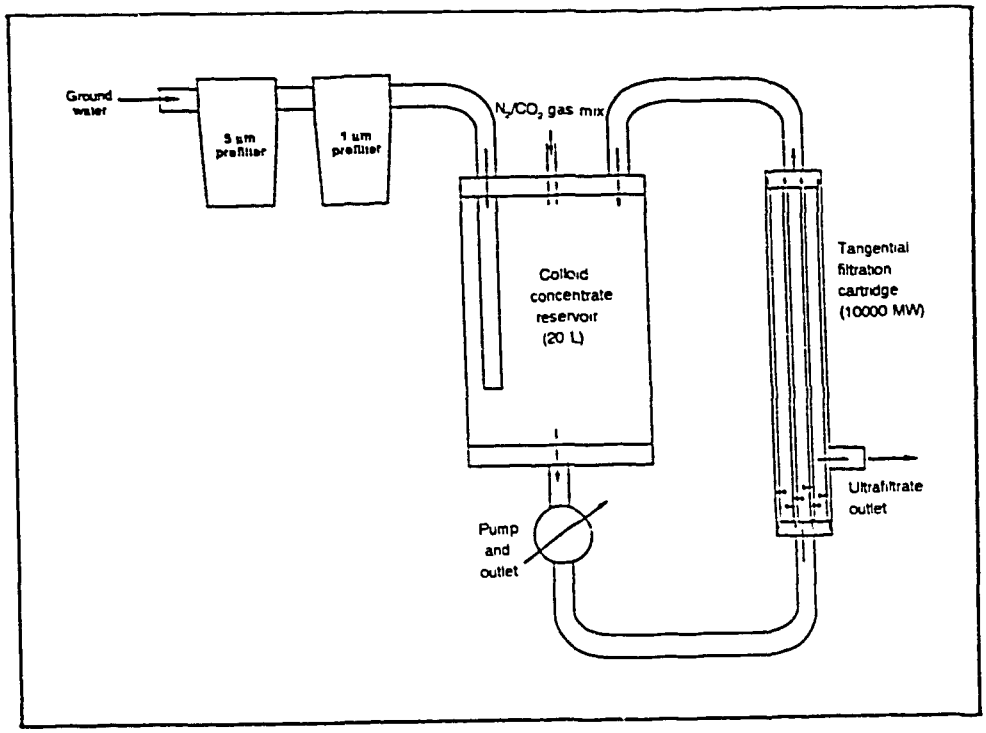

FIGURE 9.1 Hollow fibre ultrafiltration system

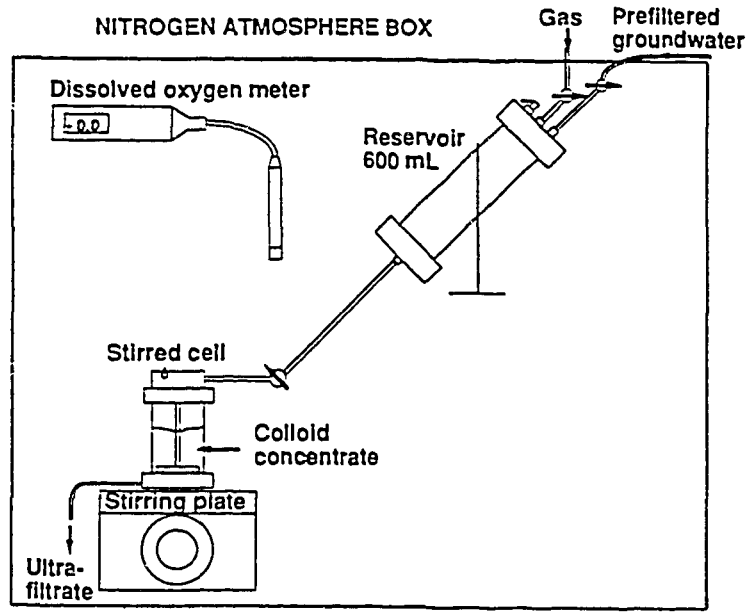

FIGURE 9.2 Stirred cell ultrafiltration system

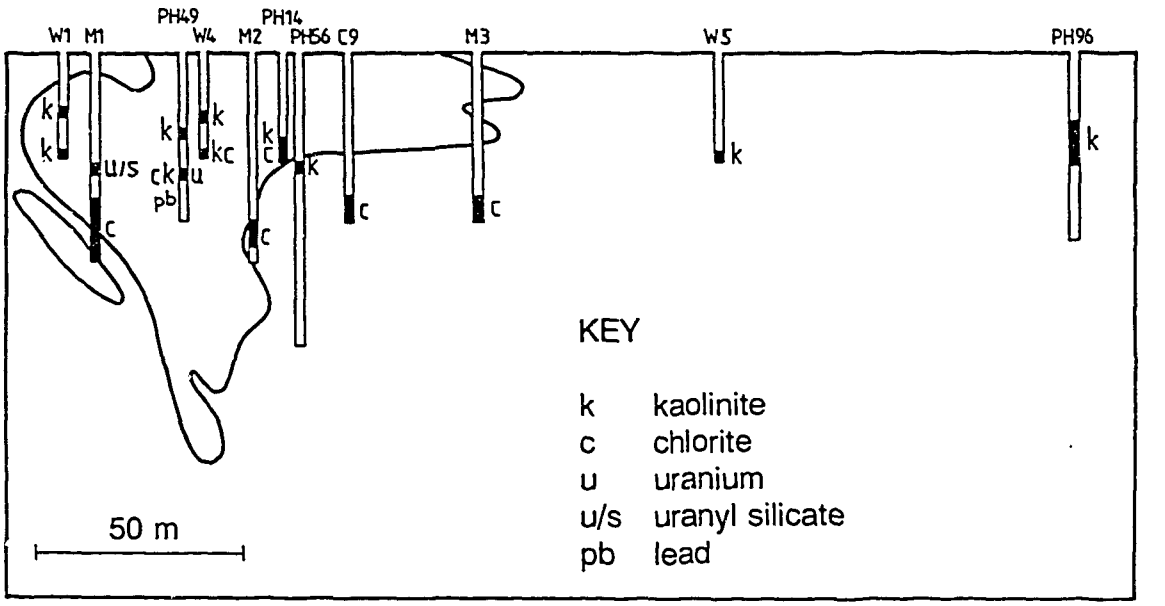

FIGURE 9.3 Distribution of some colloids detected in Koongarra groundwaters

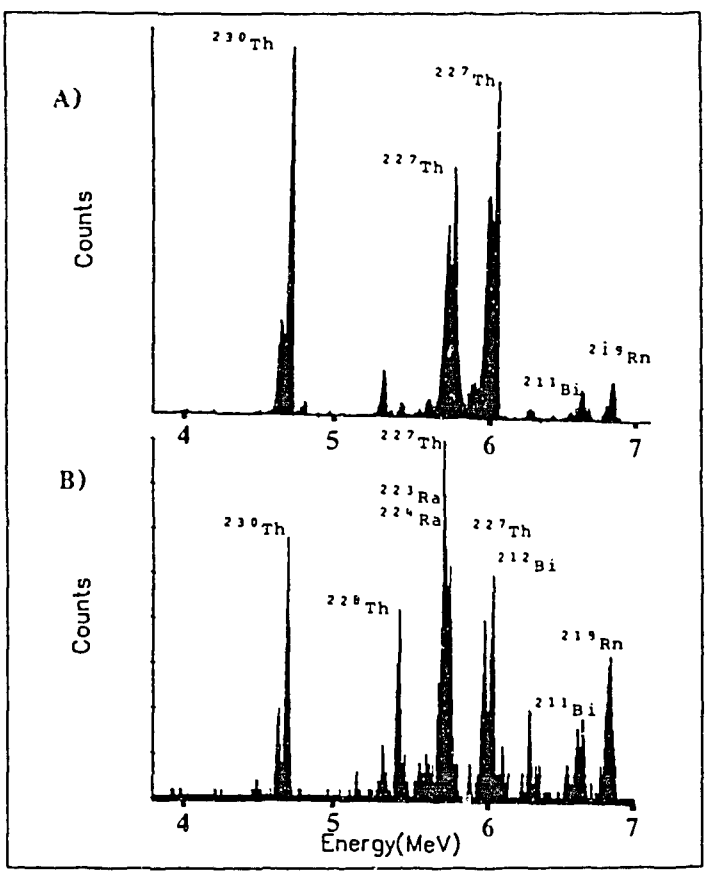

FIGURE 9.4 Thorium alpha-spectrum for PH14 samples retained by:
a) 1 μm Nuclepore filter
b) colloid filter

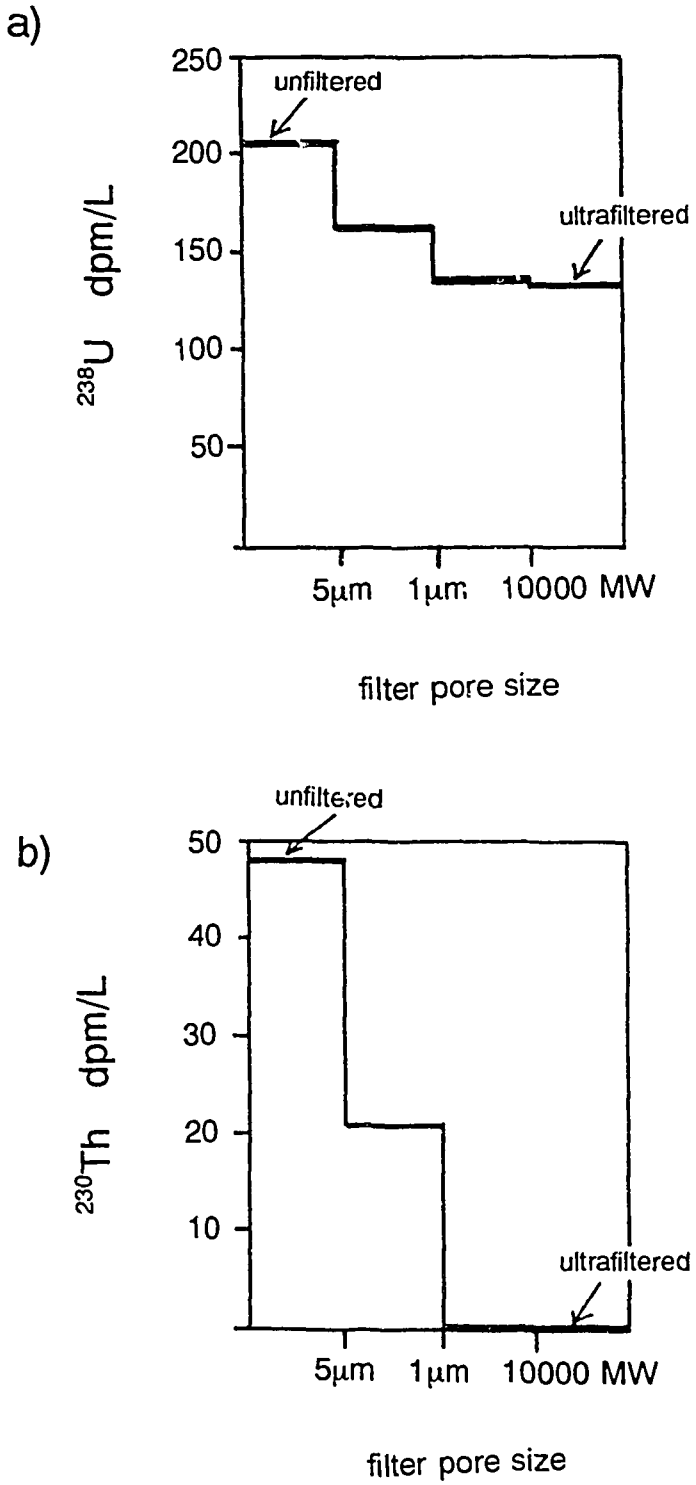

FIGURE 9.5 Effect of filtration on radionuclide levels in groundwater
a) ^{238}U b) ^{230}Th

10 DISCUSSION

10.1 Groundwater Sources and Flow-paths

The scenario emerging from this study is that groundwater moves from the vicinity of the fault zone, into the orebody. The trends in groundwater chemistry and isotopic composition suggest that a significant proportion of groundwater which enters the region of the No. 1 orebody originates from fractures in the Kombolgie sandstone and moves across the fault zone. However, downward infiltration in the fault zone, and in the region between the fault and the orebody, may also be a source of groundwater entering the flow system of the orebody. The groundwater which enters the orebody is characterised by low levels of ^{14}C, high $p(CO_2)$, low pH, and is relatively deficient in ^{2}H. The groundwater chemistry is altered by mineral-solid interactions within the immediate vicinity of the orebody, which appears to be in a zone of active weathering. After passing through the orebody, the groundwater chemistry and isotopic composition are further modified by mixing with local recharge, which permeates through the surficial sand and clay layers causing mixing and dilution. Hence, moving down-gradient, there is a gradually reducing $p(CO_2)$, and increasing proportion of ^{14}C, together with a change of $\delta^{2}H$ to less negative values.

The groundwater chemistry directly to the south (towards PH88) closely resembles that in the orebody zone. This is reflected in factors such as its conductivity, magnesium content, bicarbonate concentration, and the concentrations of uranium and its decay products (such as ^{226}Ra and ^{222}Rn). Furthermore, the $^{234}U/^{238}U$ isotope ratio is below unity at substantial depths in PH88, whereas elsewhere at Koongarra this ratio is only below unity in the shallower weathered zone. These factors suggest that present-day groundwater movement from the region of the dispersion fan may be towards PH88. This is a slightly different direction to the uranium mineralisation in the dispersion fan, which extends more towards the south-east. This observation joins a substantial body of evidence along these lines.

Giblin and Snelling (1983), in a previous study of groundwater chemistry at Koongarra, concluded that groundwater chemistry towards PH80 and PH88 was similar to the orebody. In this study, a major parameter considered was NMg, defined as follows:

$$NMg = Mg/ (Mg + Ca + Na + K)$$

with the concentrations of the ions expressed in meq/L. This parameter is a measure of the proportion of the positive charge contributed by the Mg ion.

The values of NMg in groundwater from boreholes to the south of the orebody (such as PH80 and PH88), tended to be about 0.8 or greater. These high values were similar to the those for groundwaters taken from boreholes intersecting the orebody. In the zone near PH94, PH96 and PH139 the value of NMg was much lower.

In a study of groundwater helium values (Gole et al., 1986), elevated levels of helium had a similar distribution to that obtained with the NMg parameter, again showing a slight elongation towards PH80. However, the helium anomaly had a smaller spatial extent, and this may indicate greater mechanisms for loss in the case of the gaseous He species.

The geochemical trends in Koongarra groundwaters can also be studied using a graphical representation known as a Piper Trilinear diagram (Freeze and Cherry, 1979). In this analysis, only the major ionic components are considered (cations: Mg, Ca, and Na + K; and anions: SO_4, Cl, and CO_3+HCO_3). It should be noted that in this approach, the proportion of the total milliequivalents per litre contributed by each ion, rather than its total concentration is considered. Therefore, compositions with different TDS, but with similar ionic proportions (in other words, differing only by dilution), will plot close together in a Piper diagram. In some cases, a Piper diagram can show relationships between groundwater compositions resulting from mixing of two groundwater types

Koongarra groundwaters are plotted on a trilinear diagram in Figure 10.1. The triangle in the lower left of this figure shows the cation composition (dominated by Mg) and the other triangle represents the anion composition (dominated by HCO_3). In the upper diamond, the groundwater composition is plotted at a single point representing both its anionic and cationic composition.

On a trilinear diagram such as Figure 10.1, points corresponding to groundwater samples from various Koongarra boreholes tend to be quite close together. The similar chemistry of groundwaters from boreholes PH88 and PH49 is immediately apparent, with the points corresponding to these boreholes almost superimposed in all three parts of the diagram. PH94 and KD1 (in particular) have significantly less Mg dominance and therefore plot in a slightly separate field. Therefore, in the Koongarra case, the Piper diagram is quite successful in identifying similarities in the various groundwaters.

Thus, the various investigations of the geochemistry of Koongarra have reached essentially similar conclusions, that present groundwater flow-paths may well be towards PH80 or PH88. This is at an angle to the flow inferred from the extent of the secondary uranium mineralisation which extends more perpendicularly away from the fault. The reason for this cannot be determined by a study of groundwater chemistry alone, but it is possible that deeper weathering or fracturing has led to preferential flow-paths in this vicinity. Present flow-paths may have been sustained for a considerable geological period during the formation of the dispersion fan, or may result from a recent change in flow-patterns.

These conclusions appear to be consistent with those of geophysical investigations, which have identified a subsurface 'drainage feature' to the south of the orebody (Volume 4 of this series). Other studies carried out during the ARAP raise the possibility of seasonal changes in groundwater flow patterns. Full accounts of these investigations can be found in Volumes 5 and 6 of this series.

10.2 Depth Relationships and Seasonal Effects

It has been suggested in this volume that the chemistry of groundwaters moving through the system is modified by mixing with percolating water which travels downwards from the surface. This local recharge component is seasonal, has a low uranium content, a low pH, a low conductivity, and generally low levels of dissolved constituents such as phosphate. In short, its chemistry is not greatly modified relative to rainwater, although dissolved CO_2 may be somewhat increased due to its passage through the soil zone.

Chemical data obtained for shallow (AD-hole) groundwater samples collected during the April 1991 field trip are plotted on a Piper trilinear diagram in Figure 10.2. On this diagram, the AD-samples tend to be more scattered than were the deeper groundwaters (Figure 10.1), particularly in the cationic composition.

In Figure 10.2, samples from AD-holes have been grouped, according to their position relative to the orebody (see Figure 2.3). The groupings were:

a) outside the ore-zone (boreholes AD2, AD11, AD6, and AD8), and

b) within the ore-zone (AD14, AD13, AD1 and AD12).

Samples from AD9 could be validly included in either group, and are identified separately in Figure 10.2. The positions of rainwater, and samples from PH49 (representing the composition of groundwater from the centre of the orebody) are also shown.

The main feature of Figure 10.2 is that whilst both the cation and anion data are somewhat scattered, the combined data in the upper diamond appears to fall into separate fields corresponding to the locations from which the samples were obtained. The data for the shallow boreholes intersecting the top of the orebody appears to fall on a trend-line between rainwater and the PH49 sample. This suggests that the shallow groundwaters evolve towards the composition of deeper groundwaters as they infiltrate downwards. In contrast, the samples from AD-boreholes outside the ore-zone fall in a slightly separate field on this cross-plot of anion and cation data.

It is valid to question why the shallow groundwaters appear to fall into two separate fields in the upper diamond (or cross-plot) section of the Piper diagram, when both the anion and cation data appear rather scattered. This arises because the AD samples from outside the orebody have a low proportion of Cl, despite the presence of significant levels of Na. In contrast, AD-samples from the boreholes within the orebody either have significant quantities of both Na and Cl (tending towards Na/Cl dominance or rainwater type) or tend towards the PH49 groundwater type (where both Na and Cl are very minor constituents). In either case, these latter samples fall between rainwater and PH49 groundwater compositions on the trilinear diagram.

Although only a relatively small amount of data on the chemistry of shallow groundwaters is available, the Piper diagram is of value in showing that shallow groundwaters from the region of the orebody are geochemically different to those outside the ore-zone, and that infiltrating waters appear to evolve towards the composition of deeper samples.

Figure 10.3 presents a scenario for water movement in the Koongarra weathered zone. The seasonally saturated near-surface zone has a rainwater-like chemistry in the wet season, being slightly modified by evaporation and mineral dissolution as the water table drops back to dry season levels. Depths greater than about 12 m are permanently saturated, but the pressure head on the groundwater fluctuates with season. There are numerous field observations which show that this head is almost always higher than the water table (Volume 5 of this series). This suggests that there could be a semi-permeable layer within the weathered zone which partially confines the aquifer below. The generally low levels of tritium in deeper groundwaters also provide evidence that only limited vertical mixing occurs. Several additional lines of evidence that the major water-bearing zone at the base of the weathered zone is partially confined are presented in Volume 5 of this series. In the scenario of Figure 10.3, the laterally flowing groundwater near the base of the weathered zone is gradually mixed with, and diluted by infiltrating water moving downwards from the surface.

The geochemical data suggest that most uranium mobilisation occurs in the lower section of the weathered zone (or transition zone), where groundwater chemistry is characterised by high levels of bicarbonate, which complexes uranium. In this depth range, in the permanently saturated zone above the weathering front, the $p(CO_2)$ is elevated relative to equilibrium with the atmosphere. Conductivity, Mg, and uranium levels are relatively high compared to shallow seasonal groundwaters, and the ^{14}C content of the DIC is significantly below 100% modern, although gradually rising moving away from the orebody. The pH (close to neutral) is higher than the seasonal groundwaters, and the $^{234}U/^{238}U$ isotope ratio is generally substantially below unity. As noted above, this aquifer may be partially confined by a clay-dominated layer in the weathered zone, which allows gradual mixing with the seasonal component.

In the unweathered zone, fractures probably provide the main conduits for groundwater flow. The groundwater chemistry is not strongly depth-dependent, possibly because the layering dips very steeply. A major feature of this zone is $^{234}U/^{238}U$ exceeding unity which is in contrast to the aquifer in the weathered zone. Radium migration may be significant in this zone, but uranium appears to migrate more readily in the weathered zone.

It is possible that there could be seasonal surface transport of particles by rainfall events. This has occurred, for example, in the case of rare earths at Morro do Ferro (Lei et al., 1986). The effects of human activities, particularly drilling of boreholes, may also have had an impact in recent years. Boreholes may provide conduits for mixing of waters from different depths which would not otherwise have occurred.

The absence of a significant seasonal change in groundwater chemistry, with the exception of shallow groundwaters from AD holes, is a major result of the groundwater sampling program with important implications. In general, seasonal chemical changes do not need to be included in modelling. The limitation of seasonal variation to shallow depths confirms that there could be a semi-permeable layer allowing limited downward percolation of local recharge and mixing on timescales which are longer than the annual wet/dry season cycle.

10.3 Mineral/Groundwater Interactions

The groundwaters are all dilute waters, with up to 150 mg/L total dissolved solids, dominated by Mg^{2+} and HCO_3^-. Dissolved silica is a major constituent, reaching concentrations of 0.5 mM and often exceeding the concentration of the major cations. Bicarbonate ion dominates the anionic composition. Chloride concentrations are generally quite low, but slightly higher than the level expected for rainfall chloride, suggesting that a limited amount of evaporation for the recharge waters has occurred. Magnesium, Ca^{2+} and HCO_3^- are relatively enriched relative to chloride in the groundwaters, compared to their abundances in atmospheric deposition.

The release of alkaline earths and increased alkalinity results from mineral-solution reactions within the soil zone and within the aquifers themselves. The correlation between Mg and alkalinity (mostly HCO_3) indicates some common processes affecting Mg and the dissolved carbonate system. On the N-S transect along the line of inferred flow, both Mg and alkalinity are highest in the ore-zone but decrease down-flow of the orebody.

The types of mineral-solution reactions that most probably occur within the Koongarra groundwaters are induced by the action of CO_2 on carbonate or silicate minerals within the weathered zone or within the main aquifers. Groundwaters both within, and upgradient of, the orebody contain substantial quantities of dissolved CO_2. The ultimate source of the CO_2 may be from degradation of plant material and root respiration within the soil zone, or CO_2 produced "in situ" within the aquifer from degradation of sedimentary organic matter by bacteria.

There is potential for Mg^{2+} and HCO_3^- to be released into the waters from either dissolution of dolomite or weathering of Mg-silicates such as chlorite. Considering the geology of Koongarra, the former possibility is likely to be relatively minor in the immediate vicinity of the orebody, although it is reflected in the water chemistry some distance to the south, where there is a dolomite formation. In this region both Mg^{2+} and Ca^{2+} are present in groundwaters, and in approximately equal concentrations. This is seen in the analyses of groundwaters from borehole PH110 (Appendix 3).

Close to the orebody, the groundwater cation chemistry is dominated by Mg^{2+}, and substantial levels of Si and HCO_3^- are also present. Weathering dissolution of chlorite by CO_2-charged groundwaters would release Mg and SiO_2, while

increasing alkalinity by consuming protons to convert CO_2 to bicarbonate. A possible reaction with generalised stoichiometry, involves conversion of chlorite to kaolinite:

$$\underset{\text{chlorite}}{Mg_5Al_2Si_3O_{10}(OH)_8} + 10\ CO_2 + 3\ H_2O \rightarrow \underset{\text{kaolinite}}{Al_2Si_2O_5(OH)_4} + 5\ Mg^{2+} + SiO_2 + 10\ HCO_3^-$$

The amount of SiO_2 released depends on the stoichiometry of the minerals involved, which may vary widely.

In summary, the major ion chemistry of Koongarra groundwaters is consistent with the weathering of minerals such as chlorite to ultimately form kaolinite. These matters are discussed in more detail in Volumes 9 and 12 of this series.

10.4 Concluding Comments

Koongarra groundwaters contain elevated levels of uranium and its decay products, with uranium concentrations up to four orders of magnitude higher than background levels. Groundwaters of the weathered zone are characterised by $^{234}U/^{238}U$ isotope ratios which are often substantially below unity. These low isotope ratios are correlated to the ratios in accessible (readily leached) uranium of the solid phases. In the unweathered zone, where uranium is less mobile, the groundwater $^{234}U/^{238}U$ ratios generally exceed unity. Thorium is virtually immobile in the Koongarra system. Radium is relatively mobile in the unweathered zone. The uranium in the groundwater is in true solution, rather than as colloids, and is probably present as uranyl carbonate complexes. Overall, colloidal transport of radionuclides is of minor importance, although there is some association of both actinium and thorium with colloids.

Groundwater flow across the fault from the sandstones of the Kombolgie formation appears to provide an input of water to the system. This formation is heavily fractured and water apparently moves through the fractures, then across the Koongarra fault into the Cahill formation which hosts the uranium deposit. Evidence for conduits for water across the fault lies in the similar isotopic composition of water molecules (δ^2H values) of groundwater from the Kombolgie formation and within the mineralised zones. Groundwater loss from the system may result from evapotranspiration or down-gradient flow to the south or south-east.

The paths of groundwater flow through the region of the orebody are likely to be complex, and not necessarily constant throughout the year, or over geological timescales. The groundwater in the vicinity of PH88 has a similar geochemistry to groundwater in the orebody which suggests that this region is an exit point for water flowing through the system.

Dissolved carbon dioxide is an important agent of weathering in the immediate vicinity of the orebody. The carbon isotopes (^{14}C and ^{13}C) in the groundwater indicate that this may be derived from bacterial degradation of organic material, such as graphite, which is dispersed throughout the area of the deposit. Alternatively, the source of CO_2 in the system may be the CO_2 which is present in Kombolgie groundwaters, which may traverse the fault and enter the zone of uranium mineralisation after long transit times from the surface. Either source of CO_2 would satisfactorily explain the low ^{14}C activities of dissolved inorganic carbon in groundwaters from the immediate vicinity of the orebody.

Down-gradient of the orebody, the groundwater becomes more dilute, and the δ^2H values of the water molecules become less negative and tend to approach the average values of rainwaters and surface waters. The relationship between groundwater δ^2H values and conductivities suggests a gradual mixing with infiltrating recent rainwater. Moving away from the ore-zone, the proportion of radiocarbon increases. Tritium is present in some shallower groundwaters. These phenomena appear to be adequately explained by gradual mixing with local recharge as groundwaters move down-gradient.

In conclusion, a large amount of chemical and isotopic information has been obtained for Koongarra groundwaters. The data taken as a whole appear to present a reasonably coherent description of the flow and mixing of groundwater, and of the mineral/groundwater interactions in the system.

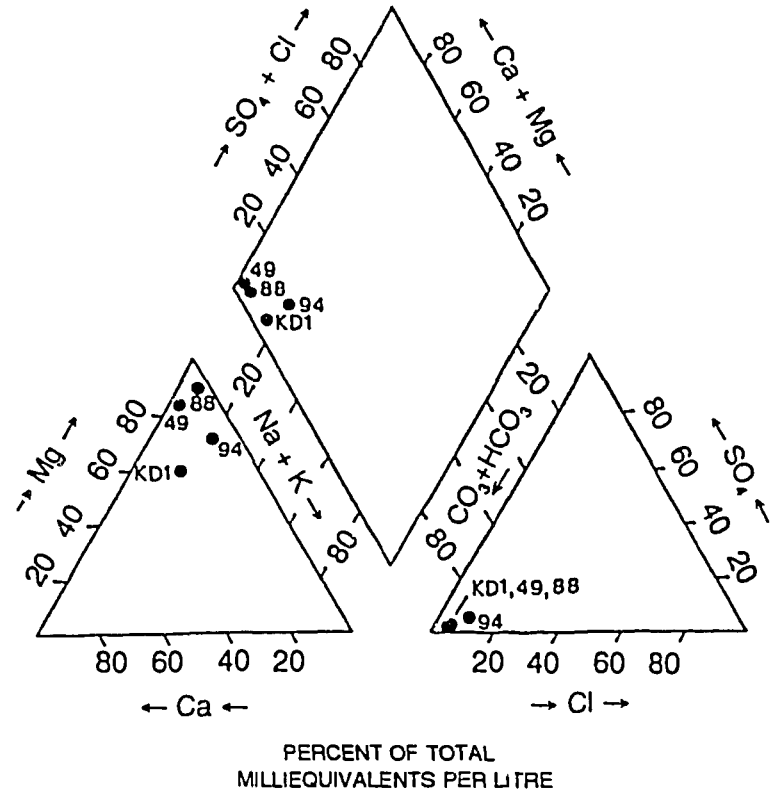

FIGURE 10.1 Selected Koongarra groundwaters plotted on a Piper trilinear diagram

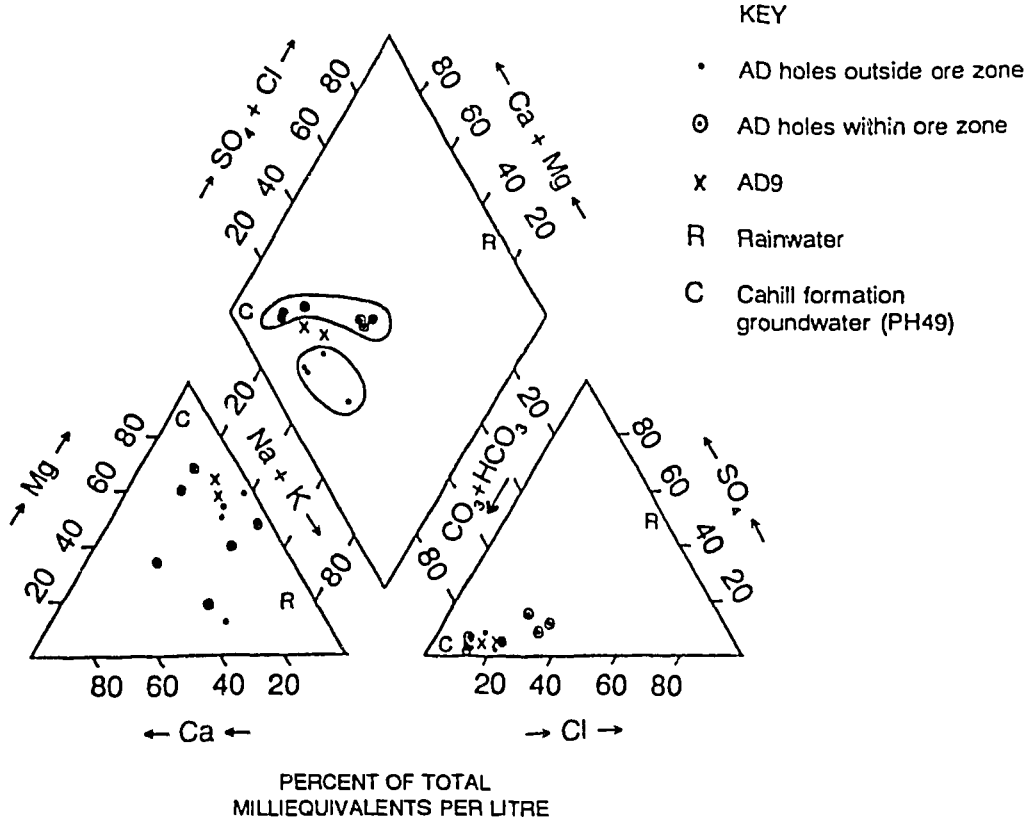

FIGURE 10.2 Samples obtained from AD-holes plotted on a Piper trilinear diagram

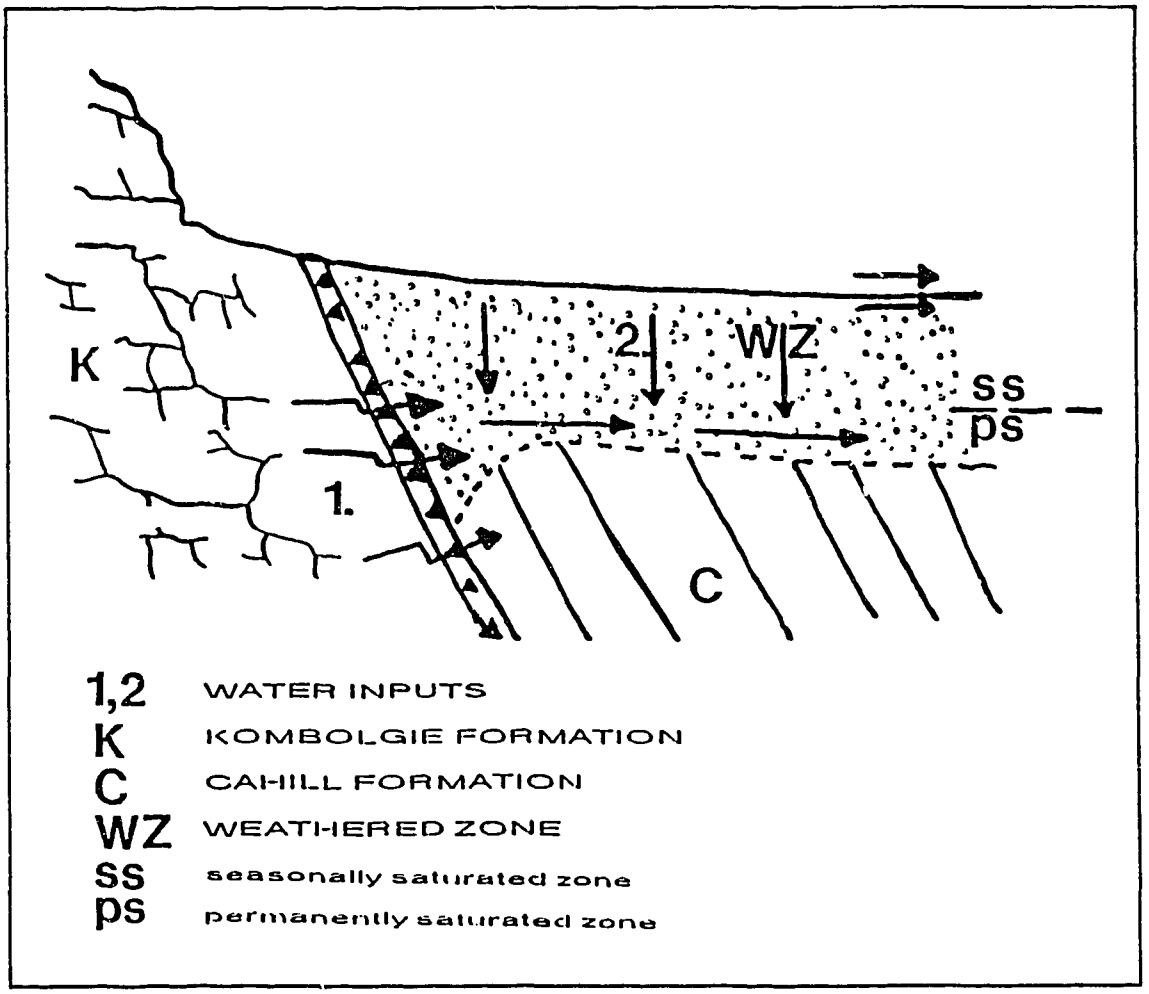

FIGURE 10.3 Proposed weathered zone groundwater flow paths

11 REFERENCES

Agemian, H. and Chau, A.S.Y. (1976) Evaluation of Techniques for the Determination of Metals in Aquatic Sediments, Analyst 101, 761-767

Allison, J.D., Brown, D.S., and Novo-Gradac, K.J. (1990) MinteqA2/ProdefA2: A Geochemical Assessment Model for Environmental Systems. Version 3.0. Users Manual. USEPA, Athens, Georgia.

Asikainen, M. (1981) State of Disequilibrium Between ^{238}U, ^{234}U, ^{226}Ra and ^{222}Rn in Groundwater from Bedrock, Geochimica et Cosmochimica Acta 45, 201-206

Asikainen, M. and Kahlos, H. (1980) Natural Radioactivity of Drinking Water in Finland, Health Physics 39, 77-83

Barnes, I. (1964) Field measurement of Alkalinity and pH. Geological Survey Water-Supply Paper 1535-H, USGPO, Washington.

Batley, G.E. and Gardner, D. (1977) Sampling and Storage of Natural Waters for Trace Metal Analysis, Water Research 11, 745-756

Brookins, D.G. (1988) Eh-pH Diagrams for Geochemistry, Springer-Verlag, New York.

Chapelle, F.H., Morris, J.T., McMahan, P.B. and Zelibor, J.L. (1988) Bacterial Metabolism and the ^{13}C Composition of Groundwater, Floridan Aquifer System, South Carolina, Geology 16, 117-121

Dearlove, J.P.L., Longworth, G., Ivanovich, M., Kim, J.I., Delakowitz, B. and Zeh, P. (1991) A Study of Groundwater-Colloids and their Geochemical Interactions with Natural Radionuclides in Gorleben Aquifer Systems, Radiochimica Acta 52/53, 83-89

Degueldre, C., Baeyans, B., Goerlich, W., Riga, J., Verbist, J. and Stadelmann, P. (1989) Colloids in Water from a Subsurface Fracture in Granitic Rock, Grimsel Test Site, Switzerland, Geochimica et Cosmochimica Acta 53, 603-610

Dickson, B.L. and Meakins, R.L. (1984) An Observation of Rapid Mobilisation of Uranium and its Decay Products, Nuclear Instruments and Methods in Physics Research 223, 593-597

Dickson, B.L. and Snelling, A.A. (1980) Movements of Uranium and Daughter Products in the Koongarra Uranium Deposit. In Ferguson, J. and Goleby, B. (eds.) Uranium in the Pine Creek Geosyncline. IAEA, Vienna.

Dongarra, G. and Langmuir, D. (1980) The Stability of UO_2OH^+ and $UO_2(HPO_4)_2^{2-}$ complexes at 25°C, Geochimica et Cosmochimica Acta 44, 1747-1751

Donnelly, T.H. and Ferguson, J (1980) A Stable Isotope Study of Three Deposits in the Alligator Rivers Uranium Field, NT. In Ferguson, J. and Goleby, B. (eds.) Uranium in the Pine Creek Geosyncline. IAEA, Vienna.

Drever, J.I. (1988) The Geochemistry of Natural Waters (second edition), Prentice-Hall, New Jersey.

Freeze, R.A. and Cherry, J.A. (1979) Groundwater. Prentice-Hall, New Jersey.

Giblin, A.M. and Snelling, A.A. (1983) Application of Hydrogeochemistry to Uranium Exploration in the Pine Creek Geosyncline, Northern Territory, Australia, Journal of Geochemical Exploration 19, 33-55

Gole, M.J., Butt, C.R.M. and Snelling, A.A. (1986) A Groundwater Helium Survey of the Koongarra Uranium Deposits, Pine Creek Geosyncline, Northern Territory, Uranium 2, 343-360

Golian, C., Nightingale, T. and Airey P.L. (1984) Protactinium-231 Measurement and Application to a Uranium-series Transport Model, Nuclear Instruments and Methods in Physics Research 223, 577-581

Grossman, E.L., Coffman, B.K., Fritz, S.J. and Wada, H. (1989) Bacterial Production of Methane and its Influence on Groundwater Chemistry in East-Central Texas Aquifers, Geology 17, 495-499

Hussain, N. and Krishnaswami, S. (1980) U-238 Series Radioactive Disequilibrium in Groundwaters : Implications to the Origin of Excess U-234 and Fate of Reactive Pollutants, Geochimica et Cosmochimica Acta 44, 1287-1291

IAEA, (1983) Isotope Techniques in the Hydrogeological Assessment of Potential Sites for the Disposal of High-level Radioactive Wastes. Technical Reports Series No. 228, International Atomic Energy Agency, Vienna.

Ivanovich, M., Duerden, P., Payne, T.E., Nightingale, T., Longworth, G., Wilkins, M.A., Hasler, S.E., Edgehill, R.B., Cockayne, D.J. and Davey, B.G. (1988) Natural Analogue Study of the Distribution of Uranium Series Radionuclides Between the Colloid and Solute Phases in the Hydrogeological System of the Koongarra Uranium Deposit, Australia. (Report AERE-R 12975) United Kingdom Atomic Energy Authority, Harwell.

Kim, J.I., Buckau, G., Baumgartner, F., Moon, H.C., and Lux, D. (1984) Colloid Generation and the Actinide Migration in Gorleben Groundwaters. In McVay, G.L. (ed) Scientific Basis for Nuclear Waste Management VII. Elsevier Science Publishers, New York.

King, P.T., Michel, J. and Moore, W.S. (1982) Ground Water Geochemistry of ^{228}Ra, ^{226}Ra and ^{222}Rn, Geochimica et Cosmochimica Acta 46, 1173-1182

Langmuir, D. (1978) Uranium Solution-Mineral Equilibria at Low Temperature with Applications to Sedimentary ore Deposits, Geochimica et Cosmochimica Acta 42, 547-569

Lee, R.D., Watson J.E. and Fong, S.W. (1979) An Assessment of Radium in Selected North Carolina Drinking Water Supplies, Health Physics 37, 777-779

Lei, W., Linsalata, P., Franca, E.P. and Eisenbud, M. (1986) Distribution and Mobilisation of Cerium, Lanthanum and Neodynium in the Morro do Ferro Basin, Brazil, Chemical Geology 55, 313-322

Lindberg, R.D. and Runnells, D.D. (1984) Ground Water Redox Reactions: An Analysis of Equilibrium State Applied to Eh Measurements and Geochemical Modelling, Science 225, 925-927

Malo, B.A. (1977) Partial Extraction of Metals from Aquatic Sediments, Environmental Science and Technology 11, 277-282

Markovic, M. and Pavkovic, N. (1983) Solubility and Equilibrium Constraints of Uranium in Phosphate Solutions, Inorganic Chemistry 22, 978-982

Miekeley, N., Jesus, H.C., Silveira, C.L.P. and Kuechler, I.L. (1989) Colloid Investigations in the Pocos de Caldas' Natural Analogue Project. In Lutz W. and Ewing R.C. (eds.) Scientific Basis for Nuclear Waste Management XII. Materials Research Society, Pittsburgh.

Murakami, T., Isobe, H. and Edis, R. (1991) Effects of Chlorite Alteration on Uranium Redistribution in Koongarra, Australia. In Abrajano, T. and Johnson, L.H. (eds.) Scientific Basis for Nuclear Waste Management XIV. Materials Research Society, Pittsburgh.

Nightingale, T.J. (1988) Mobilisation and Redistribution of Radionuclides During Weathering of a Uranium Orebody, MSC Thesis, University of Sydney, Australia.

Noller, B.N., Currey, N.A., Ayers, G.P. and Gillett, R.W. (1990) Chemical Composition and Acidity of Rainfall in the Alligator Rivers Region, Northern Territory, Australia, The Science of the Total Environment 91, 23-48

Noranda, (1978) Koongarra Project - Draft Environmental Impact Statement, Noranda Australia Limited, Melbourne.

Nordstrom, D.K. (1977) Thermochemical Redox Equilibria of ZoBell's Solution, Geochimica et Cosmochimica Acta 41, 1835-1841

Nozaki, Y. and Horibe, Y. (1983) Alpha-emitting Thorium Isotopes in Northwest Pacific Deep Waters, Earth and Planetary Science Letters 65, 39-50

Osmond, J.K. amd Cowart, J.B. (1982) Groundwater. In Ivanovich, M. and Harmon, R.S. (eds.) Uranium Series Disequilibrium: Application to Environmental Problems. Clarendon Press, Oxford.

Osmond, J.K., Cowart, J.B. and Ivanovich, M. (1983) Uranium Isotopic Disequilibrium in Groundwaters as an Indicator of Anomolies, International Journal of Applied Radiation and Isotopes 34, 283-308

Sheng, Z.Z. and Kuroda, P.K. (1986) Isotopic Fractionation of Uranium: Extremely High Enrichments of ^{234}U in the Acid Residues of a Colorado Carnotite, Radiochimica Acta 39, 131-138

Short, S.A., Lowson, R.T. and Ellis, J. (1988) $^{234}U/^{238}U$ and $^{230}Th/^{234}U$ Activity Ratios in the Colloidal Phases of Aquifers in Lateritic Weathered Zones, Geochimica et Cosmochimica Acta 52, 2555-2563

Snelling, A.A. (1980) Uraninite and its Alteration Products, Koongarra Uranium Deposit, in Uranium in the Pine Creek Geosyncline, (eds) J. Ferguson and A.B. Goleby, IAEA, Vienna.

Stenstrand, K., Annanmaki, M. and Rytomaa, T. (1979) Cytogenetic Investigation of People in Finland using Household Water with High Natural Radioactivity, Health Physics 36, 441-444

Strain, C.D., Watson, J.E. and Fong, S.W. (1979) An Evaluation of ^{226}Ra and ^{222}Rn Concentrations in Ground and Surface Water Near a Phosphate Mining and Manufacturing Facility, Health Physics 37, 779-783

Tripathi, V.S. (1983) Uranium(VI) Transport Modelling: Geochemical Data and Submodels. PhD Thesis, Stanford University, California.

Vilks, P., Cramer, J.J., Shewchuk, T.A. and Larocque, J.P.A. (1988) Colloid and Particulate Matter Studies in the Cigar Lake Natural-Analog Program, Radiochimica Acta 44/45, 305-310

GUIDE TO APPENDICES

The appendices contain details of field and analytical techniques and provide full tabulations of all data collected during the ARAP and referred to in the text of this volume.

APPENDIX 1 ANALYTICAL TECHNIQUES

APPENDIX 1

ANALYTICAL TECHNIQUES

1.1 MEASUREMENT OF URANIUM-SERIES ISOTOPES BY GAMMA SPECTROMETRY

(This analytical procedure was used at the Japan Atomic Energy Research Institute)

Groundwater samples were obtained with a submersible pump, using packers to limit the source of the sampled groundwater, as detailed in Section 3. Samples were filtered through a 1.0 μm pore-size (or smaller) membrane filter and acidified with 70% HNO_3 (10 mL HNO_3/1000 mL groundwater). Samples were stored in polycarbonate or polyethylene bottles.

Radon-222 and ^{226}Ra in the groundwater were measured directly by gamma spectrometry (hereafter referred to as the "direct method"), and the other isotopes were measured by gamma spectroscopy after evaporation of the groundwater to dryness (hereafter referred to as the "evaporation method"). The concentrations of ^{238}U and $^{234}U/^{238}U$ activity ratios in the residue of groundwater were also analysed by alpha spectrometry.

Due to the depressurisation of the groundwater upon being brought to the surface, some degassing of CO_2 may have occurred, since these groundwaters contain elevated partial pressures of CO_2 (Section 6.6). This may have resulted in some loss of ^{222}Rn, in which case the ^{222}Rn data may regarded as lower limits.

1.1.1 Direct Method

For the determination of ^{222}Rn and ^{226}Ra, about 250-500 mL of groundwater was collected in a polyethylene or polycarbonate bottle. At the time of analysis, the exact amount of the sample solutions was determined by weighing, and the amount of added HNO_3 was allowed for in subsequent calculations. They were measured using an ORTEC Ge detector (closed end coaxial type, N type crystal) for 5,000-50,000 seconds, with the count-time depending on the activity of the sample. The combined $^{222}Rn+^{226}Ra$ concentration was determined from the 352 keV peak of ^{214}Pb, or the 609 keV peak of ^{214}Bi. These are both daughter nuclides of ^{222}Rn. Figure A1.1 shows a spectrum of groundwater collected at 23-25 m in drill hole W4.

In order to check the tightness of sample bottles for ^{222}Rn gas leakage, some samples with high ^{222}Rn activities were measured repeatedly. For these samples, the ^{222}Rn activity decreased in accordance with the half-life of ^{222}Rn (3.8 days), from which it was concluded that leakage of ^{222}Rn from the sample bottles was negligible.

After two months, all the samples were measured again (for 30,000-300,000 sec), to determine the ^{226}Ra concentration (by this time several half-lifes of ^{222}Rn had elapsed, so the contribution from ^{222}Rn was insignificant). The original ^{222}Rn concentration was calculated by subtraction of the ^{226}Ra activity from the ^{222}Rn+^{226}Ra concentration. Appropriate corrections for radioactive decay from the time of sampling to the commencement of the measurements, and during the measurements, were included in all calculations.

The detector was calibrated by the measurement of a ^{226}Ra standard solution obtained from Amersham, UK, with the same conditions as for the sample measurement. The same samples were then analysed by the evaporation method described in the next section.

1.1.2 Evaporation Method

The groundwater samples (500-2000 mL) for the determination of ^{238}U, ^{226}Ra and ^{210}Pb, were weighed, then evaporated to about 100 mL in a glass beaker. They were then transferred to a plastic vessel (inner diameter 32 mm or 24 mm), and the evaporation was continued to near dryness using an infra-red lamp. The dried residual sample was sealed and measured by gamma spectrometry using an ORTEC LO-AX detector (51 mm and 19 mm in diameter and thickness, respectively). Uranium-238, ^{226}Ra and ^{210}Pb were determined from the gamma-ray peaks at 63 keV (of ^{234}Th), 186 keV and 46.5 keV respectively. For the determination of ^{226}Ra in the residual sample, the contribution to the 186 keV peak from ^{235}U was subtracted. This was done using the counts in the 63 keV peak, using a constant activity ratio ($^{235}U/^{238}U$=0.046), which was calculated from the natural abundance of ^{235}U (0.720 atom%) and ^{238}U (99.275 atom%). The 352 keV or 609 keV peaks (used for determinations in the direct method) were not used in this case, as a waiting time for the equilibration between ^{222}Rn and daughter nuclides (^{214}Pb and ^{214}Bi) would have been required. Furthermore, leakage of ^{222}Rn from the measurement vessel may have introduced a source of error.

The detector was calibrated by the measurement of ^{238}U and ^{226}Ra powder rock standards obtained from NBL (New Brunswick Laboratory), USA, with the same conditions as for the sample measurement. Figure A1.2 shows a spectrum of the residue of groundwater collected at 23-25 m in W4 drill hole.

For the subsequent analysis of ^{238}U and ^{234}U, ^{232}U yield tracer and 6 M HCl were then added to the residue used in the previous determination. After more than 2 weeks, the liquid phase was filtered through a 0.45 μm Millipore membrane. The uranium leached from the residue was purified by chemical separation and measured by alpha spectrometry, using similar procedures to those described in the following section.

1.2 URANIUM, THORIUM, AND ACTINIUM MEASUREMENT BY ALPHA SPECTROMETRY

(These procedures were used at Environmental Science Program, ANSTO)

1.2.1 Field Sampling

Filtered groundwater samples were obtained using the procedures outlined in Section 3.1. The standard filter pore-size was 0.45 μm. For uranium analysis, a sample of 1000 mL was usually sufficient to provide adequate uranium for determination by alpha spectrometry, but in some cases 2 L or 5 L samples were obtained. Samples were acidified to pH < 1.5 by adding HNO_3 (70 % - A.R. grade or better), using 10 mL per litre of sample.

Because of the low levels of thorium isotopes in filtered groundwater, much larger samples (20 L or 50 L) were required for the accurate determination of thorium. In some cases (when uranium levels were low), these larger samples were also used for measuring ^{238}U concentrations and $^{234}U/^{238}U$ ratios. Thorium (and uranium) were co-precipitated from these samples with $Fe(OH)_3$. It was preferable to do this precipitation in the field, as several samples (totalling hundreds of litres) could be reduced to a few small bottles by this means. Drums were rinsed with acidified groundwater before use and covered by plastic film during the procedure.

The co-precipitation procedure is as follows:

1) Wash sample drum, a 1 L bottle and any other containers to be used thoroughly with acidified sample water.

2) Fill the drum with groundwater, seal and remove from the vicinity of the ore-body, which is a potential source of airborne radionuclide-bearing dust contamination.

3) Determine the mass sampled, either by filling to a known volume or by weighing.

4) Acidify using A.R. HNO_3.

5) Add contents of a previously prepared Fe/tracer vial, containing a $Fe(NO_3)_3/HNO_3$ solution with a known amount of tracer for Th and/or U.

6) Shake, allow to stand for at least one hour to equilibrate.

7) Add concentrated A.R. ammonia and continue to shake until a red colour appears. Add a slight excess (to pH about 7).

8) Shake thoroughly and allow the precipitate to settle for a day or more. Repetitively decant off as much of the supernatant as possible, allowing time to settle after each step.

9) When volume is below about 5 litres, start to transfer the slurry into the previously washed one litre plastic bottle.

10) Allow the precipitate to settle in this second bottle, decant the supernate, then add more slurry from the drum. Repeat until all the $Fe(OH)_3$ is in the small bottle.

While maximum recovery of the $Fe(OH)_3$ is desirable, quantitative recovery is not required as the tracers are added before the precipitation step. For thorium analyses, ^{229}Th was used as a tracer. For low-level uranium determinations, ^{236}U or ^{232}U can be used, the latter only being suitable if ^{228}Th is not being determined.

1.2.2 Analysis Procedure

The procedures are based on standard radio-chemical techniques (Korkisch, 1969; Lally, 1982).

If tracer has not already been added, add ^{236}U, ^{232}U, or ^{229}Th as required. Evaporate samples to about 50 mL volume on a hotplate, then add concentrated A.R. grade HCl sufficient to bring the HCl to between 6 M and 9 M. Filter any precipitate which may result (Silica and other species usually precipitate during the evaporation or upon addition of HCl).

The sample is then passed through a Bio-Rad^R AG1-X8 anion exchange column, in the 6 - 9 M HCl solution. Uranium is retained, whereas thorium and radium isotopes pass through. The uranium fraction is washed off the column using 1.0 M HCl. This ensures that other impurities (eg Po if present) are retained by the column. The uranium fraction will also contain the Fe, which may be present in substantial amounts, particularly if $Fe(OH)_3$ precipitation has been used to concentrate the sample. The Fe must be removed, by extraction from 9M HCl solution into di-isopropyl ether. Note that an explosion and fire hazard exists with this reagent. This extraction should be repeated until there is no yellow colour in the 9 M HCl. The sample is then carefully evaporated to dryness, dissolved in an electrolyte (0.20 M Ammonium Acetate/0.27 M HNO_3), and electrodeposited onto a stainless steel disc for α-spectrometry.

The >6 M HCl fraction containing thorium and radium (which passed through the AG1-X8 column), is then evaporated repeatedly to dryness with 8 M HNO_3 to drive off all traces of Cl. At the same time, a second AG1-X8 column is prepared, and repeatedly conditioned by washing with 8 M HNO_3. This conditioning should continue until the effluent from the column is negative to a test for Cl. The presence of any Cl will prevent the retention of thorium by the column. The Th/Ra fraction is then passed through the conditioned column in 8 M HNO_3. The Ra passes through, and the Th is retained. The thorium fraction is then washed off the column with 1.0 M HCl, and slowly evaporated to dryness. The sample is finally taken up in the ammonium acetate electrolyte and electrodeposited on a stainless steel planchette for alpha spectrometry.

The counting system used was an ORTEC Alpha-King^{R} Spectrometer interfaced via a Multi-channel Buffer to a personal computer. Data collection and manipulation were facilitated using the Spectrum-Master^{R} software package.

Reagent blank solutions were also carried through the separation and analysis procedure and, where necessary, data were corrected for any blank contribution. Whilst routinely required in thorium analysis, corrections to uranium data were not needed.

For ^{227}Ac determination, the time at separation of the daughter ^{227}Th from the ^{227}Ac should be recorded to allow for corrections to be made for decay during chemical separations and counting. Most of the other isotopes analysed by alpha spectrometry had sufficiently long half-lives that this was not required.

1.2.3 Data Treatment

The α-spectra for uranium were straightforward to interpret, since the peaks of ^{238}U, ^{236}U, and ^{234}U are well separated in energy, and the electrodeposited samples gave well resolved spectra. The count-rates were corrected for a very minor detector background, and allowance was made for peaks of ^{235}U, which are in the same energy range as ^{236}U. This correction is readily made, because the peak of ^{235}U is in a fixed proportion to that of ^{238}U. In cases where ^{232}U was used, this peak appeared at a higher energy than the other uranium isotopes and was again well resolved.

The thorium spectra for groundwater samples generally had very low count-rates. This was due to the very low mobility of thorium in groundwater. Usually a ^{230}Th peak was discernible, and in some cases, a peak of ^{232}Th. These isotopes were quantified by their count-rates relative to the peak of ^{229}Th. Peaks of ^{228}Th were invariably seen in the α-spectrum, but this was attributed to the presence of its parent ^{228}Ra in the groundwater at the time of sampling. During sample storage, ingrowth of ^{228}Th from this source probably swamped the ^{228}Th originally in the sample. Therefore, the ^{228}Th was not quantified from the thorium α-spectrum.

The thorium spectra for some of the fine-particle and colloid fractions discussed in Section 9 showed an unusual feature - substantial peaks of ^{227}Th were present, as well as peaks from its daughters ^{219}Rn, ^{215}Po and ^{211}Bi (Figure 9.4). These are all members of the ^{235}U decay chain and are not normally prominent in α-spectra on account of the much higher activity of isotopes in the ^{238}U series. The peaks of ^{227}Th indicated the presence of ^{227}Ac in the samples (since the half-life of ^{227}Th is only 19 days and the samples had been stored for some months at the time of analysis).

The amount of ^{227}Ac was determined using the integral of the higher energy ^{227}Th doublet at 5.9-6.1 MeV, thus avoiding the more complex corrections in the 5.6-5.9 MeV energy region (Golian et al., 1984). The count rate was corrected for a minor contribution of ^{211}Bi, and allowance was made for the decay of unsupported ^{227}Th after separation from its parent.

1.3 URANIUM DETERMINATION USING THE KINETIC PHOSPHORESCENCE ANALYSER (KPA)

The Kinetic Phosphorescence Analyser (KPA) enables rapid determination of uranium concentrations to be made in aqueous samples, with good sensitivity and accuracy provided that interferences are not present.

The KPA instrument (KPA-10) installed at ANSTO, Lucas Heights was manufactured by Chemchek Instruments (USA). In the KPA, a laser pulse is used to electronically excite uranyl-containing ions. The excited phosphor then returns to the ground state with the emission of a photon, following first order kinetics. The KPA measures the time-dependent decay of light intensity, and, by extrapolation to time zero (ie. the end of the laser pulse) calculates the initial intensity, which is proportional to the uranium concentration. For good precision, several hundred laser pulses are used in each measurement and the results averaged.

The operation of the KPA is straightforward, and is controlled through a personal computer. One, or preferably several standards spanning the concentration range of interest are used to calibrate the instrument. In each case, 1.0 mL of standard and 1.5 mL of uraplex (a proprietary complexing agent) are placed in a 1.0 cm square sample cell and the emission intensity measured.

After calibration, samples are measured in a similar manner. The KPA is essentially a sealed box and no operator adjustments other than sample changing are required.

Groundwater samples from Koongarra proved to be extremely suitable for uranium analysis using the KPA, with no treatment other than acidification with HNO_3 being required prior to measurement. The results obtained were in excellent agreement with the other techniques, namely ICPMS and α-spectrometry. Figure A1.3 and Table A6.2 shows a good correspondence between data obtained by the KPA and by ICPMS over a wide concentration range. The KPA detection limit for uranium was about 0.1 ppb and the accuracy was about ±3 % at 50 ppb.

Further investigations with groundwater samples from other areas showed that interferences (particularly chloride) caused results obtained for saline groundwaters to be highly unreliable. Treatment of such samples to remove chloride appears to be promising, but as yet has not been fully successful.

In summary, the KPA provided an accurate, fast, and reliable instrument for measuring total uranium concentrations in Koongarra groundwaters. These groundwaters do not contain high levels of elements which interfere with this analysis. Interferences should be considered when assessing the suitability of KPA for other applications. In addition, it should be noted that techniques such as ICPMS or α-spectrometry provide data on a suite of elements and isotopes, rather than a single element, as is the case for the KPA.

1.4 RADIUM ANALYSIS PROCEDURE USED AT ANSTO

(Procedure used in the ANSTO Low-level Laboratory for ARAP samples)

1 Obtain the sample in 900 mL water with no acid concentration (of any type - HCl, HNO_3 or $HClO_4$) > 1 M. If the original sample does not contain at least 50 mg of Ba, add 100 mg Ba^{2+} carrier. ^{133}Ba tracer (~70 nCi) should also be present from dissolution of the original sample.

2 Add 20 mL CH_2SO_4 and 100 mL 20% Na_2SO_4.

3 Slowly add, with stirring 100 mg Pb^{2+} carrier (in 0.1 M acid) as 10 mL x 10 mg/mL solution.

4 Allow $Pb/Ba/RaSO_4$ precipitate to settle overnight.

5 Remove supernatant by suction with a water pump.

6 Transfer the fine white precipitate to a 50 mL centrifuge tube with 50% ethanol.

7 Centrifuge to pack down the $Pb/Ba/RaSO_4$ precipitate, and discard supernatant.

8 Wash walls of centrifuge tube down with 95% ethanol to collect any precipitate scum. Centrifuge to pack down, then discard wash.

9 Add 5 mL of 0.2 M Na_5 DTPA (pH 10.5) and 1 drop of universal indicator. Add drops of 10 M NaOH if necessary to render pH > 7. Warm to dissolve all sulphate precipitate.

10 Pass through a 0.45 μm disposable membrane filter into a clean, pre-rinsed polystyrene vial.

11 Add 5 mL 20% Na_2SO_4.

12 Add 2 mL 1:1 acetic acid/water rapidly to the solution.

13 Immediately add 1 mL $BaSO_4$ seeding suspension. Sit vial in cold water bath for a minimum 30 minutes.

14 Collect colloidal $Ba/RaSO_4$ precipitate on a shiny-surfaced Millipore "VV" type 25 mm diameter 0.1 μm filter (if ^{228}Ra analysis is to follow) or a Gelman "Supor" 25 mm 0.1 μm filter in a Gelman filter apparatus.

15 Rinse vial and filter funnel walls with a little 95% ethanol to ensure collection of all precipitate.

16 Disassemble filter unit and dry filter (face-up) on a filter pad.

17 Collect gamma spectrum for 10 minutes and measure ^{133}Ba using the 386 keV peak.

18 Collect an alpha spectrum for ^{226}Ra analysis.

Notes:

i Do not use cellulose nitrate/acetate conventional membrane filters (eg Millipore VC or VM). Supor membranes are not compatible with subsequent ^{228}Ra analysis.

ii If Th and Ra analyses are required (but not U) the Th co-precipitates with the $PbSO_4$ and may be recovered by evaporation and digestion (with 5 mL $CHClO_4$/5 mL $CHNO_3$) of the retained filtrate from the $Ba/RaSO_4$ source preparation.

- S. Short (ANSTO)

1.5 MEASUREMENT OF PHOSPHATE IN KOONGARRA GROUNDWATERS

Phosphate in Koongarra groundwaters is below the detection limit (1 mg/L) of ion-exchange chromatography. Therefore, during the ARAP, a spectrophotometric method was adopted (with slight modifications) and a detection limit of 5 μg/L was achieved.

Initially, samples were taken in duplicate and stored in iodine-impregnated polyethylene bottles (Heron, 1962). This enabled measurements of both 'dissolved reactive phosphorus' and 'dissolved acid-hydrolysable phosphorus' to be made. It was concluded that the latter was a preferable and reproducible measure of the amount of phosphate present, since it was free from the problem of post-sampling oxidation of dissolved Fe^{2+}. The resulting precipitation of ferric hydroxides could cause removal of phosphate from solution by adsorption. Therefore, subsequent determinations were made on samples which were acidified at the time of collection using concentrated HCl (0.5 mL in 250 mL sample) and only total phosphate was measured.

The method used was a standard ascorbic acid /molybdenum blue method (APHA, 1985). Orthophosphate reacts with ammonium molybdate and potassium antimonyl tartrate under acidic conditions to form phosphomolybdic acid which is reduced to molybdenum blue by ascorbic acid. The absorbance was measured at 880 nm, and at least one standard was measured with each set of groundwater samples. Long path-length cells (50 mm) were used to maximise sensitivity. Blank measurements were made on de-ionised water samples which had been treated in the same way as the groundwater samples. These blanks invariably yielded

apparent phosphate contents below the detection limit. Measurements were made using a Shimadzu UV-240 spectrophotometer. The calibration curve of absorbance against the PO_4 concentration of known standards was linear.

For comparative purposes some in-field determinations were made using the Chemette^R phosphate test-kit. Excellent agreement with laboratory measurements was demonstrated (Table A1.1), although the precision of the in-field measurements was substantially lower, as might be expected.

1.6 QUANTITATIVE AND SEMI QUANTITATIVE ANALYSES BY INDUCTIVELY-COUPLED PLASMA MASS SPECTROMETRY (ICPMS)

(Analyses carried out by CSIRO, Lucas Heights)

The development of ICPMS in the 1970s and the introduction of commercial instruments in the early 1980s provided the analytical chemist with a powerful tool for the analysis of a wide range of elements at the trace and ultra-trace levels of concentration. This was brought about by the successful interfacing of the inductively-coupled plasma (ICP) and the quadrupole mass spectrometer. The ICP is a high temperature source in which most elements are highly ionised.

The ions are extracted from the source through the interface and separated by the fast scanning mass spectrometer. Ion currents are measured by conventional pulse counting electronics. The combination of these two components results in an instrument which has extremely high powers of detection for most elements. Since it uses a conventional ICP nebulisation system for sample introduction the sample throughput is high.

The instrument in operation at the Lucas Heights Research Laboratories is a VG Plasmaquad PQ2. A schematic diagram of the instrument components is shown in Figure A1.4. The facility is jointly owned by the CSIRO Divisions of Exploration Geoscience and Fuel Technology, the Australian Nuclear Science and Technology Organisation (ANSTO) and the Office of the Supervising Scientist (OSS).

It is operated for the partners by Fuel Technology's Centre for Advanced Analytical Chemistry. A wide range of applications is therefore covered. These include materials characterisation, geochemical studies of mineral deposits, uranium mining and processing, environmental monitoring of aquatic systems and studies in occupational health and hygiene.

The major advantages of the application of ICPMS over other instrumental methods of analysis are the very low detection limits (0.1 to 0.01 parts per billion) for most elements, good precision and especially its multi-element capability. A number of different analytical procedures can be employed, eg full semi-quantitative analysis for up to 70 elements, quantitative analysis of any selected suite of elements, isotope abundance measurements and isotope dilution analysis for high precision and accurate analysis.

1.6.1 Semi-quantitative scan

In this procedure a full mass range scan is made of the sample. Data from up to 100 sweeps of the mass range are accumulated in about one minute. The sample is spiked with an internal standard, which is usually indium at a concentration of 0.1 ppm. Indium is chosen because of its very low abundance in nature and because its major isotope is at mass 115 which is about the middle of the mass range. Its purpose is to monitor the sample transport into the ICP and account for any matrix effects arising from sample components. The concentrations of all other elements are determined by direct interpolation of the counts for specified isotopes of the elements with the In-115 isotope counts. As this procedure does not take into account differences in relative sensitivities arising mainly from the ionisation potentials of the elements, and uses a one point calibration, the results are semi-quantitative only. While these data lack accuracy, the precision is quite good. The good reproducibility indicates that this type of analysis is suitable for survey analysis and for monitoring trends in a batch of samples.

1.6.2 Quantitative analysis

The semi-quantitative scan may be used to identify elements of interest in a sample. These elements may then be determined using a quantitative procedure based on standard calibration curves. In this type of procedure a suite of elements is determined by measuring selected isotopes of the elements and an internal standard isotope using a peak jump mode rather than scanning. A calibration curve is developed for each element. Using this type of procedure the precision is generally about 5 per cent with a sample measurement time of three to four minutes. Higher precision may be achieved by increasing the measurement time. By optimising the instrumental conditions and measurement parameters, detection limits of five parts per trillion are possible.

Another method of quantitative analysis is based on scanning. This procedure, used for the ARAP project, involves scanning samples over the full mass range. Standards covering the elements of interest in the appropriate concentration range are also scanned. Quantitative analysis is then performed for the nominated elements. The advantage of this type of procedure is that both quantitative data can be produced for specific elements as well as semi-quantitative data for all other elements.

- L. Dale (CSIRO)

1.7 TOTAL ORGANIC CARBON MEASUREMENT

(Analyses carried out by CSIRO, Lucas Heights)

The waters were analysed using the Photocatalytic Oxidation (PCO) technique. The oxidation is effected by the powerful photocatalytic properties of titanium dioxide excited by bandgap (<380 nm) illumination. All organic matter in the water is converted to carbon-dioxide under the analytical conditions and transferred through a gas interface to a calibrated high sensitivity conductivity cell.

The pH of each water sample was adjusted to 3.5 before analysis to remove inorganic carbonate and to ensure that during the PCO organic carbon was converted to the molecular form of CO_2 in solution. The pH adjustment was with dilute $HClO_4$ or dilute KOH according to whether the initial pH of the water was acid or alkaline.

The blank of the method was 0.25±0.03 μg/g (0.25±0.03 mg/L). Precision was ±6% at the 1 μg/g level.

- R. Matthews (CSIRO)

References

American Public Health Association (1985) Standard Methods for the examination of Water and Wastewater. Sixteenth Edition.

Golian, C., Nightingale, T. and Airey, P.L. (1984), Protactinium-231 Measurement and Application to a Uranium-Series Transport Model, Nuclear Instruments and Methods in Physics Research, 223, 577-581.

Heron, J. (1962) Determination of phosphate in water after storage in polyethylene. Limnol. Oceanogr. 7, 316-321.

Korkisch, J. (1969) Modern Methods for the Separation of Rarer Metal Ions. Pergamon, Oxford.

Lally, A. E. (1982) Chemical Procedures. In: Ivanovich, M. and Harmon R.S. (eds.) Uranium Series Disequilibrium - Applications to Environmental Problems. Clarendon Press, Oxford.

TABLE A1.1

LABORATORY AND FIELD PHOSPHATE DETERMINATIONS

(May 1990 Field Trip)

Bore	Depth (m)	Lab PO_4 mg/L	Field Chemettes mg/L
W1a W1b	13-15 23-25	<.005 0.360	0.0 0.5
W2a W2b	13-15 23-25	0.030 0.105	0.0 0.1
W4a W4b	13-15 23-25	0.010 0.075	0.0 0.05/0.1
W5a W5b	13-15 23-25	0.530 0.515	0.6/0.7 0.6
W7a W7b	13-15 23-25	0.100 0.415	0.1 0.3/0.4
PH49	18-20	0.140	0.1/0.2
C9	28-30	0.095	0.1
M1	27-29	0.085	<0.1
M2	42-44		0.0
M4	28-30	0.575	0.4/0.6
KD1	65-76	<0.005	0.0

The chemettes technique is a colorimetric analysis based on comparisons of colour intensity. Therefore it is dependent on the observer. Two values are given when borderline values were obtained.

Laboratory values by spectrophotometry (see text).

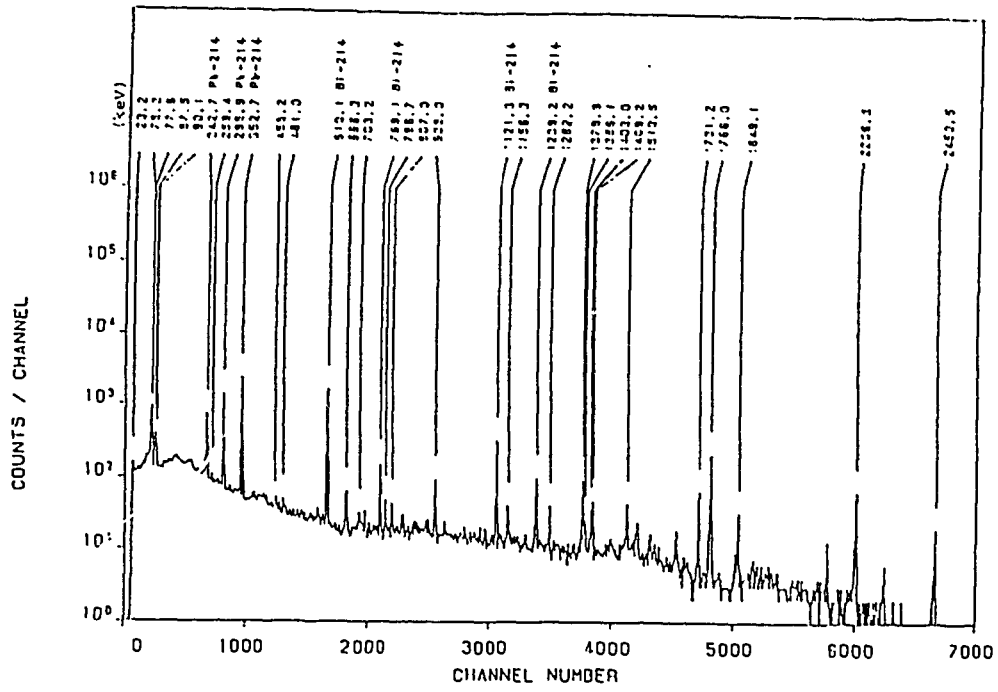

FIGURE A1.1 Gamma-ray spectrum of W4 (23-25 m) groundwater sample measured by the direct method.

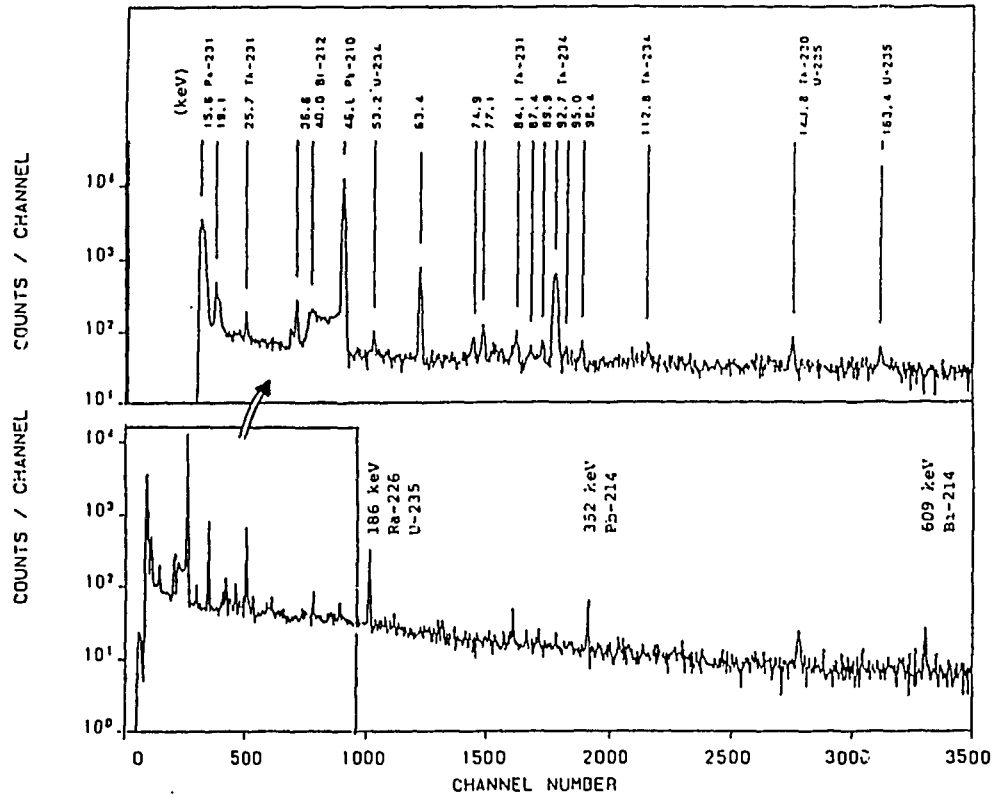

FIGURE A1.2 Gamma-ray spectrum of W4 (23-25 m) groundwater residue measured by the evaporation method.

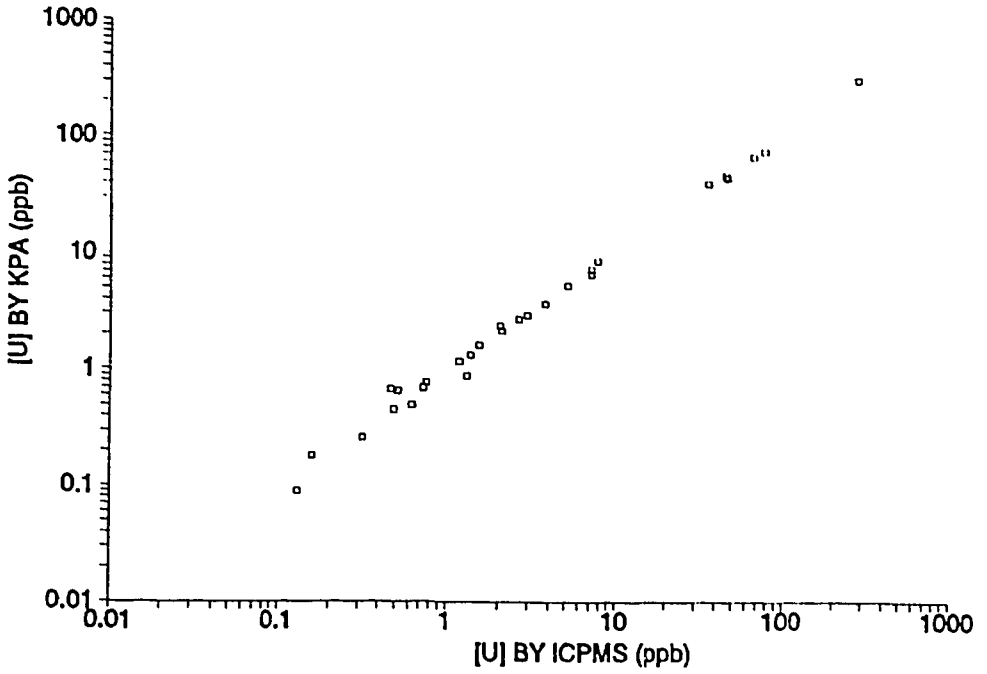

FIGURE A1.3 Comparison of KPA and ICPMS [U] data

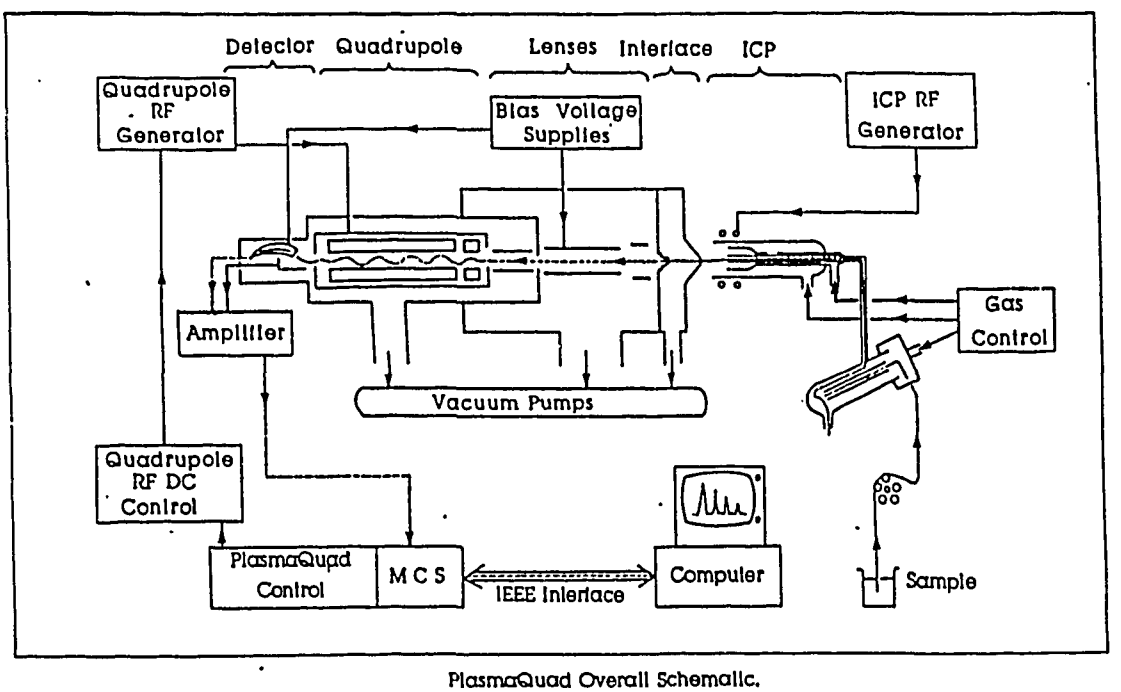

FIGURE A1.4 Overall schematic of Plasmaquad[R] ICPMS instrument

APPENDIX 2 ISOTOPIC DATA

Note: For groundwater samples collected during ARAP, total uranium concentrations were routinely measured by quantitative ICPMS. All ICPMS data for total uranium concentration is tabulated in Appendix 3. Appendix 2 includes data for uranium-series isotopes obtained by radiochemical techniques.

TABLE A2.1

^{238}U CONCENTRATIONS AND $^{234}U/^{238}U$ ACTIVITY RATIOS IN KOONGARRA GROUNDWATER SAMPLES DETERMINED BY ALPHA-SPECTROMETRY

(Technique in Appendix 1.2)

		May 1988 Field Trip		November 1988 Field Trip	
Borehole	Depth (m)	[U] µg/L	$^{234}U/^{238}U$	[U] µg/L	$^{238}U/^{238}U$
PH14	20-26	54.0(2.6)	0.73(0.03)	17.8(0.8)	0.88(0.05)
PH15	19-21	141.1(4.6)	1.00(0.02)	30.6(0.9)	0.99(0.03)
PH49	28-30	274.1(6.9)	1.064(0.013)	101.5(3.0)	1.015(0.023)
PH49	44-46	310.0(8.1)	1.197(0.013)	130.4(3.5)	1.080(0.020)
PH55	26-28	0.42(0.03)	0.97(0.08)	0.62(0.04)	1.12(0.05)
PH55	40-42	1.04(0.05)	1.03(0.03)	1.01(0.07)	1.11(0.06)
PH56	26-28	12.3(0.3)	0.824(0.012)	7.71(0.26)	0.86(0.03)
PH56	43-45	11.8(0.3)	1.095(0.022)	4.33(0.12)	1.01(0.02)
PH58	25-27	1.66(0.08)	0.91(0.06)	2.02(0.11)	1.01(0.04)
PH58	38-40	0.58(0.03)	1.41(0.10)	1.01(0.05)	1.14(0.08)
PH61	26-28	4.08(0.16)	0.93(0.02)	2.95(0.15)	0.95(0.04)
PH61	43-45	5.67(0.28)	1.15(0.05)	2.15(0.11)	1.02(0.06)
PH80	17-20	13.6(0.4)	0.744(0.013)	4.54(0.27)	0.82(0.03)
PH88	28-30	2.19(0.08)	0.93(0.03)	2.93(0.08)	0.81(0.02)
PH88	38-40	3.71(0.15)	0.78(0.02)	2.69(0.15)	0.76(0.05)
PH94	26-28	0.176(0.009)	1.38(0.08)	0.230(0.019)	1.26(0.24)
PH94	40-42	0.587(0.017)	1.006(0.022)	0.256(0.040)	1.26(0.24)
PH96	16-26	0.260(0.011)	1.06(0.04)	0.304(0.016)	0.91(0.06)
KD1	40-42	4.75(0.012)	1.122(0.009)	0.49(0.04)	1.00(0.04)
KD1	80-82	3.69(0.015)	1.11(0.04)	-	-
KD1	70-72	-	-	0.49(0.04)	1.21(0.09)

(Errors are given in brackets)

TABLE A2.1 (Continued)

W-Series Boreholes (October 1989 Field Trip)

Borehole	[U] μg/L	$^{234}U/^{238}U$
W1 a	3.2(0.1)	0.87(0.03)
W1 b	65.9(1.9)	0.78(0.02)
W2 a	16.1(0.6)	0.646(0.020)
W2 b	79.4(2.7)	0.660(0.006)
W3 a	5.50(0.17)	0.91(0.03)
W3 b	1.58(0.07)	0.97(0.05)
W4 a	412(10)	0.81(0.01)
W4 b	431(11)	1.21(0.01)
W5 a	0.42(0.04)	0.88(0.03)
W5 b	1.89(0.07)	0.83(0.03)
W7 a	0.12(0.02)	0.88(0.05)
W7 b	0.22(0.01)	0.77(0.03)

SAMPLES FROM APRIL 1991 FIELD TRIP

Borehole	Depth (m)	[U] (μg/L)	$^{234}U/^{238}U$
AD1	9.5	8.60 (0.45)	0.72 (0.04)
AD6	4.0	0.57 (0.04)	0.91 (0.06)
AD8	9.0	0.85 (0.06)	0.84 (0.05)
C1	22-23	6.32 (0.48)	0.95 (0.07)
C6	23-24	3.46 (0.28)	1.23 (0.10)
M2	36-40	40.55 (2.01)	1.51 (0.05)

(Errors are given in brackets)

TABLE A2.2

CONCENTRATIONS OF ^{238}U, ^{226}Ra and ^{210}Pb BY THE EVAPORATION METHOD COUPLED WITH GAMMA SPECTROMETRY
(Technique in Appendix 1.1.2)

Drill Hole	Depth (m)	Sample Volume (L)	Sampling Date	Concentration (Bq/L)		
				^{238}U	^{226}Ra	^{210}Pb
PH49	18-20	2.64	8. 5.90	1.2 (3.0)	7.1 (1.4)	39.0 (0.5)
	16-28	0.25	15. 5.88	1.9 (3.6)	9.8 (1.6)	34.9 (0.8)
	28-30	1.07	15. 5.88	2.7 (1.8)	7.2 (1.5)	52.2 (0.5)
	28-30	0.25	16.11.88	0.67 (19)	1.5 (3.2)	45.4 (0.8)
	44-46	0.56	15. 5.88	3.7 (2.3)	4.4 (3.7)	99.9 (0.4)
	44-46	1.76	15. 5.88	1.9 (1.6)	11.6 (0.7)	67.1 (0.3)
	44-46	0.25	16.11.88	2.4 (5.5)	9.0 (3.3)	20.9 (2.4)
PH15	19-21	1.92	15. 5.88	1.8 (1.1)	2.0 (1.8)	17.2 (0.4)
	19-21	0.25	15.11.88	2.0 (4.8)	1.0 (17)	3.1 (8.5)
	19-21	0.25	15.11.88	2.3 (4.5)	1.1 (17)	2.0 (14)
PH14	20-26	1.92	15. 5.88	0.71(2.2)	1.2 (2.6)	9.2 (0.7)
	20-26	0.25	16.11.88	0.31(23)	1.6 (9.2)	6.7 (3.6)
	20-26	0.59	10. 4.91	<0.086	1.3 (5.2)	1.8 (6.0)
PH80	17-20	1.83	15. 5.88	0.16(8.7)	0.065(39)	3.9 (1.4)
PH88	38-40	1.91	15. 5.88	0.050(20)	0.068(28)	2.6 (1.4)
PH55	26-28	1.86	15. 5.88	<0.022	0.11 (14)	1.5 (1.9)
	40-42	0.54	15. 5.88	<0.080	0.13 (43)	0.096(25)
PH56	26-28	1.00	15. 5.88	0.14(10)	0.34 (8.6)	1.6 (3.0)
PH61	26-28	1.02	15. 5.88	0.092(20)	0.16 (23)	0.54 (11)
	43-45	1.03	15. 5.88	0.077(21)	0.35 (9.5)	0.92 (5.8)
PH58	25-27	0.54	15. 5.88	<0.070	0.12 (39)	0.069 (26)
PH93	22-23	2.07	6.11.90	<0.024	0.15 (14)	0.028(27)
PH94	26-28	1.05	15. 5.88	<0.041	0.047(55)	0.059 (21)
	40-42	0.98		<0.068	0.62 (8.9)	0.034 (8.4)
PH96	16-26	0.84	15. 5.88	<0.054	0.073(50)	<0.050
KD1	40-42	2.40	15. 5.88	0.11 (7.2)	0.20 (7.8)	0.056(11)
	65-76	2.53	8. 5.90	0.049(12)	0.34 (3.8)	0.030(14)
KD2	24-32	1.58	2.11.90	<0.032	0.22 (12)	<0.029
	24-26	0.59	15. 4.91	<0.080	0.13 (48)	0.20 (46)
W1 a	13-15	2.62	8. 5.90	0.056(6.8)	0.22 (5.2)	0.67 (2.7)
	13-15	2.00	31.10.90	0.076(11)	0.076 (19)	0.31 (7.3)
W1 b	23-25	2.40	8. 5.90	0.67 (2.1)	0.82 (3.6)	2.5 (2.0)
	23-25	2.03	31.10.90	0.72 (2.6)	0.34 (9.8)	1.1 (4.7)
	23-25	0.53	12. 4.91	0.65 (4.7)	1.2 (6.1)	2.9 (4.1)
W2 a	13-15	2.51	8. 5.90	0.57 (2.1)	0.087(23)	1.5 (2.3)
	13-15	2.03	30.10.90	0.52 (3.2)	0.065(44)	0.94 (4.8)
	13-15	1.95	7.11.90	0.58 (1.8)	0.058(31)	1.5 (2.0)
	13-15	0.58	9. 4.91	0.51 (7.9)	0.24 (34)	1.9 (6.5)

Drill Hole	Depth (m)	Sample Volume (L)	Sampling Date	Concentration (Bq/L)		
				^{238}U	^{226}Ra	^{210}Pb
W2 b	23-25	2.59	8. 5.90	0.99 (1.1)	0.028(59)	1.8 (1.5)
	23-25	2.05	30.10.90	0.87 (2.1)	0.057(54)	1.7 (2.9)
	23-25	0.59	9. 4.91	0.86 (4.8)	0.16 (48)	1.4 (9.0)
	23-25	0.59	9. 4.91	0.82 (3.7)	0.14 (45)	1.7 (5.6)
W3 b	23-25	2.58	8. 5.90	0.13 (4.6)	0.25 (5.8)	0.14 (4.1)
W4 a	13-15	2.65	8. 5.90	5.4 (0.6)	2.9 (1.7)	34.9 (0.3)
	13-15	1.03	31.10.90	4.4 (1.0)	4.6 (1.8)	22.0 (0.7)
	13-15	0.58	11. 4.91	5.2 (1.8)	3.9 (4.4)	46.8 (0.7)
	13-15	0.53	11. 4.91	4.9 (1.8)	4.0 (3.8)	48.5 (0.7)
W4 b	23-25	2.57	8. 5.90	4.1 (0.9)	1.8 (3.1)	53.1 (0.3)
	23-25	0.985	31.10.90	3.3 (2.5)	1.5 (9.3)	55.5 (0.6)
	23-25	0.59	11. 4.91	3.5 (2.3)	2.6 (5.4)	91.3 (0.4)
W5 a	13-15	2.00	29.10.90	<0.019	0.023(67)	0.032(71)
W5 b	23-25	2.49	8. 5.90	<0.013	0.022(34)	0.029(38)
	23-25	2.03	29.10.90	<0.028	0.037(53)	<0.025
	23-25	0.59	12. 4.91	<0.089	0.072(98)	0.107(98)
W7 a	13-15	1.90	7.11.90	<0.030	0.069(32)	0.035(24)
W7 b	23-25	2.65	8. 5.90	<0.019	0.038(36)	0.071(29)
	23-25	1.95	27.10.90	<0.024	0.028(78)	0.054(60)
	23-25	0.59	10. 4.91	<0.067	0.10 (46)	0.14 (51)
M1	27-29	1.02	8. 5.90	5.1 (0.93)	1.2 (6.4)	5.6 (2.1)
M2	42-44	2.59	8. 5.90	0.54(1.9)	2.8 (1.1)	1.4 (1.1)
M4	28-30	2.58	8. 5.90	0.044(11)	0.52 (2.0)	0.047(6.8)
M5	27-29	2.03	2.11.90	0.014(27)	0.23 (9.4)	0.102(8.8)
C1	22-23	2.08	5.11.90	0.052(12)	0.087(16)	0.103 (20)
	22-23	0.59	17. 4.91	0.062(54)	0.095(56)	0.60 (14)
C4	23-40	2.06	5.11.90	<0.028	0.083(26)	0.53 (6.5)
C6	23-25	2.05	3.11.90	<0.022	0.12 (17)	<0.024
	23-24	0.53	16. 4.91	0.081(70)	0.18 (30)	<0.067
C9	28-30	1.14	8. 5.90	0.53 (4.6)	2.1 (3.0)	4.2 (2.4)
AD8	9	1.57	8.11.90	<0.040	0.75 (4.6)	0.27 (5.2)

The figures in parenthesis denote counting error (%).

TABLE A2.3
CONCENTRATIONS OF ^{238}U AND $^{234}U/^{238}U$ ACTIVITY RATIOS DETERMINED BY ALPHA SPECTROMETRY
Techniques in Appendix 1.1.2 (JAERI) and Appendix 1.2 (ANSTO)

Drill Hole	Depth (m)	Sampling Date	^{238}U Concentration (Bq/L)		$^{234}U/^{238}U$ Activity Ratio	
			JAERI	Ansto	JAERI	Ansto
PH49	16-28	May 88	2.1(5.4)	---	1.07(4.6)	---
	28-30	May 88	3.0(3.9)	3.4(2.5)	1.10(3.1)	1.06(1.2)
	28-30	Nov 88	0.59(2.7)	1.3(2.9)	1.03(1.8)	1.02(2.3)
	44-46	May 88	5.2(4.0)	3.8(2.6)	1.26(2.9)	1.20(1.1)
	44-46	May 88	2.0(3.7)		0.99(3.0)	
	44-46	Nov 88	2.2(2.4)	1.6(2.7)	1.01(1.3)	1.08(1.9)
PH15	19-21	May 88	1.9(2.2)	1.7(3.2)	1.03(0.9)	1.00(2.0)
	19-21	Nov 88	2.0(3.3)	0.38(3.0)	0.98(2.5)	0.99(3.0)
	19-21	Nov 88	2.1(2.6)		1.02(1.6)	
PH14	20-26	May 88	0.79(2.5)	0.67(4.7)	0.73(1.5)	0.73(4.1)
	20-26	Nov 88	0.31(2.6)	0.22(4.5)	0.79(1.8)	0.88(5.7)
PH80	17-20	May 88	0.18(5.1)	0.17(3.0)	0.76(4.7)	0.74(1.7)
	17-20	Nov 88	---	0.056(5.9)	---	0.82(3.7)
PH88	28--30	May 88	---	0.027(3.7)	---	0.93(3.2)
	28-30	Nov 88	---	0.036(2.8)	---	0.81(2.5)
	38-40	May 88	0.056(2.3)	0.046(4.0)	0.77(1.1)	0.78(2.6)
	38-40	Nov 88	---	0.033(5.5)	---	0.76(6.6)
PH55	26-28	May 88	0.0067(4.1)	0.0052(6.5)	1.02(3.7)	0.97(8.2)
	26-28	Nov 88	---	0.0077(6.5)	---	1.12(4.5)
	40-42	May 88	0.0068(5.1)	0.013(5.2)	1.30(5.6)	1.03(2.9)
	40-42	Nov 88	---	0.013(6.7)	---	1.11(5.4)
PH56	26-28	May 88	0.15(2.2)	0.15(2.4)	0.81(1.0)	0.82(1.5)
	26-28	Nov 88	---	0.096(3.3)	---	0.86(3.5)
	43-45	May 88	---	0.15(2.7)	---	1.10(2.0)
	43-45	Nov 88	---	0.054(2.8)	---	1.01(2.0)
PH61	26-28	May 88	0.093(3.6)	0.051(4.0)	0.84(3.0)	0.93(2.2)
	26-28	Nov 88	---	0.037(5.0)	---	0.95(4.2)
	43-45	May 88	0.063(2.4)	0.070(5.0)	1.16(1.3)	1.15(4.3)
	43-45	Nov 88	---	0.027(5.0)	---	1.02(5.9)
PH58	25-27	May 88	0.020(5.1)	0.021(4.9)	0.92(5.2)	0.91(6.6)
	25-27	Nov 88	---	0.025(5.3)	---	1.01(4.0)
	38-40	May 88	---	0.0072(4.7)	---	1.41(7.1)
	38-40	Nov 88	---	0.013(6.7)	---	1.14(7.0)
PH94	26-28	May 88	0.0026(7.2)	0.0022(5.3)	1.25(8.5)	1.38(5.8)
	26-28	Nov 88	---	0.0029(8.2)	---	1.26(19)
	40-42	May 88	0.0073(5.3)	0.0073(3.0)	1.07(5.7)	1.01(2.2)
	40-42	Nov 88	---	0.0032(16)	---	1.26(19)
PH96	16-26	May 88	0.0029(7.2)	0.0032(4.1)	0.91(9.2)	1.06(3.8)
	16-26	Nov 88	---	0.0038(5.3)	---	0.91(6.6)
KD1	40-42	May 88	0.095(3.1)	0.059(2.5)	1.11(2.4)	1.12(0.8)
	40-42	Nov 88	---	0.0060(5.6)	---	1.00(4.0)
	80-82	May 88	---	0.046(4.0)	---	1.11(3.6)
		Nov 88	---	0.0060(8.3)	---	1.21(7.4)

The figures in parenthesis denote counting error (%).
--- No data
Note: data obtained by JAERI and ANSTO were for different samples. Due to possible time-dependent fluctuations, these data are not directly comparable.

TABLE A2.4

CONCENTRATIONS OF ^{222}Rn AND ^{226}Ra BY THE DIRECT METHOD COUPLED WITH GAMMA SPECTROMETRY (Technique in Appendix 1.1.1)

Drill Hole	Depth (m)	Sample Volume (L)	Sampling Date	Concentration (Bq/L)	
				^{226}Ra	^{222}Rn ($\times 10^3$)
PH49	18-20	0.51	7 . 5.90	7.3 (2.0)	83 (0.9)
	28-30	0.25	16.11.88	195 (1.6)*	72 (1.1)
	44-46	0.25	16.11.88	35 (1.7)*	32 (1.2)
PH15	19-21	0.25	15.11.88	5.8 (9.2)*	4.5 (1.9)
	19-21	0.25	15.11.88	22 (1.9)*	2.6 (2.3)
PH14	20-26	0.25	16.11.88	21 (3.4)*	9.7 (1.8)
	20-26	0.59	10 . 4.91	0.99(10)	4.3 (1.0)
PH61		0.51	8 . 5.90	<0.34	0.12 (2.3)
KD2	24-26	0.59	15 . 4.91	<0.33	0.31 (1.8)
W1 a	13-15	0.52	9 . 5.90	<0.35	1.4 (1.0)
	13-15	0.50	7.11.90	<0.51	0.90 (1.4)
W1 b	23-25	0.51	9 . 5.90	0.62(19)	4.4 (1.0)
	23-25	0.53	12 . 4.91	0.58(15)	5.7 (1.1)
	23-25	0.53	12 . 4.91	1.0(12)	7.6 (1.0)
W2 a	13-15	0.51	7.11.90	<0.52	3.7 (1.0)
	13-15	0.58	9. 4.91	<0.31	4.4 (1.1)
W2 b	23-25	0.51	9 . 5.90	<0.35	5.5 (1.0)
	23-25	0.59	9 . 4.91	<0.28	3.5 (1.2)
	23-25	0.59	9 . 4.91	<0.30	4.3 (1.2)
W3 b	23-25	0.51	9 . 5.90	<0.32	0.40 (1.1)
W4 a	13-15	0.51	7 .11.90	2.7 (4.3)	33 (0.9)
	13-15	0.58	11 . 4.91	3.4 (3.8)	120 (1.1)
	13-15	0.53	11 . 4.91	3.4 (4.2)	110 (1.0)
W4 b	23-25	0.51	9 . 5.90	1.3 (9.4)	140 (0.8)
	23-25	0.59	11. 4.91	1.6 (0.6)	230 (1.1)
W5 a	13-15	0.51	7 .11.90	<0.47	0.066 (24)
W5 b	23-25	0.59	12 . 4.91	<0.32	0.22 (1.7)
W7 a	13-15	0.51	7. 11.90	<0.57	0.093 (24)
W7 b	23-25	0.59	10. 4.91	<0.26	0.20 (2.2)
M1	27-29	0.51	10. 5.90	1.0 (12)	19 (0.9)
M2	42-44	0.51	8 . 5.90	2.7 (5.4)	4.4 (1.0)
C1		0.59	17 . 4.91	<0.26	0.35 (2.0)
	22-23				0.38 (2.0)
C4	23-40	0.51	5 .11.90	<0.51	3.9 (1.1)
C6	23-24	0.53	16 . 4.91	<0.32	0.053 (3.1)

The figures in parenthesis denote counting error (%).

* There are large contributions to ^{226}Ra concentrations from ^{222}Rn which had not decayed out completely at the time of measurement.

TABLE A2.5

COMPARISON OF ^{226}RA CONCENTRATIONS BETWEEN THE DIRECT AND EVAPORATION METHODS COUPLED WITH GAMMA SPECTROMETRY

Drill Hole	Depth (m)	Sampling Date	^{226}Ra Concentration (Bq/L)	
			Direct	Evaporation
PH49	18-20	May 90	7.3 (2.0)	7.1 (1.4)#
	28-30	Nov 88	195 (1.6)*	2.5 (3.2)
	44-46	Nov 88	35 (1.7)*	9.0 (3.3)
PH15	19-21	Nov 88	5.8 (9.2)*	1.0 (27)
	19-21	Nov 88	22 (1.9)*	1.1 (17)
PH14	20-26	Nov 88	21 (3.4)*	1.6 (9.2)
	20-26	Apr 91	0.99(10)	1.3 (5.2)
W1 b	23-25	May 90	0.62(19)	0.82 (3.6)#
	23-25	Apr 91	1.0 (12)	1.2 (6.1)
W4 a	13-15	Nov 90	2.7 (4.3)	4.6 (1.8)#
	13-15	Apr 91	3.4 (3.8)	3.9 (4.4)
	13-15	Apr 91	3.4 (4.2)	4.0 (3.8)
W4 b	23-25	May 90	1.3 (9.4)	1.8 (3.1)#
	23-25	Apr 91	1.6 (0.6)	2.6 (5.4)
M1	27-29	May 90	1.0 (12)	1.2 (6.4)#
M2	42-44	May 90	2.7 (5.4)	2.8 (1.1)#

The figures in parenthesis denote counting error (%).

* There are large contributions to ^{226}Ra concentrations from ^{222}Rn which had not decayed out completely at the time of measurement.

\# The sampling times of samples analysed by both the methods were different, but the samples were collected on the same field trip.

TABLE A2.6

^{226}Ra DATA FOR KOONGARRA GROUNDWATER SAMPLES (mBq/L)

(Technique in Appendix 1.4)

Borehole	Depth (m)	Nov 88	Oct 89	May 90	Apr 91
AD1	9.5				37 (2)
AD2	9.0				14 (1)
AD11	2.5				38 (2)
AD12	5.0				9 (1)
AD13	9.0				168 (3)
AD14	10.5				656 (9)
C1	22-23				74 (3)
C5	25-27		340(10)		
C6	23-24				66 (3)
C7	25-27		1160(20)		
KD1	70-72	602 (8)			
KD1	65-76			450 (9)	
M2	37-39		2700(50)		
PH14	20-26	1220(20)			
PH15	19-21	838(10)			
PH49	25-27		5060(60)		
PH49	28-30	5680(60)			
PH49	44-46	4660(50)			
PH49	45-47		2410(40)		
PH55	28-28	82 (3)			
PH55	40-42	72 (2)			
PH56	26-28	467 (9)			
PH56	43-45	988 (12)			
PH58	25-27	65 (2)			
PH58	38-40	80 (3)			
PH61	26-28	52 (2)			
PH61	43-45	63 (3)			
PH80	17-20	93 (3)			
PH88	28-30	65 (2)			
PH88	38-40	77 (3)			
PH94	26-28	29 (2)			
PH94	40-42	12 (1)			
PH96	16-26	58 (3)			
W1 a	13-15		512 (8)		55 (2)
W1 b	23-25		760 (10)		830 (10)
W2 a	13-15		77 (2)		68 (3)
W2 b	23-25		27 (1)		86 (3)
W3 a	13-15		92 (2)		
W3 b	23-25		123 (2)		
W4 a	13-15		3780(50)		3820(50)
W4 b	23-25		1730(20)		1960(30)
W5 a	13-15		7.4 (0.7)		40 (2)
W5 b	23-25		24 (1)		91 (3)
W6 a	13-15				
W6 b	23-25				48 (1)
W7 a	13-15		1.3 (0.2)		10.5(0.9)
W7 b	23-25		5.2 (0.3)		23.2(0.8)

(Errors are given in brackets)

TABLE A2.7

ACTIVITY RATIOS OF ^{238}U, ^{226}Ra AND ^{210}Pb TO ^{222}Rn IN KOONGARRA GROUNDWATERS

Drill Hole	Depth (m)	Sampling Date	Activity Ratio		
			$^{238}U/^{222}Rn$ ($\times10^{-5}$)	$^{226}Ra/^{222}Rn$ ($\times10^{-5}$)	$^{210}Pb/^{222}Rn$ ($\times10^{-5}$)
PH49	18-20	May 90	5.9 (3.3)	1.2(1.6)	47(1.0)
	28-30	Nov 88	2.3 (19)	4.7(3.4)	63(1.4)
	44-46	Nov 88	3.8 (6.4)	0.36(3.5)	65(2.7)
PH15	19-21	Nov 88	0.52(17)	0.43(17)	70(2.7)
	19-21	Nov 88	0.50(17)	0.23(17)	78(14)
PH14	20-26	Nov 88	5.3 (25)	0.60(9.3)	69(4.0)
	20-26	Apr 91	<13	0.33(5.3)	42(6.0)
KD1	65-76	May 90	76 (12)	---	---
KD2	24-26	Apr 91	>1.4	0.24(48)	66(46)
W1 a	13-15	May 90	3.9 (8.6)	0.65(5.3)	48(2.9)
	13-15	Nov 90	1.0 (22)	1.2 (19)	35(7.5)
W1 b	23-25	May 90	1.2 (4.2)	0.54(3.8)	38(4.2)
	23-25	Nov 90	0.47(10)	---	---
	23-25	Apr 91	1.9 (7.7)	0.62(6.2)	25(4.9)
W2 a	13-15	May 90	0.15(23)	---	---
	13-15	Nov 90	0.13(44)	5.7(44)	25(4.9)
	13-15	Nov 90	0.10(31)	6.4(31)	41(2.2)
	13-15	Apr 91	0.47(35)	1.9(34)	44(6.6)
W2 b	23-25	May 90	0.028(59)	19 (59)	33(1.8)
	23-25	Nov 90	0.65(54)	---	---
	23-25	Apr 91	0.19(48)	2.1(48)	39(9.1)
	23-25	Apr 91	0.17(45)	3.1(45)	40(5.7)
W3 b	23-25	May 90	2.0 (7.4)	0.16(5.9)	36(4.2)
W4 a	13-15	May 90	0.54(1.8)	---	---
	13-15	Nov 90	1.1 (2.1)	0.72(2.0)	67(1.1)
	13-15	Apr 91	0.75(4.8)	3.1(4.6)	39(1.3)
	13-15	Apr 91	0.82(4.2)	2.7(4.0)	44(1.2)
W4 b	23-25	May 90	0.44(3.2)	7.6(3.2)	38(0.9)
	23-25	Nov 90	0.45(3.2)	---	---
	23-25	Apr 91	0.75(5.8)	8.8(5.5)	40(1.2)
W5 a	13-15	Nov 90	>1.1	0.29(71)	49(75)
W5 b	23-25	Apr 91	>0.71	0.30(98)	49(98)
W7 a	13-15	Nov 90	>2.1	0.14(40)	38(34)
W7 b	23-25	Apr 91	>1.3	0.19(46)	70(51)
M1	27-29	May 90	0.23(6.5)	1.7(6.5)	29(2.3)

Drill Hole	Depth (m)	Sampling Date	Activity Ratio		
			$^{238}U/^{222}Rn$ ($\times10^{-5}$)	$^{226}Ra/^{222}Rn$ ($\times10^{-5}$)	$^{210}Pb/^{222}Rn$ ($\times10^{-5}$)
M2	42-44	May 90	5.1 (2.2)	0.16(1.5)	33(1.5)
M4	28-30	May 90	12 (11)	---	---
M5	27-29	Nov 90	16 (29)	---	---
C1	22-23	Nov 90	1.7 (20)	0.40(16)	30(20)
	22-23	Apr 91	1.5 (59)	0.40(56)	158(14)
C4	23-40	Nov 90	>2.7	4.7(20)	14(6.6)
C6	23-24	Apr 91	2.2(34)	0.029(30)	<130
C9	28-30	May 90	3.9 (5.5)	---	---

The figures in parenthesis denote counting error (%).
--- No data
For the calculation of activity ratios, the concentrations of ^{238}U, ^{226}Ra and ^{210}Pb were determined by the evaporation method, and that of ^{222}Rn was determined by the direct method.

TABLE A2.8
SEASONAL VARIATIONS OF THE CONCENTRATIONS OF URANIUM-SERIES RADIONUCLIDES (MEASURED BY GAMMA SPECTROMETRY)

Drill Hole	Depth (m)	Sampling	Concentration (Bq/L)			
			^{238}U	^{226}Ra	^{210}Pb	^{222}Rn ($\times 10^3$)
PH49	28-30	May 88	2.7 (1.8)	7.2 (1.5)	52.2 (0.5)	
	28-30	Nov 88	0.67 (19)	1.5 (3.2)	45.4 (0.8)	
	44-46	May 88	3.7 (2.3)	4.4 (3.7)	99.9 (0.4)	
	44-46	May 88	1.9 (1.6)	11.6 (0.7)	67.1 (0.3)	
	44-46	Nov 88	2.4 (5.5)	9.0 (3.3)	20.9 (2.4)	
PH15	19-21	May 88	1.8 (1.1)	2.0 (1.8)	17.2 (0.4)	
	19-21	Nov 88	2.0 (4.8)	1.0 (17)	3.1 (8.5)	
	19-21	Nov 88	2.3 (4.5)	1.1 (17)	2.0 (14)	
PH14	20-26	May 88	0.71 (2.2)	1.2 (2.6)	9.2 (0.7)	
	20-26	Nov 88	0.31 (23)	1.6 (9.2)	6.7 (3.6)	9.7 (1.8)
	20-26	Apr 91	<0.086	1.3 (5.2)	1.8 (6.0)	4 3 (1.0)
KD2	24-32	Nov 90	<0.032	0.22 (12)	<0.029	
	24-26	Apr 91	<0.080	0.13 (48)	0.20 (46)	
W1 a	13-15	May 90	0.056(6.8)	0.22 (5.2)	0.67 (2.7)	1.4 (1.0)
	13-15	Nov 90		0.076(19)	0.31 (7 3)	0.90(1.4)
W1 b	23-25	May 90	0.67 (2.1)	0.82 (3.6)	2.5 (2.0)	4.4 (1.0)
	23-25	Nov 90	0.72 (2.6)	0.34 (9.8)	1.1 (4.7)	
	23-25	Apr 91	0.65 (4.7)	1.2 (6.1)	2.9 (4.1)	5.7 (1.1)
	23-25	Apr 91				7.6 (1.0)
W2 a	13-15	May 90	0.57 (2.1)	0.087(23)	1.5 (2.3)	
	13-15	Nov 90	0.52 (3.2)	0.065(44)	0.94 (4.8)	3.7 (1.0)
	13-15	Nov 90	0.58 (1.8)	0.058(31)	1.5 (2.0)	
	13-15	Apr 91	0.51 (7.9)	0.24 (34)	1.9 (6.5)	4.4 (1.1)
W2 b	23-25	May 90	0.99 (1.1)	0.028(50)	1.8 (1.5)	5.5 (1.0)
	23-25	Nov 90	0.87 (2.1)	0.057(54)	1.7 (2.9)	
	23-25	Apr 91	0.86 (4.8)	0.16 (48)	1.4 (9.0)	3.5 (1.2)
	23-25	Apr 91	0.82 (3.7)	0.14 (45)	1.7 (5.6)	4.3 (1.2)
W4 a	13-15	May 90	5.4 (0.6)	2.9 (1.7)	34.9 (0.3)	
	13-15	Nov 90	4.4 (1.0)	4.6 (1.8)	22.0 (0.7)	33 (0.9)
	13-15	Apr 91	5.2 (1.8)	3.9 (4.4)	46.8 (0.7)	120 (1.1)
	13-15	Apr 91	4.9 (1.8)	4.0 (3.8)	48.5 (0.7)	110 (1.0)
W4 b	23-25	May 90	4.1 (0.9)	1.8 (3.1)	53.1 (0.3)	140 (0.8)
	23-25	Nov 90	3.3 (2.5)	1.5 (9.3)	55.5 (0.6)	
	23-25	Apr 91	3.5 (2.3)	2.6 (5.4)	91.3 (0.4)	230 (1.1)
W5 b	23-25	May 90	<0.013	0.022(34)	0.029(38)	
	23-25	Nov 90	<0.028	0.037(53)	<0.025	
	23-25	Apr 91	<0.089	0.072(98)	0.107(98)	
W7 b	23-25	May 90	<0.019	0.038(36)	0.071(29)	
	23-25	Nov 90	<0.024	0.028(78)	0.054(60)	
	23-25	Apr 91	<0.067	0.10 (46)	0.14 (15)0	
C1	22-23	Nov 90	0.052(12)	0.087(16)	0.103(20)	0.35(2.0)
	22-23	Apr 91	0.062(54)	0.095(56)	0.60 (14)	0.38(2.0)
C6	23-25	Nov 90	<0.022	0.12 (17)	<0.024	
	23-24	Apr 91	0.081(70)	0.18 (30)	<0.067	

The figures in parenthesis denote counting error (%).

TABLE A2.9
PERCENT MODERN CARBON (PMC) FOR KOONGARRA GROUNDWATER

Bore Hole	Depth (m)	PMC	Error (%)	Field Trip
C5	25-27	60.8	5.7	Oct 89
C7	25-27	65.6	8.9	Oct 89
C8	38-40	78.9	7.0	May 89
C9	34-40	75.6	6.4	May 89
C9	28-30	79.2	6.6	May 90
C10	27-40	54.5	4.7	May 89
KD1	?	63.8	0.8	USNRC
KD1	80-82	82.9	9.4	May 88
M1	24-26	65.4	5.9	May 89
M1	35-50	68.6	6.0	May 89
M2	40-46	51.0	4.4	May 89
M3	34-40	78.5	7.6	May 89
M4	34-40	76.0	7.7	May 89
M4	28-30	86.1	7.4	May 90
PH14	?	59.5	1.4	USNRC
PH14	20-26	69.3	8.3	May 88
PH15	19-21	69.0	7.7	May 88
PH49	?	50.6	0.6	USNRC
PH49	27-29	37.1	3.6	May 89
PH55	?	91.6	2.2	USNRC
PH55	26-28	84.8	9.7	May 88
PH55	40-42	88.4	9.9	May 88
PH56	26-28	75.5	8.6	May 88
PH58	25-27	90.9	10.6	May 88
PH61	26-28	79.2	8.9	May 88
PH80	17-20	84.5	9.6	May 88
PH88	28-30	100.5	12.0	May 88
PH88	38-40	101.9	12.2	May 88
PH94	?	101.3	1.1	USNRC
PH94	26-28	93.5	11.6	May 88
W1 a	13-15	95.7	8.1	Oct 89
W1 a	13-15	95.7	8.1	May 90
W1 b	23-25	85.4	7.2	Oct 89
W1 b	23-25	86.9	7.3	May 90
W2 b	23-25	82.6	7.8	Oct 89
W2 b	23-25	80.4	7.2	May 90
W3 a	13-15	89.3	8.3	Oct 89
W3 b	23-25	77.4	7.0	Oct 89
W4 a	13-15	80.5	6.9	May 90
W4 a	13-15	85.4	7.1	Oct 89
W4 b	23-25	65.5	5.6	May 89
W4 b	23-25	62.9	5.6	May 90
W5 a	13-15	87.1	7.4	Oct 89
W5 a	13-15	90.9	7.8	May 90
W5 b	23-25	90.5	7.7	Oct 89
W7 b	23-25	88.0	7.8	Oct 89
W7 b	23-25	97.2	8.6	May 90

USNRC - Refers to data obtained during the USNRC - sponsored project which preceded the ARAP, reported in: Quarterly Report No. 7 on Radionuclide Migration Around Uranium Ore Bodies - Analogue of Radioactive Waste Repositories, AAEC Report C38 (1983).

TABLE A2.10

^{13}C, DEUTERIUM AND ^{18}O DATA

1 May 1988 field trip

Borehole	Depth (m)	$\delta^{13}C$	$\delta^{2}H$	$\delta^{18}O$
PH14	20-26	-20.89	-36.7	-6.04
PH15	19-21	-19.62	-39.1	-6.04
PH49	28-30		-37.9	-6.34
PH49	44-46		-41.6	-6.69
PH55	26-28	-20.64	-36.9	-5.48
PH55	40-42	-20.28	-35.5	-5.86
PH56	26-28	-20.69	-35.5	-6.02
PH56	43-45		-33.7	-5.95
PH58	25-27	-19.83	-36.6	-5.47
PH58	40-42		-36.5	-5.49
PH61	26-28	-20.07	-34.1	-6.01
PH61	43-45		-37.2	-5.78
PH80	17-20	-20.79	-35.9	-5.81
PH88	28-30	-20.41	-33.3	-5.57
PH88	38-40	-19.86	-31.3	-5.48
PH94	26-28	-21.08	-32.0	-5.54
PH94	40-42		-32.2	-5.32
KD1	40-42		-38.6	-6.31
KD1	80-82	-20.65	-40.7	-6.33

TABLE A2.10 (continued)

2 May 1989 Field Trip

Borehole	Depth (m)	δ^2H	$\delta^{13}C$
W4(b)	23-25	-37.9	-21.7
PH49	27-29	-37.5	
PH49	33-35	-39.1	
PH80	17-19	-34.2	
PH146	17-89	-39.6	
C8	24-26	-35.5	
C8	38-40	-31.8	-19.8
C9	34-40	-37.4	-19.7
C10	27-40	-37.2	-18.9
M1	24-26	-37.9	-19.5
M1	35-50	-38.8	-20.1
M1	46-48	-34.1	
M2	40-46	-38.5	-19.7
M3	20-22	-33.0	
M3	26-28	-34.1	
M3	34-40	-35.2	
M4	34-40	-24.7	
Koongarra Creek		-24.5/-24.3	
Rainwater		-22.0/-22.7	

TABLE A2.10 (continued)

3 October 1989 Field Trip

Borehole	Depth (m)	δ^2H	$\delta^{13}C$
W1 a	13-15	-36.7	-21.3
W1 b	23-25	-36.4	-18.6
W2 b	13-15	-30.3	
W2 b	23-25	-32.1	
W3 a	13-15	-34.9	-14.7
W3 b	23-25	-33.5	-18.7
W4 a	13-15	-34.1	-20.5
W4 b	23-25	-37.9	
W5 a	13-15	-32.0	-17.1
W5 b	23-25	-31.8	-19.0
W7 a	13-15	-30.7	
W7 b	23-25	-29.9	-16.1
PH49	25-27	-41.9	-16.1
PH49	45-47	-39.0/-39.3	
C5	25-27	-32.4	-18.2
C7	25-27	-37.8	
M2	37-39	-27.6	

4 April 1991 Field Trip

Borehole	Depth (m)	δD	$\delta^{18}O$
AD1	9.5	-35.8	-5.46
AD1*	9.5	-33.9	-5.19
AD9	7.0	-31.7	-5.26
AD12	5.0	-31.8	-5.22
AD13	9.0	-36.2	-6.00
AD14	10.5	-36.8	-5.95
W6(b)	23-25	-35.0	-5.98
Creek near KD1		-30.2	-5.01

1 $\delta^{13}C$ is given as ‰ difference relative to PDB standard
1 σ = 0.1‰ (May 1988 sample set)
1 σ = 0.05‰ (subsequent sample sets)

2 δ^2H is ‰ relative to V-SMOW
(1 σ = 1.0‰)

3 $\delta^{18}O$ is ‰ relative to V-SMOW
(1 σ = 0.1‰)

TABLE A2.11

TRITIUM DATA

Bore Hole	Depth (m)	Tritium (TU)	Field Trip
AD1	9.5	2.8	May 91
AD2	9.0	2.5	May 91
AD12	5.0	2.5	May 91
AD13	9.0	1.0	May 91
AD14	10.5	0.7	May 91
C1	22-23	0.8	Nov 90
C4	23-40	1.5	Nov 90
C5	25-27	0.1	Oct 89
C6	23-25	0.1	Nov 90
C7	25-27	0.1	Oct 89
C9	28-30	0.4	May 90
KD1	40-42	0.0	May 88
KD1	80-82	0.4	May 88
KD1	65-76	0.1	May 90
KD2	24-32	0.5	Nov 90
M1	27-29	0.3	May 90
M4	28-30	0.7	May 90
M5	28-40	0.3	Nov 90
PH14	20-26	0.3	May 88
PH15	19-21	0.3	May 88
PH49	18-20	0.7	May 90
PH49	16-28	0.3	May 88
PH49	28-30	0.3	May 88
PH55	26-28	0.2	May 88
PH55	40-42	0.2	May 88
PH56	26-28	0.3	May 88
PH56	43-45	0.3	May 88
PH58	25-27	0.2	May 88
PH58	38-40	0.4	May 88
PH61	26-28	0.2	May 88
PH61	43-45	0.0	May 88
PH80	17-20	0.4	May 88
PH88	28-30	0.8	May 88
PH88	38-40	1.2	May 88
PH93	22-23	0.5	Nov 90
PH94	26-28	2.0	May 88

Maximum measurement error 0.3 TU

TABLE A2.11 (continued)

TRITIUM DATA

		Tritium (TU)		
Bore Hole	Depth (m)	Oct 89	May 90	Apr 91
W 1 a	13-15	0.6	1.0	
W 1 b	23-25	0.2	0.3	0.2
W 2 a	13-15		0.3	0.6
W 2 b	23-25	0.5	0.6	0.7
W 3 a	13-15	2.8		
W 3 b	23-25	0.9		
W 4 a	13-15	1.2	1.3	
W 4 b	23-25		1.4	1.3
W 5 a	13-15	0.1	0.2	
W 5 b	23-25	0.3	0.3	0.3
W 6 a	13-15			
W 6 b	23-25			
W 7 a	13-15		3.0	
W 7 b	23-25	0.9	1.3	1.0

Maximum measurement error 0.3 TU

APPENDIX 3 MAJOR CHEMICAL DATA

Data grouped by field trip - full details are given in Table 3.1

In this Appendix, the following usage is adopted:

Blank space	no data / not measured
[ ]	imprecise or doubtful data
¦	data not reported due to evidence of contamination, analytical error, reporting error, etc.

Note that some shallow depths in W-holes (13-15 m sampling interval) showed evidence of contamination by materials used in sealing the sampling interval (see text). In these cases the data was omitted from the tabulations.

TABLE A3.1.1

FIELD DATA AND ANIONS: MAY 88

Bore	Depth m	pH	Eh mV	EC µS/cm	HCO_3^- mg/L	Cl^- mg/L	F^- mg/L	SO_4^{2-} mg/L	PO_4^{3-} µg/L
PH14	20-26	6.42	162	207	128	5.8	0.10	<1.0	[160]
PH15	19-21	6.66	115	227	137	2.7	0.15	3.0	[560]
PH49	16-28	6.44	155	204	130	4.9	0.15	<1.0	
PH49	28-30	6.74	130	236	154	3.7	0.17	2.0	[310]
PH55	26-28	6.57	110	193	127	3.7	0.12	3.0	[650]
PH55	40-42	6.53	125	198	124	3.8	0.20	<1.0	
PH56	26-28	6.50	145	177	108	4.7	0.18	<1.0	[385]
PH56	43-45	6.95	120	169	113	3.1	0.13	1.0	
PH58	25-27	6.57	100	198	125	3.9	0.24	3.0	[260]
PH58	38-40	6.60	145	172	114	3.8	0.10	2.0	
PH61	26-28	6.92	170	170	107	2.8	0.18	<1.0	[190]
PH61	43-45	7.03	160	225	151	2.6	0.20	1.0	[145]
PH80	17-20	6.31	160	163	96	4.3	0.09	<1.0	[230]
PH88	28-30	6.54	127	148	88	3.6	0.12	1.0	
PH88	38-40	6.62	90	134	81	3.8	0.10	[8.0]	[185]
PH94	26-28	7.17	250	74	38	2.2	0.09	1.0	
PH94	40-42	6.77	125	90	56	3.8	[1.20]	2.0	[185]
PH96	16-26	6.55	120	98	56	3.5	0.15	<1.0	
KD1	40-42	5.95	165	106	69				[<5]
KD1	80-82	5.82	235	124	43	2.6	0.05	<1.0	

TABLE A3.1.2

MAJOR CATIONS, U and Si: MAY 88

Bore	Depth m	Mg mg/L	Na mg/L	K mg/L	Ca mg/L	Si mg/L	Fe mg/L	Mn µg/L	U µg/L
PH14	20-26	20.3	1.32	0.62	5.0	10.9	1.11	420	52.3
PH15	19-21	21.5	1.01	0.59	3.6	8.2	0.42	350	137
PH49	16-28	20.1	1.32	0.53	3.1	9.9	0.82	182	
PH49	28-30	26.4	1.35	0.68	3.9	8.9	0.78	154	265
PH55	26-28	17.9	3.16	1.05	4.4	14.0	5.60	142	0.40
PH55	40-42	18.3	1.57	1.65	3.7	12.1	0.70	97	1.00
PH56	26-28	16.0	1.15	0.47	3.6	10.1	0.87	40	12.0
PH56	43-45	16.7	1.17	0.53	4.4	9.4	0.53	35	11.4
PH58	25-27	18.0	2.30	1.43	4.3	14.4	0.52	111	1.61
PH58	38-40	17.7	2.22	1.45	3.7	15.8	0.28	87	0.56
PH61	26-28	16.4	0.96	0.59	2.7	8.1	0.05	7	3.95
PH61	43-45	18.0	1.12	1.00	8.8	7.2	0.26	54	5.49
PH80	17-20	16.2	1.15	0.37	1.3	10.9	0.35	234	13.2
PH88	28-30	14.1	1.52	0.56	1.4	14.5	0.32	20	2.13
PH88	38-40	13.0	1.62	0.63	1.0	14.1	1.05	67	3.60
PH94	26-28	5.7	1.99	1.00	1.4	12.1	0.04	8	0.17
PH94	40-42	6.1	3.53	2.00	3.8	10.4	0.19	23	0.57
PH96	16-26	7.0	2.18	1.37	2.1	13.6	0.41	55	0.25
KD1	40-42	3.6	1.09	0.37	3.1	6.1	18.90	189	4.61
KD1	80-82	2.4	0.99	0.18	2.0	6.5	0.10	9	3.57
Blank		0.001	<0.02	0.002	0.002	<0.02	0.02	<1	
Blank		0.001	<0.02	0.003	0.004	0.02	0.02	<1	
Blank		0.001	<0.02	0.003	0.006	0.02	0.02	<1	

Limited data for a PH49 (44-46 m) sample was obtained on this field trip:
Mg - 28.7, Na - 1.36, K - 0.81, Ca - 7.9, Si - 9.8, Fe - 0.46, Mn - 0.032 (mg/L)

TABLE A3.2.1

FIELD DATA AND ANIONS: NOV 88

Bore	Depth m	pH	Eh mV	EC µS/cm	HCO_3 mg/L	Cl^- mg/L	F^- mg/L	SO_4^{2-} mg/L	PO_4^{3-} µg/L
PH14	20-26	6.80	70	235	157	9.1	0.24	0.32	130
PH15	19-21	7.05	120	207	149	6.0	0.37	0.04	295
PH49	28-30	6.84	130	230	159	8.5	0.34	0.29	90
PH49	44-46	7.01	280	247	180	2.0	0.38	0.11	60
PH55	26-28	6.55	105	179	117	6.2	0.24	0.20	475
PH55	40-42	6.60	75	180	120	5.5	0.24	0.24	445
PH56	26-28	6.72	120	167	116	7.3	0.23	0.24	215
PH56	43-45	6.93	135	183	120	5.7	0.29	0.18	175
PH58	25-27	6.70	115	188	118	6.1	0.21	0.16	685
PH58	38-40	6.59	135	187	114	6.2	0.20	0.10	665
PH61	26-28	7.24	45	208	140	4.6	0.36	0.04	110
PH61	43-45	7.30	80	227	156	5.1	0.36	0.22	130
PH80	17-20	6.68	130	163	99	6.6	0.17	0.43	305
PH88	28-30	6.92	120	138	87	5.5	0.21	0.08	105
PH88	38-40	6.82	90	141	92	3.2	0.22	<0.02	155
PH94	26-28	7.06	225	74	38	2.8	0.14	0.08	285
PH94	40-42	6.94	225	75	38	3.4	0.11	0.84	200
PH96	16-26	7.14	145	102	66	4.6	0.21	0.37	210
KD1	40-42	6.07	140	126	81	3.1	0.12	<0.02	10
KD1	70-72	6.18	220	108	67	3.4	0.29	0.20	5
*PH27	20m	6.88	120	151	108	3.2	0.18	<0.02	5
*PH92	20m	7.20	120	147	99	3.8	0.17	0.17	385
*PH96	20m	6.94	130	96	66	2.8	0.15	0.16	280
*PH110	20m			161	116	5.8	0.15	0.14	65
*PH139	20m	7.10	100	121	79	4.9	0.18	0.11	255

* - Samples obtained using a small-volume electric pump without packers.

TABLE A3.2.2

MAJOR CATIONS, U and Si: NOV 88

Bore	Depth m	Mg mg/L	Na mg/L	K mg/L	Ca mg/L	Si mg/L	Fe mg/L	Mn µg/L	U µg/L
PH14	20-26	25.0	1.2	0.85	4.7	10.3	3.80	230	15.6
PH15	19-21	24.0	1.2	0.83	2.7	8.1	0.53	90	30.5
PH49	28-30	25.0	1.2	0.75	5.2	9.2	1.10	140	93.9
PH49	44-46	24.0	1.3	0.91	8.5	8.7	0.45	67	127
PH55	26-28	19.0	1.4	1.00	2.0	14.7	2.30	59	0.66
PH55	40-42	19.0	1.4	1.10	2.7	14.5	3.50	96	0.98
PH56	26-28	18.0	2.3	0.64	3.5	10.0	0.93	36	7.19
PH56	43-45	19.0	1.3	0.85	6.8	8.8	0.71	32	4.30
PH58	25-27	19.0	2.2	1.30	2.2	15.2	2.40	86	2.04
PH58	38-40	18.0	2.2	1.30	2.1	15.7	1.10	75	1.05
PH61	26-28	19.0	1.0	0.52	7.1	6.6	0.83	82	2.97
PH61	43-45	21.0	1.5	1.10	11.0	6.5	0.59	67	2.38
PH80	17-20	17.4	1.1	0.39	0.9	10.7	1.30	280	4.64
PH88	28-30	15.0	1.6	0.72	0.7	14.9	1.10	73	2.83
PH88	38-40	15.0	1.6	0.74	0.7	14.9	1.20	71	2.37
PH94	26-28	6.0	2.1	0.84	0.6	12.1	0.06	5	0.24
PH94	40-42	6.1	2.1	1.00	0.7	12.1	0.05	6	0.28
PH96	16-26	9.5	2.1	1.60	2.3	15.7	0.78	55	0.30
KD1	40-42	4.8	1.0	0.41	2.3	5.3	22.00	120	0.52
KD1	70-72	8.9	8.5	0.22	4.6	8.2	1.60	5	0.55
*PH27	20m	13.8	1.0	1.10	4.1	3.1	3.60	160	0.15
*PH92	20m	16.0	2.1	0.85	1.9	16.6	0.60	13	0.27
*PH96	20m	9.5	2.2	1.30	2.3	15.3	0.25	13	0.24
*PH110	20m	13.0	1.5	1.40	12.7	10.6	0.41	8	0.28
*PH139	20m	12.0	3.3	0.91	1.9	15.8	1.60	36	[0.07]

* - Samples obtained using a small-volume electric pump without packers

TABLE A3.3.1

FIELD DATA AND ANIONS: MAY 89

Bore	Depth m	pH	Eh mV	EC µS/cm	HCO_3^- mg/L	Cl^- mg/L	F^- mg/L	SO_4^{2-} mg/L	PO_4^{3-} µg/L
PH14	20-26	6.51	160	217	125	6.77	0.14	0.58	160
PH49	27-29	7.01	-80	216	143	5.00	0.16	0.12	140
PH49	33-35	7.04	120	202	153	4.84	0.20	0.39	135
PH80	17-19	[5.64]	160	176	90	4.97	0.29	<0.02	285
PH146	17-89	6.62	100	204	133	3.64	0.43	0.40	585
PH146*	17-89	6.63	250	208	142	3.52	0.32	0.67	
C6	35-40	7.12	¦	189	116	4.25	0.14	0.49	30
C8	24-26	6.25	225	188	104	4.43	0.36	0.28	85
C8	38-40	6.92	280	190	111	4.41	0.37	0.31	15
C9	34-40	6.70	[95]	[284]	[142]	¦	[0.22]	¦	[120]
C10	27-40	7.16	350	181	95	2.86	0.26	0.37	<5
M1	24-26	7.10	205	275	162	5.53	0.39	0.34	40
M1	35-50	7.15	260	225	162	3.93	0.24	0.94	190
M1	46-48	7.06	230	256	160	5.67	0.45	0.46	635
M2	40-46	7.01	130	247	156	5.06	0.28	[1.10]	135
M3	20-22	6.65	200	161	87	4.93	0.28	0.50	<5
M3	26-28	6.68	265	160	88	4.61	0.19	0.59	<5
M3	34-40	6.59	380	167	88	4.29	0.23	0.53	5
M4	34-40	6.89	130	189	110	3.31	0.13	<0.02	300
W4	23-25	6.51	200	279	156	6.12	0.08	0.24	70
KCrk		6.9		17	8	2.94	0.09	0.14	25

* - Denotes second sample set at PH146

TABLE A3.3.2

MAJOR CATIONS, U and Si: MAY 89

Bore	Depth m	Mg mg/L	Na mg/L	K mg/L	Ca mg/L	Si mg/L	Fe mg/L	Mn µg/L	U µg/L
PH14	20-26	21.1	1.3	0.66	2.44	10.2	0.85	412	46.6
PH49	27-29	20.4	1.2	0.64	3.08	8.5	0.93	155	107
PH49	33-35	21.6	1.3	0.64	4.04	8.5	0.66	125	71.2
PH80	17-19	14.5	1.2	0.40	0.85	9.9	0.81	184	14.9
PH146	17-89	18.9	0.9	0.89	2.99	7.2	1.67	46	1.58
PH146*	17-89	21.6	0.9	0.46	4.08	6.6	0.036	39	0.48
C6	35-40	17.9	1.5	0.81	1.76	4.1	0.007	143	12.6
C8	24-26	16.0	1.5	0.75	1.27	13.0	0.138	114	9.71
C8	38-40	15.4	1.6	0.86	1.63	9.5	0.016	155	2.27
C9	34-40	17.7	1.3	1.12	¦	10.8	3.09	126	26.4
C10	27-40	14.1	1.8	0.73	2.21	2.9	0.014	213	0.70
M1	24-26	21.9	1.1	0.52	2.53	4.3	0.007	120	128
M1	35-50	24.4	1.2	0.55	2.69	5.1	0.028	71	248
M1	46-48	21.3	1.2	0.47	3.08	6.1	<0.001	25	109
M2	40-46	21.7	1.7	1.45	[5.86]	6.0	0.192	34	3.11
M3	20-22	14.4	1.4	0.45	0.53	10.7	0.006	171	22.0
M3	26-28	13.2	1.4	0.57	0.72	11.5	0.016	104	28.8
M3	34-40	14.0	1.4	0.48	0.62	12.4	0.021	121	31.0
M4	34-40	14.9	2.0	1.74	2.09	13.3	2.98	266	4.08
W4	23-25	24.3	1.4	0.74	1.36	8.5	0.32	69	395
K Creek		0.46	1.4	0.10	0.18	3.9	0.133	7	0.21
Blank		0.002	0.02	0.01	<0.01	0.02	0.001	4	0.02

* - Denotes second sample set at PH146

TABLE A3.4.1

FIELD DATA AND ANIONS: OCT 89

Bore	Depth m	pH m	Eh mV	EC µS/cm	HCO_3^- mg/L	Cl^- mg/L	F^- mg/L	SO_4 mg/L	PO_4 µg/L
W1 a	13-15	6.55	220	195	98	7.43	0.12	[4.1]	<5
W1 a*	13-15	6.80	195	200	93	6.21	0.20	[3.1]	10
W1 b	23-25	7.09	255	230	120	8.20	0.14	1.85	415
W1 b*	23-25	6.75	235	215	107	6.88	0.25	1.52	370
W2 a	13-15	¦	¦	[230]	119	5.24	0.18	[2.7]	<5
W2 b	23-25	6.48	235	160	98	3.29	0.19	0.36	110
W3 a	13-15	¦	¦	[130]	41	6.13	0.30	[5.5]	25
W3 b	23-25	7.08	100	148	89	10.30	0.19	<0.02	180
W4 a	13-15	5.85	330	135	66	5.80	0.09	[0.8]	30
W4 a*	13-15	5.75	305	133	60	6.44	0.11	[0.8]	35
W4 b	23-25	6.80	140	240	165	2.86	0.14	0.43	90
W4 b*	23-25	6.85	125	250	159	4.05	0.23	0.34	80
W5 a	13-15	¦	¦	[165]	101	2.13	0.15	[0.8]	590
W5 b	23-25	6.80	185	125	82	9.71	0.12	<0.02	545
W7 a	13-15	¦	¦	[67]	27	2.76	0.12	[2.3]	80
W7 b	23-25	7.15	220	93	52	1.95	0.15	1.36	450
M2	37-39	7.26	160	247	156	[2.20]	0.26	0.56	105
C5	25-27	7.05	145	150	87	1.76	0.27	0.51	60
C7	25-27	7.02	115	153	93	2.20	0.26	0.43	125
PH49	25-27	6.75	115	255	159	3.05	0.35	0.17	175
PH49	45-47	7.10	80	275	183	3.10	0.39	1.03	125

* - Denotes second sample set

TABLE A3.4.2

MAJOR CATIONS, U and Si: OCT 89

Bore	Depth m	Mg mg/L	Na mg/L	K mg/L	Ca mg/L	Si mg/L	Fe mg/L	Mn µg/L	U µg/L
W1 a	13-15	¦	1.88	1.43	¦	6.7	0.049	4.7	2.51
W1 a*	13-15	¦	1.96	1.84	¦	6.8	0.022	4.1	7.33
W1 b	23-25	¦	3.44	2.08	¦	6.7	0.006	16	38.6
W1 b*	23-25	¦	3.31	2.08	¦	6.9	0.002	20	50.5
W2 a	13-15	¦	2.11	0.72	¦	14.2	0.001	2.5	14.1
W2 b	23-25	16.3	1.32	0.45	0.77	15.5	0.015	11	71.2
W3 a	13-15	¦	1.54	0.52	¦	6.8	0.003	27	4.11
W3 b	23-25	13.2	0.98	0.42	3.34	10.5	0.190	498	1.33
W4 a	13-15	12.3	1.70	0.54	2.08	9.8	0.017	421	414
W4 a*	13-15	11.4	1.70	0.49	2.19	9.7	0.037	537	439
W4 b	23-25	27.3	1.11	0.60	2.95	9.7	0.035	60	364
W4 b*	23-25	26.8	1.22	0.66	1.72	9.7	0.510	69	318
W5 a	13-15	[11.6]	1.95	0.62	¦	18.7	0.002	22	0.38
W5 b	23-25	12.6	1.88	0.53	1.51	19.0	0.049	108	1.82
W7 a	13-15	¦	1.19	0.27	¦	8.9	0.001	1.4	0.13
W7 b	23-25	7.4	1.17	0.36	2.77	14.7	0.001	3.3	0.22
M2	37-39	23.6	1.94	1.21	6.41	6.4	0.016	23	7.35
C5	25-27	15.1	1.00	0.35	1.09	7.8	0.036	32	7.94
C7	25-27	14.5	0.98	0.37	1.17	6.3	0.055	45	5.49
PH49	25-27	25.9	1.23	0.67	4.40	9.0	0.610	143	108
PH49	45-47	26.9	1.28	0.75	8.15	8.6	0.040	43	131

* - Denotes second sample set

TABLE A3.5.1

FIELD DATA AND ANIONS: MAY 90

Bore	Depth m	pH	Eh mV	EC µS/cm	HCO_3^- mg/L	Cl^- mg/L	F^- mg/L	SO_4^{2-} mg/L	PO_4^{3-} µg/L
W1 a	13-15	6.80	245	[200]	108	5.46	0.63	[8.2]	<5
W1 b	23-25	6.50	260	168	93	6.34	0.64	3.20	360
W2 a	13-15	¦	¦	[222]	133	3.39	0.66	2.42	30
W2 b	23-25	6.58	225	165	100	3.12	0.60	1.08	105
W4 a	13-15	5.97	305	136	66	8.01	0.49	1.64	10
W4 b	23-25	6.81	120	220	154	2.90	0.72	0.97	75
W5 a	13-15	[7.8]	[170]	[164]	101	2.61	0.53	1.10	530
W5 b	23-25	6.76	175	126	79	2.77	0.52	0.92	515
W7 a	13-15	¦	¦	[70]	36	1.97	0.41	2.21	100
W7 b	23-25	7.16	280	89	51	2.27	0.50	0.72	415
PH49	18-20	6.62	95	225	141	3.61	0.71	0.93	140
C9	28-30	6.69	175	[258]	130	5.22	0.70	¦	95
M1	27-29	6.96	220	249	160	2.36	0.85	1.12	85
M2	42-44	7.28	120	300	194	2.37	0.85	0.81	
M4	28-30	6.93	65	173	106	3.22	0.58	0.76	575
KD1	65-76	6.05	250	116	67	1.93	0.57	1.27	<5

TABLE A3.5.2

MAJOR CATIONS, U and Si: MAY 90

Bore	Depth m	Mg mg/L	Na mg/L	K mg/L	Ca mg/L	Si mg/L	Fe mg/L	Mn µg/L	U µg/L
W1 a	13-15	¦	1.54	1.16	¦	6.4	0.014	4.4	4.64
W1 b	23-25	[10.5]	2.07	1.29	¦	6.4	0.026	13	63.0
W2 a	13-15	¦	1.48	0.65	¦	14.0	0.003	26	59.6
W2 b	23-25	16.0	1.36	0.45	0.84	14.1	0.012	9.4	95.5
W4 a	13-15	11.6	1.72	0.52	1.83	8.7	0.079	531	511
W4 b	23-25	24.1	1.15	0.68	1.31	8.6	0.478	55	389
W5 a	13-15	[10.9]	1.80	0.68	¦	16.8	<0.002	20	0.22
W5 b	23-25	11.5	1.79	0.55	1.50	16.6	0.110	104	0.38
W7 a	13-15	¦	1.05	0.27	¦	8.5	<0.002	1.6	5.40
W7 b	23-25	7.3	1.21	0.39	1.39	13.4	<0.002	0.4	0.56
PH49	18-20	21.0	1.23	0.54	2.62	8.8	2.770	322	118
C9	28-30	21.0	1.24	1.13	[8.4]	11.0	0.117	79	57.2
M1	27-29	24.7	1.00	0.41	3.12	6.1	0.007	81	489
M2	42-44	27.7	1.12	0.90	6.48	6.7	0.019	50	52.2
M4	28-30	15.0	2.10	1.16	1.98	15.9	2.392	154	3.85
KD1	65-76	8.0	1.02	0.54	4.60	6.1	0.047	253	3.43
Blank		<0.001	0.01	<0.01	0.001	0.01	0.002	0.1	0.005

EFFECT OF PUMPING TIME (Depths as Above)

Bore	Time (hrs)	Mg mg/L	Na mg/L	K mg/L	Ca mg/L	Si mg/L	Fe mg/L	Mn µg/L	U µg/L
W4 a	2	11.5	1.65	0.51	1.87	8.7	0.106	569	508
W4 a	3	12.0	1.61	0.53	1.82	8.6	0.081	576	516
W4 a	3.5	11.6	1.72	0.52	1.83	8.7	0.079	531	511
W4 a	4	11.5	1.65	0.51	1.80	8.7	0.069	498	532
W4 a	5	12.0	1.66	0.51	1.68	8.6	0.058	456	526
W4 b	0.5	24.8	1.09	0.61	1.44	8.4	0.811	88	233
W4 b	1	24.6	1.09	0.63	1.39	8.4	0.558	66	359
W4 b	2	24.3	1.12	0.64	1.30	8.5	0.482	56	395
W4 b	2.5	24.1	1.15	0.68	1.31	8.6	0.478	55	389
W4 b	3	24.3	1.16	0.68	1.30	8.6	0.402	45	422
W4 b	5	24.3	1.20	0.73	1.29	8.7	0.357	38	483
PH49	1.5	20.9	1.22	0.55	2.22	8.8	2.77	327	68
PH49	3	20.9	1.21	0.54	2.40	8.7	2.74	308	100
PH49	3.5	21.0	1.23	0.54	2.62	8.8	2.77	322	118
PH49	4	21.1	1.24	0.52	2.64	8.8	2.52	312	115
PH49	5.5	21.0	1.25	0.53	2.59	8.8	2.41	319	127

TABLE A3.6.1

FIELD DATA AND ANIONS: NOV 90

Bore	Depth (m)	pH	Eh mV	EC µS/cm	HCO_3^- mg/L	Cl^- mg/L	F^- mg/L	SO_4^{2-} mg/L	PO_4^{3-} µg/L
W1 a	13-15	¦	¦	195	97	5.28	0.72	¦	[115]
W1 b	23-25	6.64	270	179	104	6.49	0.71	[3.2]	425
W2 a	13-15	[7.50]	[70]	160	124	3.25	0.70	[3.0]	55
W2 b	23-25	6.47	185	160	98	3.09	0.68	1.26	130
W4 a	13-15	5.66	295	113	41	11.2	0.54	[3.0]	35
W4 b	23-25	6.75	120	247	163	4.66	0.81	1.10	80
W5 a	13-15	[7.56]	[200]	158	99	2.77	0.61	1.20	545
W5 b	23-25	6.72	125	127	81	2.84	0.59	0.94	445
W7 a	13-15	¦		67	31	1.88	0.49	[3.1]	95
W7 b	23-25	6.94		85	48	2.25	0.53	0.79	425
C1	22-23	7.45		166	106	3.01	0.68	1.31	120
C4	23-40	7.01		140	85	2.91	1.02	0.82	10
C6	23-25	[8.16]		175	110	3.34	0.76	0.83	70
M5	27-29	6.89		124	73	3.12	0.72	0.87	325
M5	28-40	6.92		123	72	2.98	0.62	0.88	300
PH93	22-23	6.82		112	68	2.94	0.56	0.89	115
KD2	24-32	7.22		174	107	2.95	0.69	0.67	430
AD1	9.5m	6.71		110	53	5.15	0.64	1.32	10
AD2	9.0m	7.69		191	119	3.54	1.09	1.81	35
AD8	9.0m	6.59		97	50	2.44	0.86	0.94	20

TABLE A3.6.2

MAJOR CATIONS, U and Si: NOV 90

Bore	Depth (m)	Mg mg/L	Na mg/L	K mg/L	Ca mg/L	Si mg/L	Fe mg/L	Mn µg/L	U µg/L
W1a	13-15	¦	1.68	1.40	¦	¦	0.003	0.5	8.83
W1b	23-25	[11.5]	1.65	1.12	¦	¦	0.013	16	106
W2a	13-15	[11.4]	1.39	0.73	¦	¦	0.004	35	83.3
W2b	23-25	14.5	1.59	0.62	0.92	¦	0.038	25	107
W4a	13-15	7.8	1.81	0.72	2.33	¦	0.074	326	459
W4b	23-25	22.3	1.08	0.78	1.20	¦	0.538	75	355
W5a	13-15	10.1	1.82	0.77	[8.9]	¦	0.004	23	0.63
W5b	23-25	10.9	1.76	0.69	1.46	¦	0.085	117	0.83
W7a	13-15	¦	1.16	0.32	[5.8]	¦	0.017	1.9	1.30
W7b	23-25	7.1	1.23	0.40	1.01	¦	0.006	1.1	0.59
C1	22-23	14.3	1.31	0.62	1.85	¦	0.139	179	7.52
C4	23-40	12.1	1.08	0.30	0.41	¦	0.207	681	13.1
C6	23-25	15.1	1.34	0.83	1.45	¦	0.010	63	5.21
M5	27-29	10.4	1.61	0.67	0.71	¦	0.155	47	3.72
M5	28-40	10.5	1.62	0.65	0.69	¦	0.132	42	5.17
PH93	22-23	8.7	1.84	0.90	0.85	¦	0.740	109	1.42
KD2	24-32	13.8	1.57	0.73	1.53	¦	3.610	85	2.87
AD1	9.5m	12.1	1.79	1.12	1.15	¦	0.003	402	52.5
AD2	9.0m	13.1	3.28	1.89	0.91	¦	0.005	171	2.55
AD8	9.0m	4.0	2.68	2.47	1.05	¦	1.320	2013	1.13
Blank								0.3	0.004

TABLE A3.7.1

FIELD DATA AND ANIONS: APR 91

Bore	Depth m	pH	Eh mV	EC µS/cm	HCO_3^- mg/L	Cl^- mg/L	F^- mg/L	SO_4^{2-} mg/L	PO_4^{3-} µg/L
W1 a	13-15	¦	¦	197	109	3.86	0.77	¦	115
W1 b	23-25	6.60	190	187	107	2.74	0.71	3.10	425
W2 a	13-15	[7.2]	[145]	166	102	3.32	0.68	3.37	25
W2 b	23-25	6.45	215	166	99	3.14	0.70	1.30	130
W4 a	13-15	5.82	310	120	50	9.43	0.53	1.47	30
W4 b	23-25	6.78	135	246	154	4.09	0.73	1.01	65
W5 a	13-15	[7.4]	[185]	166	100	2.85	0.64	1.19	545
W5 b	23-25	6.76	150	136	81	2.83	0.62	0.90	480
W6 b	23-25	[8.1]	[235]	[180]	100	1.92	0.66	2.93	110
W7 a	13-15	¦	¦	87	46	2.56	0.51	1.36	75
W7 b	23-25	6.98	310	82	43	2.24	0.56	1.15	395
C1	22-23	7.39	155	168	102	2.86	0.64	0.97	55
C6	23-24	7.68	240	195	121	3.11	0.75	0.77	20
M2	36-40	7.39	215	278	176	2.45	1.01	1.81	25
PH14	20-26	7.21	-5	261	164	2.97	0.84	0.70	55
PH146	17-89	6.65	140	221	140	2.09	0.89	1.14	565
KD2	24-26	6.79	120	161	99	3.01	0.68	0.89	200
AD1	9.5m	5.90	380	30	11	2.78	0.42	2.22	<5
AD1*	9.5m	5.70	400	31	10	3.07	1.03	1.15	<5
AD2	9.0m	6.70	255	62	31	2.90	0.47	0.74	<5
AD6	4.0m	6.40	305	56	21	3.19	0.45	0.69	<5
AD8	9.0m	6.44	330	60	30	2.54	0.51	0.92	<5
AD9	7.0m	5.96	325	42	18	1.90	0.43	1.05	<5
AD9*	7.0m	5.68	335	38	14	2.22	0.42	0.85	<5
AD11	2.5m	5.74	290	33	14	1.42	0.42	1.32	<5
AD12	5.0m	6.76	180	115	54	4.20	0.63	3.58	<5
TAD12	1.5m	5.55	355	24	6	2.02	0.40	0.96	<5
AD13	9.0m	6.43	205	149	76	6.87	0.65	2.42	<5
AD14	10.5m	5.80	235	101	41	6.87	0.56	2.43	<5
RAIN		5.2	555	17					
CREEK NEAR KD1		4.6	485	18	<5	1.90	0.36	0.68	10

* - Denotes second sample set
TAD12 was a temporary sampling point close to AD12

TABLE A3.7.2

MAJOR CATIONS, U and Si: APR 91

Bore	Depth m	Mg mg/L	Na mg/L	K mg/L	Ca mg/L	Si mg/L	Fe mg/L	Mn µg/L	U µg/L
W1 a	13-15	¦	1.94	1.16	¦	5.5	0.002	1	7.76
W1 b	23-25	12.4	1.94	1.06	[8.9]	6.5	0.078	11	45.9
W2 a	13-15	11.3	1.64	0.57	¦	13.5	0.003	14	47.0
W2 b	23-25	14.8	1.62	0.59	0.99	13.9	0.053	20	67.3
W4 a	13-15	9.0	1.92	0.51	2.10	8.0	0.091	208	393
W4 b	23-25	23.0	1.39	0.71	1.39	8.0	0.369	47	287
W5 a	13-15	[11.0]	2.32	0.75	[9.5]	16.9	0.006	26	1.37
W5 b	23-25	11.4	2.30	0.58	1.77	16.7	0.094	75	2.08
W6 b	23-25	¦	¦	¦	¦	¦	¦	¦	2.63
W7 a	13-15	¦	2.06	0.25	¦	8.7	0.005	3	1.18
W7 b	23-25	6.7	1.40	0.46	0.93	12.8	0.005	1	0.32
C1	22-23	14.7	1.64	0.59	2.15	9.1	0.023	147	7.14
C6	23-24	17.6	1.82	0.99	1.94	3.1	0.007	77	3.75
M2	36-40	23.9	1.44	1.07	6.30	4.7	0.004	74	36.1
PH14	20-26	20.3	1.61	0.74	6.60	7.5	3.600	550	¦
PH146	17-89	19.4	1.00	0.38	3.60	6.9	1.200	28	0.77
KD2	24-26	13.6	1.79	0.50	1.31	12.9	1.640	58	1.54
AD1	9.5m	1.33	2.41	0.36	0.93	4.4	0.012	36	5.14
AD1*	9.5m	0.54	2.50	0.46	1.60	6.2	0.187	2	7.14
AD2	9.0m	3.86	4.30	0.29	1.49	4.4	0.108	63	0.73
AD6	4.0m	2.46	2.62	0.19	0.18	5.6	0.040	55	0.49
AD8	9.0m	2.89	2.84	1.87	1.44	5.0	0.006	950	0.63
AD9	7.0m	2.22	1.60	0.15	0.61	4.9	0.008	165	0.13
AD9*	7.0m	1.84	1.65	0.27	0.58	5.2	0.014	166	0.16
AD11	2.5m	0.55	4.50	0.33	2.35	2.6	0.610	86	1.31
AD11*	2.5m	0.26	2.71	0.30	0.41	2.3	0.580	68	0.43
AD12	5.0m	7.63	3.60	0.50	2.47	7.5	0.004	151	2.03
TAD12	1.5m	1.11	1.97	0.14	0.17	3.4	0.029	6	0.47
AD13	9.0m	9.20	3.60	2.24	5.60	10.4	1.220	370	77.9
AD14	10.5m	3.23	3.00	1.55	6.60	6.8	2.730	208	2.94
CREEK NEAR KD1		0.14	1.29	0.21	0.12	3.0	0.183	3	0.52
Blank		<0.001	0.06	<0.04	0.001		0.002	<1	<0.01

* - Denotes second sample set
TAD12 was a temporary sampling point close to AD12

APPENDIX 4

TRACE CONSTITUENTS (quantitative data)

Data grouped by Field Trip - full details are given in Table 3.1

Note: Data units in this Appendix are µg/L (ppb)

In this Appendix, the following usage is adopted:

Blank space	no data / not measured
[ ]	imprecise or doubtful data
¦	data not reported due to evidence of contamination, analytical error, reporting error, etc.

Note that some shallow depths in W-holes (13-15 m sampling interval) showed evidence of contamination by materials used in sealing the sampling interval (see text). In the case of major ions (presented in Appendix 3), anomalous results could be readily identified and were rejected. In this Appendix, raw analytical data are presented, and the possibility of erroneous data for the shallow sampling intervals (ie W1a, W2a, W3a, W4a, W5a, W7a) should be considered in interpreting the results. All other boreholes (PH, C-, M-, KD-, and AD- holes) were constructed without the use of sealing materials, therefore these samples were unaffected by this source of error.

TABLE A4.1

TRACE CONSTITUENTS (Quantitative Data): MAY 88

Bore	Depth m	Al µg/L	As µg/L	B µg/L	Ba µg/L	Pb µg/L	Ti µg/L	V µg/L	Zn µg/L
PH14	20-26	<20	<20	20	76	<30	5	<3	70
PH15	19-21	20	<20	20	49	<30	1	<3	1380
PH49	16-28	20	<20	30	9	<30	2	<3	2
PH49	28-30	240	<20	40	17	<30	6	<3	25
PH55	26-28	<20	<20	60	204	<30	2	<3	58
PH55	40-42	120	<20	30	70	<30	7	<3	12
PH56	26-28	40	<20	40	10	<30	5	<3	2
PH56	43-45	150	<20	40	21	<30	1	<3	17
PH58	25-27	30	<20	30	42	<30	5	<3	207
PH58	38-40	30	<20	30	67	<30	3	<3	6
PH61	26-28	20	<20	30	9	<30	1	<3	2
PH61	43-45	20	<20	40	54	<30	1	<3	3
PH80	17-20	30	<20	30	2	<30	1	<3	2
PH88	28-30	<20	<20	30	6	<30	2	<3	2
PH88	38-40	20	<20	30	8	<30	1	<3	<2
PH94	26-28	<20	<20	20	7	<30	2	<3	<2
PH94	40-42	20	<20	40	7	<30	1	<3	<2
PH96	16-26	20	<20	20	14	<30	6	<3	<2
KD1	40-42	20	<20	20	9	<30	1	<3	8
KD1	80-82	<20	<20	40	6	<30	2	<3	14
Blank		20		20	<1		1		<2
Blank		<20		10	<1		5		<2
Blank		20		10			5		<2

TABLE A4.2

TRACE CONSTITUENTS (Quantitative Data): NOV 88

Bore	Depth m	Al µg/L	As µg/L	B µg/L	Ba µg/L	Cu µg/L	Pb µg/L
PH14	20-26	<10	0.4	15	41	<3	3.3
PH15	19-21	<10	1.2	4	9	<3	1.3
PH49	28-30	<10	0.7	14	11	<3	1.1
PH49	44-46	<10	0.7	23	10	<3	0.3
PH55	26-28	<10	1.0	11	20		0.4
PH55	40-42	<10	0.4	9	23		0.7
PH56	26-28	10	0.3	15	9		0.5
PH56	43-45	10	0.3	17	17		0.6
PH58	25-27	10	0.4	14	42	<3	1.3
PH58	38-40	<10	1.2	8	49	<3	0.7
PH61	26-28	<10	0.4	9	30		1.0
PH61	43-45	<10	0.6	18	52		0.7
PH80	17-20	<10	0.2	11	5	<3	0.9
PH88	28-30	<10	0.2	15	7		0.7
PH88	38-40	<10	<0.1	8	10		0.9
PH94	26-28	<10	0.6	12	5	<3	[26.1]
PH94	40-42	<10	0.3	9	3		1.1
PH96	16-26	<10	1.0	4	11		2.1
KD1	40-42	<10	0.9	6	5	<3	1.0
KD1	70-72	<10	0.6	10	7		1.1
PH27*	20m	<10	<0.1	11	22		1.0
PH92*	20m	<10	0.3	11	10		0.8
PH96*	20m	<10	0.3	3	10		0.8
PH110*	20m	<10	0.7	9	16		1.9
PH139*	20m	<10	0.2	7	45		0.7
BLANK						2	

* - Samples obtained using a small-volume electric pump without packers.

TABLE A4.2 (Continued)

TRACE CONSTITUENTS (Quantitative Data): NOV 88

Bore	Depth m	Se µg/L	Th µg/L	Ti µg/L	V µg/L	Zn µg/L
PH14	20-26	<1	0.07	<2	0.9	40
PH15	19-21	<1	0.07	<2	1.6	2650
PH49	28-30	1	0.07	<2	1	6
PH49	44-46	<1	0.06	<2	1.1	<2
PH55	26-28	2	0.06	<2	1	<2
PH55	40-42	<1	0.06	<2	0.7	<2
PH56	26-28	<1	0.07	<2	1	6
PH56	43-45	<1	0.07	<2	0.7	<2
PH58	25-27	<1	0.08	<2	0.9	6
PH58	38-40	4	0.06	<2	1.4	4
PH61	26-28	<1	0.07	<2	0.8	<2
PH61	43-45	<1	0.06	<2	0.8	<2
PH80	17-20	<1	0.1	<2	0.7	3
PH88	28-30	<1	0.06	<2	2.3	16
PH88	38-40	<1	0.07	<2	1.5	18
PH94	26-28	<1	0.06	<2	4.1	2
PH94	40-42	<1	0.1	<2	2.2	<2
PH96	16-26	3	0.06	<2	3.1	<2
KD1	40-42	3	0.09	<2	0.6	<2
KD1	70-72	<1	0.06	<2	0.8	5
*PH27	20m	<1	0.15	<2	0.4	680
*PH92	20m	<1	0.07	<2	0.5	<2
*PH96	20m	<1	0.21	<2	1.8	4
*PH110	20m	1	0.06	<2	1.2	2
*PH139	20m	<1	0.08	<2	0.4	<2

* - Samples obtained using a small-volume electric pump without packers.

TABLE A4.3

TRACE CONSTITUENTS (Quantitative Data): MAY 89

Bore	Depth m	Al µg/L	B µg/L	Ba µg/L	Co µg/L	La µg/L	Mo µg/L	Nd µg/L	Pb µg/L
PH14	20-26	<2	25	65.6	3.2	0.82	0.6	0.1	0.7
PH49	27-29	<2	31	22	1.6	0.21	0.5	0.1	0.5
PH43	33-35	<2	27	23	1	0.33	0.7	0.1	0.4
PH80	17-19	<2	22	5.8	0.5	0.05	0.3	0.1	0.3
PH146	17-89	<2	20	4	0.4	0.09	0.2	0.1	0.9
PH146*	17-89	<2	26	2.5	1	0.1	0.4	0.2	0.5
C6	35-40	<2	19	23.5	0.1	0.24	0.8	0.1	0.3
C8	24-26	<2	24	8.7	0.3	0.18	0.2	0.2	0.5
C8	38-40	<2	13	25.6	0.4	0.3	0.6	0.1	0.5
C9	34-40	<2	20	21.1	0.2	0.34	0.9	0.1	0.5
C10	27-40	<2	24	5.7	0.4	0.12	0.3	0.1	0.3
M1	24-26	<2	26	7.1	0.3	0.12	0.8	0.3	0.4
M1	35-50	<2	23	8.9	0.2	0.14	0.5	0.2	0.4
M1	46-48	<2	23	7.3	0.1	0.27	0.5	0.2	0.3
M2	40-46	<2	38	12.7	0.1	0.16	6.7	0.1	0.3
M3	20-22	<2	18	7.3	0.4	0.1	0.3	0.1	0.5
M3	26-28	<2	25	7.1	0.3	0.15	0.2	0.1	0.4
M3	34-40	<2	17	8.1	0.4	0.11	0.2	0.1	0.3
M4	34-40	<2	17	52.6	0.3	0.71	0.7	0.1	1.4
W4	23-25	<2	38	15.9	0.5	0.22	1.1	0.1	0.6
K Creek		<2	14	0.3	0.3	0.04	0.2	0.2	1
Blank		<2	9	0.2	<0.1	0.02	0.1	0.1	0.2
Blank		<2	7	0.4	0.1	0.06	0.2	0.1	0.2

* - Denotes second sample set at PH146

TABLE A4.3 (Continued)

TRACE CONSTITUENTS (Quantitative Data): MAY 89

Bore	Depth m	Rb µg/L	Se µg/L	Sr µg/L	Th µg/L	Ti µg/L	V µg/L	Zn µg/L	Zr µg/L
PH14	20-26	1.3	<5	3.9	0.01	<2	2	95	0.1
PH49	27-29	3.3	<5	5.8	0.01	<2	0.8	74	0.1
PH49	33-35	2.6	<5	7.6	0.02	<2	0.8	78	0.1
PH80	17-19	1.1	<5	2.6	0.05	<2	1.8	36	0.3
PH146	17-89	1.2	<5	4.8	0.04	<2	1	21	<0.1
PH146*	17-89	1.4	<5	7.2	0.01	<2	1.3	21	0.2
C6	35-40	1.5	<5	3	0.01	2	0.9	15	0.1
C8	24-26	1	<5	2.6	0.02	<2	1.6	31	0.1
C8	38-40	1.6	<5	3.2	0.01	6	0.8	34	0.1
C9	34-40	3.3	<5	19.2	0.01	4	1.1	36	<0.1
C10	27-40	2.9	<5	3.6	0.02	<2	0.5	15	0.1
M1	24-26	3.1	<5	2.6	0.02	2	0.8	19	0.1
M1	35-50	2.8	<5	2.5	0.01	<2	3	16	0.1
M1	46-48	1.8	<5	2.5	0.03	<2	8.7	11	0.2
M2	40-46	4.3	<5	17.4	0.01	3	1.1	15	0.1
M3	20-22	0.8	<5	0.8	0.02	2	0.7	19	0.1
M3	26-28	1.4	<5	1.3	<0.01	2	0.4	42	0.1
M3	34-40	1.5	<5	1.2	0.01	<2	0.7	35	0.1
M4	34-40	7.7	<5	8.8	0.02	3	0.6	65	0.1
W4	23-25	3.9	<5	1.8	0.02	<2	2	22	0.1
K Creek		0.7	<5	1.4	0.03	<2	0.6	18	0.2
Blank		<0.1	4	0.1	0.01	2	0.4	15	0.1
Blank		0.1	5	0.1	0.01	2	0.4	20	0.1

* - Denotes second sample set at PH146

TABLE A4.4

TRACE CONSTITUENTS (Quantitative Data): OCT 89

Bore	Depth m	Al µg/L	B µg/L	Ba µg/L	Br µg/L	Ce µg/L	Co µg/L	Cr µg/L	Cu µg/L
W1 a	13-15	43.00	19.00	6.23	38.71	0.00	0.13	0.52	0.60
W1 a*	13-15	90.00	20.00	5.58	44.61	0.00	0.25	0.37	0.99
W1 b	23-25	28.00	23.00	9.74	77.12	0.00	0.52	0.71	0.56
W1 b*	23-25	31.00	20.00	10.17	72.78	0.01	0.60	0.71	2.09
W2 a	13-15	5.00	15.00	14.52	24.04	0.01	0.09	0.21	3.87
W2 b	23-25	2.00	14.00	4.76	38.74	0.00	0.13	0.19	0.58
W3 a	13-15	37.00	23.00	9.36	35.85	0.01	0.12	0.27	2.29
W3 b	23-25	4.00	38.00	29.06	29.60	0.00	1.51	0.21	2.67
W4 a	13-15	4.00	23.00	18.88	63.78	0.00	18.07	0.25	0.62
W4 a*	13-15	3.00	22.00	23.58	63.98	0.00	24.08	0.23	1.13
W4 b	23-25	15.00	39.00	15.58	30.04	0.00	0.33	0.31	0.60
W4 b*	23-25	13.00	42.00	17.61	59.61	0.00	0.43	0.24	1.38
W5 a	13-15	10.00	11.00	12.15	19.88	0.00	0.11	0.19	0.56
W5 b	23-25	5.00	13.00	21.75	34.05	0.00	0.07	0.16	2.77
W7 a	13-15	2.00	21.00	5.27	27.90	0.00	0.10	0.18	0.67
W7 b	23-25	2.00	17.00	5.37	17.73	0.00	0.07	0.42	0.90
M2	37-39	15.00	43.00	12.32	17.33	0.00	0.18	0.11	1.03
C5	25-27	4.00	23.00	6.42	21.09	0.00	0.07	0.22	3.82
C7	25-27	3.00	22.00	7.46	47.52	0.00	0.25	0.33	6.07
PH49	25-27	6.00	35.00	10.99	85.64	0.00	1.43	0.40	0.67
PH49	45-47	7.00	35.00	7.31	110.56	0.00	0.29	0.27	2.18

* - denotes second set of samples

TABLE A4.4 (Continued)

TRACE CONSTITUENTS (Quantitative Data): OCT 89

Bore	Depth m	I µg/L	La µg/L	Mn µg/L	Mo µg/L	Nd µg/L	Ni µg/L	Pb µg/L	Rb µg/L
W1 a	13-15	9.15	0.04	4.69	2.49	0.16	2.33	0.47	4.70
W1 a*	13-15	8.11	0.14	4.10	1.86	0.17	1.86	0.52	5.19
W1 b	23-25	7.04	0.07	15.82	0.73	0.10	3.63	0.89	5.78
W1 b*	23-25	7.14	0.04	20.42	0.79	0.05	3.56	0.32	5.83
W2 a	13-15	3.86	0.09	2.52	0.93	0.10	5.42	0.60	1.21
W2 b	23-25	5.46	0.06	11.35	0.13	0.12	0.98	0.66	0.53
W3 a	13-15	13.28	0.07	27.28	0.84	0.07	1.50	0.43	2.23
W3 b	23-25	4.33	0.26	498.02	0.40	0.16	1.00	0.21	2.46
W4 a	13-15	13.20	0.02	420.95	0.23	0.06	31.20	0.89	2.21
W4 a*	13-15	16.86	0.12	536.63	0.35	0.08	30.40	0.92	1.94
W4 b	23-25	9.94	0.04	60.05	0.82	0.05	0.95	0.95	2.27
W4 b*	23-25	11.64	0.08	68.86	0.45	0.06	1.11	0.64	2.34
W5 a	13-15	4.80	0.08	22.35	0.23	0.08	1.08	0.35	1.05
W5 b	23-25	6.73	0.08	108.69	0.12	0.13	1.09	0.53	1.26
W7 a	13-15	21.46	0.03	1.37	0.96	0.14	0.69	0.28	0.11
W7 b	23-25	6.01	0.04	3.25	0.16	0.06	1.27	0.29	0.29
M2	37-39	8.07	0.10	23.49	5.98	0.14	1.19	3.46	2.39
C5	25-27	5.43	0.20	31.54	0.31	0.19	1.38	0.47	1.19
C7	25-27	6.34	0.05	44.75	0.87	0.08	1.13	0.89	1.14
PH49	25-27	6.50	0.08	142.72	1.42	0.14	1.47	2.61	2.02
PH49	45-47	5.11	0.17	42.73	1.02	0.07	1.37	1.19	1.84

TABLE A4.4 (Continued)

TRACE CONSTITUENTS (Quantitative Data): OCT 89

Bore	Depth m	Se µg/L	Sm µg/L	Sr µg/L	Th µg/L	Ti µg/L	U µg/L	V µg/L	Zn µg/L	Zr µg/L
W1 a	13-15	8.26	0.03	37.86	0.00	<1	2.51	5.81	11.25	0.12
W1 a*	13-15	5.84	0.09	40.89	0.01	<1	7.33	4.89	7.32	0.08
W1 b	23-25	2.95	0.10	33.84	0.01	<1	38.62	4.67	6.70	0.08
W1 b*	23-25	7.07	0.09	38.90	0.02	<1	50.46	5.43	11.39	0.49
W2 a	13-15	8.85	0.06	33.13	0.00	<1	14.05	2.20	10.38	0.13
W2 b	23-25	6.62	0.07	1.69	0.01	<1	71.18	2.21	7.78	0.07
W3 a	13-15	4.29	0.04	19.50	0.02	<1	4.11	5.44	8.09	0.07
W3 b	23-25	3.71	0.07	35.28	0.02	<1	1.33	0.21	6.81	0.07
W4 a	13-15	7.89	0.07	3.41	0.01	<1	413.99	2.80	28.24	0.06
W4 a*	13-15	3.75	0.05	3.92	0.01	<1	438.53	1.70	29.40	0.07
W4 b	23-25	8.41	0.06	3.22	0.01	<1	364.36	1.85	9.10	0.11
W4 b*	23-25	11.11	0.05	2.00	0.01	<1	318.25	1.34	8.79	0.04
W5 a	13-15	1.43	0.05	9.83	0.01	<1	0.38	3.54	9.43	0.06
W5 b	23-25	7.28	0.11	6.80	0.01	<1	1.82	0.37	28.12	0.10
W7 a	13-15	7.37	0.06	2.88	0.01	<1	0.13	7.11	4.89	0.07
W7 b	23-25	1.50	0.06	3.97	0.01	<1	0.22	6.49	5.94	0.10
M2	37-39	2.20	0.06	18.43	0.01	<1	7.35	0.35	8.38	0.09
C5	25-27	2.95	0.12	2.50	0.01	<1	7.94	0.49	15.10	0.07
C7	25-27	3.75	0.09	2.87	0.01	<1	5.49	0.31	9.13	0.05
PH49	25-27	4.45	0.06	7.42	0.02	<1	107.90	0.33	27.57	0.06
PH49	45-47	3.91	0.05	12.15	0.01	<1	130.72	0.51	9.41	0.10

TABLE A4.5

TRACE CONSTITUENTS (Quantitative Data): MAY 90

Bore	Depth (m)	Al µg/L	As µg/L	B µg/L	Ba µg/L	Bi µg/L	Br µg/L	Cd µg/L	Ce µg/L	Co µg/L	Cr µg/L
W1 a	13-15	73.63	0.14	24	4.58	0.01	125.46	0.03	0.00	0.19	0.40
W1 b	23-25	9.19	0.13	31	10.82	-0.01	142.65	-0.01	0.00	0.57	0.15
W2 a	13-15	39.25	0.10	21	11.78	0.00	140.48	-0.05	0.00	0.19	0.04
W2 b	23-25	7.10	0.06	26	4.03	-0.01	118.92	-0.01	0.00	0.12	0.02
W4 a	13-15	7.67	0.20	29	19.56	0.00	279.24	-0.05	0.01	22.23	0.02
W4 b	23-25	23.39	0.13	34	15.90	-0.01	127.31	0.27	0.00	0.45	0.03
W5 a	13-15	5.76	0.20	31	12.71	0.00	81.45	-0.05	0.00	0.05	0.02
W5 b	23-25	3.08	0.10	16	21.12	0.02	138.59	-0.05	0.00	0.08	0.04
W7 a	13-15	5.16	0.18	23	5.81	0.01	145.49	0.21	0.00	0.04	0.03
W7 b	23-25	0.94	0.07	26	5.84	-0.01	85.67	0.12	0.00	0.01	0.19
PH49	18-20	1.07	0.38	36	11.43	0.00	135.54	0.08	0.00	3.09	0.02
C9	28-30	0.53	1.29	31	24.30	-0.01	239.54	-0.05	0.00	0.15	0.02
M1	27-29	0.83	0.12	32	5.57	0.01	55.24	0.15	0.00	0.26	0.02
M2	42-44	8.92	0.43	47	8.12	0.00	244.21	0.11	0.00	0.20	0.04
M4	28-30	2.96	0.15	13	44.04	0.02	141.96	0.04	0.00	0.12	0.01
KD1	65-76	-0.38	0.75	25	12.25	0.00	304.61	0.13	0.00	6.38	0.08
BLANK		-0.55	0.03	<3	0.61	0.02	5.18	-0.02	0.00	0.00	0.01

TABLE A4.5 (Continued)

TRACE CONSTITUENTS (Quantitative Data): MAY 90

Bore	Depth (m)	Cu	Dy	Er	Eu	Gd µg/L	Ho	I	La	Lu	Mn
W1 a	13-15	0.24	0.02	-0.01	0.01	-0.02	0.01	3.78	-0.06	0.01	4.40
W1 b	23-25	0.04	-0.01	-0.01	0.03	0.01	0.01	4.15	-0.08	0.00	13.32
W2 a	13-15	0.18	0.01	-0.01	0.02	0.00	0.00	2.95	-0.10	-0.01	25.72
W2 b	23-25	-0.25	0.01	-0.01	0.02	-0.02	0.00	3.14	-0.02	0.01	9.41
W4 a	13-15	0.12	0.02	-0.01	0.02	0.04	0.01	15.44	0.00	0.00	530.97
W4 b	23-25	-0.11	0.02	-0.01	0.02	0.01	0.01	10.11	-0.06	0.01	54.69
W5 a	13-15	-0.03	0.04	-0.01	0.03	0.01	0.01	2.07	-0.08	0.01	19.72
W5 b	23-25	0.18	0.01	-0.01	0.05	0.00	0.00	2.40	-0.08	0.00	104.22
W7 a	13-15	-0.04	0.04	0.07	0.02	0.01	0.01	3.91	-0.04	-0.01	1.58
W7 b	23-25	-0.10	0.01	-0.01	0.00	0.06	0.00	3.52	-0.06	-0.01	0.45
PH49	18-20	-0.17	0.02	-0.04	0.01	0.04	0.00	8.48	-0.08	0.01	322.88
C9	28-30	-0.10	0.03	-0.01	0.03	0.00	0.02	7.70	-0.08	0.00	79.34
M1	27-29	-0.15	-0.01	0.02	0.02	-0.01	0.00	7.97	-0.04	0.00	80.74
M2	42-44	0.29	0.02	-0.01	0.02	0.01	0.01	7.89	-0.06	0.00	49.55
M4	28-30	-0.09	-0.01	-0.04	0.04	-0.02	0.00	3.40	-0.03	-0.01	153.92
KD1	65-76	0.23	0.05	-0.01	0.03	0.00	0.02	4.73	-0.10	0.00	252.66
BLANK		-0.08	0.00	-0.03	0.01	0.06	0.00	-0.73	-0.08	0.00	0.08

TABLE A4.5 (Continued)

TRACE CONSTITUENTS (Quantitative Data): MAY 90

Bore	Depth (m)	Mo	Nd	Ni	Pb	Pr µg/L	Rb	Sb	Se	Sm	Sr
W1 a	13-15	3.58	0.02	4.18	0.27	-0.01	3.79	0.08	1.86	0.03	33.08
W1 b	23-25	0.62	-0.03	4.01	1.03	-0.02	4.27	0.04	0.56	-0.01	25.65
W2 a	13-15	0.72	-0.03	4.07	0.09	-0.02	0.69	0.14	-0.33	0.03	19.17
W2 b	23-25	0.06	0.02	0.17	-0.06	-0.01	0.51	-0.04	-0.36	-0.01	1.47
W4 a	13-15	0.35	0.08	28.71	0.49	-0.01	2.07	-0.02	-0.36	0.06	2.63
W4 b	23-25	0.60	0.02	0.30	0.07	-0.01	2.67	0.04	0.80	0.02	1.84
W5 a	13-15	0.16	0.14	1.13	0.10	-0.01	1.05	-0.04	-0.67	-0.01	10.04
W5 b	23-25	0.10	0.02	0.30	0.52	-0.01	1.11	0.01	-0.67	0.06	5.77
W7 a	13-15	0.64	0.02	0.81	-0.02	-0.01	0.14	0.08	-0.66	-0.04	3.75
W7 b	23-25	0.11	0.02	0.17	-0.06	-0.02	0.30	-0.01	-0.33	-0.01	2.21
PH49	18-20	1.25	0.08	0.92	-0.04	-0.01	2.05	-0.07	0.28	0.06	4.22
C9	28-30	1.14	0.09	1.14	0.04	-0.02	2.41	0.15	0.35	-0.01	6.88
M1	27-29	0.46	0.02	0.97	0.08	0.00	1.75	0.09	-0.40	-0.04	2.34
M2	42-44	7.21	-0.03	0.87	0.47	-0.02	2.16	0.04	-0.38	0.05	8.17
M4	28-30	0.27	-0.03	0.23	-0.02	-0.01	4.05	0.09	0.43	-0.04	6.91
KD1	65-76	0.13	0.09	4.28	-0.01	0.01	1.35	-0.04	0.03	-0.01	15.47
BLANK		-0.02	0.01	0.06	-0.12	0.00	0.00	-0.05	-0.44	-0.04	0.05

TABLE A4.5 (Continued)

TRACE CONSTITUENTS (Quantitative Data): MAY 90

Bore*	Tb	Te	Th	Ti	Tm	U µg/L	V	Y	Yb	Zn	Zr
W1 a	0.02	0.41	0.00	<2	0.01	4.64	7.08	0.01	-0.04	5.35	-0.01
W1 b	0.00	0.11	0.10	<2	0.00	62.96	4.34	0.00	0.00	12.97	-0.01
W2 a	0.01	0.74	0.03	<2	0.00	59.57	2.84	0.02	0.00	7.82	0.00
W2 b	0.00	-0.14	-0.02	<2	0.01	95.51	2.39	0.00	0.00	1.22	0.00
W4 a	0.00	0.11	0.04	<2	0.00	511.35	2.11	0.09	0.04	22.78	0.00
W4 b	0.01	0.10	0.04	<2	0.01	389.46	1.24	0.00	-0.02	7.18	0.03
W5 a	0.01	1.00	0.02	<2	0.00	0.22	1.74	0.01	0.00	2.58	0.04
W5 b	0.01	0.11	-0.02	<2	0.01	0.38	0.20	0.00	0.00	7.99	0.17
W7 a	0.00	0.43	-0.02	<2	0.01	5.40	4.54	0.00	-0.02	0.27	-0.01
W7 b	0.01	1.05	-0.02	<2	0.00	0.56	6.57	-0.01	-0.04	1.83	0.03
PH49	0.01	0.41	0.00	<2	0.01	117.55	0.25	-0.01	-0.02	21.25	0.01
C9	0.03	-0.14	-0.04	<2	0.00	57.25	0.45	0.00	-0.04	14.63	0.00
M1	0.01	0.09	-0.02	<2	0.00	489.43	0.92	-0.01	0.02	5.93	0.03
M2	0.01	0.38	0.04	<2	0.00	52.20	0.27	-0.01	0.00	10.42	0.00
M4	0.00	0.48	-0.04	<2	0.01	3.85	0.16	0.00	-0.02	16.19	0.00
KD1	0.02	-0.14	0.05	<2	0.00	3.43	0.08	-0.01	0.01	26.05	0.00
BLANK	0.00	0.07	0.00	<2	0.00	0.01	0.01	-0.01	-0.03	1.89	0.01

* - sample depths are as shown on p167

TABLE A4.6

TRACE CONSTITUENTS (Quantitative Data): NOV 90

Bore	Depth (m)	Al µg/L	As µg/L	B µg/L	Ba µg/L	Bi µg/L	Br µg/L	Cd µg/L	Ce µg/L	Co µg/L	Cr µg/L
W1 a	13-15	3156.04	0.24	20.0	1.80	0.01	257.43	0.00	0.00	0.18	0.74
W1 b	23-25	19.41	0.31	20.0	21.58	0.00	393.03	0.33	0.00	0.65	0.55
W2 a	13-15	66.50	0.18	10.00	15.52	0.00	358.97	0.23	0.00	0.20	0.14
W2 b	23-25	2.96	0.00	20.00	9.58	0.01	286.91	0.10	0.00	0.25	0.12
W4 a	13-15	3.59	0.08	20.00	22.85	-0.01	568.21	0.05	0.01	20.24	0.08
W4 b	23-25	8.98	0.31	40.00	18.78	0.01	343.27	0.08	0.00	0.65	0.12
W5 a	13-15	8.50	0.42	20.00	13.56	-0.01	290.72	-0.01	0.00	0.08	0.09
W5 b	23-25	3.99	0.15	20.00	25.80	0.01	230.39	0.04	0.00	0.11	0.16
W7 a	13-15	15.13	0.16	20.00	7.06	0.02	201.44	0.02	0.00	0.06	0.04
W7 b	23-25	1.66	0.08	10.00	5.34	0.03	261.76	0.02	0.00	0.04	0.15
C1	22-23	4.61	0.26	31.00	4.74	-0.02	359.57	0.11	0.00	0.12	0.14
C4	23-40	3.77	0.03	10.00	7.70	0.01	315.93	0.24	0.00	0.50	0.12
C6	23-25	19.41	0.03	20.00	13.43	0.00	309.24	-0.01	0.00	0.04	0.57
M5	27-29	1.35	0.12	20.00	6.31	0.01	243.78	0.15	0.00	0.16	0.09
M5	28-40	2.25	0.13	20.00	6.89	0.02	247.55	-0.05	0.00	0.25	0.14
PH93	22-23	9.02	0.00	20.00	11.60	0.01	241.88	0.18	0.01	0.34	0.05
KD2	24-32	1.44	0.33	20.00	9.83	0.01	254.28	0.04	0.00	0.07	0.09
AD1	9.5	1.22	0.04	10.00	39.62	0.02	1188.80	0.20	0.00	3.47	0.15
AD2	9.0	1.09	0.18	20.00	45.88	-0.01	507.90	0.11	0.00	1.37	1.03
AD8	9.0	11.40	0.38	20.00	197.93	-0.01	2144.72	1.17	0.04	29.02	0.92
BLANK		0.39	0.05	30.00	0.02	0.03	20.15	0.05	0.01	0.05	0.01

TABLE A4.6 (Continued)

TRACE CONSTITUENTS (Quantitative Data): NOV 90

Bore	Depth (m)	Cu µg/L	Dy µg/L	Er µg/L	Eu µg/L	Gd µg/L	Ho µg/L	I µg/L	La µg/L	Lu µg/L	Mn µg/L
W1 a	13-15	0.80	0.03	-0.04	0.01	0.03	0.00	6.41	-0.10	0.00	0.49
W1 b	23-25	2.12	0.03	-0.02	0.02	0.04	0.01	6.77	-0.10	0.01	15.98
W2 a	13-15	0.85	0.06	-0.02	0.05	0.04	0.03	2.02	0.03	0.00	35.20
W2 b	23-25	0.65	0.01	-0.03	0.02	0.00	0.00	4.29	-0.05	0.01	25.00
W4 a	13-15	1.16	0.07	-0.03	0.02	0.07	0.01	26.78	0.02	0.01	325.55
W4 b	23-25	0.27	0.01	-0.01	0.05	-0.02	0.03	18.20	-0.06	0.01	74.91
W5 a	13-15	0.56	0.02	-0.04	0.04	0.00	0.00	3.93	-0.02	0.00	22.79
W5 b	23-25	0.63	-0.01	0.01	0.05	0.01	0.00	4.34	-0.01	0.00	117.19
W7 a	13-15	0.66	-0.01	-0.04	0.03	-0.01	0.00	5.06	-0.08	0.01	1.89
W7 b	23-25	0.71	0.08	-0.02	0.03	0.02	0.00	2.97	-0.06	0.00	1.12
C1	22-23	0.27	0.03	0.00	0.06	0.04	0.00	8.76	-0.05	0.01	179.44
C4	23-40	0.35	0.09	-0.04	0.03	0.03	0.01	9.75	-0.03	-0.01	680.87
C6	23-25	0.21	0.03	-0.03	0.04	0.00	0.00	4.99	-0.08	0.00	62.85
M5	27-29	0.34	0.03	0.00	0.05	0.04	0.02	9.53	-0.10	0.01	46.85
M5	28-40	0.41	0.01	0.07	0.00	0.06	0.00	12.28	-0.02	0.03	41.57
PH93	22-23	0.21	0.03	-0.04	0.02	-0.02	0.03	8.08	-0.10	0.00	109.02
KD2	24-32	0.26	0.01	-0.04	0.04	0.00	0.00	4.91	-0.04	-0.01	84.65
AD1	9.5	2.89	0.01	0.00	0.10	0.00	0.01	24.53	-0.10	0.00	402.04
AD2	9.0	16.67	0.01	0.00	0.06	0.06	0.01	23.95	-0.02	0.00	171.00
AD8	9.0	8.24	0.04	0.00	0.26	0.02	0.01	54.87	0.67	0.03	2013.38
BLANK		0.20	0.06	0.00	0.02	0.04	0.01	-0.15	0.01	0.02	0.32

TABLE A4.6 (Continued)

TRACE CONSTITUENTS (Quantitative Data): NOV 90

Bore	Depth (m)	Mo µg/L	Nd µg/L	Ni µg/L	Pb µg/L	Pr µg/L	Rb µg/L	Sb µg/L	Se µg/L	Sm µg/L	Sr µg/L
W1 a	13-15	7.65	0.17	5.19	0.08	0.01	5.21	0.34	1.56	0.04	38.77
W1 b	23-25	0.67	0.12	8.49	1.05	0.04	5.37	0.00	1.82	0.04	44.40
W2 a	13-15	0.85	0.04	8.45	0.06	-0.02	0.93	-0.04	-0.15	0.05	23.33
W2 b	23-25	0.12	0.10	3.63	0.46	-0.01	0.73	-0.01	0.47	0.04	2.69
W4 a	13-15	0.97	0.17	59.18	0.79	0.03	2.99	-0.04	0.83	-0.04	4.46
W4 b	23-25	0.58	0.08	2.31	0.25	0.00	3.10	-0.01	-0.67	-0.01	1.79
W5 a	13-15	0.26	0.02	1.16	0.19	-0.02	0.94	0.04	-0.10	-0.04	11.24
W5 b	23-25	0.09	0.03	5.20	0.17	-0.02	1.79	-0.07	2.45	-0.01	7.40
W7 a	13-15	0.60	0.01	1.92	0.22	-0.01	0.12	0.00	0.03	0.04	3.50
W7 b	23-25	0.03	-0.03	4.15	0.24	-0.02	0.29	-0.05	0.35	0.02	2.28
C1	22-23	1.01	0.04	0.67	0.19	0.00	2.86	0.00	-0.19	-0.04	5.54
C4	23-40	0.25	0.24	0.77	0.13	0.01	1.10	0.03	0.43	0.00	2.92
C6	23-25	1.10	0.10	0.64	-0.04	0.00	2.09	0.09	0.43	0.11	3.38
M5	27-29	0.24	-0.03	2.13	0.13	-0.01	0.38	0.03	-0.24	-0.04	4.71
M5	28-40	0.26	-0.03	4.33	0.48	0.00	0.52	0.19	0.60	0.00	5.04
PH93	22-23	0.18	0.03	0.70	0.25	-0.01	1.10	0.02	0.05	0.03	6.22
KD2	24-32	0.26	0.09	0.66	-0.02	0.00	0.67	-0.04	1.71	0.07	8.47
AD1	9.5	5.72	0.03	22.58	0.58	-0.02	2.11	0.35	2.01	0.00	4.23
AD2	9.0	10.62	0.12	12.13	0.40	-0.02	1.91	0.69	0.64	0.04	3.80
AD8	9.0	1.52	0.13	63.46	40.76	0.13	8.24	2.79	1.57	0.09	7.96
BLANK		0.01	0.06	0.01	0.59	0.02	-0.01	-0.03	-0.93	-0.02	0.01

TABLE A4.6 (Continued)

TRACE CONSTITUENTS (Quantitative Data): NOV 90

Bore*	Tb µg/L	Te µg/L	Th µg/L	Ti µg/L	Tm µg/L	U µg/L	V µg/L	Y µg/L	Yb µg/L	Zn µg/L	Zr µg/L
W1 a	0.00	0.85	0.01	<0.5	0.00	8.83	23.18	0.00	0.01	3.22	0.03
W1 b	0.03	0.96	0.01	<0.5	0.01	105.76	5.27	0.01	0.04	18.33	0.05
W2 a	0.01	0.60	0.07	<0.5	0.01	83.31	4.00	0.00	-0.04	2.35	0.09
W2 b	0.01	0.50	0.08	<0.5	0.01	106.52	2.18	0.02	0.01	7.78	0.06
W4 a	0.01	0.16	0.03	<0.5	0.00	459.48	2.25	0.17	0.06	39.88	0.01
W4 b	0.00	-0.14	0.00	0.50	0.01	354.73	1.38	0.01	0.11	25.27	0.10
W5 a	0.01	0.37	-0.04	0.50	0.00	0.64	1.94	0.00	0.02	1.74	0.01
W5 b	0.02	0.14	0.03	<0.5	0.01	0.83	0.28	0.00	0.01	6.51	0.06
W7 a	0.01	0.05	-0.01	2.20	0.00	1.30	5.45	0.04	0.03	2.16	0.10
W7 b	0.01	0.57	0.07	1.00	0.01	0.59	6.95	0.00	-0.02	7.76	0.03
C1	0.01	0.19	0.04	<0.5	0.00	7.52	0.33	0.00	-0.01	3.13	0.00
C4	0.00	0.49	0.03	<0.5	0.01	13.10	0.48	0.00	-0.02	8.02	0.03
C6	0.01	0.49	0.08	<0.5	0.00	5.21	0.35	0.00	0.01	3.12	0.01
M5	0.00	0.17	0.03	<0.5	0.00	3.73	1.77	0.00	0.06	14.08	0.01
M5	0.03	-0.14	0.01	0.60	0.00	5.17	3.79	-0.01	0.12	17.30	0.03
PH93	0.00	-0.14	-0.04	<0.5	0.00	1.42	0.32	-0.01	-0.02	15.80	0.01
KD2	0.01	0.13	-0.02	<0.5	0.01	2.87	0.24	-0.01	-0.02	30.22	0.04
AD1	0.02	0.17	0.01	<0.5	0.00	52.50	2.94	0.00	0.14	9.45	0.00
AD2	0.01	-0.14	0.01	<0.5	0.01	2.55	11.96	0.00	-0.01	6.05	0.07
AD8	0.04	0.62	-0.01	<0.5	0.00	1.13	0.26	0.10	-0.04	132.13	0.02
BLANK	0.03	0.28	0.01	0.60	0.01	0.00	0.01	0.01	0.01	-0.24	0.04

* - sampling depths are as shown on page 171

TABLE A4.7

TRACE CONSTITUENTS (Quantitative Data): APR 91

Bore	Depth (m)	Al	B	Ba[a]	Ba[b]	Ce µg/L	Co	Cr	Dy	Eu	Ga
W1 a	13-15	890	17	1.6	1.38	0.00	0.15	0.12	0.00	0.00	32.16
W1 b	23-25	7	15	11.8	10.05	0.01	0.46	0.67	0.00	0.00	0.53
W2 a	13-15	24	10	7.7	6.76	0.00	0.15	0.21	0.00	0.00	0.43
W2 b	23-25	1	8	5.8	4.89	0.00	0.14	-0.13	0.00	0.01	0.18
W4 a	13-15	1	16	15.2	13.19	0.00	12.95	0.99	0.01	0.01	0.52
W4 b	23-25	1	27	13.2	11.16	0.00	0.34	1.12	0.00	0.00	0.39
W5 a	13-15	14	18	11.3	9.96	0.00	0.06	0.28	-0.01	0.01	0.33
W5 b	23-25	13	16	17	15.14	0.02	0.06	0.64	0.00	0.00	0.39
W6 b	20-25	6	25	44	43.23	0.02	0.09	0.85	0.02	0.02	1.65
W7 a	13-15	3	21	7.8	6.98	0.00	0.01	0.79	0.01	0.00	0.29
W7 b	23-25	3	6	4.2	3.64	0.00	0.02	0.40	0.00	0.00	0.20
C1	22-23	2	13	4.4	4.50	0.01	0.07	1.15	0.01	0.00	0.10
C6	23-24	2	22	7.2	7.17	0.01	0.02	0.72	0.03	0.00	0.15
M2	36-40	5	30	7.9	7.23	0.00	0.22	2.04	0.00	0.01	0.26
PH14	20-26	6	28	53	43.09	0.01	0.89	0.76	0.01	0.03	1.68
PH146	17-89	3	11	1.2	1.35	0.00	0.39	1.96	0.00	0.00	0.01
KD2	24-26	3	12	7.2	6.22	0.00	0.14	0.11	0.00	0.00	0.24
AD1	9.5m	1	68	3.4	3.39	0.02	4.69	0.10	0.01	0.00	0.13
AD1*	9.5m	22	390	0.5	0.50	0.02	0.29	1.12	0.03	0.01	0.03
AD2	9.0m	86	81	1.8	1.98	0.00	0.52	0.52	0.00	0.00	0.01
AD6	4.0m	1	24	4.2	3.86	-0.01	2.22	1.21	0.01	0.00	0.09
AD8	9.0m	1	17	138	123.58	0.03	26.06	1.53	0.01	0.06	4.88
AD9	7.0m	2	20	8.4	8.72	0.02	11.74	2.10	0.03	0.00	0.25
AD9*	7.0m	2	28	1.4	1.42	0.01	12.58	0.64	0.03	0.01	0.04
AD11	2.5m	30	167	1.6	1.28	0.04	6.58	1.17	0.00	0.00	0.01
AD11*	2.5m	19	44	1.4	1.17	0.01	4.42	0.62	0.02	0.00	-0.04
AD12	5.0m	1	132	5.2	4.86	0.03	0.80	0.57	0.02	0.01	0.16
TAD12	1.5m	46	50	0.3	0.32	0.05	0.21	0.43	0.00	0.01	-0.05
AD13	9.0m	10	89	20.6	20.42	0.02	18.79	1.61	0.01	0.00	0.54
AD14	10.5m	19	58	16	15.99	0.04	2.83	1.36	0.04	0.01	0.41
CREEK NR. KD1		3	16	3	0.59	0.09	0.18	0.42	0.01	0.00	-0.06
BLANK A mg/L		<1	13	<0.2	-0.01	0.00	0.01	0.00	-0.02	0.00	0.00
BLANK B mg/L		<1	14	<0.2	0.00	0.00	0.01	-0.09	0.02	0.01	0.00

[a] - ICPAES [b] - ICPMS

TABLE A4.7 (Continued)

TRACE CONSTITUENTS (Quantitative Data): APR 91

Bore	Depth (m)	La	Lu	Mn	Nd	Ni µg/L	Pb	Rb	Re	Sc	Se
W1 a	13-15	0.01	0.00	3.82	-0.01	0.83	-0.18	1.65	-0.01	-6.08	1.25
W1 b	23-25	0.00	0.00	20.58	0.00	2.08	-0.20	1.72	0.00	-5.90	2.18
W2 a	13-15	0.00	0.00	20.24	0.01	1.33	-0.08	0.24	0.01	-5.90	2.84
W2 b	23-25	0.00	0.00	21.49	0.01	0.19	0.61	0.29	-0.01	-6.08	4.89
W4 a	13-15	0.00	0.00	211.00	-0.01	26.72	0.59	0.85	0.01	-6.08	0.81
W4 b	23-25	0.00	0.00	65.04	-0.01	-0.26	-0.09	1.34	0.02	-6.08	1.24
W5 a	13-15	0.00	0.00	35.63	-0.01	0.25	-0.04	0.49	-0.01	-6.08	1.37
W5 b	23-25	0.00	0.00	79.33	0.01	-0.09	-0.15	0.65	-0.01	-6.08	1.08
W6 b	23-25	0.01	0.00	1.57	-0.04	4.56	2.47	42.94	0.00	-	-25.56
W7 a	13-15	0.00	0.00	8.87	-0.01	0.37	-0.23	0.08	0.00	-6.08	2.27
W7 b	23-25	0.00	0.00	5.78	-0.01	-0.19	-0.08	0.17	0.00	-5.72	1.50
C1	22-23	0.00	0.00	138.67	-0.03	0.28	-0.12	0.59	0.01	-	-14.01
C6	23-24	-0.01	0.00	76.27	-0.04	0.50	-0.24	1.03	0.02	-	-22.56
M2	36-40	0.00	0.00	94.95	-0.01	0.47	0.02	1.11	0.04	-6.08	1.12
PH14	20-26	0.00	0.00	619.65	-0.01	0.06	-0.06	0.55	0.01	-6.08	1.41
PH146	17-89	0.00	0.00	82.21	0.01	0.12	-0.23	0.21	-0.01	-6.08	0.76
KD2	24-26	0.00	0.00	37.39	0.01	-0.08	-0.23	0.08	0.00	-6.08	-0.10
AD1	9.5m	0.00	0.00	34.95	-0.02	15.96	1.94	0.39	0.01	-	-3.69
AD1*	9.5m	0.04	0.00	2.12	-0.04	3.21	2.24	0.17	0.03	-	-19.60
AD2	9.0m	0.00	0.00	65.95	-0.01	4.61	0.40	0.17	0.00	-5.78	1.53
AD6	4.0m	0.00	0.00	64.82	-0.01	6.49	-0.08	0.16	0.00	-6.08	0.86
AD8	9.0m	0.02	0.00	1024.46	0.06	103.81	1.22	2.61	0.00	-6.08	2.18
AD9	7.0m	0.00	0.00	157.94	-0.02	86.21	0.21	0.20	0.01	-	-29.46
AD9*	7.0m	-0.01	0.00	163.87	-0.03	80.33	0.17	0.36	0.02	-	-18.89
AD11	2.5m	0.02	0.01	106.86	0.01	216.79	-0.06	0.22	0.00	-6.08	2.67
AD11*	2.5m	0.00	0.00	83.21	0.00	145.50	-0.07	0.20	0.00	-6.08	-0.54
AD12	5.0m	0.01	0.00	154.72	0.01	8.04	-0.02	0.26	0.01	-5.96	1.35
TAD12	1.5m	0.01	0.00	8.15	0.01	0.33	-0.17	0.14	0.00	-5.78	0.96
AD13	9.0m	0.00	0.00	380.14	-0.01	305.89	0.53	1.09	0.04	-	-22.24
AD14	10.5m	0.00	0.00	199.39	0.01	222.65	1.06	0.64	0.01	-	-18.54
CRK NEAR KD1		0.02	0.00	2.90	0.01	0.76	2.27	0.19	0.01	-	-30.26
BLANK A		0.01	0.00	0.03	-0.02	0.07	-0.16	-0.02	0.00	-	-12.59
BLANK B		0.00	0.00	0.00	0.02	0.09	-0.18	-0.01	0.00	-	-10.17

TABLE A4.7 (Continued)

TRACE CONSTITUENTS (Quantitative Data): APR 91

Bore	Depth (m)	Sm	Sr	Tb	Th	Ti	U µg/L	W	Yb	Zn	Zr
W1 a	13-15	-0.03	23	0.00	0.00	<2	7.76	0.22	0.00	5.04	0.01
W1 b	23-25	-0.01	31	0.01	0.00	<2	45.89	0.05	0.00	7.06	0.01
W2 a	13-15	-0.02	12	0.00	0.00	<2	46.96	0.01	0.01	1.30	0.02
W2 b	23-25	-0.02	2	0.01	0.00	<2	67.26	0.03	0.01	11.88	0.00
W4 a	13-15	-0.02	3	0.01	0.00	<2	393.20	0.02	0.00	28.93	0.00
W4 b	23-25	-0.01	2	0.00	0.00	<2	287.10	0.04	0.01	3.61	0.01
W5 a	13-15	-0.02	9	0.00	0.00	<2	1.37	0.04	0.00	1.96	0.00
W5 b	23-25	-0.01	6	0.00	0.00	<2	2.08	0.00	0.01	3.23	0.01
W6 b	23-25	0.02	690	0.00	0.00	<2	2.63	9.61	0.01	2.03	0.01
W7 a	13-15	-0.01	6	0.00	0.01	<2	1.18	0.03	0.00	4.54	0.03
W7 b	23-25	-0.02	2	0.00	0.00	<2	0.32	0.02	0.00	16.29	0.01
C1	22-23	-0.02	3	0.00	-0.01	<2	7.14	0.04	-0.01	2.87	-0.01
C6	23-24	-0.02	3	0.00	0.03	<2	3.75	0.09	0.02	1.77	-0.01
M2	36-40	-0.01	9	0.00	-0.01	<2	36.19	0.08	0.01	2.56	0.01
PH14	20-26	0.00	12	0.01	0.00	<2	3.08	0.24	0.00	361.50	0.01
PH146	17-89	0.00	5	0.00	0.00	<2	0.77	0.44	0.00	23.11	0.02
KD2	24-26	-0.03	3	0.01	0.00	<2	1.54	0.01	0.00	96.22	0.00
AD1	9.5m	-0.04	11	0.01	-0.01	<2	5.14	0.01	0.01	8.53	0.00
AD1*	9.5m	0.00	12	0.01	0.03	3	7.14	0.01	0.00	35.60	0.02
AD2	9.0m	-0.01	1.5	0.01	0.00	<2	0.73	0.02	0.01	2.36	0.02
AD6	4.0m	-0.02	0.6	0.00	0.00	<2	0.49	-0.02	0.00	21.93	0.03
AD8	9.0m	-0.01	5.2	0.00	0.00	<2	0.53	0.01	0.00	24.69	0.00
AD9	7.0m	0.00	1.8	0.01	0.02	5	0.13	0.07	0.07	21.13	0.01
AD9*	7.0m	-0.02	1.6	0.00	-0.02	<2	0.16	-0.02	0.02	33.68	0.00
AD11	2.5m	-0.01	2.1	0.01	0.00	<2	1.31	-0.01	0.03	14.39	0.03
AD11*	2.5m	-0.03	0.7	0.01	0.00	<2	0.43	-0.01	0.01	36.64	0.00
AD12	5.0m	0.02	2.6	0.01	0.00	<2	2.03	0.08	0.01	2.53	0.02
TAD12	1.5m	0.04	0.5	0.01	0.00	<2	0.47	0.02	0.00	1.50	0.01
AD13	9.0m	0.02	6.6	0.01	0.01	<2	77.90	0.06	0.02	117.85	0.01
AD14	10.5m	0.01	7.1	0.00	0.01	<2	2.94	0.01	0.00	116.94	0.01
CRK NEAR KD1		0.00	0.9	0.01	-0.01	<2	0.52	0.02	0.01	6.30	0.03
BLANK A		0.01	<0.1	0.00	0.00	<2	0.00	0.00	-0.05	0.27	0.03
BLANK B		0.01	<0.1	0.00	0.01	<2	0.00	0.04	-0.03	0.55	0.01

APPENDIX 5 SEMI-QUANTITATIVE ICPMS DATA

Important note:

Semi-quantitative ICPMS data was obtained from a general ICPMS scan, as detailed in Appendix 1.6.1. It gives an indication of the presence of particular species, accurate to within a factor of 2. The detection limit is, at best, 0.01 ppb, and may be much higher than this for some elements.

It is emphasised that the major reason for obtaining this data was to assess which elements were present at levels which justified the use of other, quantitative techniques, including quantitative ICPMS. For most elements which were present at such levels, reporting of semi-quantitative data was not necessary as quantitative data subsequently became available.

Therefore, most of the constituents which were present at significant levels were measured by other, quantitative techniques.

An important consideration in assessing this data was that many species were present at levels comparable to, or below, levels in the blanks which were also submitted for analysis. In such cases, the data has been omitted from these compilations, leading to numerous blank spaces in the tables. These blank spaces should be interpreted as meaning that these elements were not present at measurable levels. Maximum blank values are given in Table A5.1.

Tables A5.2 and A5.3 illustrate the kind of data provided by qualitative ICPMS. They show that the majority of elements which were not measured quantitatively were present at negligible levels (comparable to the levels in blanks), or below detection limits. The data from these scans (and similar data for samples collected on other field trips) enabled the suite of elements for which quantitative data was obtained to be modified to include almost all elements present at potentially quantifiable levels. Therefore, on subsequent field trips, quantitative analyses of almost all elements shown as non-zero values on tables A5.2 or A5.3 were performed.

In conclusion, it can be stated that during the ARAP, every element present at levels detectable by ICPMS or any other technique in these groundwaters was determined quantitatively for at least one set of groundwater samples.

TABLE A5.1

MAXIMUM ELEMENT CONCENTRATIONS IN MULTI-ELEMENT SCANS OF BLANK SAMPLES SUBMITTED WITH KOONGARRA GROUNDWATERS

Element	Isotope	Elemental Concentration (ppb)
Ag	109	0.1
As	75	1
Au	197	0.2
Bi	219	0.1
Br	81	10
Cd	111	0.5
Ce	140	0.1
Cr	52	2
Cs	133	0.05
Cu	63	5
Dy	163	0.1
Er	166	0.05
Eu	153	0.05
Ga	69	0.2
Gd	158	0.2
Ge	72	2
Hf	178	0.1
Hg	202	1
Ho	165	0.05
I	127	5
Ir	193	0.05
Lu	175	0.05
Nb	93	0.05
Ni	60	2
Os	192	0.1
Pd	106	0.2

Element	Isotope	Elemental Concentration (ppb)
Pr	141	0.05
Pt	195	0.2
Re	187	0.05
Rh	103	0.05
Ru	102	0.2
Sb	121	0.05
Sc	45	2
Sm	152	0.2
Sn	120	0.5
Ta	181	0.02
Tb	159	0.02
Te	128	0.2
Tl	205	0.05
Tm	169	0.05
W	182	0.5
Y	89	0.05
Yb	172	0.1

These figures indicate the highest values recorded in 5 blank samples submitted with Koongarra water samples. Reflecting the accuracy of these analyses, they were rounded up, with only one significant figure reported.

TABLE A5.2

SEMI-QUANTITATIVE ICPMS DATA
(May 1989 Field Trip)

(Accurate to within a factor of 2 of the true value)

Bore-hole	Depth (m)	Elemental Concentration (ppb)									
		Br	Cu	Er	Eu	Ga	I	Ni	Os	Sb	W
Blank		10	2	0.05	0.02	0.05	1	1	0.05	0.05	0.2
PH14	20-26	34	6		0.05	1.1	14	3			
PH49	27-29	23				0.17	7				1.2
PH49	33-35	41	5		0.04	0.4	7				0.9
PH80	17-19	41	9		0.05		7				
PH146	17-89	21	7		0.11	0.12	4	3			0.9
PH146*	17-89	18			0.04		7			0.1	0.7
C6	35-40	260	5		0.05	0.3	9			0.23	0.4
C8	24-26	21			0.05	0.13	5	3			
C8	38-40	45				0.3	6	3		0.13	
C9	34-40	36			0.08	0.2	10	3			
C10	27-40	93	6	0.11			7	3	0.13		
M1	24-26	38	9	0.13	0.08	0.24	10		0.2	0.11	0.3
M1	35-50	29			0.05	0.15	6			0.12	0.3
M1	46-48	23		0.16	0.1		8		0.14		
M2	40-46	31	4			0.2	4		0.14		
M3	20-22	30	6	0.13	0.04	0.11	8			0.1	
M3	26-28	69				0.2	14				
M3	34-40	38			0.06	0.2	8				
M4	34-40	61	14	0.15	0.05	0.6	6				
W4	23-25	110	5	0.1	0.04	0.4	14	14		0.13	
K Ck		113			0.06		8			0.2	

The remaining elements, not included on this table, were below the blank values given in Table A5.1.

TABLE A5.3

SEMI-QUANTITATIVE ICPMS DATA
(October 1989 Field Trip)

units - ppb
(Accurate to within a factor of 2 of the true value)

Bore-hole	Depth (m)	Bi	Cd	Cs	Ga	Re	Sb	W	Yb
W1 a	13-15			0.06	9.49			0.29	
W1 a	13-15	0.03		0.07	8.63			0.09	
W1 b	23-25			0.22	0.66				
W1 b	23-25			0.18	0.99				
W2 a	13-15				0.02				
W2 b	23-25								
W3 a	13-15							0.28	0.04
W3 b	23-25								0.05
W4 a	13-15			0.06	0.05				
W4 a	13-15								
W4 b	23-25				0.04			0.02	
W4 b	23-25								
W5 a	13-14			0.02					
W5 b	23-25								
W7 a	13-15								
W7 b	23-25								
PH49	25-27	0.02					0.05	2.58	
PH49	45-47					0.08		2.44	
C5	25-27								
C7	25-27								
C7	25-27								0.01
M2	37-39	22.5	1.54					0.06	

All other elements listed in Table A5.1 were comparable to, or below the blank values.

APPENDIX 6 MISCELLANEOUS DATA TABULATIONS

TABLE A6.1

COMPARISON OF GROUNDWATER DATA OBTAINED BY PNC (JAPAN) AND CSIRO, LUCAS HEIGHTS, AUSTRALIA
(May 1988 Groundwater Samples)

Bore	Depth mg/L	Mg mg/L	Na mg/L	K mg/L	Ca mg/L	Si mg/L	Fe mg/L	Mn µg/L	Lab
PH14	20-26	20.3	1.32	0.62	5.0	10.9	1.11	420	CSIRO
		21.0	1.30	0.60	2.5	10.7	1.06	430	PNC
PH15	19-21	21.5	1.01	0.59	3.6	8.2	0.42	350	CSIRO
		22.0	1.10	0.53	2.1	7.9	0.35	370	PNC
PH49	16-28	20.1	1.32	0.53	3.1	9.9	0.82	182	CSIRO
		21.0	1.40	0.49	1.8	9.0	0.78	190	PNC
PH49	28-30	26.4	1.35	0.68	3.9	8.9	0.78	154	CSIRO
		26.0	1.30	0.60	4.5	8.9	0.84	160	PNC
PH55	26-28	17.9	3.16	1.05	4.4	14.0	5.60	142	CSIRO
		18.4	3.20	1.10	2.7	12.9	5.70	150	PNC
PH55	40-42	18.3	1.57	1.65	3.7	12.1	0.70	97	CSIRO
		19.9	1.60	2.00	4.3	11.4	0.68	100	PNC
PH56	43-45	16.7	1.17	0.53	4.4	9.4	0.53	35	CSIRO
		17.3	1.10	0.53	5.2	9.0	0.53	40	PNC
PH58	38-40	17.7	2.22	1.45	3.7	15.8	0.28	87	CSIRO
		18.2	2.20	1.20	2.3	14.1	0.26	90	PNC
PH61	26-28	16.4	0.96	0.59	2.7	8.1	0.05	7	CSIRO
		17.1	1.10	0.54	3.4	7.7	0.05	<10	PNC
PH61	43-45	18.0	1.12	1.00	8.8	7.2	0.26	54	CSIRO
		19.7	1.20	1.00	10.8	6.7	0.25	60	PNC
PH80	17-20	16.2	1.15	0.37	1.3	10.9	0.35	234	CSIRO
		16.8	1.20	0.35	0.8	10.4	0.30	250	PNC
PH94	26-28	5.7	1.99	1.00	1.4	12.1	0.04	8	CSIRO
		6.0	2.20	1.00	1.0	11.1	0.06	10	PNC
PH94	40-42	6.1	3.53	2.00	3.8	10.4	0.19	23	CSIRO
		6.1	3.80	2.00	4.4	9.4	0.19	30	PNC
KD1	40-42	3.6	1.09	0.37	3.1	6.1	18.90	189	CSIRO
		3.8	1.10	0.33	1.9	5.7	20.00	200	PNC
KD1	80-82	2.4	0.99	0.18	2.0	6.5	0.10	9	CSIRO
		2.5	1.10	0.26	1.2	6.0	0.09	<10	PNC

TABLE A6.2

COMPARISONS OF U AND Mn DATA OBTAINED BY VARIOUS TECHNIQUES

April 1991 Sample Set

Bore	Depth (m)	Mn AES µg/L	Mn ICPMS µg/L	U ICPMS µg/L	U KPA µg/L
W1 a	13-15	1	4	7.76	8.59
W1 b	23-25	11	21	45.9	45.9
W2 a	13-15	14	20	47.0	44.3
W2 b	23-25	20	21	67.3	66.1
W4 a	13-15	208	211	¦	393
W4 b	23-25	47	65	287	300
W5 a	13-15	26	36	1.37	1.32
W5 b	23-25	75	79	2.08	2.13
W7 a	13-15	3	9	1.18	1.16
W7 b	23-25	1	6	0.32	0.26
C1	22-23	147	139	7.14	7.27
C6	23-24	77	76	3.75	3.64
M2	36-40	74	95	36.1	39.3
PH14	20-26	550	620		
PH146	17-89	28	82	0.77	0.77
KD2	24-26	58	97	1.54	1.61
AD1	9.5	36	35	5.14	5.22
AD1*	9.5	2	2	7.14	6.55
AD2	9.0	63	66	0.73	0.69
AD6	4.0	55	65	0.49	0.45
AD8	9.0	950	1024	0.63	0.49
AD9	7.0	165	158	0.13	0.09
AD9*	7.0	166	164	0.16	0.18
AD11	2.5	86	107	1.31	1.34
AD11*	2.5	68	83	0.43	0.40
AD12	5.0	151	155	2.03	2.33
TAD12	1.5	6	8	0.47	0.67
AD13	9.0	370	380	77.9	74.6
AD14	10.5	208	199	2.94	2.91

* - Denotes second sampling

TABLE A6.3

TOTAL ORGANIC CARBON DATA

(Measurement procedure described in Appendix 1)

Detection limit 0.3 mg/L

Borehole	Depth (m)	Field Trip	TOC (mg/L)
AD1	9.5	May 91	0.90
AD2	9	May 91	0.90
AD12	5	May 91	3.10
AD13	9	May 91	1.00
C6	35-40	May 89	0.46
C8	24-26	May 89	0.61
C8	38-40	May 89	0.81
C9	34-40	May 89	0.66
C10	27-40	May 89	1.62
KD1	40-42	Nov 88	1.42
M1	24-26	May 89	0.75
M1	35-50	May 89	0.97
M1	46-48	May 89	1.70
M2	40-46	May 89	0.71
M3	20-22	May 89	0.86
M3	34-40	May 89	0.53
M4	34-40	May 89	0.63
PH14	20-26	Nov 88	0.97,0.57,1.24
PH15	19-21	Nov 88	1.74,1.10
PH49	28-30	Nov 88	1.51
PH49	33-35	May 89	0.87,0.97
PH49	44-46	Nov 88	1.24,0.84,0.98
PH55	26-28	Nov 88	1.30
PH55	40-42	Nov 88	1.38
PH56	26-28	Nov 88	1.09
	43-45	Nov 88	1.33
PH58	25-27	Nov 88	2.16
PH58	38-40	Nov 88	1.24
PH61	26-28	Nov 88	1.69
PH61	43-45	Nov 88	1.34
PH80	17-20	Nov 88	0.97
PH80	17-20	May 89	0.53
PH88	28-30	Nov 88	1.66
PH88	38-40	Nov 88	0.94
PH94	26-28	Nov 88	0.87
PH94	40-42	Nov 88	1.58
PH96	16-26	Nov 88	0.76
PH146	17-89	May 89	0.76,0.48

Borehole	Depth (m)	Field Trip	TOC (mg/L)
W1a	13-15	Nov 90	1.20
W1b	23-25	Apr 91	0.50
W2a	13-15	Nov 90	1.30
W2b	23-25	Apr 91	0.70
W4a	13-15	Nov 90	2.80
W4b	23-25	Apr 91	1.70
W7a	13-15	Nov 90	1.60
W7b	23-25	Apr 91	1.60